TECHNISCHE UNIVERSITÄT MÜNCHEN

Lehrstuhl für Physiologie

Secondary plant metabolites and gut health: functional studies on porcine small intestine *in vitro* models

Jakob Maximilian Müller

Vollständiger Abdruck der von der Fakultät Wissenschaftszentrum Weihenstephan für Ernährung, Landnutzung und Umwelt der Technischen Universität München zur Erlangung des akademischen Grades eines

Doktors der Naturwissenschaften

genehmigten Dissertation.

Vorsitzender:		Univ.-Prof. Dr. D. R. Treutter
Prüfer der Dissertation:	1.	Univ.-Prof. Dr. M. W. Pfaffl
	2.	Priv.-Doz. Dr. A. K. Büttner
		(Friedrich-Alexander-Universität Erlangen-Nürnberg)

Die Dissertation wurde am 18.04.2012 bei der Technischen Universität München eingereicht und durch die Fakultät Wissenschaftszentrum Weihenstephan für Ernährung, Landnutzung und Umwelt am 24.07.2012 angenommen.

Für meinen verstorbenen Doktorvater Prof. Dr. Dr. Heinrich H. D. Meyer

Content

Abbreviations

3´-UTR: Three prime untranslated region

67LR: 67kDa laminin receptor

COPD: Chronic obstructive pulmonary disease

CV: Coefficient of variation

DAC: Decitabine

DCs: Dendritic cells

DMEM: Dulbecco's modified eagle medium

DNMT: DNA methyltransferases

EGCG: Epigallocatechin gallate

FBS: Fetal bovine serum

GALT: Gut-associated lymphoid tissue

GC-MS: Gas chromatography-mass spectrometry

GFP: Green fluorescent protein

IBD: Inflammatory bowl disease

IECs: Intestinal epithelial cells

IgA: Immunoglobulin A

kbp: Kilo base pairs

kDa: Kilo dalton

LB-agar: Lysogeny broth agar

LC-MS: Liquid chromatography-mass spectrometry

LPS: Lipopolysaccharid

M-cells: Microfold cells

MOI: Multiplicity of infection

PAMPs: Pathogen associated molecular patterns

PBS: Phosphate buffered saline

PCA: Principal component analysis

PRRs: Pattern recognition receptors

qPCR: Quantitative real-time polymerase chain reaction

RIN: RNA integrity number

RNAi: RNA interference

RT: Reverse transcription

SAFE: Solvent assisted flavor evaporation

SEM: Standard error of the mean

shRNA: Small hairpin RNA

USDA: U.S. department of agriculture

VP: Viral particles

Abstract

Secondary plant metabolites are the most ethnic medicative agents. If taken up by nutrition for steady health promotion or ingested aimed during an acute disease, their major effectiveness is mediated trough the epithelial of the gastrointestinal tract. Two candidates as representatives for a pharmacological drug and a food component were investigated in this work due to its curative potential employing *in vitro* models of the small intestine. Thereby, the major volatile compound of eucalyptus oil (*Eucalyptus spec.*), cineole was focussed as being an established medication in respiratory diseases. Regarding the health impact of a daily green tea diet, the prime secondary plant metabolite of *Camellia sinensis*, epigallocatechin gallate (EGCG) was selected as the infusion of this plant represents the second most consumed beverage globally next to water.

Porcine cell lines as IPEC-J2 (jejunal) and IPI-2I (ileal) served as monogastric models of the intestinal epithelium. By employment of gas chromatography-mass spectrometry (GC-MS) initial metabolization of cineole in the small intestine, immediate to absorption was evaluated. Appliance of electric cell-substrate impedance sensing (ECIS) further monitored the herbal influence by means of toxicity and in general processes on cellular level. For questioning the locally mediated immune response to both investigated secondary plant metabolites reverse transcriptase quantitative real time polymerase chain reaction (RT-qPCR) based gene expression analysis was applied. For a better understanding of involved molecular drug targets the cell culture models were physiologically manipulated by adenoviral induced RNA interference (RNAi) in terms of loss-of-function studies. In particular therewith the EGCG and also metastasis related membrane bound 67 kDa laminin receptor (67LR) was examined, as well as its involvement in TLR4 signaling. Additionally for the tea catechin the scope was extended to epigenetic level and its potential to alter inherit methylation patterns was measured using luminometric methylation assay (LUMA).

The outcome reveals distinct cytotoxicity parameters within the *in vitro* approach as well as for cineole dosage by determining a sharp cell detaching concentration level. Noteworthy for the pharmacological compound no measurable corresponding immune reactions could be assigned close to this threshold. In contrast, considering primary pathways of innate immunity EGCG evoked cytokine up-regulations on mRNA level independently from predicted molecular pathways in concentrations as evaluated for tea beverages, as well as applied in

much lower doses. Consecutive considerations of anti-tumorigenic properties of EGCG showed its potential to alter global methylations and further, related to the 67LR, could show a significant suppressive potential in synergy with regulatory small RNAs even in very low concentrations.

In this view the measurable intestinal health promotion through the focussed secondary plant metabolites in this work is ambivalent. The immediate benefit of cineole applied orally for cure of respiratory diseases could not be assigned to physiological activities within the small intestine epithelium. For EGCG a promising new gateway in metastasis prevention is accessed what calls for follow up studies employing cancer cell lines, not only of the gastrointestinal tract.

Zusammenfassung

Sekundäre Pflanzenstoffe stellen die ursprünglichste Art medikativer Anwendungen dar. Ob für eine stetige Gesundheitsförderung mit der Nahrung aufgenommen, oder als gezielte Einnahme im akuten Krankheitsfall, wird ihre primäre Wirksamkeit über das Epithel des Gastrointestinaltrakts vermittelt. Zwei sekundäre Pflanzeninhaltsstoffe wurden während dieser Arbeit als Vertreter eines pharmakologischen Wirkstoffes, beziehungsweise eines Nahrungsbestandteiles, bezüglich ihrer heilsamen Eigenschaften in *in vitro* Modellen des Dünndarms untersucht. Einerseits wurde Cineol untersucht welches Hauptbestandteil des Öls der Eukalyptuspflanze (Eucalyptus spec.) ist und als gebräuchliche Medikation bei Erkrankungen der respiratorischen Organe eingesetzt wird. Andererseits wurde hinsichtlich des Einflusses einer täglichen Diät der Hauptmetabolit des Sekundärstoffwechsels der Teepflanze (*Camellia sinensis*), Epigallochatechin gallate (EGCG) ausgewählt, da grüner Tee das weltweit am zweit häufigsten konsumierte Getränk nach Wasser darstellt.

Die porcinen Zellinien IPEC-J2 (jejunum) und IPI-2I (ileum) dienten dabei als Modelle monogastrischer Darmepithelien. Durch Gaschromatographie-Massenspektrometrie (GC-MS) wurde die eingängige Verstoffwechselung von Cineol unmittelbar nach der Aufnahme im Dünndarm untersucht. Weiterhin wurden mittels Electric Cell-substrate Impedance Sensing (ECIS) Pflanzeninhaltsstoff induzierte Einflüsse auf Zellulärer Ebene aufgezeichnet, sowie die im Modell verursachte Zytotoxizität untersucht. Zur Fragestellung nach den lokal im intestinalen Epithel vermittelten Immunantworten beider Sekundärer Pflanzenstoffe wurden Reverse Transkriptase quantitative Echtzeit Polymerase Kettenreaktion (RT-qPCR) basierte Genexpressionsanalysen durchgeführt. Zum besseren Verständnis der tangierten molekularen Ziele der Drogen diente die physiologische Manipulation der Zellkulturmodelle mit Hilfe von adenoviral vermittelter RNA Interferenz (RNAi) für Funktions-Verlust-Analysen. Im Speziellen stand dabei der sowohl mit EGCG als auch mit Metastasenbildung in Verbindung stehende 67 kDa Laminin Rezeptor (67LR) im Mittelpunkt. Im Weiteren wurde die Beteiligung dieses Proteins an der TLR4-Signaltransduktion untersucht. Um die Beeinflussung epigenetischer Methylierungsmuster durch das Teecatechin zu untersuchen wurde der Luminometric Methylation Assay (LUMA) herangezogen und somit die Betrachtung auf die epigenetische Ebene erweitert.

Es zeigten sich prägnante Zytotoxizitätsparameter sowohl verursacht durch den *in vitro* Versuchsansatz selbst als auch durch die Cineolgabe, wobei sich dabei ein scharf definiertes letales Konzentrationsniveau ermitteln lies. Bemerkenswerterweise verursachte der Arzneistoff nahe dieses Grenzwertes keine damit zusammenhängende, messbare Immun-Reaktion im Zellkulturmodell. Dahingegen rief die EGCG-Gabe den angeborenen Immunstoffwechsel betreffend verstärkte Zytokin Expression auf mRNA Ebene hervor, welche unabhängig von postulierten Stoffwechselwegen zu beobachten war. Diese Effekte waren unter EGCG-Konzentrationen messbar welche wie auch hier gezeigt denen von frisch aufgebrühtem grünen Tee entsprechen, als auch in sehr viel geringeren Dosen. Anschließende Untersuchungen zu der Tumorbildung entgegenwirkenden Eigenschaften von EGCG konnten ein die globale Methylierung veränderndes Potenzial zeigen. Im Zusammenhang mit dem 67LR konnte außerdem für sehr niedrige Konzentrationen ein signifikantes Vermögen von EGCG festgestellt werden in Synergie mit regulierenden small RNAs die 67LR Expression zu supprimieren.

Im Anbetracht der Ergebnisse ergeben sich ambivalente Befunde bezüglich der gesundheits-fördernden Eigenschaften der hier untersuchten Sekundären Pflanzenstoffe vermittelt im Dünndarmbereich. Ein unmittelbarer positiver Effekt durch die orale Einnahme von Cineol bei respiratorischen Erkrankungen kann nicht klar an eine Wirkungsvermittlung über das Dünndarmepithel gekoppelt werden. Dahingegen eröffnet EGCG einen viel versprechenden neuen Ansatz für die Forschung zur Prävention von Metastasenbildung welcher Folgestudien an nicht nur dem Verdauungssystem entsprungenen Krebszelllinien nahelegt.

Background

Secondary plant metabolites and gut health

Long before mankind was aware of molecules the effectiveness of plants on human health was discovered. With rising knowledge and more elaborate analytical methods the detailed composition of medications containing herbal ingredients was elucidated. Today, modern drug screening reveals numerous candidate molecules derived from plants all over the world which serve as leads for the pharmacological industry. This field gets particularly interesting if a potentially active agent of a traditionally used plant extract is characterized and can then retrospectively be assigned to its physiological function in health promotion.

Weather ingested directly with the food or more specifically by pharmacologically processed preparations, the most common path of drug delivery for herbal administrations is the oral intake. Accordingly the interest in how natural products contribute to the improvement or development of gastric well being is immense. Thereby, by means of immunity the most important section of the gastrointestinal tract is the small intestine. Located between the stomach and the large intestine (Figure 1) the small intestine represents that part of the digestive system where nutrients are depleted from the previously chemically and enzymatically down broken ingested matter. Hence the small intestine represents the major epithelium for selective absorption of extracorporeal substances into the organism. This circumstance carried along that during evolution this body interior interface developed a crucial role in immunity (Groschwitz & Hogan 2009).

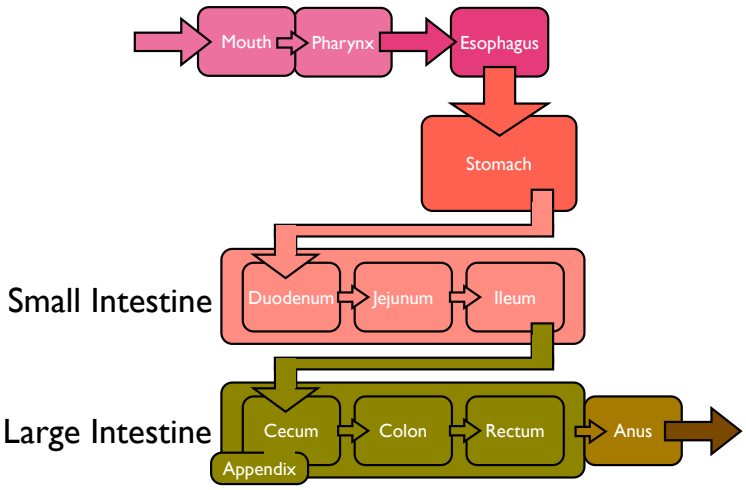

Figure 1 Alimentary canal

Along with the daily food intake not only primary nutrients but also secondary plant metabolites, anorganic compounds and withal a multitude of microbes enter our body. All enclosed pathogens which pass the stomach without degradation by the gastric acid continue their noxious passage into the small intestine. In case of an injury on the surface of the body that breaks the physical lining of the outer epithelium a local inflammation is induced as reaction of the innate immune system to concomitant bacterial infections. Secondary responses of the acquired immune system are then mediated outgoing from the body wide network of lymph nodes to the peripheral located lesion. Immune cells including macrophages, dendritic cells (DCs), B-cells and T-cells are recruited, activated and dispatched to act upon the site of infection (Ley et al. 2007). In case of the body interior lining epithelial where a permanent changing microbial environment must be separated from the desired nutrients determined for absorption, a more specialized tissue has developed. Enclosing it is called gut-associated lymphoid tissue or GALT. This assemblage of epithelial and immune cell linages represents a partially autonomous acting part of the immune system. Among the basic intestinal epithelial cells (IECs) reside embedded paneth cells, goblet cells, enterocytes and enteroendocrine cells (Abreu 2010) and thus form the mucosal coated physical boundary of the small intestine. Characteristically positioned within the sub-section of the ileum the follicular structures of the peyer's patches perform a locally mediated humoral immune response by processing antigens directly out of trans-epithelial phagocytosed and digested pathogens through microfold cells (M-cells) (Owen 1999). Pro-inflammatory cytokine/chemokine signaling what includes primary (IL1β, TNFα) (Galley & Webster 1996) and secondary (IL6, IL8) (Pitman & Blumberg 2000) mediators leads to the recruitment of macrophages and DCs and in turn T-cells and B-cells which initiate Immunoglobulin A (IgA) production in the underlying lamina propria (Fagarasan & Honjo 2003; Underdown & Schiff 1986). Beneath minor influence on obsonization processes and complement system activation, the subsequent secretion of IgA into the gut lumen then primarily prevents the mucosa of bacterial colonization. Recognized pathogens get coated with IgA and consecutively flushed out.

In the more worse case when microorganisms pass the mucosal barrier and intrude the underlying tissue another defense mechanism becomes effective. On both apical and basolateral surfaces of the gut epithelium as well as on the membrane of macrophages and DCs within the tissue Pattern Recognition Receptors (PRRs) are expressed. Those receptor

bind Pathogen Associated Molecular Patterns (PAMPs) which represent small molecular conserved motifs present on the surface of microbes (Akira et al. 2006). A prominent candidate which triggers the bacterial Lipopolysaccaride (LPS) is the Toll like receptor 4 (TLR4). The subsequent cast cascade leads to the expression of genes signaling an acute inflammation. In case of TLR4 the bound LPS two crucial MyD88- and TRIF-dependent physiological pathways are involved: The MAPK-Pathway and the Nfκb-Pathway (Akira 2009). By activation of transcription factors and further their translocation into the nucleus Cytokines like IL1β, IL6, IL12β and TNFα indicating an acute inflammation are produced (Platt & Mowat 2008). By the LPS induced signal also T-Cells can be attracted to PAMP activated DCs what is depending on expression of membrane proteins (CD40, CD80 & CD86) and simultaneous antigen presentation (Iwasaki & Medzhitov 2004). Accordingly the TLR-Pathway represents a crucial link between innate and acquired immunity what expand the importance of the GALT for the whole immune system.

However already beyond the active threat by microbial attacks the gastrointestinal tract takes a key role basic physical condition of an organism. Its physical constitution determines between healthiness or chronic illness. When the pre-processed chymus reaches the small intestine it contains beside microbial contents still a variety of secondary plant metabolites originating from the food. Dietary habits often carry along a self-imposed monotony. This may carry along an amplification of weak herbal originated physiological effects over time and result in health promotion or insidious toxification.

The basic functionality of the intestinal mucosa is based on permanent renewal what becomes apparent in one of the quickest turnover rates of all tissues. This balance between growth and mortification is distinct regulated by the interplay of proliferation, differentiation and finally apoptosis (J. N. Rao et al. 2010). By maintaining the programmed cell death the signaling through of initiator-caspases (like Casp9) and in turn effector-caspases (like Casp3) regulates the IEC-homeostasis (Earnshaw et al. 1999).

Regarding in further context disorders like inflammatory bowel disease or gastrointestinal cancer, the question if proliferation or contrarily apoptosis promoting factors are affected by the constant impact of nutritionally or medicatively ingested matter becomes crucial. Beside a role in Crohn's disease (Maclachlan 2008) the expression of Cyclin D1 is related to uncontrolled G1/S phase transition and thus develops an oncogenic function (Fu 2004).

Considering the second cell cycle checkpoint prior to mitosis entry the regulation of Cyclin B1 takes a similar position related to gastric cancer (Begnami et al. 2010). Fatally disorders of cytokine mediated regulation via the transforming growth factor beta (TGFβ) are even supposed link the state of chronic inflammation to cancerogenesis (Hong 2010).

The common entity of all these processes is that they all act locally in the GALT. Hence the impact from locally enriched physiologically active compounds of herbal origin is self-evident. Therefore this work is dedicated to the investigation of two secondary plant compounds which evolve their health promoting potential in the gut.

A popular medical administration traditionally and indeed applied orally in respiratory diseases therapy is cineole or containing preparations. The impact on epithelial development, its immunomodulatory potential as well as the immediate metabolisation by IECs are examined here in a combinatory methodical approach.

Green tea is ubiquitous consumed almost all over the world. Therefore the second candidate chosen is epigallocatechin gallate, the major flavonoid of the tea plant. This compound was object of multiple studies concerning health promoting effects mediated through gut epithelium.

Cineole, respiratory therapy in the gut

Cineole or 1,8-cineole (see Figure 2) is a cyclic monoterpenoid (IUPAC-nomenclature: 1,3,3-trimethyl-2-oxabicyclo[2.2.2]octane) and a secondary plant metabolite also known as eucalyptol, what refers to its major natural source, the eucalyptus tree (*Eucalyptus spec.*). Oil from this plant can contain up to 84% of the volatile compound (Sadlon & Lamson 2010). Cineole is a colorless and liquid lipophilic volatile aroma compound with a density of 0.93 g/cm3 (at 20 °C) and can be dissolved in water with up to 3.5 g/L (at 21 °C). It has a melting point of 1 - 2 °C, a flash point of 49 °C and a boiling point of 174 - 177 °C. The empirical formula of cineole is $C_{10}H_{18}O$ at a molecular weight of 154.25 g/mol.

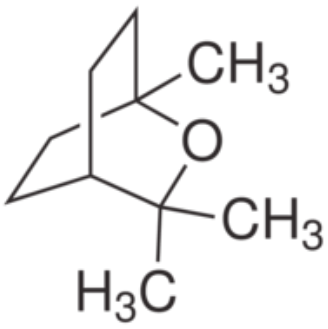

Figure 2 Cineole (1,3,3-trimethyl-2-oxabicyclo[2.2.2]octane)

However, other plants like laurel (*Laurus spec.*), oregano (*Origanum spec.*), basil (*Ocimum spec.*), rosemary (*Rosmarinus spec.*), thyme (*Thymus spec.*), sage (*Salvia spec.*) or cardamom (*Elettaria spec.*) commonly used as cuisine herbs also contain this substance but in far fever amounts (Sertel et al. 2011; Asbaghian et al. 2011; Ben Farhat et al. 2009). Once ingested orally the metabolization of cineole is maintained by the cytochrome P450 system in the mammalian liver as studies revealed (Duisken et al. 2005; Miyazawa et al. 2001). Australian scientists could identify a multitude of urinary cineole metabolites (2,9-Dihydroxy-, 2,10-dihydroxy-, 2α,4-Dihydroxy-, 2α,7-dihydroxy-, 7,9-Dihydroxy-, 7-Hydroxy-1,8-cineole and 7-cineolic acid) from brushtail possums (*Trichosurus vulpecula*) feed with a cineole rich diet (Boyle et al. 2000; Carman & Klika 1992; Bull et al. 1993) (& follow up studies). Similar results were gained from human plasma or urine samples after experimental application of sage tea (2-hydroxy-, 3-hydroxy-, 7-hydroxy- and 9-hydroxy-1,8-cineole) (Horst & Rychlik 2010).

Actually the employment of cineole is manifold. Beneath seasoning, cosmetical or even cleaning issues the use as pharmacological agent has a long tradition in many cultures as the Australian or Chinese (Whitehouse et al. 1998; Chiang et al. 2005). Nowadays, cineole has gained a distinct role all around the world as non-prescription mucolytic medication in disorders like Bronchitis, Sinusitis or Chronic Obstructive Pulmonary Disease (COPD) (Juergens et al. 2003; Worth et al. 2009). Described more abstract in the context of mucosal epithelial affection. Customary well known products in Germany are Soledum® (Klosterfrau Healthcare Group, Köln, Germany) or GeloMyrtol® (G. Pohl-Boskamp GmbH & Co, Hohenlockstedt, Germany) for example. Both preparations have in common that they are applied orally as enteric coated capsules, and hence evolve their curative potential beyond their passage through the stomach within the small intestine.

The development of an expectorant effect of cineole by inhalation through the respiratory tract is empirically proven and a major application. Conventional preparations like Transpulmin® (MEDA Pharma GmbH & Co. KG, Bad Homburg v.d. Höhe, Germany) can be either used by straight slathering onto the torso or direct inhaling with steaming water. Concomitant physiological impacts are scientifically examined. An inhibitory effect for cytokines TNFα, IL1β, IL6 and IL8 on cultured human lymphocytes and monocytes has been described (Juergens et al. 2004) as well as on a murine macrophage cell line (Chao et al. 2005). Further anti-inflammatory and anti-nociceptive activities of cineole were evaluated *in vivo* by inflammation experiments in rats (F. A. Santos & V. S. Rao 2000).

The rising question is now, if cineole is applied orally, what effects are mediated locally in the gut epithelium? Antimicrobial activity of 1,8-cineole or containing oils is described manifold (Nascimento et al. 2000; Prabuseenivasan et al. 2006). Cytotoxicity in cancer cell culture models is also evident (Foray et al. 1999; Loizzo et al. 2007). Is it thus health promoting or harmful? What dose is lethal for IECs and what effects arise before? Are regulatory factors determining the destiny of an epithelial cell affected by cineole or thereout metabolized molecular compounds? May immunomodulation trough cineole in the GALT have far more impact on an organism than curing a cold?

Green tea, epigallocatechin gallate and its receptor

Flavonoids are a very versatile class of secondary plant metabolites which provide a variety of marvelous skills. Popular members like the anthocyanidins provoke the color of leaves and fruits, what shields from damage caused by ultraviolet radiation and at the same time attract auxiliary insects for pollination. Another abundant member of the flavonoids are the catechins (or flavan-3-ols, see Figure 3) which are capable to act allelopathic, what means they harm other competing or hostile species (Baldwin 2003). However, following Paracelsus` famous principle, *the dose makes the poison*, these catechins do not affect malicious only. A characteristic of all flavonoids is the phenolic core scaffold (Mota et al. 2009) that makes them potent antioxidants (Valcic et al. 1999). This is utilized positively for the plants protection against oxidative stress, as well as for the plants consumer. Therefrom many healthy effects are assigned to enriched consumption of this compound class or containing vegetal food respectively.

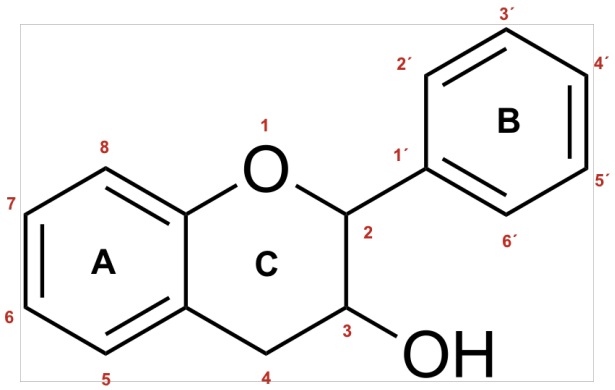

Figure 3 Catechin core scaffold (Flavan-3-ol)

If we now face the question what the richest source of Flavonoids is, the basic worldwide consumption of a particular aliment must be considered. Hence, due to be the second most drank liquid on earth, tea and within its quantitatively major secondary plant compound Epigallocatechin gallate (EGCG) contributes with most substantial impact. According to a study of the U.S. Department of Agriculture (USDA) wherein an extensive database of flavonoid containing habitual biomaterials was compiled (Government 2011) the EGCG content of green tea (*Camellia sinensis*) is only exceeded by the carob fruit (Ceratonia siliqua) (Figure 4), but carob is certainly far less consumed. Other food plants, like red berries, apples or nuts which have still noteworthy EGCG contents follow distant by several powers of ten.

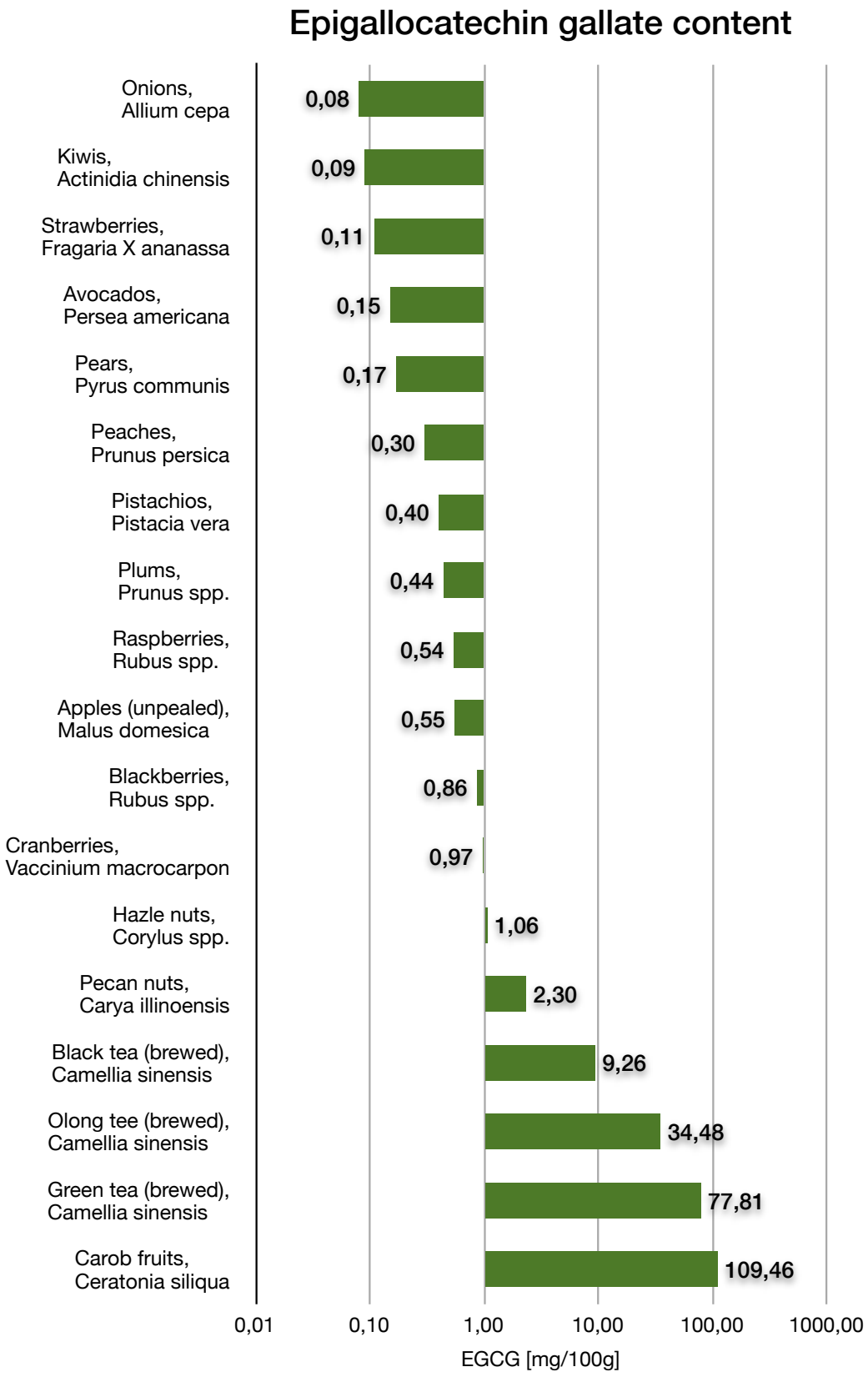

Figure 4 Epigallocatechin gallate content of all comprising vegetal biomaterials listed in the USDA-database.

from: U.S. Department of Agriculture - "USDA Database for the Flavonoid Content of Selected Foods" (Release 2.1 - January 2007); URL: http://www.nal.usda.gov/fnic/foodcomp/Data/Flav/Flav02-1.pdf

The EGCG molecule itself (Figure 5) is a white solid salt. Its empirical formula is $C_{22}H_{18}O_{11}$ at a molecular weight of 458.37 g/mol. The prefix *Epi-* refers to the diastereoisomeric enantiomes which are present throu C atoms 2 & 3 of the C ring, whereas *-gallo-* marks an extra hydroxyl group at the 3´ C atom of the B-ring of the catechin scaffold that is esterified with gallic acid at C atom number 3 of the C-ring. When EGCG is solved in water the color turns to a brownish, greenish yellow (Flavonoid originates from latin, *flavus* meaning yellow) and tastes bitter, attended by an adstringent effect similarly as a green tee infusion (Kielhorn & Thorngate 1999).

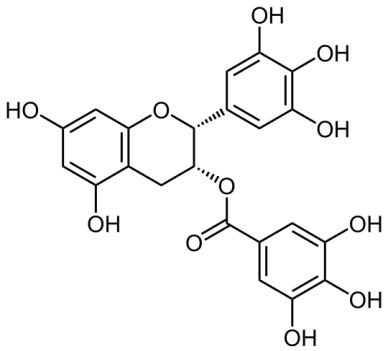

Figure 5 Epigallocatechin gallate ((2R,3R)-2-(3,4,5-Trihydroxyphenyl)-3,4-dihydro-1(2H)-benzopyran-3,5,7-triol-3-(3,4,5-trihydroxybenzoat))

Green and black tea are both made from the same plant, *Camellia sinensis*. Green tea is immediately steamed and roasted what prevents it from fermentation. Exactly this is what is desired in black tea production. The characteristic darker, more orange or brown color of black tea rises from enzymatic oxidation and hydrolysis of catechin constituents of the tea leaves. The result is the formation of theaflavins (Figure 6) which are polycyclic polyphenols formed by quinonic condensation of the catechin molecules (Tanaka & Kouno 2003) and which evoke the unique flavor of black tea (H. N. Graham 1992). The lighter color of green tea compared to black tea get comprehensible by comparing the catechin patterns of both tea preparations as shown in Figure 7 (Government 2011).

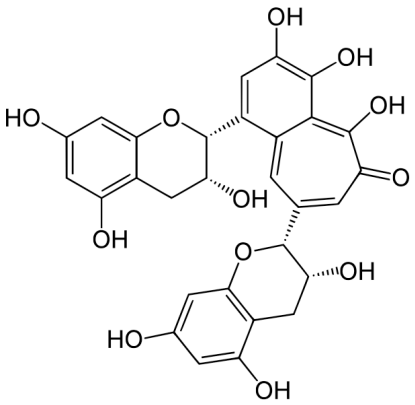

Figure 6 Theaflavin (3,4,5-trihydroxy-1,8-bis[(2R,3R)-3,5,7-trihydroxy-2-chromanyl]-6-benzo[7]annulenone)

Flavan-3-ol composition (including Theaflavin) in *Camelia sinensis* dry leaves and infusion, raw (green) or fermented (black)

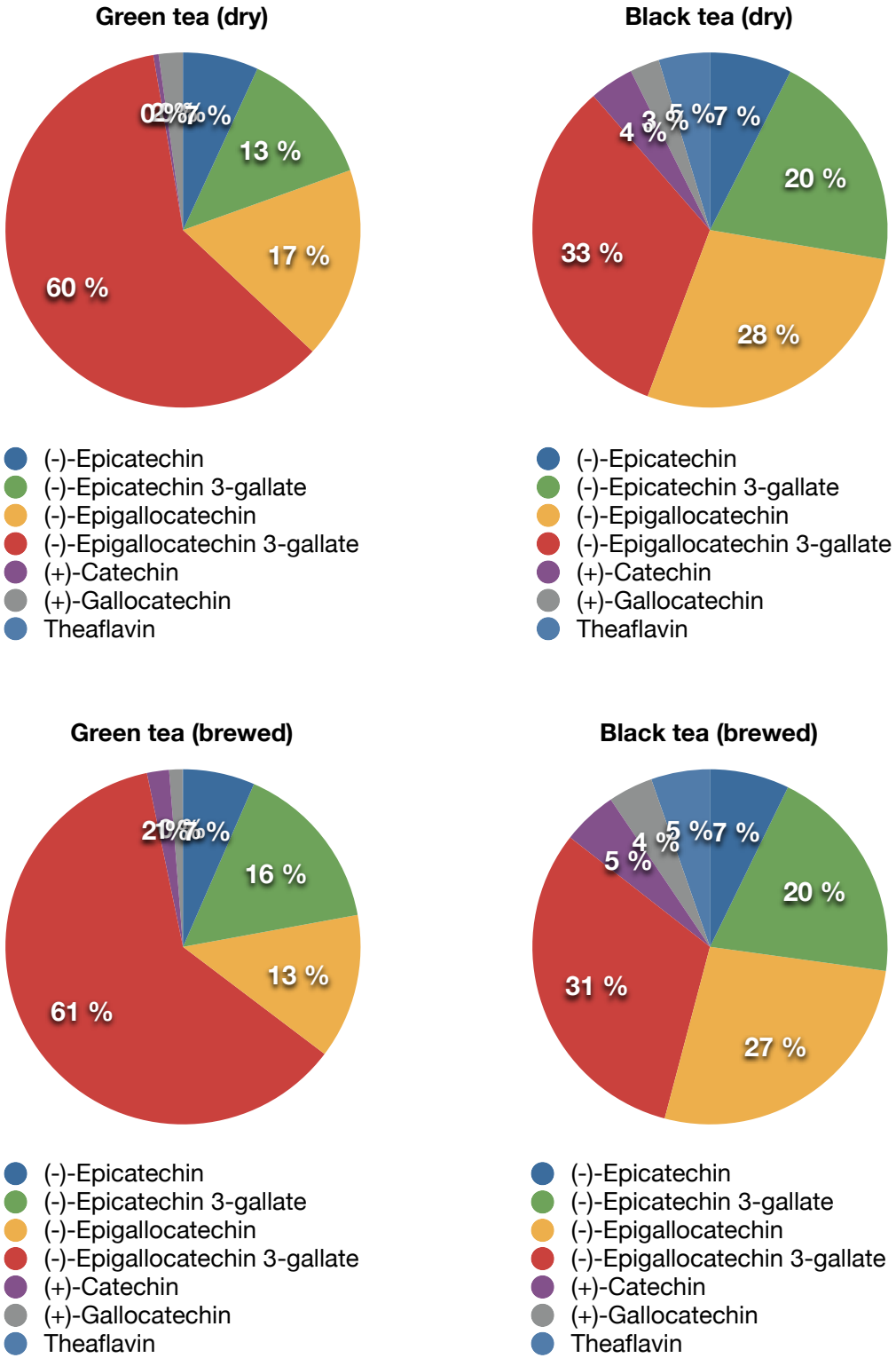

Figure 7 Major catechin (Flavan-2-ol) composition of green and black tea, dry matter or brewed.

from: U.S. Department of Agriculture - "USDA Database for the Flavonoid Content of Selected Foods" (Release 2.1 - January 2007); URL: http://www.nal.usda.gov/fnic/foodcomp/Data/Flav/Flav02-1.pdf

Several intermediate processing levels are known today as the so called semi-fermented Oolong teas or specially treated tea specialities. Among these are for example the Pu-Erh tea which is extra microbial treated black tea that ferments for several years at room temperature (Q. Wang et al. 2011) or preparations like the Kombucha what is made by using a combination of bacterials and yeasts applied on pre-sweetened black tea (Greenwalt et al. 2000).

Evaluating the innumerable studies on tea polyphenols, for healthy issues the consumption of green tea is supposed to have more positive effects compared to black tea (Cheng 2006). An obvious reason is the higher antioxidant potential which is, measured in Vitamin C equivalents, 1.8 times higher for unfermented tea than for fermented (K. W. Lee et al. 2002a). Another reason may be the enriched caffeine content in black tea, what rises parallel and reciprocal to the oxidative degradation of EGCG in the tea leafs during the fermentation processes (Y.-S. Lin et al. 2003). Concretely many findings reporting health promoting properties of tea consumption including issues of cardiovascular diseases, referring to total or LDL cholesterol levels (Deka & Vita 2011), the potential to prevent obesity by influencing adipogenesis (Moon et al. 2007) and counteractions in various vicious viral induced diseases, among Hepatitis C (Dhiman 2011) and Herpes simplex (Isaacs et al. 2011) as well as inhibitory activities on the life cycle of the HI-virus (Yamaguchi et al. 2002; S. Li et al. 2011) or its infectivity (Hauber et al. 2009).
The worldwide *per capita* consumption of green tea is approximated with 120 mL/day (Babu & D. Liu 2008). Accordingly the alimentary aspects of green tea or EGCG intake and further diseases related to the gastrointestinal tract are obvious. Statistically, no other secondary plant metabolite should have a more consequential influence by means of steadiness and moderate dosage. Interestingly, regarding the initial impact in the consumer´s mouth, an epidemiological study could show that the potential to develop esophageal cancer was reduced dependent on the drinking temperature of tea (Wu et al. 2009) and recommended lukewarm drinking. On the proximate passage through the gastrointestinal tract EGCG is more or less unchallenged as studies show that only weak down breaking activity can be observed by saliva (Tsuchiya et al. 1997) or within the stomach due to the non-oligomeric character of this particular class of polyphenols (Spencer et al. 2000).

Commonly flavanoids in nature are conjugated to β-glycosidic carbohydrates what requires β-glycosidase activity prior to absorption. Exceptionally flavan-3-ols are mostly present non-glycosylated. Hence their uptake for further circulation through the mesenteric tissue proceeds immediately in the small intestine (Spencer 2003). With regard to local disorders like mucosal ulcers or lesions, healing properties could be attributed to tea catechins in animal studies (Hamaishi et al. 2006; Sato et al. 2002). The more general syndrome of Inflammatory bowl disease (IBD) is mediated by alteration of the pattern of resident microbes interacting with the intestinal mucosa and the consequential interplay of environmental and/or host factors (Xavier & Podolsky 2007). Antibiotic and probiotic properties balancing the gut flora (Su et al. 2008) were assigned to green tea consume and further it has already been recommended as a therapeutical appliance concerning Crohn's Disease (Alic 1999). The IBD underlying pathways follow LPS induced activation of the adaptive immune system, what recruits dendritic cells and macrophages via TLR4 signaling, whereupon the transcription factors Nfκb and AP1 become effective (Akira & Takeda 2004). In consequence as described above (see chapter "*Secondary plant metabolites and gut health*") the inflammatory cytokine cascade is initiated. Thereby an immunomodulatory role of EGCG by affecting not only the involved leukocytes (Ahn et al. 2004; Wilkins et al. 2011) but also the epithelial cells of the small intestine (F. Yang et al. 2001) through inhibition of the Nfκb effector kinase Iκkb has already been described.

If these inflammation pathways are chronically stressed an enhanced risk for development of intestinal cancer is given (Angel & Karin 1991; Eferl & Wagner 2003; Dolcet et al. 2005; Akira 2009). In this context manifold publications report and review the preventive potential of EGCG in probably all kinds of cancer, but especially by molecular targeting and inhibition of the Nfκb- and MAPK pathways (J. K. Lin et al. 1999; Chung et al. 1999; Kazi et al. 2002; J.-K. Lin 2002; Donaldson 2004; Beltz et al. 2006; Shankar et al. 2007; C. S. Yang & H. Wang 2011; C. S. Yang et al. 2011; Yuan et al. 2011). What remains despite of all studies unclear, are the distinct mechanisms of how EGCG effects the oncogenic targets. The question is how the interaction is mediated.

A potential milestone in all EGCG research was the postulation of a membrane-embedded receptor by Hirofumi Tachibana in 2004, that specifically reacts to EGCG contact, but not to other close related catechins (Tachibana et al. 2004). His discovery refers to a quite

ambiguous gene which has been mainly linked to metastasis formation so far (Liotta 1986; Castronovo 1993). The 67kDa laminin receptor (67LR), also known as LAMR1, RPSA and with multiple other names. This gene is peculiar indeed as it poses a mystery around its processing during expression. Derived from a genomic sequence, encoding a 32.8 kDa protein, it is translated into a 37 kDa precursor and subsequently appears as a 67 kDa protein. Further it is conspicuous because of its high redundancy. Found as conserved sequence almost allover the five kingdoms it emerges everywhere: intra-nuclear, cytosolic, ribosomal, membrane-embedded although no typical transmembrane segment is present, as well as secreted into the surrounding media (Castronovo et al. 1991; Montuori & Sobel 1996; Nelson et al. 2008). By means of gastric cancer and in particular metastasis it has been shown that the expression level of this gene positively correlates with enhanced progression of the disease (W. A. Lee et al. 1996; L. Liu et al. 2010). Thereby, in its nature as laminin receptor, the 67LR mediates over-expressed in the membrane of circulating cancer cells through specific surface binding while target tissue invasion, as briefly reviewed (Müller n.d.).

The question now is, if the above cited molecular targets involved in multiple intestinal inflammatory disorders are stimulated by EGCG autonomously, via the 67LR, or on another and still ambiguous way? What represents the detailed mode of action on molecular pathway level? Ahead follows the task to deal with the issue evolving when the anti-cancerogenic potential of the green tea polyphenol EGCG faces the interplay with a so far metastasis correlated receptor. Does the 67LR act separately by a novel signaling linked to EGCG, or emerges a new synergy, not preconceived without being aware of the ligand/receptor relation? Maybe the observations referring to EGCG as cancer preventive agent made until today must be viewed in a different light.

In vitro approach

The scientific analysis of secondary plant metabolite induced effects on physical health in particular mediated through the initial reactions following the uptake in the immuno-linked gastrointestinal system requires an abstract model. Therefore cell culture provides a potent and convenient application for basic research, not only indicating the final effects post application, but also allowing more specified and isolated considerations of molecular-physiological issues. The pig as a monogastric animal matches best the physiology of the human being. Hence the utilization of a porcine epithelial cell line represents a very universal model to provide information valuable for diverse interest groups. There among animal health as an economic factor as well as human health as ubiquitous demanded.
Accordingly the epithelial cell lines used in this work, IPI-2I (ileum) and IPEC-J2 (jejunum), being progenies of porcine small intestine tissues provide a versatile platform for analysis of both, initial metabolization of secondary plant compounds by the small intestine and resulting immunomodulatory effects which affect biochemical pathways.

Non-invasive online monitoring via electric cell-substrate impedance sensing

Studying physiological processes in an isolated manner requires enhanced methods. Metabolite profiles raised by GC-MS-analysis or RT-qPCR expression patterns can be acquired following an application after the desired incubation time by posterior sampling of tissue or cells respectively. More diagnostic information needs monitoring of the kinetics decrypting the proceeding effects after an application. Therefore in regard to the cell culture based *in vitro* approach this study employs the electric cell-substrate impedance sensing technology (ECIS) (Giaever & Keese 1984).
This method utilizes a device that functions as impedance meter (as described in section *Experimental*). Electrodes and counter-electrodes implemented into the substrate area of special cell culture dishes or “arrays“ measure the change in impedance through the inserted media. Co-applied cells which settle onto the surface alter the signal in dependence from the adjusted frequency of the applied current. The present frequency allows to catch events in different heights above the ground what provides more specified insights into different cell activities. Among cell migration and proliferation (Lo et al. 1993; Lundien et al. 2002) signal

transduction (Reddy et al. 1998), cell attachment (Giaever & Keese 1984), invasion or extravasation (Keese et al. 2002), the barrier function of cell layers (Tiruppathi et al. 1992) or even the cell behavior under a continuous media flow (DePaola et al. 2001).

The output is a visualization mirroring all changes over time expressed as normalized impedance. However, information must be interpreted by consulting microscopy and cell counts for example in order to evaluate what the signal shift corresponds to. If finally the data curves are assigned to a certain cell state detailed real time data of how a treatment develops its physiological potential over time can be acquired. Toxicity levels of applied treatments, if intended or provoked by technical side effects can be determined in a dose dependent manner (Müller et al. 2011; Almstätter et al. n.d.). Lethality establishing over a certain time under a certain dosage of a substance is measured not only at the end point but already at the onset of toxicity what reflects the cellular situation true-to-life.

Switching physiological pathways by RNA interference

Real time recording of the events of cellular level is one grave conception, but to reveal the underlying principles on molecular level requires a more sophisticated assay set up. Applying a treatment is dedicated to evoke an effect. After emergence it can be recorded and evaluated due to the desired parameters. However, when analyzing biochemical pathways the more meaningful knowledge lies within the black box between the stimulus and the reaction. Therefore, with regard to metabolic questions the identification of the bottleneck within a regulatory pathway is the key target of investigation. The necessary tool is an application that can block such a physiological relay in order to identify the effector drug target.

For this task the method of choice, when working in cell culture models and also in this study, is RNA interference (RNAi). This evolutionarily conserved and ubiquitous phenomenon in eukaryotes and in protists (Cerutti & Casas-Mollano 2006; Marraffini & Sontheimer 2010) was first described in 1998 by the group of the two scientists Andrew Zachary Fire and Craig Cameron Mello (Fire et al. 1998). Nowadays the underlying mechanism which induces posttranscriptional gene silencing is assigned as a natural protection against viral or transposonal threat (Buchon & Vaury 2005).

The process of RNAi is initiated by exogenous double strained shRNA inside the nucleolus. These shRNA-precursors, normally of viral origin, are initially recognized by an enzyme called Drosha (Y. Lee et al. 2003; Han et al. 2006). This ribonuclease finds the loop secondary structure and subsequently cleaves the precursor producing a 3´-prime two nucleotide overhang (see Figure 8). The so pre-processed ribooligonucleotide is then transferred outside the nucleolus via GTP dependent Exportin V (Zeng & Cullen 2004). In the cytosol this small shRNA is in turn recognized by a second ribonuclease called Dicer. Therefrom the whole processing is called “dicing“. The target detection is “cis-acting“ actuated, what means it is driven by recognition located on the same molecule (Y. Wang et al. 2007). In this step the loop is removed determining the second end of the remaining now so called small interfering RNA (siRNA). Likewise a 5´-prime two nucleotide overhang is produced (Myers et al. 2003). In following events a cumulative process starts wherein a couple of proteins, among members of the argonaut family or the dsRNA binding protein R2D2 play an important role (Q. Liu et al. 2003; Song et al. 2003). They are recruited and assemble an Enzyme complex called RISC (from *RNA-induced silencing complex*) (Schwarz et al. 2003; Pham & Sontheimer 2005). Now the siRNA-duplex is selectively unwinded and the 5´-prime thermodynamic more labile RNA fragment is incorporated into the RISC as “guide strand“ (Khvorova et al. 2003). With this siRNA loaded the RISC can bind its mRNA target derived from the same progenitor and thus faces its enemy. Thereupon the messenger transcript is cleaved and subsequently degraded, how the silencing effect is initiated (Ameres et al. 2007). This perfect matching siRNA can be recycled within the RISC and evokes more RNA interference (Murchison & Hannon 2004).

Since its discovery in 1998 RNA interference has been developed to a practicable biotechnological tool based on the discovery of the German scientist Thomas Tuschl and his colleagues (Elbashir, Harborth, et al. 2001a). Anterior problems in transferring the phenomenon by applying siRNAs or inducing its expression arouse from unintended random interferon reactions of host organisms to “longer“ shRNA constructs. In 2001 Tuschl´s workgroup could show that employment of explicitly 21 base pair “short“ constructs leads to absence of the disturbing immune responses (Tuschl 2001). Today the derived technology has further developed and is now even utilized for approaches of therapeutical gene silencing (Bumcrot et al. 2006).

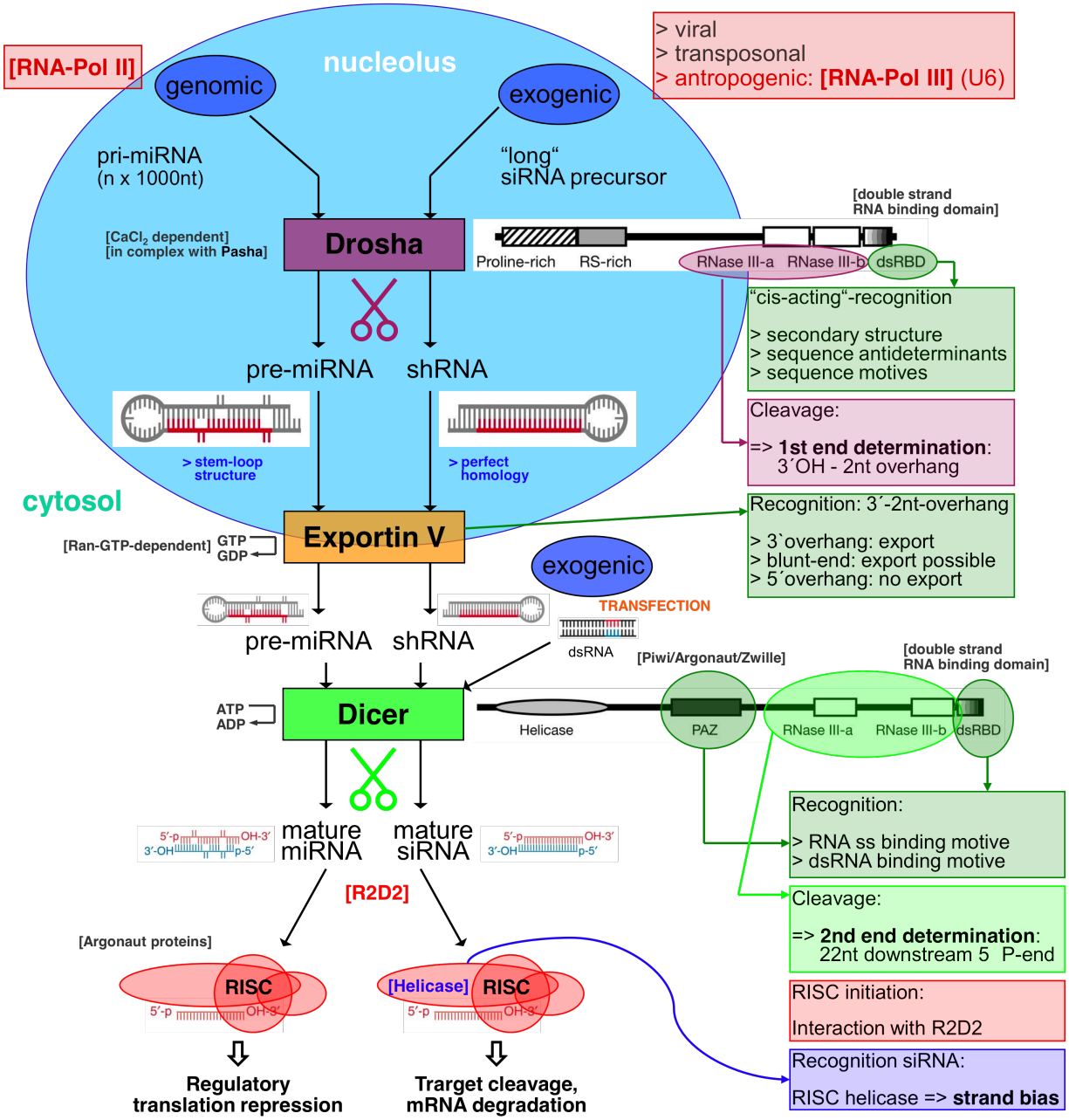

Figure 8 Small RNA pathways. Figure made 2008 by Jakob Müller with information from literature research (Krinke & Wulff 1990; Zhang & Nicholson 1997; Filippov et al. 2000; Elbashir, Lendeckel, et al. 2001b; Hammond et al. 2001; Nykänen et al. 2001; Blaszczyk et al. 2001; Conrad & Rauhut 2002; Hannon 2002; Y. Lee et al. 2002b; Hutvágner & Zamore 2002; Myers et al. 2003; Y. Lee et al. 2003; Q. Liu et al. 2003; Schwarz et al. 2003; Lingel et al. 2003; Yan et al. 2003; Song et al. 2003; Zeng & Cullen 2004; Y. S. Lee et al. 2004b; Pham et al. 2004; Lingel et al. 2004; Murchison & Hannon 2004; Joshua-Tor 2004; Y. Lee et al. 2004a; Landthaler et al. 2004; Pham & Sontheimer 2005; Han et al. 2006; Y. Wang et al. 2007; van Rooij & Olson 2007; Kapadia et al. 2008; Grosshans & Filipowicz 2008).

A task within this work is to examine how the secondary tea compound EGCG contributes to the health state of an organism and in particular how it establishes its positive effect within the small intestine epithelia or GALT. In this context based on cell culture models, RNAi can auxiliary be applied for drug target screening by designing “loss-of-function“-studies. As described above (Chapter “*Background*“) the pathogen related structure molecule LPS is a potent inductor of an acute immune responses which occur causally in the small intestine due to its nature as interface for nutrient absorption and likewise protective lining. The triggered signaling is described to runs via two pathways, engaging the transcription factors AP1 and Nfκb and induce primary mediators of the inflammatory cascade namely TNFα, IL1β, IL6 and IL12β. Within these pathways the expression of the transcription factors is crucial for signal transduction. In regard of the objective drug, the green tea polyphenol EGCG the known effector is Nfκb. Further the postulation of the membrane-embedded EGCG receptor (67LR) (Tachibana et al. 2004) complements the analytic setting (see Figure 9). By questioning if a LPS induced immune signal stops provoking an immune response when one of these key players (Nfκb, AP1, 67LR) is blocked, or loses its functionality through RNAi silencing, the detailed role of EGCG in intestinal inflammation can be distinguished.

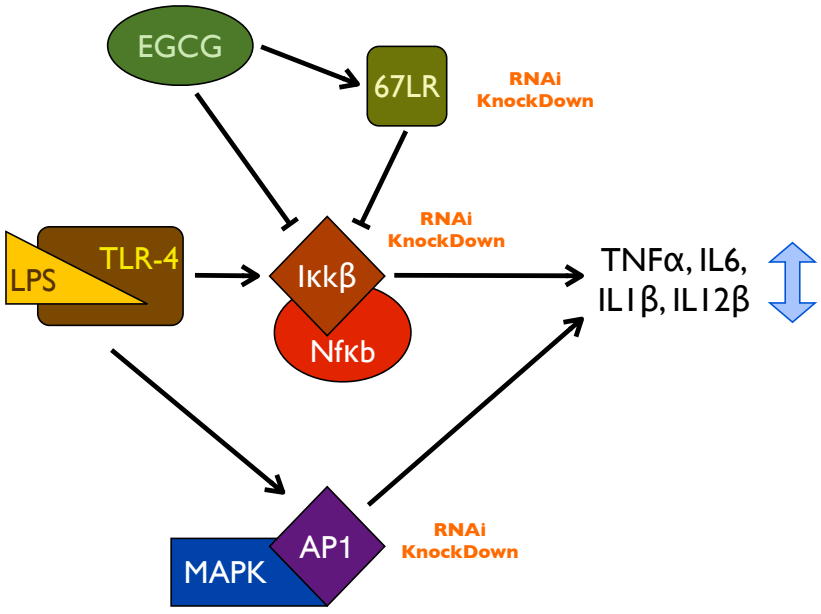

Figure 9 Loss-of-function scenario. Figure made 2012 by Jakob Müller with information from the KEGG pathway database (Kyoto Encyclopedia of Genes and Genomes; http://www.genome.jp/kegg/) and from literature (Angel & Karin 1991; Karin 1995; Takeuchi & Akira 2001; Fujihara et al. 2003; Karin et al. 2004; Tachibana et al. 2004; Akira et al. 2006; Akira 2009).

Extending scope to epigenetic level

The RNAi mediated knockdown model described in the precedent chapter provides a test system for elucidation of drug targets involved in inflammation within the porcine small intestine cell culture. The basic principle is to switch physiological pathways by inhibiting the functionality of key genes within and thus evaluate the pursued path of signal transduction by absence of expected effects induced by the treatment. In this manner, for more information about how the objective secondary plant metabolites affect, another kind of gene silencing can be utilized. It insists in the alteration of present methylation patterns by an analyte. Generally to such processes is referred as epigenetics (Berger et al. 2009). Methylation occurs covalent bound to genomic DNA, thereby causing stable inherited phenotypes but without changing the DNA sequence itself. These patterns are mounted, removed and maintained by a group of enzymes called the DNA methyltransferases (DNMTs). Subspecies are the DNMT 1 which is postulated to perform general *maintenance* work (Mortusewicz et al. 2005; T. Chen & E. Li 2006) and DNMTs 3a & 3b which are meant to be essential *de novo* methylators (Okano et al. 1998). By means of physiological pathways these enzymes gain more and more importance linked to cancerogenesis (Esteller 2007). Abnormal hypomethylation of promotor regions of tumor-suppressor genes results in cancer promotion due to awakened expression. Accordingly a disturbance in DNMT activity can result in pro- or anticancerogen effects. A potent inhibitor of the DNMTs is decitabine (Flotho et al. 2009). This compound represents a cytidine analog (Figure 10) that evolves its inhibitory functionality when phosphorylated to a triphosphate nucleotide and then incorporated into the DNA (Szyf 2010).

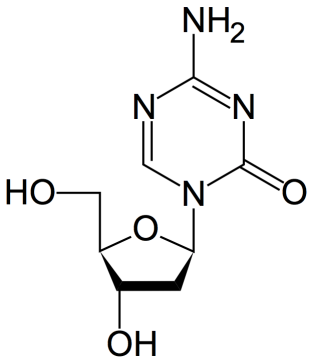

Figure 10 Decitabine (5-aza-2'-deoxycytidine)

When DNMTs interact with the genomic DNA, they form stable complexes with the cytosine analogs and thus enzymes are trapped (Christman et al. 1985). Reactivation of silenced tumor suppressor genes has already been shown to inhibit cell growth in various cancer cell lines (F. P. S. Santos et al. 2010; M.-Y. Chen et al. 2011). Logically the effectivity is coupled to the basic cell turnover as being induced during proliferation.

As described above there are manifold findings of anticancerogenic or at least cancer preventive properties of EGCG (see chapter "*Green tea, epigallocatechin gallate and its receptor*"). As further described the 67LR might provide the *missing link* by playing a double role, as EGCG receptor as well as in target tissue recognition during metastasis. Recently it has been reported that the anticancerogene potential of EGCG might originate from a direct interaction and inhibition of the DNMTs with the tea catechin. DNMTs can provoke DNA demethylation comparable to decitabine and in turn can provoke tumor suppressor gene reactivation in cancer cell lines (Fang et al. 2003).

Hence, in regard of the intestinal cell culture model an add-on approach for physiological analyses concerning the health promoting effects of EGCG is the investigation of evoked alterations in methylation patterns. If this epigenetic aspect is paired with RNAi loss-of-function scenarios targeting the different key players of DNA methylation on the one hand and the metastasis plus EGCG related 67LR on the other, we face an approach bearing a high potential of new discoveries. Complemented with decitabine as a control inhibitor the potential oncogenic signaling network between the EGCG-receptor and epigenetic regulation of tumor suppressors by DNA methyltransferases might be elucidated and provide more insights in how Epigallocatechin gallate acts in cancer (Figure 11).

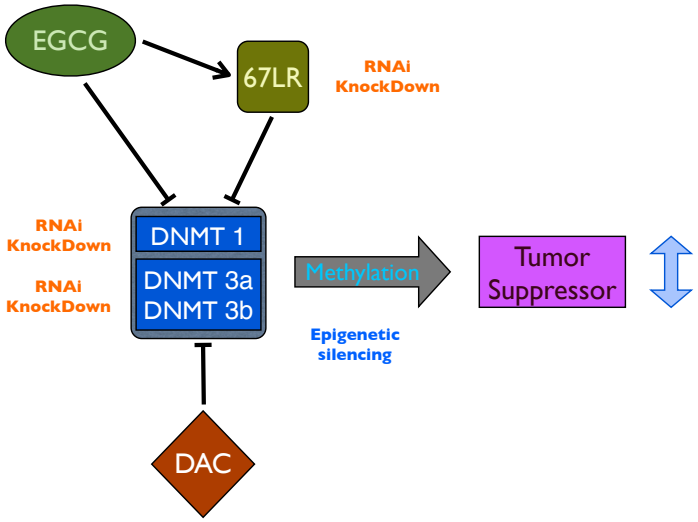

Figure 11 Epigenetic silencing combined with RNA interference. Figure made 2012 by Jakob Müller from information given and cited in chapter "Extending scope to epigenetic level".

Aim of the study

The studies intend to deliver more insights in how secondary plant metabolites act in health promotion through the small intestine epithelium. Inherently positive effects of the here investigated substances cineole and epigallocatechin gallate are already empirically proofed or manifold attributed by scientific, clinic and epidemiological studies. However, what misses is detailed knowledge of specifically attended physiological pathways or triggering intermediate metabolites. Therefore the aim of this study was to employ *in vitro* models which can be manipulated on demand in order to establish clarifying test settings for distinct screening of molecular drug targets and thereby provide the necessary physiological conditions to attain and evaluate a near *in vivo* drug turnover.

The epithelial cell lines IPI-2I (ileum) and IPEC-J2 (jejunum) as progenies of porcine small intestine tissues supply a versatile platform for analysis of both, intestinal metabolization and subsequent immunomodulatory effects induced by secondary plant compounds. By appliance of nutritional, pharmacological and in order to obtain magnified effects overbid concentrations, the cells are stimulated, resulting metabolite profiles are assessed and potential drug targets are scheduled to be identified by permutation of loss-of-function scenarios in a combined methodical approach.

Experimental

Cell culture

Basic maintenance

All cell cultures in this work were maintained at 37°C, 100% humidity and 5 % CO2. Cells were subcultured all 72 h at 80 % of confluence. For routine passaging 75 cm^2 (250 mL) cell culture dishes (Greiner Bio-One, Frickenhausen, Germany) served as platform. Therefore cells were washed with pre-warmed (37 °C) Phosphate buffered saline (PBS) and subsequently detached with pre-warmed (37 °C) 0.25 % trypsin/EDTA (PAA, Pasching, Austria). Only cells passaged less than ten times were used. Three different kinds of cells were applied using different medias:

IPI-2I

Dulbecco's modified eagle medium (DMEM) (PAA) supplemented with 10% fetal bovine serum (FBS) (PAA), 4 mM L-glutamine (PAA), 0.024 U/mL insulin (Sigma–Aldrich, St. Louis, USA) and 100 U/mL penicillin/streptomycin (PAA). The IPI-2I are porcine jejunal epithelial cells transformed with the SV40 plasmid (pSV3-neo) for immortalisation (Kaeffer et al. 1993) and derive from an adult miniature male boar. They were supplied by Health Protection Agency Culture Collections, Salisbury, UK.

IPEC-J2

DMEM/Ham's F-12 (1:1) (PAA) supplemented with 5 % FBS (PAA), 2 mM L-glutamine (PAA) and 100 U/mL penicillin/streptomycin (PAA). The IPEC-J2 are non-transformed porcine ileal epithelial cells (Schierack et al. 2006) and originate from a neonatal unsuckled piglet. They were generously supplied by Dr. Karsten Tedin (FU Berlin).

HEK-293

DMEM (PAA) supplemented with 10% FBS (PAA), 4 mM L-glutamine (PAA) and 100 U/mL penicillin/streptomycin (PAA). The Hek-293 are human kidney cells (F. L. Graham et al. 1977) cells were originally drawn by Cell Lines Service (Eppelheim, Germany) but supplied by SIRION-BIOTECH GmbH (Martinsried, Germany).

Metabolite assays

Metabolite profiling

For assessment of the metabolisation of cineole by the gut epithel $1x10^6$ IPEC-J2 cells were seeded in 75 cm^2 (250 mL) cell culture dishes (Greiner Bio-One) containing 20 mL of cell culture medium. After 72 h the medium was renewed when the cells attained a confluence level of 95 %. Subsequently the cells were treated by adding 1 mL or 100 µL of the cineole stock solution so that the resulting final concentrations were 0.1 g/L and 1.0 g/L. The cineole stock solution was continuously stirred due to weak solubility of cineole in water. The different treatments were performed in duplicates. After incubation for 0 h, 3 h, 6 h, 9 h and 24 h the cells were detached using a cell scrapper together with the surrounding medium and transferred into a glass separating funnel.

Immediately the harvested cells were mixed with 20 mL of dichloromethane (1:1) and an internal standard (tri-fold deuterated 2-α-hydroxy-1,8-cineole, 400 ng/mL) was added. By mixing and separating the hydrophilic and hydrophobic phases the extraction was carried out. This procedure was carried out tree times under repeated addition of 20 mL of dichloromethane.

Subsequently the samples were stored at -20 °C until Solvent assisted flavor evaporation (SAFE) (Engel et al. 1999) processing and microdistillation (Bemelmans & Land 1979) previous to Gas chromatography-mass spectrometry analysis (see chapter "*Gas chromatography-mass spectrometry*").

Physiological profiling

For the question if cineole may alter the expression pattern of epithelial gut cells a approach on a smaller platform was chosen. $1x10^5$ IPEC-J2 cells were seeded in 48 well cell culture dishes (Greiner Bio-One) 600 µL of cell culture medium. After 48 h , at 80 % confluence the medium was changed when and subsequently washed with 600 µL of PBS. Then cineole in three different concentrations (0.0 g/L, 0.1 g/L and 1.0 g/L) was applied mixed with fresh cell culture media. All treatments were performed in triplicates. Thereafter the cell culture returned into the incubator. After 0, 3, 6, or 9 h wells were sampled by aspirating the supernatant and washing the cell layer with pre-warmed PBS and proximate addition of lysis buffer RLT (RNeasy® Mini Kit, Qiagen, Hilden, Germany). Then RNA was extracted according to the manufacturers manual and stored at -80 °C.

Knockdown assay

For knockdown studies a cell culture assay based on 48-well tissue culture plates (Greiner Bio-One) was established. Therefore 500 µL of a homogenized cell suspension containing 1 x 10^5 cells (IPEC-J2 or IPI-2I) was applied per well. After 48 h of settlement the cell culture medium was removed and the cell layer was washed with 600 µL of pre-warmed (37 °C) PBS. Subsequently 500 µL of treatment containing medium was added to the cells what represents the starting point of the incubation time or the virus infection. The incubation times were fitted to the particular issue of an assay. All treatments were performed in triplicates (three wells).

If multiple treatments were inserted during one assay at different points of time the first treatment was applied with 350 µL (e.g. EGCG) and the second treatment with another 150 µL (e.g. LPS) of cell culture medium.

With elapsing of the particular incubation time the cell layer was washed with another 600 µL of PBS and 350 µL of pre-warmed lysis buffer RLT (RNeasy® Mini Kit, Qiagen) was applied with regard to the following total RNA extraction. If the extraction was not carried out recently the lysis buffer treated 48-well plates were sealed with Parafilm® (Pechiney Plastic Packaging Company, Chicago, USA) and then stored at -20 °C until extraction.

Virus application

Adenoviral vectors were stored as glycerol stocks at -80 °C in 30 µL aliquots. For application in the assays an aliquot was thawed on ice and then a pre-dilution in cell culture medium was mixed in order to minimize the pipetting error. Using this pre-dilution the working solutions containing the desired MOI for the particular assay were prepared.

For determination of the need amount of virus each assay plate contained “count-wells“. These were extra wells mounted with the same cell suspension as all other wells in an equal volume. They were harvested with 400 µL of trypsin solution post to the PBS washing step. In this manner exclusively vital cells still attached to the substrate were obtained and then counted using a Neubauer Hemocytometer. For that cell count always three wells were pooled for an average result representing the mean cell number over the tissue culture plate at the time of treatment.

After virus application the cell culture wells were incubated for 48 h until an optimal RNA interference gene knockdown was established (see chapter “*Adjusting the effector to firm parameters*“) or incubation time was fitted to the particular issue of an assay (indicated in results if altered). Then another PBS washing step was implemented and subsequently further treatments were applied.

Drug treatments

50 mg of solid EGCG (Sigma–Aldrich) were solved in 10 mL H_2O and stored in aliquots at -20 °C. From this stock solution the working solutions for the cell culture assays were prepared in medium.

For induction of the cells 10 mg of LPS (Sigma–Aldrich) were solved in 10 mL cell culture medium and stored in stock solution aliquots at -20 °C.

The inserted final concentration of each applied substance is displayed in the plot for every single experiment shown.

Methylation assays

Alteration of methylation patterns by manipulation of physiological pathways

For the methylation experiments $1x10^5$ IPEC-J2 cells were seeded into 6-well tissue culture plates (Greiner Bio-One) containing 3 mL of cell culture medium. After 48 h the medium was aspirated and the cells were washed with 2 mL of PBS. Along with 3 mL of fresh medium the virus application was applied at a MOI of 400. If knockdown viruses for several genes were added simultaneously into one well each virus was inserted with a MOI of 400. Accordingly the negative control virus (Ad5-U6stop) was applied in an equal amount what means summing up the total viral dose for one particular well. That way all wells obtained the same viral load in order to potentially bear equal side-effects caused by the viral infection.
After the virus infection the cells were cultivated for another 24 h, allowing expression of the transfected shRNA and manifestation of the knockdown. At this point of time cells were treated with 2 mg/L, 20 mg/L EGCG or 5 µM DAC (Sigma–Aldrich). Therefore 100 µL of a stock solution were added to the 3 mL medium. As both, EGCG and DAC was solved in H_2O control wells in this assay were treated with H_2O only. Each treatment was performed in triplicates.
After 72 h the cells were harvested and used for RNA or DNA extraction (see *"Nucleic acid analysis" & "Luminometric methylation assay"*). RNA was used for RT-qPCR to confirm gene knockdown and analyze gene expression alterations induced by different treatments. DNA was employed for global methylation analyses.

Methylation inhibition by physiological active substances

For DNMT inhibitor treatment experiments without any gene knockdown a slightly different approach was used. $5x10^4$ IPEC-J2 cells were seeded in 12-well tissue culture dishes (Greiner Bio-One) applying 2 mL of cell culture medium. After 24 h of incubation the cells were treated with EGCG (20 mg/L), DAC (5 µM) or H_2O as control. The cells were harvested after another 72 h and RNA respectively DNA was extracted.

Nucleic acid analysis

Virus titration by absolute quantification of whole adenoviral particles

This chapter deals with the question how to titrate virus preparations in an accurate and time efficient way. The applied method (Müller et al. 2011) was developed during this doctoral work and is therefrom not cited by external publications. The titration procedure includes the targeted extraction of encapsulated adenoviral genomes which are subsequently quantified selectively among the DNA yield by quantitative real-time PCR.

Extraction of intact viral genomes

The aim of this step is to gain all unharmed genomes among the total DNA present in a sample of an adenovirus preparation (The preparation procedure is described in chapter "*RNA Interference*"). Therefore a virus aliquot is initially DNase I (New England Biolabs GmbH, Ipswich, USA) digested in order to degrade all free adenoviral genomes present out of broken viral particles. After thermal and chemical inactivation of the nuclease the sample is proteinase K treated what triggers the capsids of the remaining intact viral particles and releases the included viral genomes into the reaction vessel. Proteinase is inactivated afterwards. The overall DNA concentration of the so processed samples is then in the first instance quantified using the NanoDrop® ND-1000 spectrophotometer (PEQLab Biotechnologie GmbH, Erlangen, Germany). Due to DNase I being a endonuclease that amount finally differs from the effective content of viral genomes which are hypothesized to correlate viral particles in this titration method.

Quantitative real-time polymerase chain reaction (qPCR)

Proximate to the selective extraction procedure the adenoviral genomes inhered in the gathered total DNA undergo an absolute quantification versus a standard curve. Thereby a plasmid based standard is deployed derived from pAd/PL-DEST (Invitrogen, Karlsruhe, Germany). This plasmid was also used during the production process of the adenoviral vectors as described in chapter "*RNA Interference*").

The qPCR triggers the Ad5-pTP-Gene (see Primers in Table 1) a genus-common gene for *Adenoviridae* involved in DNA replication (Davison et al. 2003). The average yield measured from virus preparations done during this work is 1 x 10^8 VP/µL (CV = 42 %). Evaluation of the accuracy of this method is included in the corresponding publication (Müller et al. 2011).

Relative quantification of gene expression levels

Total RNA extraction and quality control

All RNA samples in this work were extracted according to the manufacturers guidelines using the RNeasy® Mini Kit (Qiagen). Doing the final step of this kit the RNA was eluted from the column using 53 µL of RNase free H_2O and subsequently concentration was determined using the NanoDrop® ND-1000 spectrophotometer (PEQLab). In regard to the RT-qPCR measurements the RNA concentration was adjusted to 10 ng/µL in H_2O.
Precedent small aliquots of higher concentrations (3-5 µL à 50-100 ng/µL, depending on the RNA-yield) were saved for RNA quality control. Therefore the 2100 Bioanalyzer (Agilent Technologies, Santa Clara, USA) with a RNA nano LABchip (Agilent Technologies, Santa Clara, USA) was utilized. The mean RIN value for RNA spot test from cell cultures was 9.45 (SEM = 0.09, n = 80). RNA was stored until further measurements at -80 °C.

Reverse transcription quantitative real-time polymerase chain reaction (RT-qPCR)

For all RT-qPCR experiments the Corbett Rotorgene 3000 (Corbett Life Science, Sydney, Australia) served as platform in combination with the SuperSkript® III Platinum® SYBR® Green One-Step qRT-PCR Kit (Invitrogen). The used sample volume was 10 µL containing 38ng RNA, 5 µL SYBR-Mix and 10 pmol primermix (forward + reverse primers) (Eurofins MWG Operon, Ebersberg, Germany).
The cycler program included a 10 min reverse transcription reaction at 50 °C followed by a 5 min denaturation step at 95 °C. Under continuous fluorescence measurement 40 amplification cycles (denaturation 95 °C/10s, annealing 60 °C/10 sec, extension 72 °C/15 sec) and a subsequent melting curve from 40 °C to 95 °C (in 0.5 °C steps with a dwell time of 2 sec) were recorded.

All RT-qPCR measurements were performed in duplicates. The data was collected with Rotor-Gene 6 software (Corbett) and subsequently relative change in gene expression was determined under the terms of the ΔΔCq-method (Livak & Schmittgen 2001) versus stable expressed reference genes (see Table 1).

Table 1 Primers used during this work

	gene name	abbreviation		primer sequence	fragment	accession number
refernce genes	Actin, beta	ActB	fwd	AACTCCATCATGAAGTGTGAC	234	NM_173979.3
			rev	GATCCACATCTGCRGGAAGG		
	Glyceraldehyde-3-phosphate dehydrogenase	GAPDH	fwd	AGCAATGCCTCCTGTACCAC	187	NM_001206359.1
			rev	AAGCAGGGATGATGTTCTGG		
	Histone H3	H3	fwd	ACTGGCTACAAAAGCCGCTC	232	XM_003356519
			rev	ACTTGCCTCCTGCAAAGCAC		
	Ubiquitin	UQ	fwd	AGATCCAGGATAAGGAAGGCA	198	XM_003358301
			rev	GCTCCACCTCCAGGGTGAT		
target genes	Caspase 3	Casp3	fwd	GCAACGTTTCTAAAGAAGACCATAG	64	NM_001077840
			rev	CCATGGCTTAGAAGCACACAAATAA		
	Caspase 9	Casp9	fwd	CTGACTGCCAAGCAAATGG	104	XM_003127619
			rev	GCCTGACAGCCGTGAGAG		
	Cyclin B1	CycB1	fwd	GGATCACCAGGAACACGAAA	187	NM_001170768
			rev	GCTTCCTTTTTCAGAGGCAGT		
	Cyclin D1	CycD1	fwd	GACGAGCTGCTGCAAATG	188	XM_003480653
			rev	GAAATGAACTTCACGTCTGTGG		
	Interleukin 1 beta	IL1b	fwd	AGAAGAGCCCATCGTCCTTG	139	NM_001005149
			rev	GAGAGCCTTCAGCTCATGTG		
	Interleukin 5	IL5	fwd	TGGAGCTGCCTACGTTAGTG	105	NM_214205
			rev	TCGCCTATCAGCAGAGTT		
	Interleukin 6	IL6	fwd	GCAATGAGAAAGGAGATGTGT	138	XM_003357471
			rev	GCAGGTCTCCTGATTGAACC		
	Interleukin 8	IL8	fwd	GGCAGTTTTCCTGCTTTCTGC	153	XM_003361958
			rev	CAGTGGGGTCCACTCTCAAT		
	Transforming growth factor beta 1	TGFb	fwd	ACGTCACTGGAGTTGTGCGG	159	XM_002701901
			rev	TTCATGCCGTGAATGGTGGCG		
	tumor necrosis factor-alpha	TNFa	fwd	CCCCTGTCCATCCCTTTATT	200	NM_214022
			rev	AAGCCCCAGTTCCAATTCTT		
	Ribosomal protein SA	67LR	fwd	AGCGAGCTGTGCTGAAGTTT	257	NP_001032223.1
			rev	GTGAGCTCCCTTGTTGTTGC		
	IKBKB	IkKb	fwd	GGCGAACAGAGATTAATACACAAA	256	NM_001099935.1
			rev	GTGCCGAAGCTCCAGTAGTC		
	C-JUN protein	cJun	fwd	ATGACTGCAAAGATGGAAACG	310	NM_213880.1
			rev	TCACGTTCTTGGGGCACA		
	(cytosine-5-)-methyltransferase 1	DNMT 1	fwd	GAAAAGGCGAGCTGAAAGG	204	NM_001032355.1
			rev	GGCTGTTGACAAACCTCACA		
	(cytosine-5-)-methyltransferase 3 alpha	DNMT 3a	fwd	GAATCGCTACAGGGCTTCTG	164	NM_001097437.1
			rev	CTGGATATGCTTCTGCGTGA		
	(cytosine-5-)-methyltransferase 3 beta	DNMT 3b	fwd	GCAAGTTCTCCGAGATACCA	136	NM_001162404.1
			rev	CGTATCCTGGCTTTCTCCAG		
	pTP [Human adenovirus 5]	Ad5-titer2	fwd	CTGCTCGATTTGATAAACATCCT	102	AP_000203.1
			rev	CAGGCTAAGCATGGAATAGTTGAT		
cloning primers	pAd forward		fwd	GACTTTGACCGTTTACGTGGAGAC		
	pENTR forward		fwd	TGACTGATAGTGACCTGTTCG		
	pENTR reverse		rev	GGTGTTTCGTCCTTTCCACAA		

Luminometric methylation assay

Genomic DNA extraction

For DNA extraction the “peqGOLD Tissue DNA Kit” (PEQLab) was used following the manufacturer’s kit manual with minor variations. 400 µL DNA lysis buffer T and 20 µL Proteinase K were applied. The Lysate was transferred into a 1.5 mL tube and incubated for 1 h at 50 °C. Thereafter 15 µL of RNase A were added incubated for another 30 min. DNA was quantified using the NanoDrop® ND-1000 and qualified using the 2100 Bioanalyzer (see chapter “*Nucleic acid analysis*“).

Measurement of global DNA methylation

Global DNA methylation was determined using luminometric methylation assay (LUMA) (Karimi et al. 2006) slightly alternated (Fürst et al. 2012). In two separate reactions 500 ng of genomic DNA were digested for 20 min with isochizomere restriction enzymes: HpaII + EcoRI or MspI + EcoRI (0.5 µL (10 U/µL) enzyme (Fermentas, St. Leon-Rot, Germany), 2 µL tango buffer (Fermentas), in a total volume of 20 µL H_2O). In regard to their common target sequence CCGG HpaII is sensitive and MspI insensitive for CpG methylation.
The LUMA mesurements were performed in a 96-well format using the PSQ96 MA system (Qiagen) applying the corresponding data evaluation software. The HpaII/EcoRI respectively MspI/EcoRI ratios were calculated as (dGTP + dCTP)/dATP. The HpaII/MspI ratio was consulted for determination of DNA methylation at the investigated CCGG-sites (0 ≙ 100 % of DNA methylation, 1 ≙ 0 % of DNA methylation).

RNA interference

sh-Oligonucleotide design

The initial step in production of viral mediated gene knockdowns by RNA interference is the design of the sh-oligonucleotide that is finally the template for the siRNA precursor expressed by the target cell line induced by the U6-Promotor sequence. Therefore a 21 base pair long (Tuschl 2001) siRNA sequence must be determined for the desired target. Based on the knowledge gained from SIRION-BIOTECH GmbH (Martinsried, Germany) and further literature fundamental criteria for selection emerge:

- 3´-end has lower thermodynamic stability than the 5´-end (Khvorova et al. 2003)
- sequence must be BLAST®-checked (National Library of Medicine, Bethesda, USA) for sequential complementarity less than 15 base pairs to other genes or in crucial regions (Jackson et al. 2006; Chalk & Sonnhammer 2008)
- Potential splice variants must be considered
- The target sequence should have a GC-content of 40-55% (Chan et al. 2009)
- The whole inserted cloning cassette must not contain restriction sites of used enzymes
- Avoid stop signals for RNA-Polymerase III (≙ TTTTT)
- The target sequence should be within the coding sequence (not within the 3´-UTR)
- If several sequences for one target are designed they should not overlap
- Check for secondary structures that may disturb RNA interference (Shao et al. 2007)

Another aspect during the siRNA-sequence design process was interspecies compatibility. The target species in this work was swine (IPI-2I & IPEC-J2, see "*Cell culture*"), but looking ahead manual design opened up the possibility to choose 21-mers also complementary to Sus scrofa, Bos taurus, Mus musculus and Homo sapiens.

Using the *clustal W2* alignment algorithm (http://www.ebi.ac.uk/Tools/msa/clustalw2/) not only splice variants within one species were checked but also sequences from the species above were compared.

Due to leak of reliable algorithms the first siRNA sequences were designed manually considering the rules mentioned above. However with progression of research and

publication of validated knockdown-kits by the industry further siRNA sequences were designed using the following online tool:

BLOCK-iT™ RNAi Designer (Invitrogen)

(URL: http://rnaidesigner.invitrogen.com/rnaiexpress/setOption.do?designOption=shrna&pid=8117042879085147254)

When a 21 base pair segment was identified as candidate the corresponding sh-oligo was designed by embedding the siRNA-sequence into the need cloning cassette for plasmid integration (see Figure 12 and chapter "*Cloning*").

Figure 12 siRNA-cloning cassette. This figure shows an exemplary cloning cassette (here bearing the target sequence of 67LR; also see Tables 1 & 2) how it was used for siRNA-knockdown adenovirus production.

Subsequent the desired oligonucleotides for the cloning cassette were commissioned at Ella Biotech GmbH (Martinsried, Germany). An overview of all siRNA-sequences designed and processed for this work is given in Table 2.

The virus production is then divided in two steps. In a first phase the cassette is cloned into the a plsmid vector which bears the adenoviral genome and then in a second phase viral particles are generated by transfecting the cloning product into a production cell line. The following two chapters deal with this whole procedure.

Table 2 siRNA-sequences for RNA interfernence knockdowns

gene name	abbreviation	siRNA-sequence	accession number
RPSA	67LR-1	GCCACTGAATGGGTAGGAACA	NM_001037146.2
	67LR-2	GCCTACCATTGCTCTGTGTAA	
IKBKB	IkKb-1	GGAAATGAAAGAACGGCTTGG	NM_001099935.1
	IkKb-2	GCAAGGCGAACAGAGATTAAT	
	IkKb-3	GGGATCTGCGCAAGTACTTGA	
C-JUN	cJun-1	GCAAAGATGGAAACGACCTTC	NM_213880.1
	cJun-2	GAACTCGAGCGCCTGATAATC	
	cJun-3	GCCTGATAATCCAGTCCAGTA	
DNMT1	DNMT1-A	GCTTCAGCGTGTACTGTAAAC	NM_001032355.1
	DNMT1-B	GCAGGAGAAGATCTACATAAG	
	DNMT1-C	GCAGGATATCTCGTACAATGG	
DNMT3A	DNMT3a-A	GGACAAGAATGCCACCAAATC	NM_001097437.1
	DNMT3a-B	GGCATCCACTGTGAATGATAA	
	DNMT3a-C	GCATCCACTGTGAATGATAAG	
DNMT3B	DNMT3b-A	GCCTAAGCTCTTCCGAGAAAC	NM_001162404.1
	DNMT3b-B	GGTTTGGCGATGGCAAGTTCT	
	DNMT3b-C	GGATGAACAGGTCTGTGATAG	

Cloning

The whole cloning procedure contains three sections. In a first step the cloning-cassette is integrated into a first with 2.7 kbp relatively small and manageable plasmid, bearing a kanamycin resistance for selection. It is a derivate of Invitrogen`s pENTR™/U6 designed and provided by SIRION-BIOTECH GmbH (Martinsried, Germany). Initially the two single stranded oligonucleotides must be dissolved in H_2O and annealed by heating and cooling (95 °C then to room temperature) in order to built a cassette. Furthermore the plasmid is digested with EcoR1 and Bbs1 (both from New England Biolabs GmbH). Subsequently the open ends of the cassette are T4 Polynucleotide Kinase (New England Biolabs GmbH) treated for dephosphorylation and the open ends of the plasmid are in contrast phosphorylated using Alkaline Phosphatase, Calf Intestinal (New England Biolabs GmbH). With T4 DNA Ligase (New England Biolabs GmbH) the cassette is then integrated and the recombinant plasmid is amplified on selective LB-agar (kanamycin, Roth, Karlsruhe, Germany) using heat competent Library Efficiency® DH5α™ (Invitrogen).

In a second step the new information within the first plasmid is exchanged to another plasmid. Thereby the second plasmid (pAd/PI-DEST™, Invitrogen) bearing a ampicillin resistance delivers the adenoviral genome and hence is with 34.9 kbp relatively big and unmanageable. The exchange happens by homologue recombination using the Gateway® LR Clonase® II Enzyme mix (Invitrogen). Also this cloning product is amplified using selective LB-agar (ampicillin, Roth) applying competent DH5α cells (Invitrogen).

In a third step the gained recombinant plasmid is digested with PacI (New England Biolabs GmbH). Thereby the circular DNA is linearized and the bacterial backbone is removed. The now linear viral DNA precursor should be immediately transferred to the next section of the virus production due to frequent auto-religation processes.

Virus production

The virus production is conducted in HEK-293 cells (see chapter "*Cell culture*"). This cell line is transformed with fragments of the adenovirus type 5 (F. L. Graham et al. 1977) what serves as viral vector for mediation of RNA interference knockdowns in this work. The vector genome differs from the wildtype by gene deletions in the E1/E3 region (Davison et al. 2003)

what evokes replication deficiency. These missing genes are supplemented by the HEK-293 cell line wherefrom it is used as production cell line for adenoviral vectors (Bett et al. 1994).
The production process itself is divided into two steps. First the linearized replication deficient adenovirus genome from the previous chapter is transfected into the HEK-293 cells using jetPEI™ (Polyplus-transfection™, Illkirch-Graffenstaden, France). This happens in a relatively small scale (6-well tissue culture plates, Greiner Bio-One). Subsequently the whole virus is expressed for the first time why this step is also called “Rescue“.
When the first viral particles are gained they are used for secondary infection of HEK-293 cells in a bigger scale (15 cm diameter tissue culture plates, Greiner Bio-One) for virus amplification. This virus preparation and ultimately the virus harvest is conducted applying the ViraBind™ Adenovirus Miniprep Kit (Cell Biolaps Inc., San Diego, USA). Post production the viral preparations are stored at -80 °C in the kit elution buffer supplemented by 10 % glycerol.
The follow-up task is the virus titration. This procedure is described in chapter “*Virus titration by absolute quantification of whole adenoviral particles*“. The common yield from the here described method is 1 x 10^8 VP.

Knockdown evaluation

Once a virus with its individual siRNA-sequence is generated and titrated it needs evaluation in regard to the grade of knockdown this sequence evokes in the accordant target cell line. Prior to that question two other aspects are of importance. The first question is if the target cell line can be infected by the viral vector.
The efficacy of the transfection of the here used porcine target cell lines (IPI-2I & IPEC-J2, see chapter “*Cell culture*“) by human adenovirus 5 can be evaluated using a pENTR derivate bearing a GFP-sequence (pENTR-GFP1, SIRION Biotech GmbH). The nativity of the virus is then checked using fluorescence microscopy. Positive infection events are then indicated by comet shaped plaques (see Figure 13).

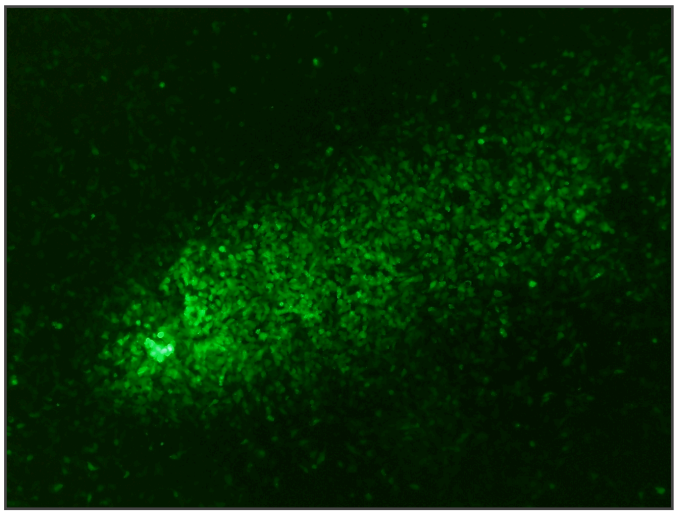

Figure 13 GFP Plaque. Typical dispersal of an GFP-virus infection on a confluent HEK-293 cell layer recorded with a Leica DM IRB microscope (Leica Microsystems GmbH, Wetzlar, Germany) in combination with an Olympus DP 72 (Olympus, Tokyo, Japan) camera system in 50 x magnification.

If a cell line is transducible by the adenoviral vector the next question is, if despite of the gene deletion the virus can replicate in the target cell line. Due to large occurrence of viral derived genome sections in the untranslated regions of higher vertebrate genomes the possibility of spontaneous reproduction exists. This incident then will lead to unrequested lysis of the target cell line.

In order to check that problem the target cell line is seeded in tissue culture dishes and is treated with the GFP-virus. After 48 hrs when infection events should be completed (Müller et al. 2011) the media is changed and the culture is incubated for another 72 hrs. Then cells are harvested using a cell scraper and undergo three frost taw cycles ($N_{2(lq)}$ vs. 37 °C) in order to release potentially originated viral particles. This whole procedure is repeated another two times. In the second or at least third passage absence of fluorescing plaques because of consumption during infection events and concomitant dilution of remaining viral particles should be observed, if no new viral particles are generated.

The next and crucial evaluation criterium in respect of the intended application is the gene silencing efficiency of the particular integrated siRNA-sequence. This is checked using the described knockdown assay (see chapter “Knockdown assay“). Thereby Ad5/U6-Stop (SIRION Biotech GmbH), a special adenovirus 5 derivate serves as control in order to keep the viral load on all cells constant. Having an empty cloning cassette this virus bears no explicit siRNA sequence and hence only mediates infection side effects.

Applying the knockdown assay different normalization modes must be considered. The underlying relative gene quantification (Logan & Edwards 2009; Livak & Schmittgen 2001) requires a differential consideration of which samples are related as treatment and

corresponding control. In the case of aiming for knockdown efficiency it is therefrom of importance to exclusively correlate sample groups of one kind of secondary treatment. That means if in an experiment are beneath several gene knockdowns also several different drug treatments are applied the net outcome for the gene down-regulation is calculated by normalizing knockdown treated samples versus ad5/U6-Stop samples separately within one drug treatment group (Müller & Pfaffl 2012; Müller n.d.). That way side effects or synergetic actions between the knockdown application and the drug treatments are regarded and thus normalized, what exposes the net effect of gene silencing. A typical layout of a knockdown assay with controls is demonstrated in Figure 14.

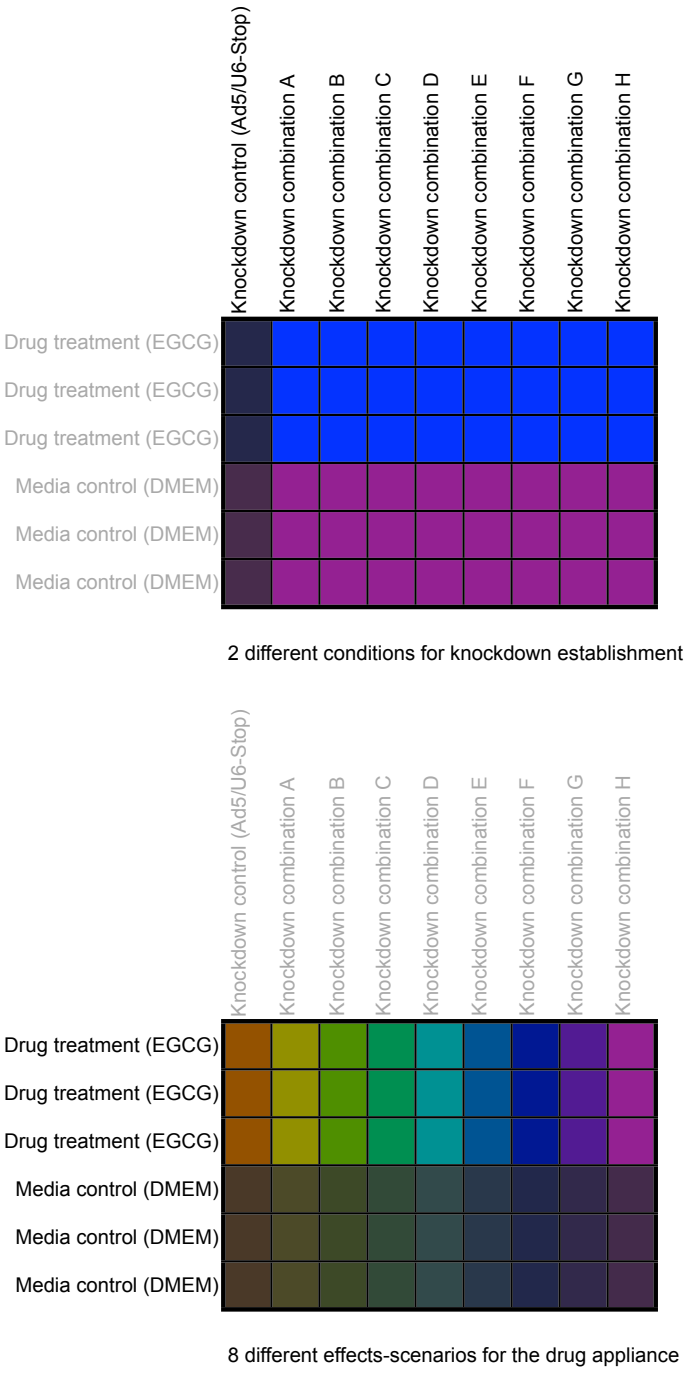

Figure 14 Knockdown assay layout. Horizontally are applied different gene knockdowns (here Ad5/U6-Stop knockdown control & knockdown combinations A to H) and vertically different drugs (here EGCG vs. DMEM). The color scheme discriminates different treatment groups. The grey shaded colors represent the controls for their highlighted partners.

Electric cell-substrate impedance sensing

For non-invasive online measurement of effects on cellular level *Electric cell-substrate impedance sensing* (ECIS) was applied (Giaever & Keese 1984). The used platform was the ECIS-1600 (Applied BioPhysics, Troy, USA) in combination with 8-well cell culture array plates (8W10E by Applied BioPhysics, distributed by Ibidi GmbH, Martinsried, Germany) which have a substrate area of 0.8 cm^2 (Figure 15). In this setup the current flow through the media filled incubation vessel (cell culture conditions see chapter "*Cell culture*") is detected by ten gold micro electrodes (250 µm diameter).

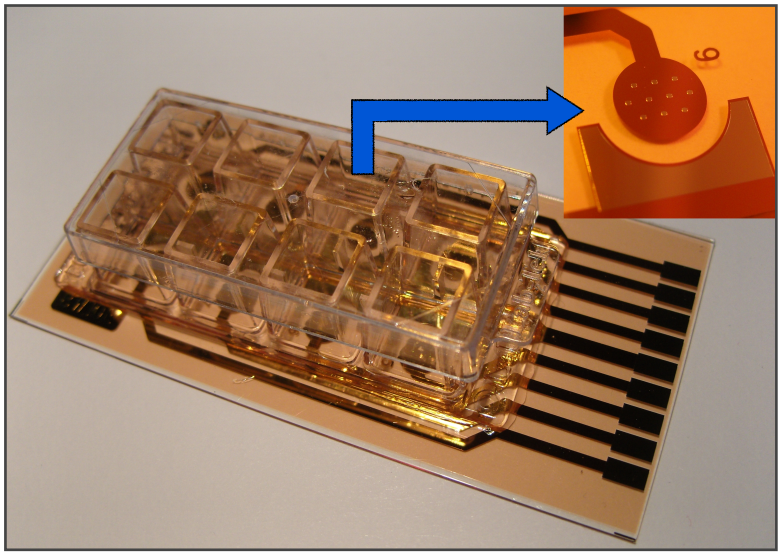

Figure 15 8W10E-array. This Figure shows a cell culture array used with Applied BioPhysics ECIS-devices. The magnified detail-picture shows the ground of one of the eight incubation vessels bearing ten micro electrodes.

After the requested cells are seeded into the array by injecting 300 µL of a homogeneous cell suspension, current is applied and the experiment is cast at a frequency of 30 kHz and a measurement interval of 60 sec. With these basic parameters all ECIS-experiments in this work are conducted. The used cell lines, their cell density and the duration of the data acquirement are adjusted according to the aim of the particular assay.

Viral cytotoxicity

For physiological studies in the manner of loss-of-function experiments adenoviral induced gene knockdowns were applied in different cell culture settings (see chapter "*Switching*

physiological pathways by RNA-interference“ & “Knockdown evaluation“). Concomitant titer dependent cytotoxicity parameters of the applied adenoviral vectors were gathered using the ECIS-device as described previously (Müller et al. 2011). In this study a viral load gradient (including MOIs of 100, 200, 400, 800 and 1600) was tested concerning the impact on proliferation inhibition and detachment of IPI-2I cells. This experiment was designed in regard to the progress of a viral infection, monitoring its incubation time and the establishment of viral effects over a period of 72 h.

Drug effects

Lethal dose determination

To approach the question of potentially harmful effects induced by a cineole treatment on the viability of epithelial gut cells the ECIS-technology was applied using the parameters as described before (Müller et al. 2012). Thereby the minimal non-lethal dose of this secondary plant metabolite for IPEC-J2 cells was titrated during a real time measurement.

Wound healing assay

Further for non-lethal cineole dosages the impact on cell morphology and wound healing were investigated using the ECIS device as described by before (Almstätter et al. n.d.). Thereby an injury of the cell layer is provoked by pointed application of an elevated electrical field (6 V, 20 sec) (Jumblatt & Neufeld 1986).

Gas chromatography-mass spectrometry

As basic platform for gas chromatography-mass spectrometry (GC-MS) analysis served an Agilent MSD quadrupole system (GC 7890A and MSD 5975C, Agilent Technologies, Waldbronn, Germany) and a GERSTEL CIS 4C injection system combined with a GERSTEL MPS 2 autosampler (GERSTEL GmbH & Co. KG, Duisburg, Germany). Data recording and analysis were conducted using the MSD ChemStation E.02.00.493 software (Agilent Technologies, Inc.). As analytical capillaries a DB-FFAP and a DB-5 were applied (30 m length, 0.25 mm inner diameter, 0.25 µm film thickness, J&W Scientific, Fisons Instruments, Mainz-Kastel, Germany).
The detailed GC-MS analytical setup and its full employment during the experiments for this work had been described earlier (Müller et al. 2012). By all means two different aims were focussed by *in vitro* metabolization assays with cineole treated epithelial gut cells:

Metabolite screening

Qualitative occurrence of 1,8-cineole metabolite patterns were compiled by comparison of retention indices (Kováts 2004) from two analytical capillaries of different polarities (DB-FFAP & DB-5) and further by comparison of EI mass spectra versus synthesized references.

Metabolite quantification

Metabolization rates in samples of cell layers and media supernatants were quantified relatively to the retrieval of an internal standard (deuterated 2-α-hydroxy-1,8-cineole) by correlating the respective areas under the curve obtained from the corresponding ion chromatograms. Thereby serial dilutions of deuterated 2-α-hydroxy-1,8-cineole served for the assessment of several metabolites found, since the quantitative aspect was only intended for a very rough estimation.

Liquid chromatography-mass spectrometry

For quantification of EGCG in tea preparations the four green tea varieties *„Yellow“ Tea*, *Green North Tukvar*, *Wu Lu* - "*Fog Tea*" and *Bi Lo Chung* (Greuther Teeladen, Vestenbergsgreuth, Germany) were brewed with 80°C warm tap water and left to draw for 15 min. The obtained tea infusions were diluted as follows: tea in H_2O 16.7 fold (600 µL tea to 1400 µL H_2O, then thereout 200 µL to 800 µL of H_2O) and then 500 µL of this aqueous dilution to 500 µL of analytic Ethanol. Dilution factors served for back calculation of the EGCG yield from the tea infusions. After dilution the samples were prepared for LC-MS analysis by filtration (0.45 µm) and subsequently measured under the parameters shown in Table 3.

Table 3 Measurement parameters for high-performance liquid chromatography (HPLC) & mass spectrometry (MS)

HPLC		
Flow rate	0.3mL/min	
Solvent A (aqueous)	90% 10mM ammonium acetate pH 7.4, 10% methanol containing 0.1% acetic acid	
Solvent B (organic)	90% methanol, 10% 10mM ammonium acetate pH 7.4 containing 0.1% acetic acid	
column	Prontosil Bischoff C18 Aq (100x2mm, 3µm)	
Oven temp.	25°C	
Autosampler temp.	15°C	
DAD	540nm	
	320nm	
	280nm	
scan	190-600nm (step width 2nm)	
Injection volume	20µL	
Solvent gradient	Time [min]	% B
	0	0
	3	70
	6	100
	11	100
	12	0
	20	0
MS		
Source	Multimode (ESI and APCI) - Polarity switch	
Gas temp.	350°C	
Vaporizer	200°C	
Drying Gas	6L/min	
Nebulizer	45psig	
Capillary Voltage positive & negative	3000V	
Corona positive & negative	2µA	
Fragmentor positive & negative	100V	
Charging Voltage	2000V	

Results and discussion

Manipulation of cell physiology by adenoviral mediated knockdowns

The task to investigate how effects derived from secondary plant compounds act within the physiological pathways of the small intestine epithelia requires isolated conditions in order to set aimed molecular test parameters. Therefore epithelial cell culture provides a suitable model. However, thereby utilized biotechnological tools must be evaluated due to its inherit potential to influence the health state of the test object. As in this work gene knockdown models are employed for elucidation of inflammatory and health questions based on adenoviral vectors the evaluation of their physiological impact was mandatory.

Adjusting the effector to firm parameters

Initially, a very basic duty is to ascertain the amount of vector that is inserted and hence affects the cells. Therefore a valid titration procedure for adenovirus was established. In accordance to this method as described in chapter "*Experimental*" the harvested virus was extracted selectively for still intact and hence infecting viral particles (VP). Subsequently these particles were titrated via absolute quantification using RT-qPCR. The example in Figure 16 shows plots from the RT-qPCR part of a titration series wherein two adenovirus-preparations were tested which were finally attributed to 6.34 x 10^6 VP/µL and 5.66 x 10^7 VP/µL respectively. The method developed during this work delivers precise information with evaluated minor faultiness as the analysis of mean errors of all steps during the titration procedure from a multitude of titrations shows (Müller et al. 2011). When the titer is assigned, the knockdown model must be adjusted. In respect to the epithelial cells, which should be harmed as few as possible, the inserted viral load must be optimized. Thereby two considerations are of importance. On the one hand a maximization of knockdown efficacy is necessary, and in contrast on the other minimal noxious impact on the cell physiology is essential. Furthermore the intended application in multi-gene loss-of-function scenarios requires additionally the realization of parallel gene silencing without a potentially toxic and disturbing viral overdosage. Hence the minimal effective MOI has to be assigned.

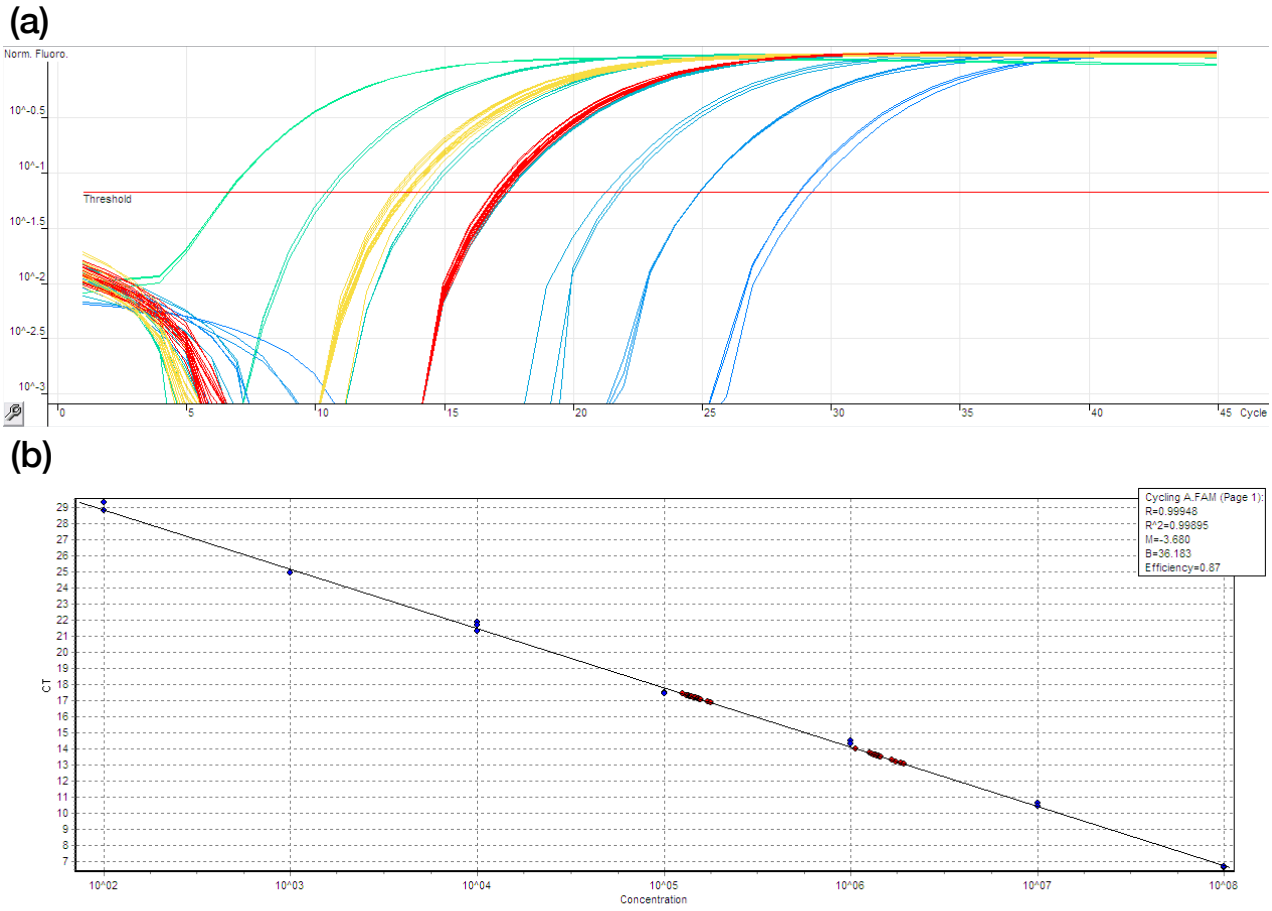

Figure 16 (a) Absolute quantification of viral particles versus a plasmid standard curve. Green to blue lines indicate the plasmid dilution (n = 3 RT-qPCR reactions) whereas yellow and red lines are the two tested viruses (n = 3 extractions x 3 RT-qPCR reactions) (b) Derived standard curve (r^2 = 0.998).

As evaluated in the assay shown in Figure 17a, the needed time for maximal knockdown development is approximately reached after 48 hours. In Figure 17b the followup assay, incubated for now 48 hours post infection shows that with a MOI of 400 a knockdown level is achieved that does not enhance determinatively when more virus is applied.

In accordance with these findings the next demand was accessed. For the need multi-gene knockdown virus mixtures were prepared. Thereby for each desired knockdown a virus quantity was contributed with the minimal MOI of 400. Figures 18 show the RT-qPCR measurements from a knockdown assay where two viruses targeting different genes were applied, both at the optimized conditions from above.

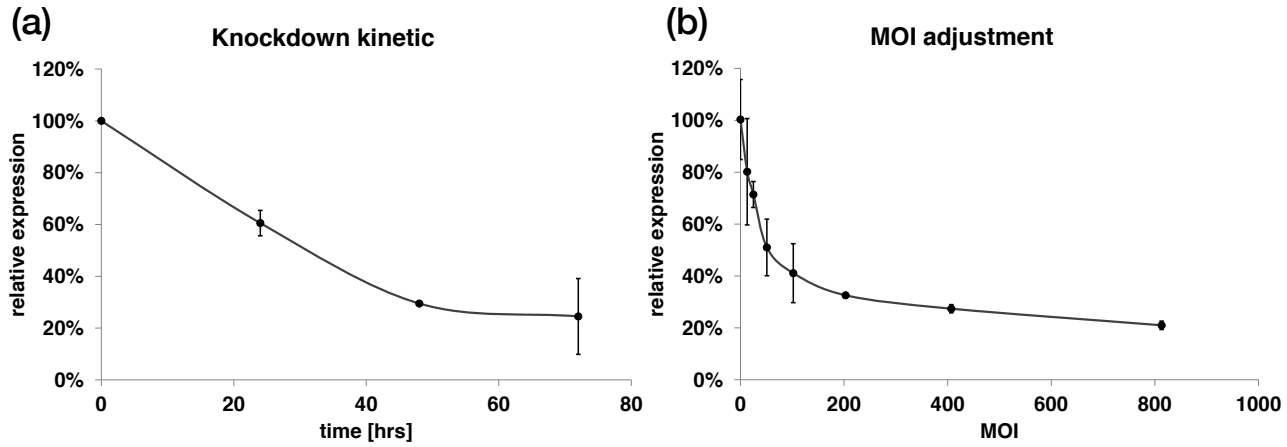

Figure 17 (a) Knockdown establishment over time at a MOI of 1000 in IPI-2I cells (n = 3 cell culture wells x 2 RT-qPCR reactions). (b) Knockdown efficiency for different MOIs 48 hours post infection in IPI-2I cells (n = 3 cell culture wells x 2 RT-qPCR reactions).

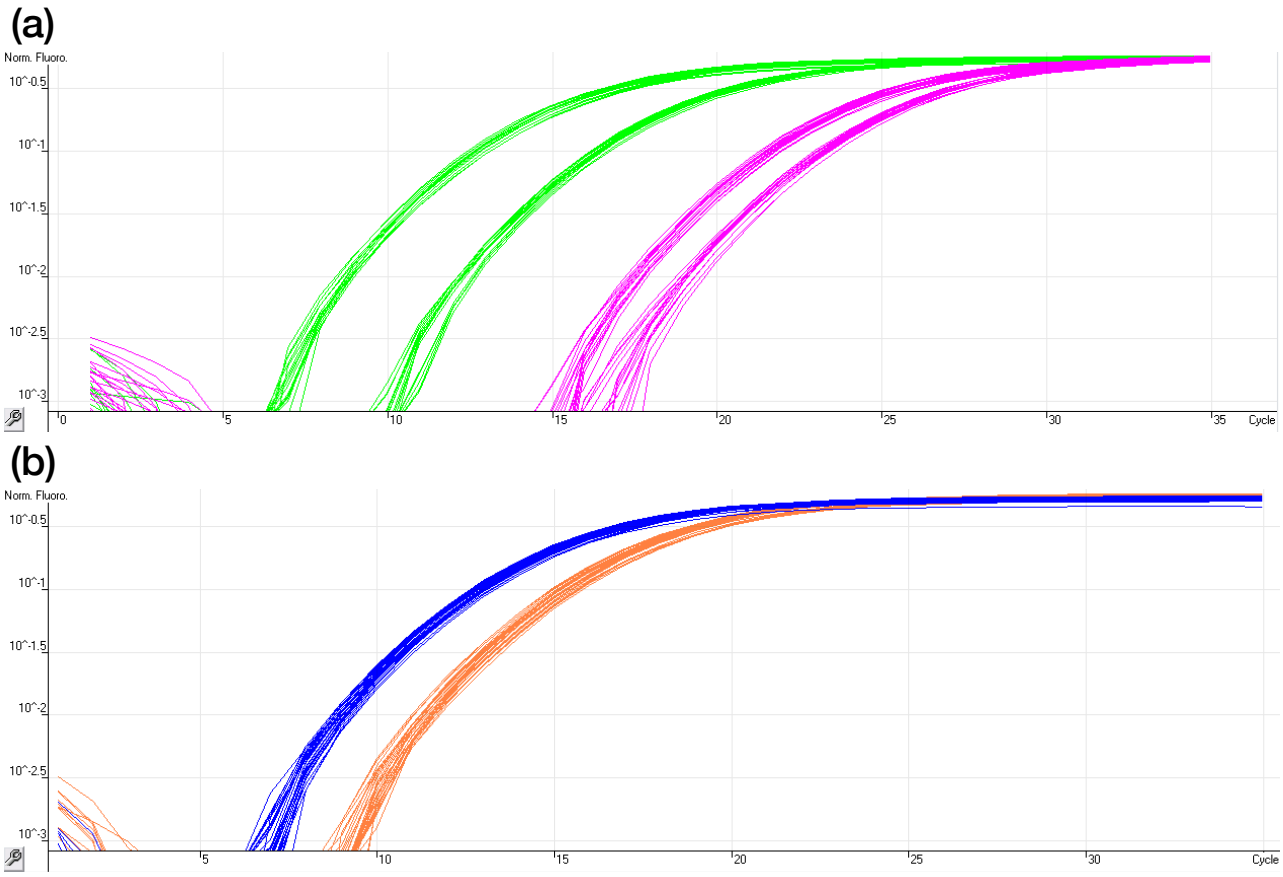

Figure 18 Multi-gene silencing. RT-qPCR data from a knockdown assay (MOI 400, 48h post infection, n = 3 cell culture wells x 2 RT-qPCR reactions) with IPEC-J2 cells and two viruses: (a) target genes (green = 67LR, pink = Ikkβ), (b) reference genes (blue = UQ, orange = GAPDH);

Thereby gets obvious that in Figure 18a the two target genes are measured and in Figure 18b two reference genes. The array of curves deriving from a target gene separates into two sub-arrays for each target gene (green or pink), whereas the array derived from a reference gene remains as a single bundle (blue or orange). For the target genes the divided curve bundles mark the particular gene knockdown.

A more general problem which must be discussed in the scope of RNAi knockdowns are the inhered off-target effects. The approach of this work tries to evaluate specifically which drug targets are affected in the used intestinal cell culture model by the RNAi mediated loss-of-function scenarios. Within this *in vitro* setups we seem to be aware of random side effects, or at least keep them in check by elaborately chosen controls. However, RNA interference as silencing tool carries along fundamental problems. A siRNA-sequence specifically designed for the desired target gene always bears the potential to bind off-target and co-silence another genes (Jackson et al. 2003; Lim et al. 2005; Jackson et al. 2006). Therefrom, when interpreting the outcome of an assay by means of physiological pathways at least the considered genes should be checked for cross reactions derived from the particular applied siRNA-sequence or RNAi mediating virus respectively. A principal component analysis (PCA) based (Jolliffe 2002) screening method has been described earlier by me (see Appendix). The underlying principle is that when data is edited according to this method and subsequently analyzed via PCA the off-target-affected and thus accidentally down-regulated genes can be filtered since they appear together with targeted genes in one data cluster (see Figure 19).

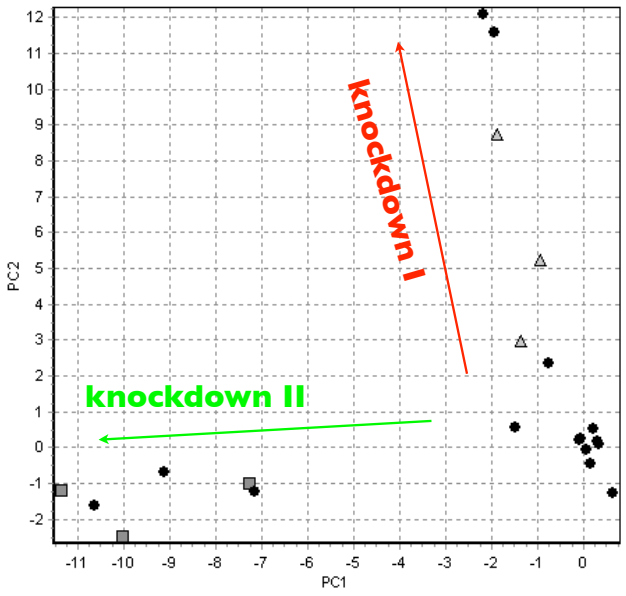

Figure 19 PCA based off-target analysis. The data points on the two axis (green & red) contain exclusively genes affected by an identical knockdown effect. Grey triangles and squares among are no targeted gens and thus bear an off-target effect (Müller & Pfaffl 2012).

Evaluate cytotoxic accessory symptoms

The precedent evaluation series was dedicated to create conditions which minimize the technical impact that may influence the health state of the cell culture model redundantly. Accordingly the minimal viral impact which still facilitates potent functional manipulations was assigned to MOI 400 and 48 hrs. Nevertheless the viral mediated knockdown application carries along the potential to harm the epithelial cells and thus disturbs the physiological investigations. In order to evaluate this extend ECIS technology was consulted and a cytotoxicity assay was designed (Müller et al. 2011) and cast with IPI-2I cells (n = 2 wells x 3 assay) using a control virus which solely induces infection but is deficient of any knockdown properties.

Figure 20a shows one of these assays. Regarding the impedance curves several physiological findings can be assigned. Firstly the point of inflection at approximately 20 hrs post cell seeding protrudes. Parallel cast optical cell enumerations (Figures 20b&c could reveal that the around 50 % of the all over signal increase must be dedicated to activities of cell settlement. Further regarding the impedance signal of infected samples versus the control wells it gets obvious that the incubation time for the adenoviral infection takes approximately 24 hrs due to the indicative signal decrease after this period of time. This matches quite well the findings from above wherein the allover incubation time for the knockdown establishment was assigned to 48 hours post infection. Another important insight in the pathology of an adenoviral infection is gained post the implied media change during this assay. The evoked cytotoxic effect lasts continuously on the epithelial cells and thus must be attributed to the inhered viral infection. Terminal cell enumerations could further show that the cells really die and not just decrease the signal by weaker adherence (Müller et al. 2011). A combined statistical evaluation could reveal a distinct correlation between the inserted viral vector and the resulting cytotoxicity level in a significantly dose dependent manner as shown in Figure 21.

The experiments so far only tested the negative impact of the control vector (Ad5-U6-Stop) on the epithelial cells. Hence, the proximal question is, if a knockdown evaluated virus is applied, does it evoke the same toxicity? In a followup assay a PPARγ targeting knockdown virus was applied versus Ad5-U6-Stop with identical MOIs.

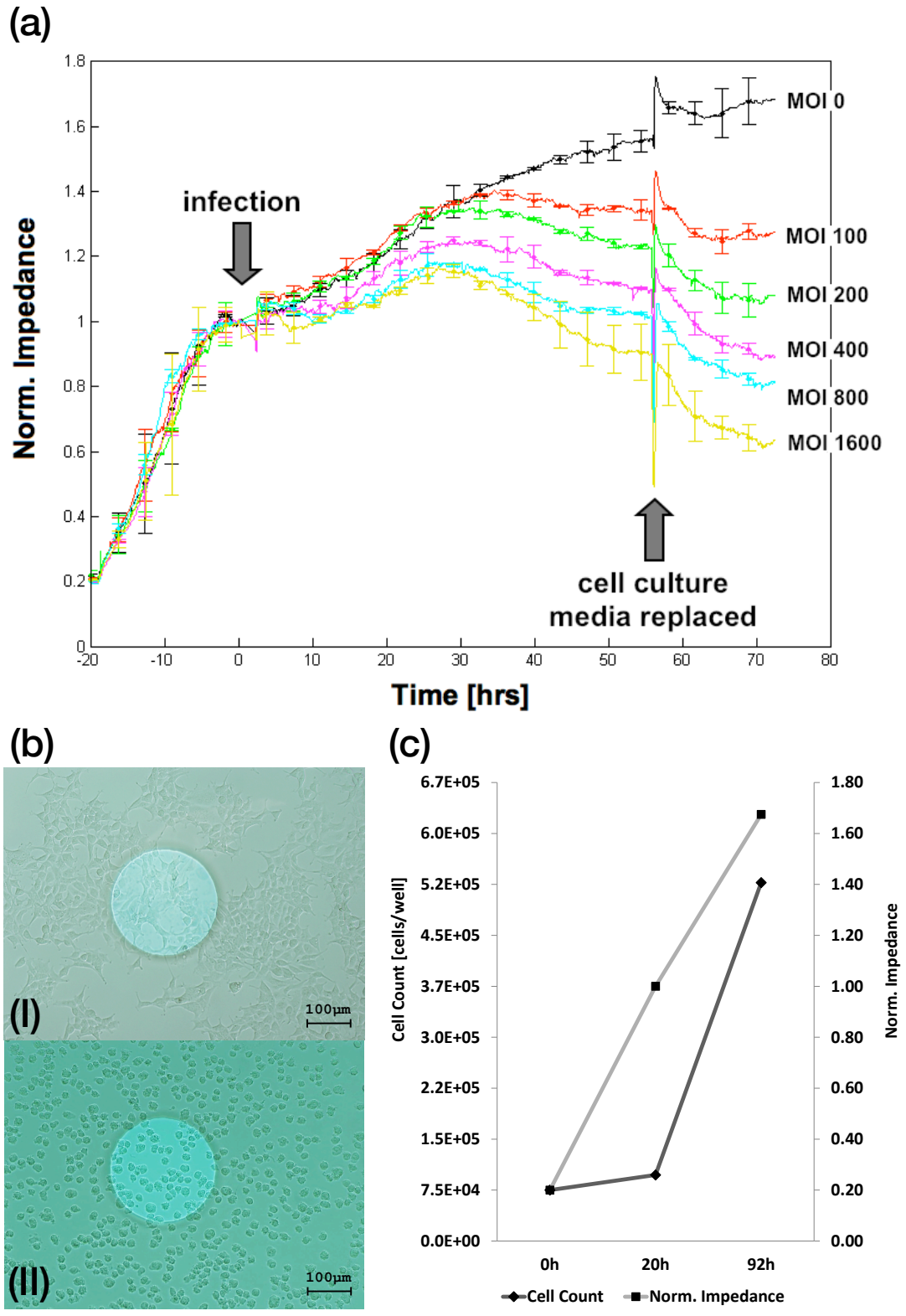

Figure 20 Cytotoxicity assay. (a) 1 x 105 IPI-2I cells seeded (t = -20 hrs) in a 8W10E ECIS array and treated (t = 0 hrs) with different concentrations (MOIs) of control virus Ad5-U6-Stop, then media changed 57 hrs post infection. (b) Microscopic picture of IPI-2I in the 8W10E cell culture dish. The lighter circle in the center is one of the 10 microelectrodes covered with (I) proliferating cells or (II) semi-trypsinated cells for optical enumeration. (c) Cell count versus impedance value over time.

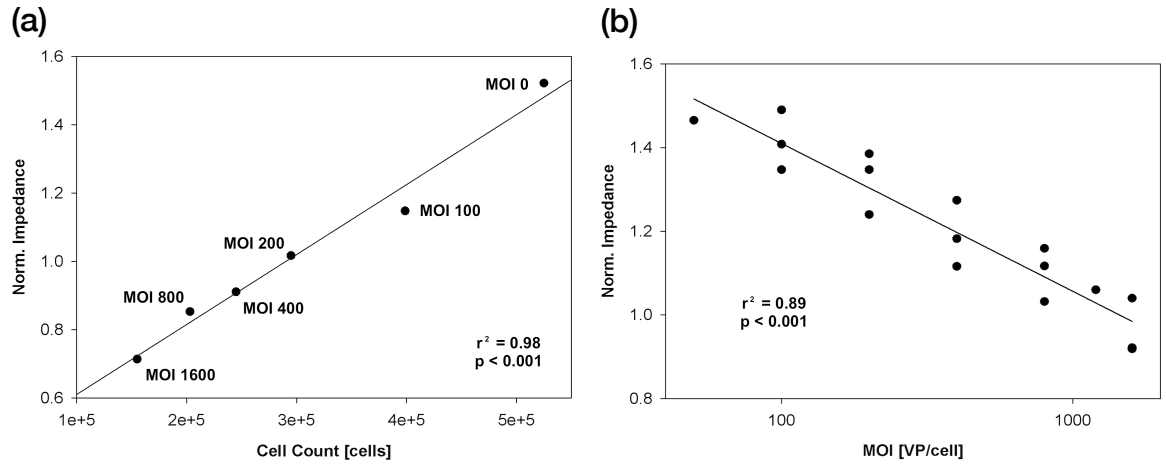

Figure 21 Dose dependency of viral adenoviral cytotoxicity. (a) End-point cell count correlated with end-point impedance values. In contrary to the first 20 hrs of the ECIS measurement the obtained impedance values correspond directly to cell numbers indicating real cell death. (b) Comparison of repeated cytotoxicity assays due to normalized impedance values after 72 h as a function of MOI on a logarithmic abscissa. The applied polynomial regression indicates high significance.

The outcome demonstrates equally evoked cytotoxicity by the disparate virus species what indicates the transferability of the base findings and further as a sideline verifies the applied titration method on a physiological level (see Figure 22).

Summing up, non-invasive ECIS measurements revealed that the applied knockdown model is not a non-invasive technique. The health state of the intestinal epithelial cells is attended when casting loss of function studies, but with the optimized set up parameters harming effects are minimized and by employing the control virus physiological findings are suitable.

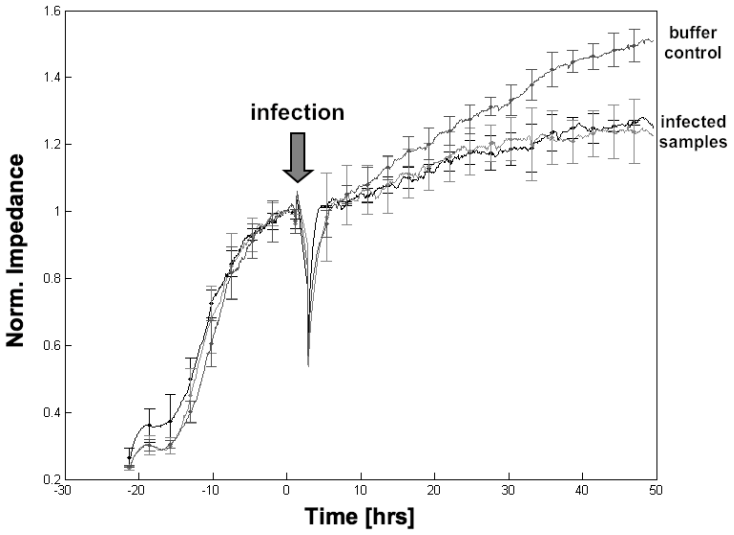

Figure 22 ECIS assay applying equal amounts of an evaluated (70 % down-regualtion) knockdown virus targeting PPARγ and the non-knockdown control virus Ad5-U6-Stop versus the buffer control (virus storage buffer).

Effects of secondary plant compounds

The first chapter of the results and discussion part was dedicated to the question if valuable physiological information can be acquired with particular this cell culture approach combined with RNAi induced gene silencing. Now, below in regard to themed issues the findings referring to positive physiological effects of the analyzed secondary plant compounds on the mimicked organ, the small intestine is discussed.

Thereby two aspects are in focus pursued by the two objective herbal derived compounds. Cineole as a major metabolite of the Eucalyptus tree is as digested application no big matter. Therefrom its represents the more pharmacological questioning as it usually has primary relevance by medicinal preparations. In an expanded view the investigation especially for metabolization within the gut epithelium this study affiliates the findings of cineole derivates after oral consumption in various body fluids.

In contrast epigallocatechin gallate as quantitatively the major secondary compound of the tea plant, aims for the food aspect of health promotion by herbal derived substances mediated in the small intestine. As “tea-science“ is a quite matured field it nevertheless bids need for research since the postulation of an EGCG-receptor, what forces the scope to molecular signaling pathways.

Both, cineole and EGCG evolve their potential in one of the most important organs maintaining basic matters of well being: The gastrointestinal tract.

Cineole

The research concerning cineole was planed and conducted in cooperation with the Fraunhofer-Institut für Verfahrenstechnik und Verpackung IVV and the Friedrich-Alexander-Universität Erlangen-Nürnberg.
This chapter deals with the assays which investigated the impact of cineole on intestinal epithelial cell lines. The combinatory approach includes a dose depending cytotoxicity assay, the assessment of metabolization profiles found qualitatively and quantitatively over time and the related physiological responses on gene expression level.

Lethal dose determination

The results in this chapter are acquired together with Isabella Almstätter during her master thesis (Almstätter 2010) guided by us in cooperation with Prof. Dr. Andrea Büttner.
An initial consideration, before questions on molecular level referring to how cineole affects the gut intestinal immunity by itself or potential metabolization products are attended, is the impact on cellular level. This was evaluated in a dose dependent manner employing the ECIS-device for non-invasive real-time tracking. Therefore cineole containing media was applied in different physiological to pharmacological concentrations (0.3, 0.5, 0.7, 1.0, 1.3, 1.7 and 2.0 g/L) into cell culture arrays pre-seeded with IPEC-J2 cells and grown close to confluence. Following an impedance measurement over 60 hrs delivered a viability plot as shown in Figure 23a.
Despite of the relatively narrow range of concentrations with seven subdivisions within about one decimal power only two groups delineated. All treatment groups with a dose of 1.0 g/L or less survived unaffected and all others with 1.3 g/L and above detached instantly what carries along the certain death in for epithelial cells in this set up. In a second measurement series (Figure 23b) utilizing a relatively very fine resolved dilution curve of applied cineole these findings were confirmed. The acute cytotoxicity of cineole for the intestinal epithelial IPEC-J2 cells established at 1.2 g/L, what was assigned as lethal dose (Almstätter et al. n.d.; Müller et al. 2012). A possible explanation for this phenomenon may be the degradation or denaturation of adhesion proteins at this critical point of 1.2 g/L. Physiological effects are unlikely due to the progression of the not affected samples. No slightly occurring toxicity can

be observed even 60 h post treatment. These finding correspond to the reaction of the measured apoptose markers (see gene expression data in chapter "*Impact on intestinal gene expression*").

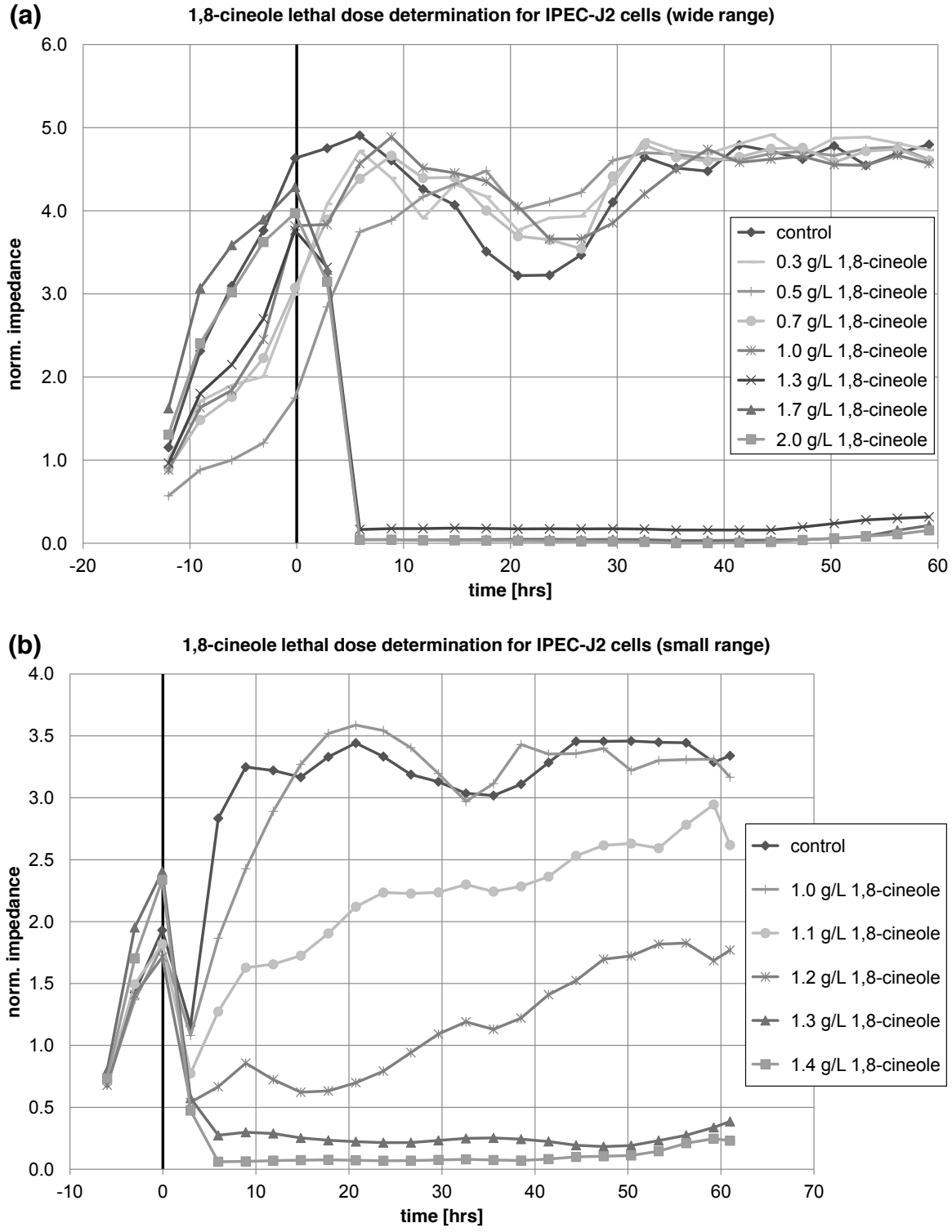

Figure 23 Electric cell-substrate impedance sensing (ECIS) measurement of JPEC- J2 cells. treated with a wide (a) and a narrow (b) range of cineole concentration applied.

Intestinal metabolization

The results in this chapter are acquired together with Natalie Gruner during her diploma thesis (Gruner 2011) guided by us in cooperation with Prof. Dr. Andrea Büttner.

Earlier works (as described in chapter *"Cineole, respiratory therapy in the gut"*) could show that cineole metabolites can be detected in body fluids as urine, blood or even mother milk post sage tea consumption. Consequently the next aim was to determine if metabolization of cineole occurs already in the intestinal epithelium and if, in which dimension. Therefore IPEC-J2 cell extractions treated with 1g/L cineole over a time course of 0, 3, 6, 9, and 24 hours, were measured by GC-MS analysis. For the intended quantification a radioactive standard (tri-fold deuterated 2-α-hydroxy-1,8-cineole) was carried along. As preliminary work, in order to gain valid data, the pure cineole and the standard were also incubated in cell free samples under similar cell culture conditions only applied in blank media or aqueous solution. For all time points comparable results were acquired. In concentrations a factor of 10^4 to 10^6 lower than the base compound cineole trace fractions of nine derivates of cineole were found as shown in Figure 24. As there were 9-hydroxy-1,8-cineole, 2-oxo-1,8-cineole, 2,3-dehydro-1,8-cineole, 7-hydroxy-1,8-cineole, α3-hydroxy-1,8-cineole, 4-hydroxy-1,8-cineole, 3-oxo-1,8-cineole, β2-hydroxy-1,8-cineole and α2-hydroxy-1,8-cineole (Kirsch et al. 2010).

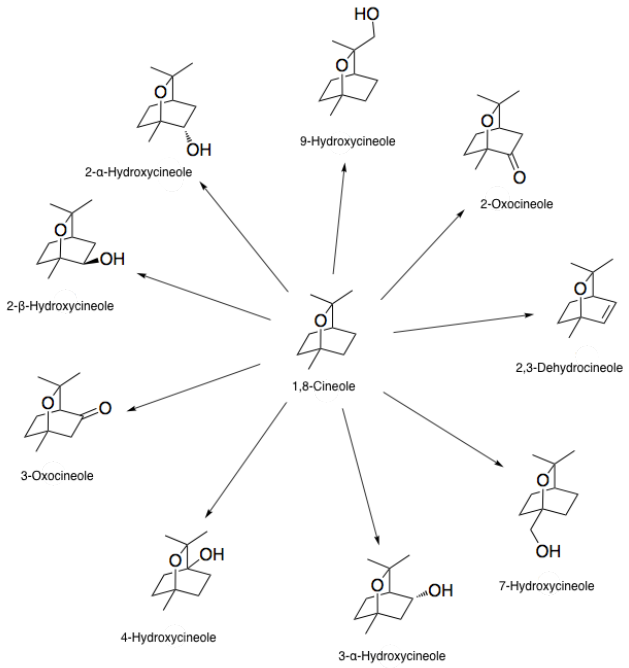

Figure 24 Quantitatively found cineole derivates from cell free media and water samples

Regarding the occurrence in all fractions, from water or media as well as at any time, the stringent implication is that these are naturally occurring derivates already present in the inserted analytes. Further comparative evaluation of the GC-MS analysis by peak integration revealed that the cineole derivative spectra remains constant over all cases and thus leads to the conclusion, that the inserted cineole as well as the found derivatives are stable under the applied experimental conditions. Nominally the values of the derivates were drastically lower than with 1 g/L those of cineole. There among 3-oxocineole and 2-oxocineole reached the highest concentrations in a range of around 200 µg/L whereas other were around 100 µg/L. With these values the derivate concentrations already reach the detection limit of the measurement. Solely α2-hydroxy-1,8-cineole noticeably showed the tendency to alter between the two host liquids with 200 µg/L in culture medium and about 100 µg/L in water.

Based on these preliminary studies and with cineole concentrations of 1.0 g/L and 0,1 g/L respectively the actual metabolization experiment was cast under identical time parameters (0, 3, 6, 9, and 24 hours), but confronting the appliance with the potential biotransformator, the intestinal epithelial IPEC-J2 cells. Obtained compound concentrations were again calculated by evaluation of the peak areas and normalized versus the cineole free controls (Figure 25).

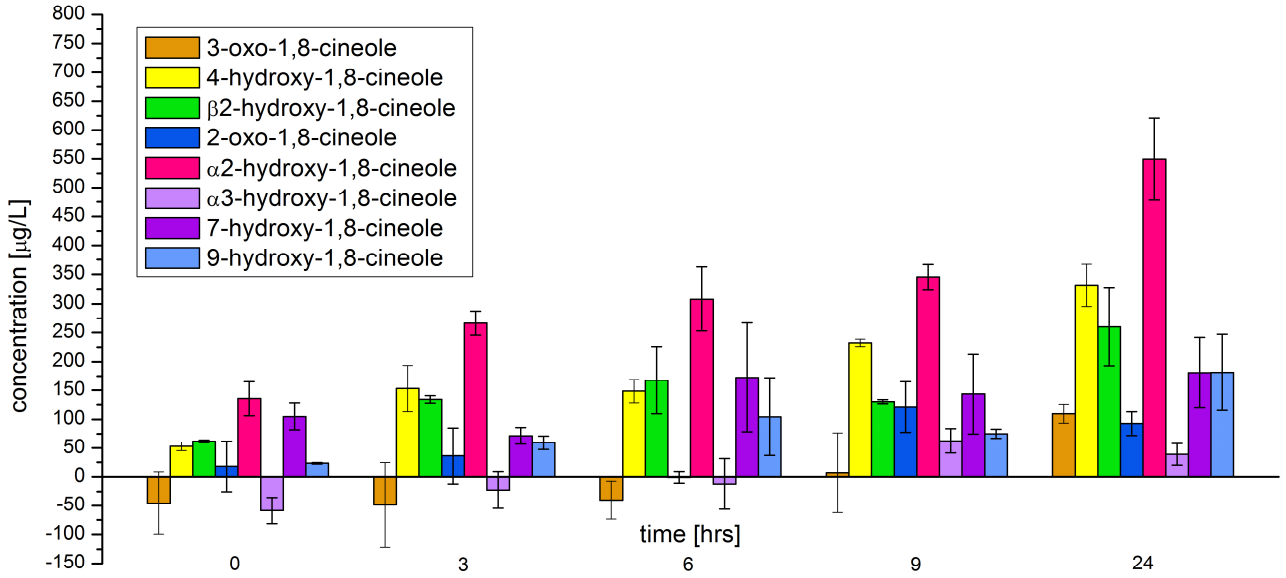

Figure 25 Metabolite profile over time at 1g/L cineole in IPEC-J2 cells

For the derivate α2-hydroxy-1,8- cineole an increase by the factor 3.7 could be assigned (from 150 µg/L to 550 µg/L) and for 4-hydroxy-1,8-cineole and 9-hydroxy-1,8-cineole even an enrichment by approximately factor 7.0 (from 50 µg/L to 350 µg/L and from 25 µg/L to 175 µg/L). In the first sight these values provide an enormous increase. However regarding the dramatically higher concentration of $1x10^6$ µg/L cineole the physiological relevance in terms of metabolization is rather questionable. Regarding the experimental set up the values are again located at the detection limit. This problem is further demonstrated by the statistical data evaluation. The standard error of means exceeds the variation in some cases and the measurement error even provokes negative concentrations by means of normalization. As the results for the lower concentration of 0.1 g/L cineole were accordingly even worse due to background noise, there is no sense in plotting them. Therefrom a slight indication of metabolic activity in the small intestine can be assigned but not more than a tendency (Müller et al. 2012). Hence the applied *in vitro* model could not provide an effective positive evidence for primary metabolization of cineole in the bowel. Thus herein induced immune reactions should directly derive from the base compound cineole and not from the impact of eventual derivates.

Impact on intestinal gene expression

From the ECIS measurements for cineole the very distinct lethal effector level of 1.2 g/L is assigned. Therefrom the obvious question is what impact results on molecular level. At a concentration of 1.0 g/L cineole what is close to the lethal one an also distinct alarming reaction on expression level should succeed. For monitoring of the cellular response marker genes related to cell cycle and proliferation (CycB1, CycD1 & TGFβ), apoptosis (Casp3 & Casp9) and for acute inflammation (TNFα, IL1β, IL6 & IL8) were evaluated by RT-qPCR. Additionally, out of academic interest IL5 was measured as it plays a role in asthmatic diseases and thus also refers to mucosal matters (Juergens et al. 2003; Takatsu 2011).The relative change in gene expression was determined in dependance to the above used cineole concentrations (1.0 g/L, 0.1 g/L) using again JPEC-J2 cells.

After data evaluation by normalizing within one point of time physiological relevant amplitudes in expression change were only found in few samples (Müller et al. 2012). There among the most distinct regulation was manifested for IL1β with a fold down-regulation of 0.7 after 3

hours of incubation with 1.0 g/L cineole and for IL8 with a 0.6 fold down-regulation after 6 hours and 1.0 g/L (Figure 26). This matches principally quite well the textbook wisdom as these genes act as primary (IL1β) and secondary (IL8) mediators in the acute inflammatory cascade. Hence an immunosuppressive effect as ascribed to cineole in this manner before (Sadlon & Lamson 2010) seems evident.

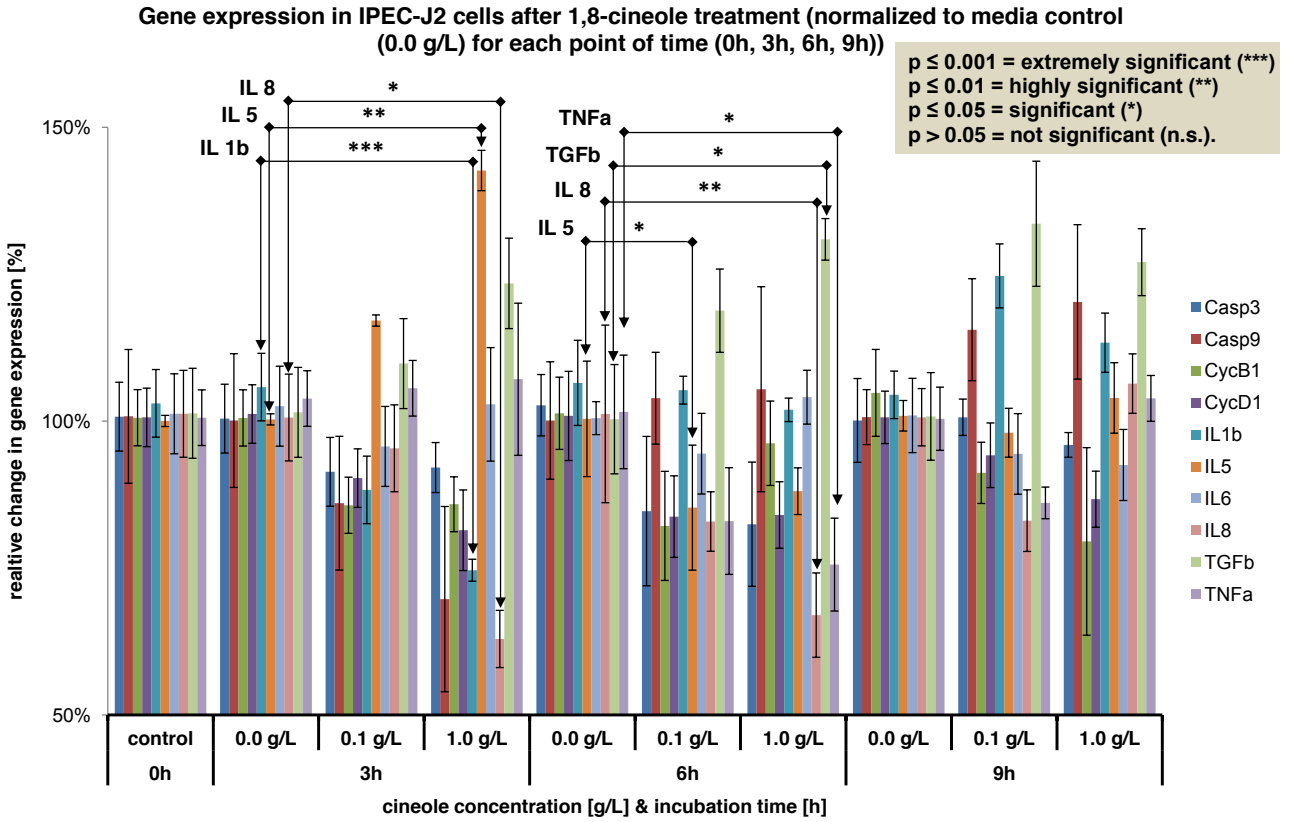

Figure 26 Gene expression pattern in cineole treated IPEC-J2 cells (normalization mode 1).

Unfortunately these alteration of IL1β and IL8 only occur distinctly within the 1.0 g/L samples and can not be distinguished in the 0.1 g/L samples. For a pharmaceutical application and thus an realistic physiological effect this concentration is far too high. Somehow in contradiction stands the leak of reactions of the apoptotic markers Casp3 and Casp9. With the near lethality dosage an amplitude was highly expected but could not be assigned. A potential explanation might be that the cell detachment observed in the ECIS measurements not originates from autocrine reactions but simply from chemical corrosion of the adhesion proteins when the cineole concentration exceeds the critical concentration of 1.2 g/L. Lethallity would be given in any case.

For deeper insights into the expression state of the apparently inert cells the so far normalization mode to one point of time and thus the reference point was changed. In Figure 27 the same data from Figure 26 is plotted, but with normalization to absolute zero, what means to the samples with an incubation time of 0 hrs and treated with 0g/L cineole. What is obtained is a plot showing the shift of relative gene expression over time. Were the regulations in the first normalization mode by physiological aspects relatively weak, except for the few and discussed candidates, the pattern now gets clearly more vivid. This proofs that the cells are not simply inert. Regulations up to 4.3 fold for CycD1at 9 h are indicated. An explanation might be that during the experiment the cells have grown into confluence and thus changed their physiology. As CycB1 being an activator of the cyclin-dependent kinase 1/cyclin B1 complex within the cell cycle during the progression from G2- to the M-phase (Castedo et al. 2002) and is further not degraded until the anaphase (Wolf et al. 2006) the incipient cell cycle arrest may temporarily cause the relative accumulation.

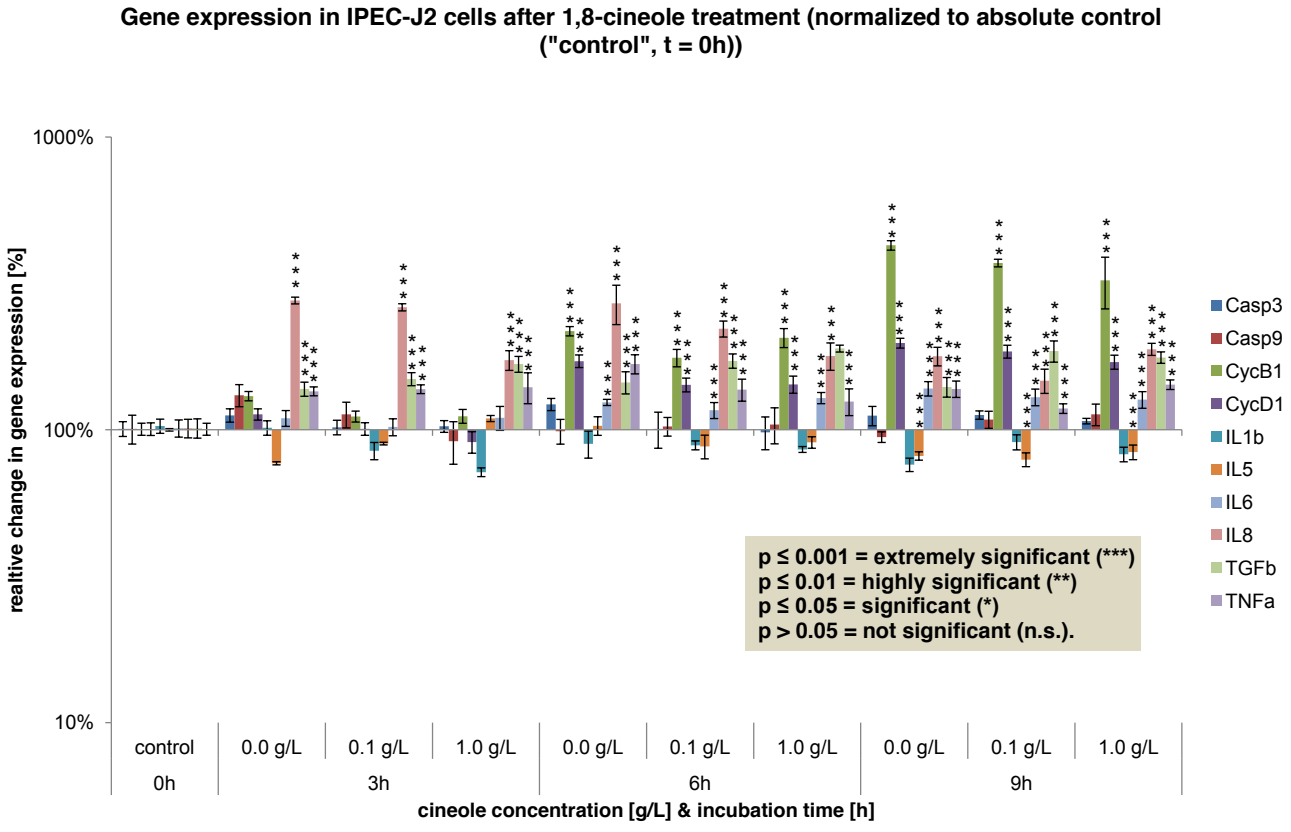

Figure 27 Gene expression pattern in cineole treated IPEC-J2 cells (normalization mode 2). Significant variations refer to the absolute control at t = 0h and hence deal with the gene shift over time.

Interestingly this up-regulation og CycB1 happens in all tree concentration levels (0.0 g/L, 0.1 g/L & 1.0 g/L,). Thus, what is monitored must be dedicated to a time effect, and therefore induced independent from the cineole treatment. This means explicitly cineole has no physiological impact on the intestinal gut cells, at least within the considered genes. This assumption from the data can be further underlined by additional analysis. The PCA here again delivers a potent tool. Considered sample wise and thus solely in respect to the amplitude of all regulative effects lying on one sample, no treatment specific normalization disturbs the obviousness of the outcome. The PCA plot in Figure 28 again deals with the same dataset as Figures 26 and 27. As the more distinct gene shift over time exceeds the week immunomodulation by cineole only the time effect gets visible after processing by the PCA algorithm. Treatment derived effects blur, as they probably do equally in the small intestine.

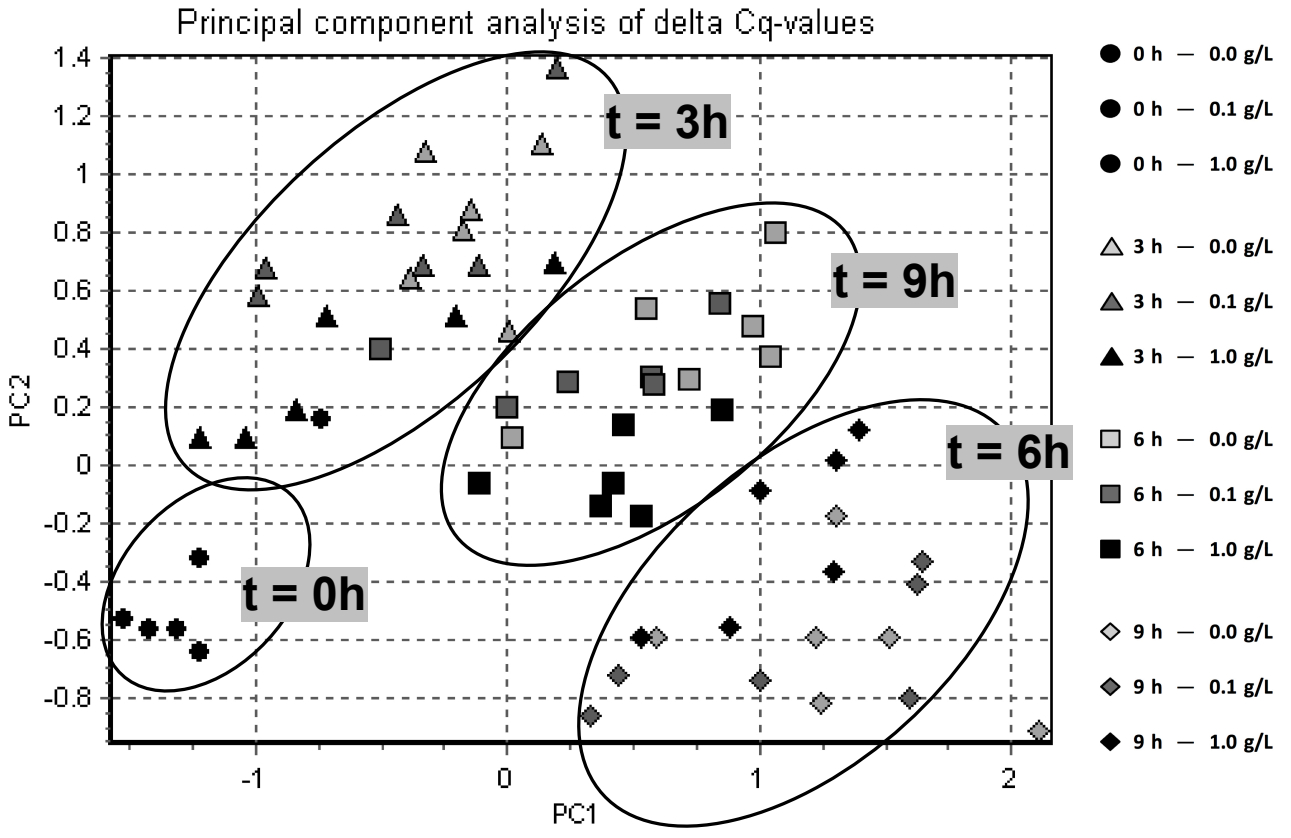

Figure 28 Cineole assay evaluated by PCA

Epigallocatechin Gallate

In this chapter the outcome of all investigations concerning EGCG as the main active agent of the tea plant *Camellia sinensis* will be reviewed. The initial determination of actual contents across different varieties of infusions will lead to the nutritional question concerning its role in basic intestinal immunity. In an expanded scope related health issues are examined especially dealing with potential reasons of its cancer preventive properties.

EGCG content of different tea varieties

A personal concern within these studies on health properties of green tea was to determine the EGCG content of individual tea preparations to clarify my actual intake of the major tea catechin. Therefore fresh brewed tea with 1 g tea dry matter on 0.1 liter of boiled water that has chilled down to 80 °C was analyzed with LC-MS (Figure 29). The outcome was that with drinking of 1 liter of the so prepared tea around 1 g EGCG is consumed, what matches with literature values quite well (Balentine et al. 1997; Harbowy & Balentine 1997). Amazingly that leads to the assumption that approximately 10 % of the dry matter of tea is EGCG. In view of this potent infusion yield the rank of tea health science is emphasized.

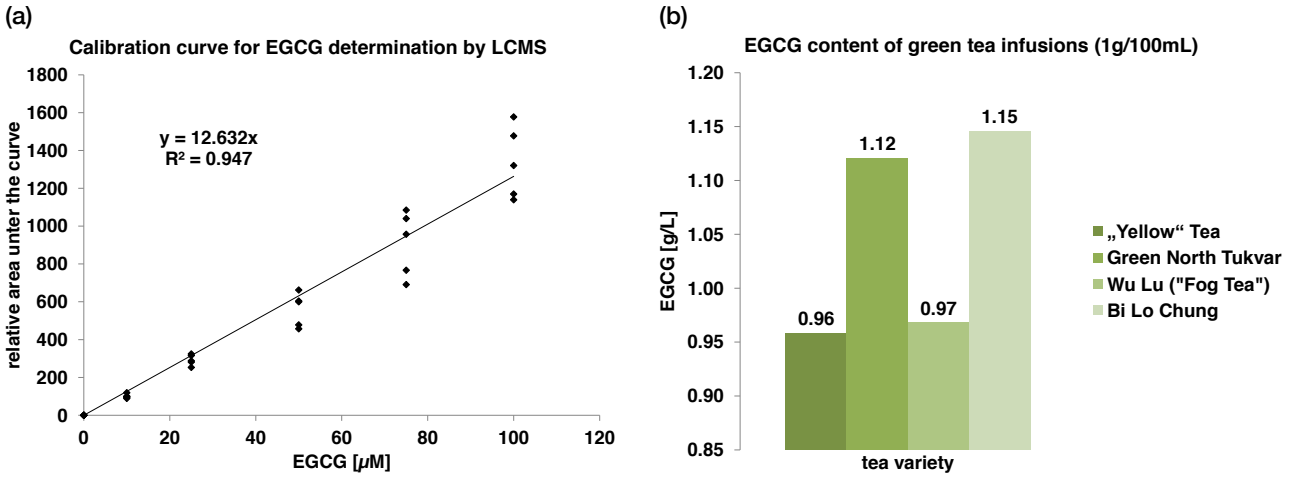

Figure 29 EGCG quantification from green tea infusions. (a) LC-MS calibration curve from pure EGCG. (b) EGCG content in fresh brewed tea (1 g dry matter / 100 mL, water at 80 °C for 15 min).

Molecular impact during intestinal immune signaling

As one question of this work was the modulation of the primary immune response by tea consumption through the gut-associated lymphoid tissue (GALT) the intestinal model was challenged with LPS. Hence, the targeted TLR4 pathway should be stimulated and primary mediators like TNFα, IL1β or IL6 should be up-regulated. For more detailed questioning which molecular targets are involved the RNAi knockdown model was applied in order to block the signal transduction through the NFκb and MAPK pathways which are primary signaling routes during inflammation. As the inhibitory impact of EGCG on the NFκb pathway has been demonstrated manifold, an additional knockdown silencing the 67LR was supposed to clarify if EGCG acts directly or through its receptor on the NFκb effector kinase IκKb or maybe via another pathway (see chapter "*Switching physiological pathways by RNA interference*").

Initially the reactivity of the cell culture model was assigned. Therefore IPEC-J2 cells were treated with different concentrations of LPS in order to provoke an immune reaction. Figure 30 shows time kinetics for inflammatory mediators post that treatment. As in preliminary studies the response was weaker than expected and limited only to the the cytokine IL6 (2.0 fold up-regulation at 1µg/ml post 3 hrs) the experiment was repeated, but unfortunately showed reproducibility (2.3 fold). As with 1µg/ml the maximal amplitude was evoked this concentration was chosen for the immune induction.

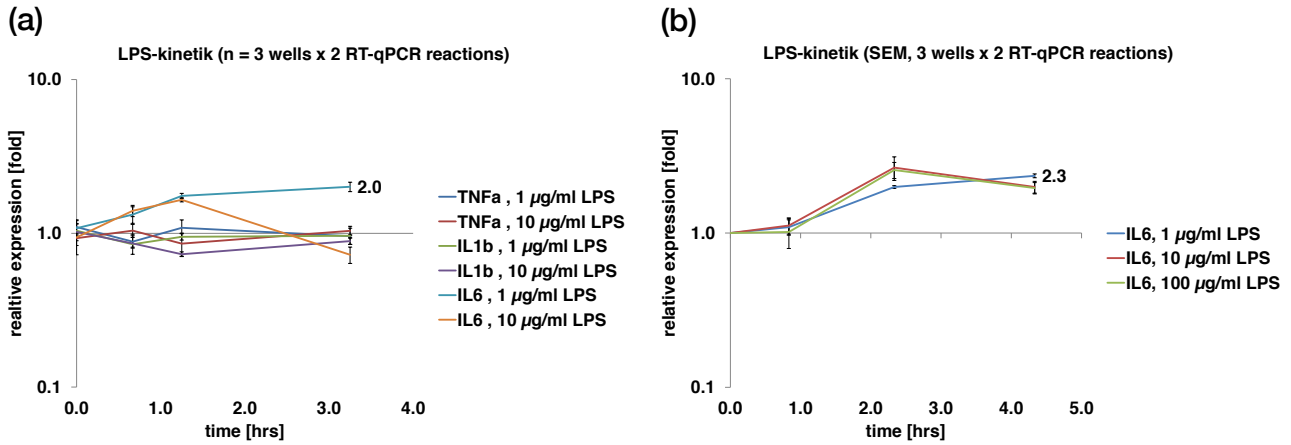

Figure 30 Assays of LPS challenged IPEC-J2. RT-qPCR analysis of TNFa, IL1b & IL6 expression.

Hence, in regard to the intended knockdown model at least one marker gene could be identified in order to test the signal disruption under "*loss-of-function*".

In a next step the specifically designed knockdown viruses for silencing of the key targets IκKb (Nfkb pathway), cJun (or "AP1", MAPK pathway) and 67LR (EGCG-receptor) had to be evaluated. Therefore, the establishment of the knockdown over time was assessed and subsequently the routine MOI of 400 was confirmed for that incubation time (see Figure 31).

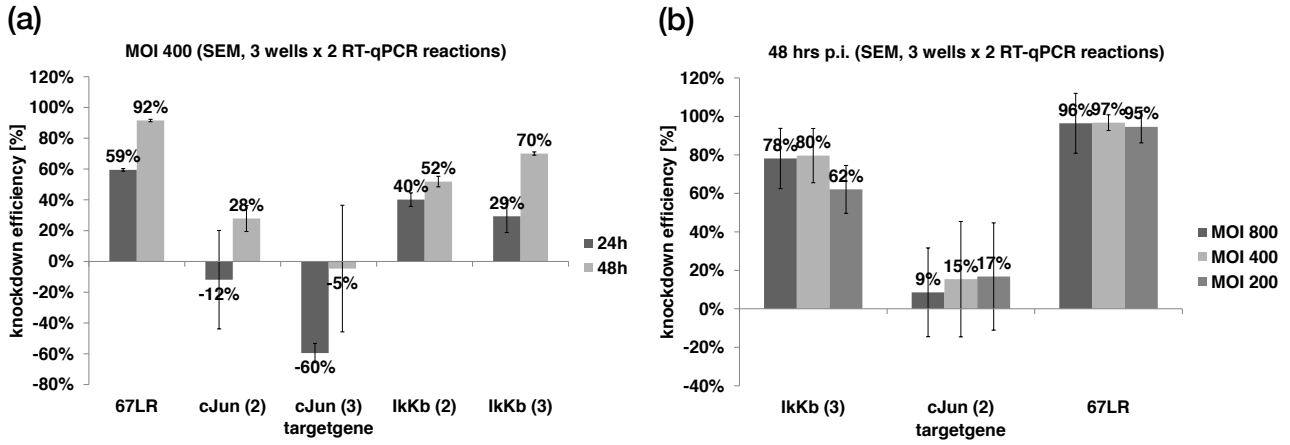

Figure 31 Knockdown evaluation series in IPEC-J2 for loss-of-function scenarios within TLR4 and 67LR signaling. (a) Time kinetic. (b) MOI gradient.

With silencing efficiencies of 80 % for IκKb and 97 % for 67LR at optimized conditions (MOI 400 & 48 hours of incubation post infection) two of the three targets knockdowns could be assigned as proper. In contrary, as it can be seen in both plots the cJun knockdown caused problems. For particular these assays already a third and fourth siRNA-sequence had been cloned, but without success. The derived knockdown was in all cases attended by uncontrolled and vivid gene regulations down as well as up. The variations among the conducted cell culture triplicates manifest in the error bars exceeding the particular effect. All in all four attempts were cast in order to silence cJun. Regarding the crucial role of the transcription factor AP1 in physiology, it seems likely that the knockdown failure and the consecutive mad reactions on transcription level derive from the try to silence this gene. On the one hand due to its abundant necessity for cell signaling (Shaulian & Karin 2002; Eferl &

Wagner 2003; Osborn & Olefsky 2012), and on the other due to the attending viral infection (Hagmeyer et al. 1993).

Subsequently, with the above adjusted parameters a knockdown assay was cast as shown in Figure 32a. Thereby the JPEC-J2 cells were infected with all viruses for all tree intended knockdown targets. Accordingly, for another try, a fourth siRNA-sequence targeting cJun was designed and processed. It repeatedly carried along identical problems as indicated in Figure 32b wherein corresponding silencing data for the presented assay is plotted.

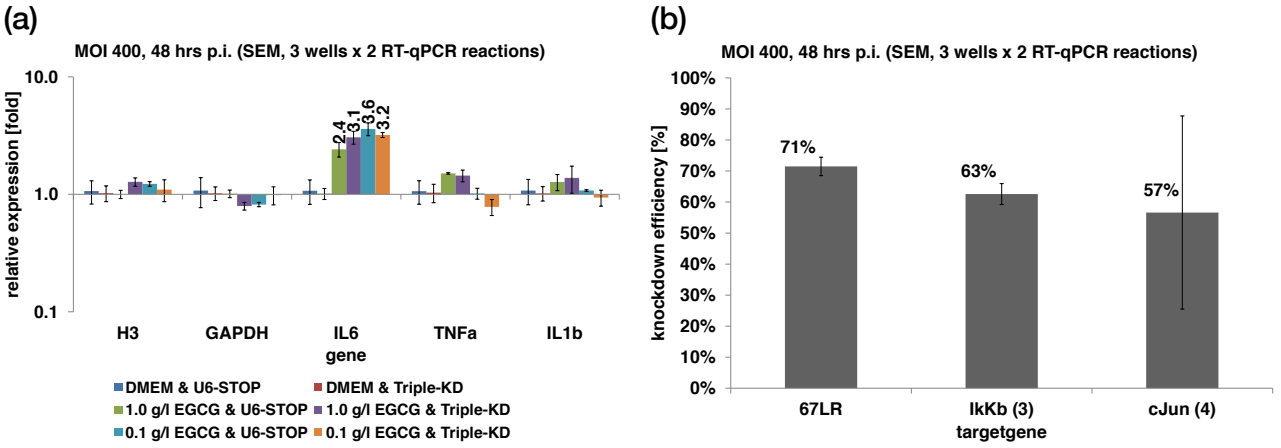

Figure 32 Loss-of-function study on EGCG in TLR4 and 67LR signaling. (a) RT-qPCR gene expression analysis (relative fold regulation) from IPEC-J2 cells. The triple knockdown treated (at MOI 400: 67LR-KD, IkKb-KD & cJun-KD versus negative control virus Ad5-U6-Stop) cell culture was pre-treated with two concentrations of EGCG (1.0 g/L & 0.1 g/L) for 3 hrs (performed in triplicates). Subsequently LPS with 1 µg/ml was added to all samples as a chalange and cells were harvested for RNA extraction post another 3 hrs. Then Inflammation marker (TNFα, IL1β & IL6) and reference gene (Histone H3 & GAPDH) transcript levels were assigned (duplicates). (b) Corresponding silencing efficiencies calculated by normalization against the negative control virus Ad5-U6-Stop.

In this experiment the cells were pre-treated with EGCG; the intention was to monitor if subsequent LPS challenge simulating a pathogen incident. Therefrom EGCG should be investigated for immunomodulatory activities as preventive agent by continuous consumption of green tea. The question was if EGCG can alter the induced immune reaction through the LPS challenge depending on the blockage of the underlying signaling pathways or depending from the presence of the postulated EGCG receptor.

The first imprint is that again the most response is given by IL6 within a physiological relevant rang (2.4 to 2.6 fold). However, it needs a closer look to get the reasons of this enhanced cytokine expression.

If we first consider the two cases wherein no EGCG and therefore the media control is applied, the red group (DMEM & Triple-KD) versus the blue group (DMEM & U6-Stop), we face the unexpected situation of an equal gene response. Here, the not knockdown attended samples should show a higher IL6 level relative to those where the TLR4 signaling pathways are interrupted.

When we now consider the scenario within the control vector group (blue, green and turquoise, as DMEM & U6-Stop, 1 g/L EGCG & U6-Stop and 1.0 g/L EGCG & U6-Stop) the finding is that the enhanced IL6 expression there is solely induced by EGCG. Thereby the lower concentration even provokes a higher IL6 response (3.6 versus 2.4 fold).

If we finally compare samples within one treatment group, for example the orange and the turquoise with the lower EGCG concentration applied (0.1 g/L EGCG & Triple-KD versus 0.1 g/L EGCG & U6-Stop) which are optionally gene silenced or not, it gets obvious that the inflammatory signal gene IL6 is up-regulated only EGCG dependent. No significant difference in relative gene expression can be attributed to the varied knockdown situation. In consequence that includes besides the TLR4 signaling pathways as well the potential signal transmission thought the 67LR as an EGCG receptor. Hence the IL6 stimulation occurs induced by the tea catechin in any case, and therefore probably regulated via another mediator.

The findings from the knockdown experiments imply that by a base treatment with EGCG the evolved IL6 response induced by LPS is blocked. However the physiological benefit is questionable confronted with the measured immune stimulation through the tea catechin. It self (re-)activates the cytokine. Hence, in regard of the not pre-treated cells, which here as well show no reaction to the LPS treatment and further considering that the whole scenery measures relative changes in gene expression, the blurring reason might be the probably much higher challenge for the intestinal epithelial cells present, what manifests in the adenoviral infection. However, it remains to assign that during these studies no difference could be noticed due to the leakage of the EGCG receptor, even with a potent 67LR knockdown applied.

67LR: a potential target for EGCG in cancer prevention?

Epigenetic issues

The results in this chapter are acquired together with Johannes Meier during his master thesis at our institute (Meier 2011).

Aiming for more insights into the associations between the 67LR, epigenetic originated silencing by DNMTs and the mutual effector molecule EGCG the involved genes were knocked down by RNAi and analyzed under permuted treatments with DNMT inhibitory DAC or EGCG respectively. In a combinatory approach gene expression and methylation levels were acquired. The thereout developing silencing scenario investigated in the intestinal IPEC-J2 model constitutes as presented in Figure 33.

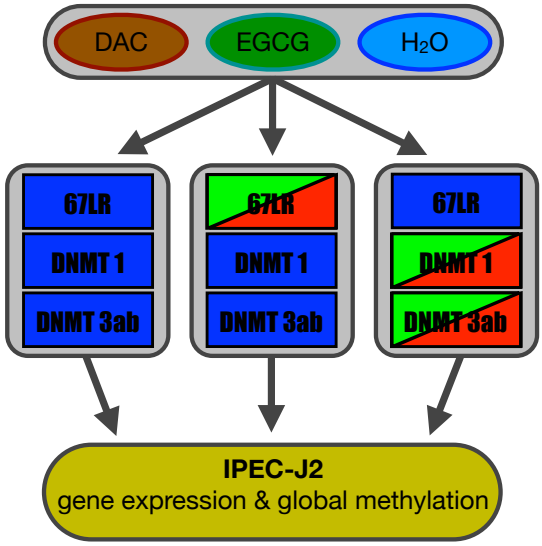

Figure 33 Epigenetics affecting silencing scenario. Blue boxes in the middle row represent genes not targeted by specific RNAi viruses whereas green/red boxes are alternated with or without specific knockdowns during an experiment.

In the first experimental series as indicated in the left column of Figure 33, the explicit influence of EGCG (20 mg/L) or DAC (5 µM) treatments on the cell culture in absence of any gene knockdown was investigated. As control H_2O was applied. In terms of gene regulatory effects the methyltransferases DNMT1, DNMT3a and DNMT3b were analyzed and additionally the impact on 67LR expression (Figure 34a). As a notable result the expression level of DNMT 1 and DNMT 3b was enhanced 3.9 fold and 7.8 fold under the impact its inhibitor DAC. Hence, these two methyltransferases seem to be more important in this context than DNMT3a, since its expression is only weakly affected. As supposed to act in an analog manner on methyltransferases like DAC (Pandey et al. 2010), a similar tendency, but

with only 2.1 fold (DNMT 1) and 1.8 fold (DNMT 3b) up-regulation not that distinct, can be observed for EGCG.

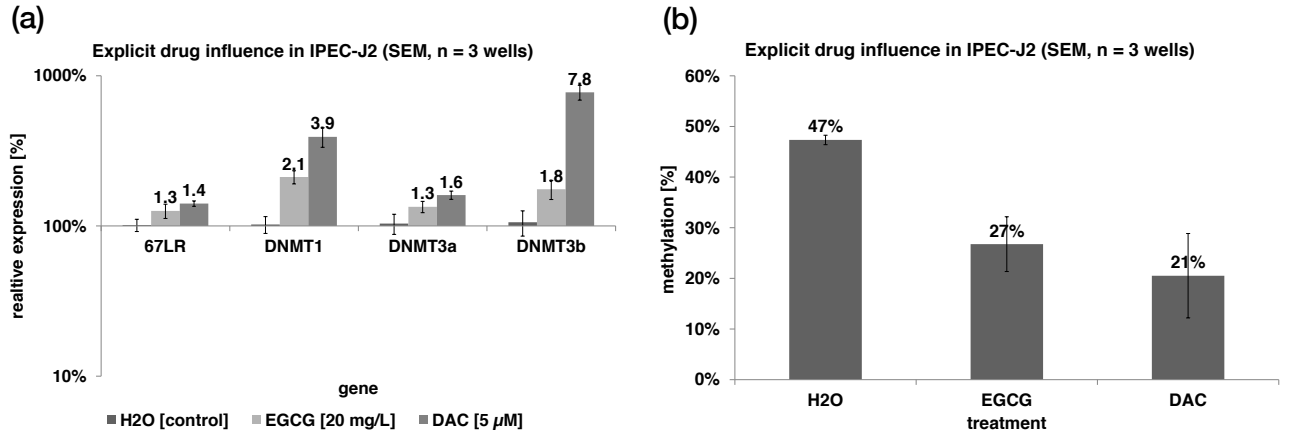

Figure 34 Isolated drug effects on IPEC-J2. (a) Relative expression levels of Methyltransferases and the 67LR post 72 hrs of drug treatment (20 mg/L EGCG or 5µM DAC). (b) corresponding global methylation values.

On methylation level the treatments showed inverse correlating effectiveness. The supposed inhibitor DAC provoked a reduction of relative global methylation of 21 % in contrary to 47 % under control conditions and EGCG still contributed with a suppression of 27 % (Figure 34b. In accordance with recent findings in cancer cell lines (Nandakumar et al. 2011) the suppressing influence of tea catechins and in particular EGCG on the global methylation state is therefrom confirmed as well for this intestinal model. In regard to the fact that the methylation is established during cell proliferation and that the gene expression levels here reflect the time point at the end of the assay, the gene expression and methylation data is consistent. An obvious explanation for the up-regulation is thus inherit. The intestinal epithelium can counter regulate disruptions in global methylation.

The experiments conducted in relation to the middle column of Figure 35 (study layout) investigate the same effects under knockdown of 67LR (MOI 400). Thereby a second EGCG concentration one potency below (2 mg/L) was considered. As indicated in Figure 35a-d the gene knockdown was present with 93 % up to 97 % and no other gene of interest was affected off-target in a distinct magnitude. Figure 35e-h shows the corresponding gene expression values post 72 hrs of drug treatment.

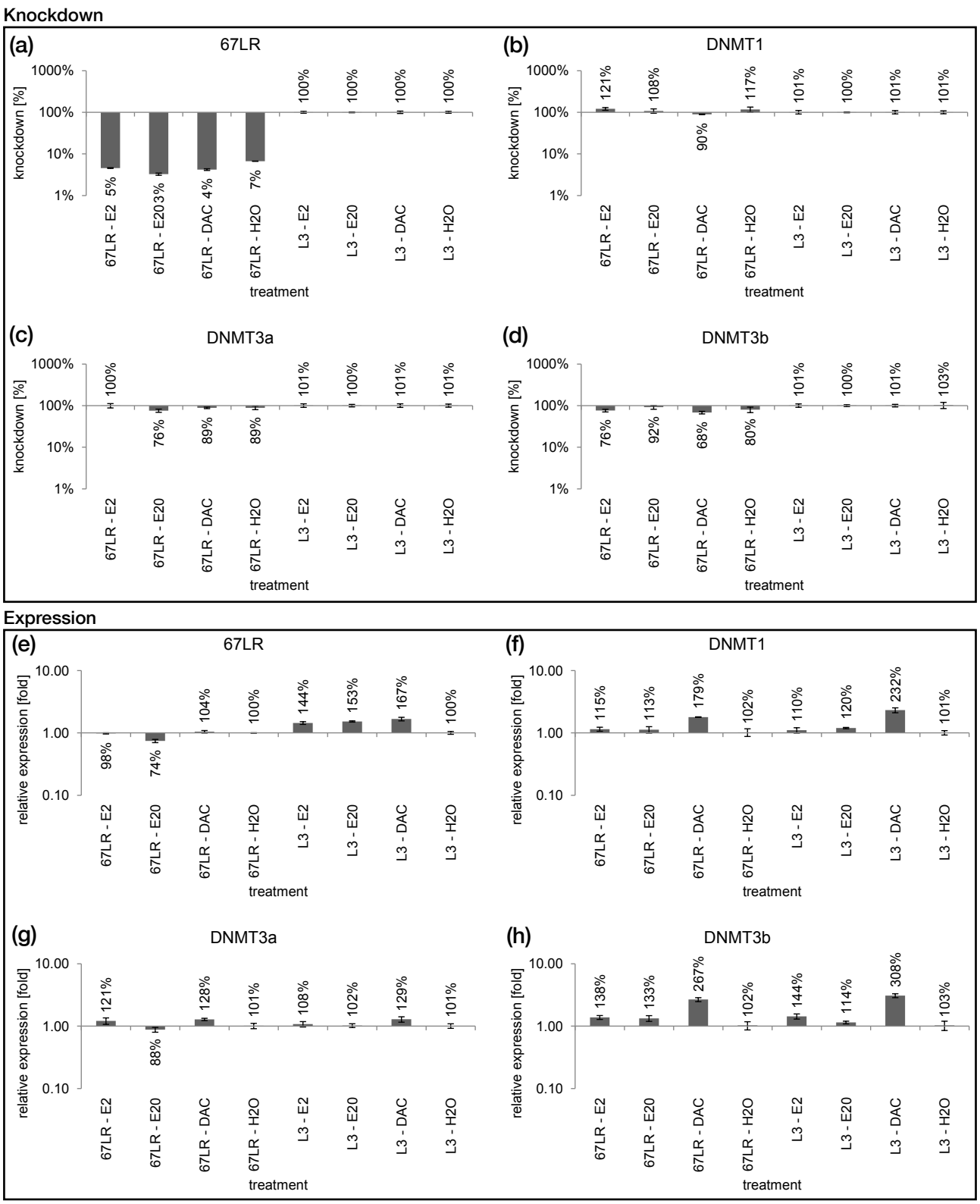

Figure 35 Drug effects (DAC, EGCG) on IPEC-J2 cells under 67LR knockdown versus knockdown control (Ad5-U6-Stop = L3; all assays n = 3 wells x 2 RT-qPCR reactions). (a-d) Net knockdown effects (MOI 400) for all treatment variants: E2 = 2 mg/L EGCG, E20 = 20 mg/L EGCG, DAC and H_2O-control on considered genes (DNMT 1, DNMT 3a, DNMT 3b and the knockdown target gene 67LR). (e-d) Corresponding net relative change in gene expression from the identical assay.

Considering the induced expression alterations under almost leakage of the EGCG-receptor, the cell physiology reacts with a comparable lag-regulation, at least in awareness of the present DNMT inhibitor DAC. Still up-regulations of DNMT 1 (2.3 fold -67LR-KD & 1.8 fold +67LR-KD) and DNMT 3b (3.1 fold -67LR-KD & 2.7 fold +67LR-KD) can be observed, although not that distinct. Again the DAC impact on DNMT 3a is higher than on DNMT 1 and vanishes for DNMT 3b. For EGCG the tendency to enhance DNMT 1 and 3b expression due to an inhibitory activity, as observed without any knockdowns can not be assigned anymore. However, the data does not clarified if this is inflicted as intended by the applied 67LR knockdown, due to neglect able levels of expression change.

Mirroring these observations to methylation states, it is more likely that EGCG has no more impact. Figure 36 shows only distinct hypo-methylation through DAC compared to the control and knockdown independent. For EGCG treatments no effect is present any more. The suppression observed in absence of adenoviral knockdowns can not be recovered under these treatment conditions. Thus the receptor dependency can not be confirmed.

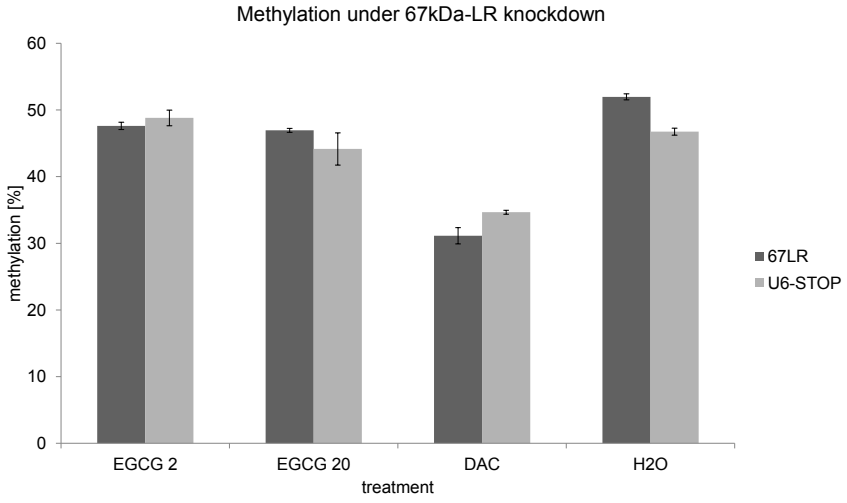

Figure 36 Global methylation values post different drug treatments (2 mg/L EGCG, 20 mg/L EGCG, DAC & H_2O-control) in IPEC-J2 under 67LR knockdown versus knockdown control Ad5-U6-Stop (n = 3 wells x 2 RT-qPCR reactions).

The experiments conducted for the final setting (left column of Figure 35 wherein the different species of DNMTs are silenced in functional groups, is reviewed in this paragraph. The drug treatment pattern is identical with the antecedent, but the applied knockdown viruses target the *maintenance* methyltransferase DNMT 1, combined the *de novo* methyltrasferases DNMT 3a & DNMT 3b or all tree considered DNMTs. Again in the first four plots the silencing efficiency is shown (Figure 37a-d).

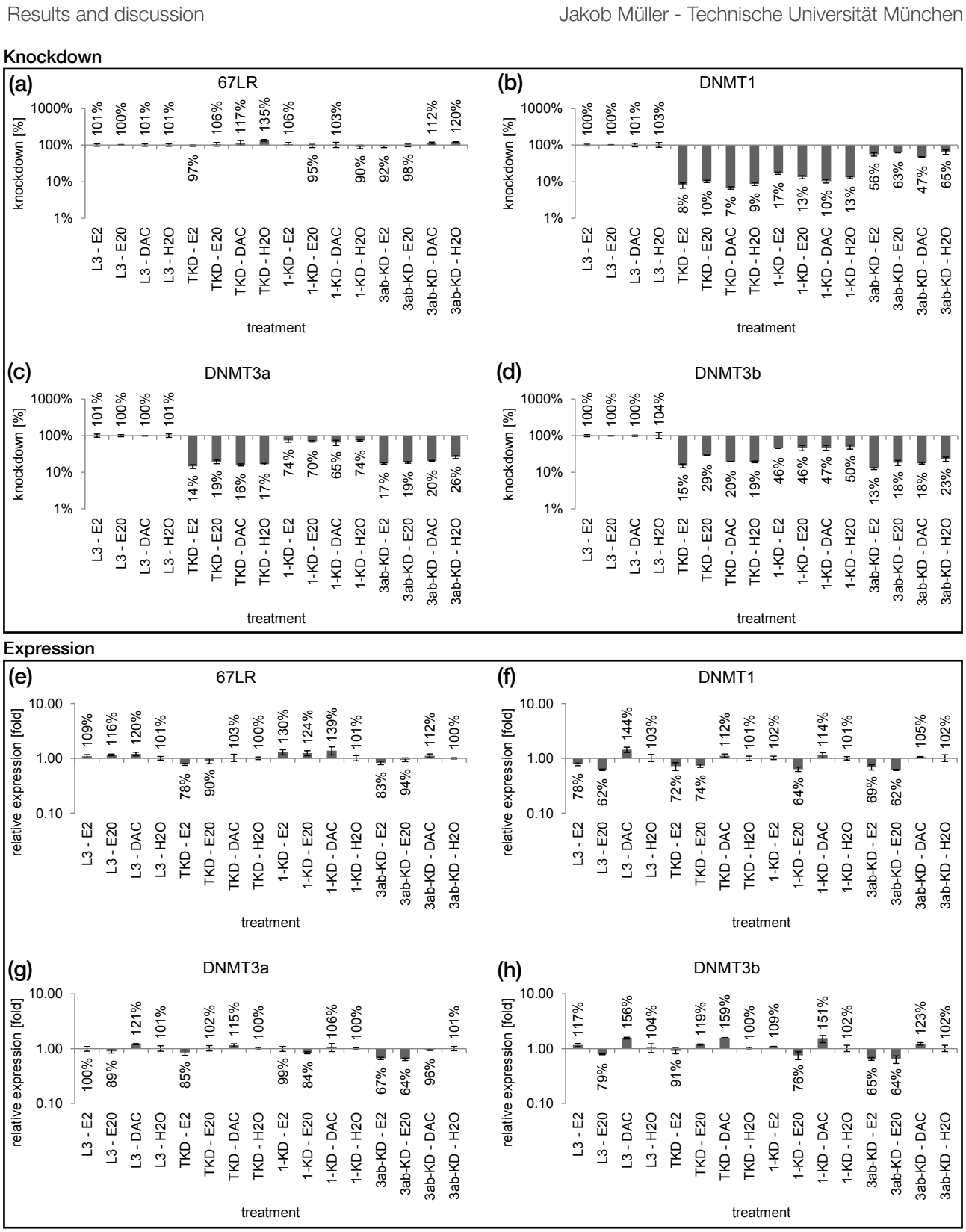

Figure 37 Drug effects on IPEC-J2 cells under DNMT knockdown combinations (*maintenance* DNMT (1), *de novo* DNMTs (3ab) or all three DNMTs (1,3a & 3b = TKD)) versus knockdown control (Ad5-U6-Stop = L3; all assays n = 3 wells x 2 RT-qPCR reactions). (a-d) Net knockdown effects (MOI 3 x 400) for similar drug treatment variants as in Figure 36 and on the same gene set. (e-d) Corresponding net relative change in gene expression out of the identical assay.

For this application of a triple-knockdown it was necessary to imply all single viruses with an MOI of 400 what leads to a combined overall MOI for one well of 1200. The intended knockdown targets are affected by mean silencing efficiencies (n = 3 wells x 2 RT-qPCR reactions) of 89 % for DNMT 1 (SEM = 1%), 81 % for DNMT 3a (SEM = 1%) and 81 % for DNMTs 3b (SEM = 2 %), whereas the 67LR was merely off-target attended reciprocal to less than -6 % (SEM = 3 %), what can be attributed to natural variation. Therefrom the silencing scenario is indeed valuable as 80 % of knockdown represent a proper threshold.

However, Inherit unveils a unintended but interesting discovery. In Figure 37b`-d` the data from Figures 37b-d is plotted in a slightly different mode. This visualization emphasizes weaker knockdown effects due to an inverted and linear ordinate. That way it is revealed, that the respective target knockdown carries along con-natural and remarkable developed off-target effects.

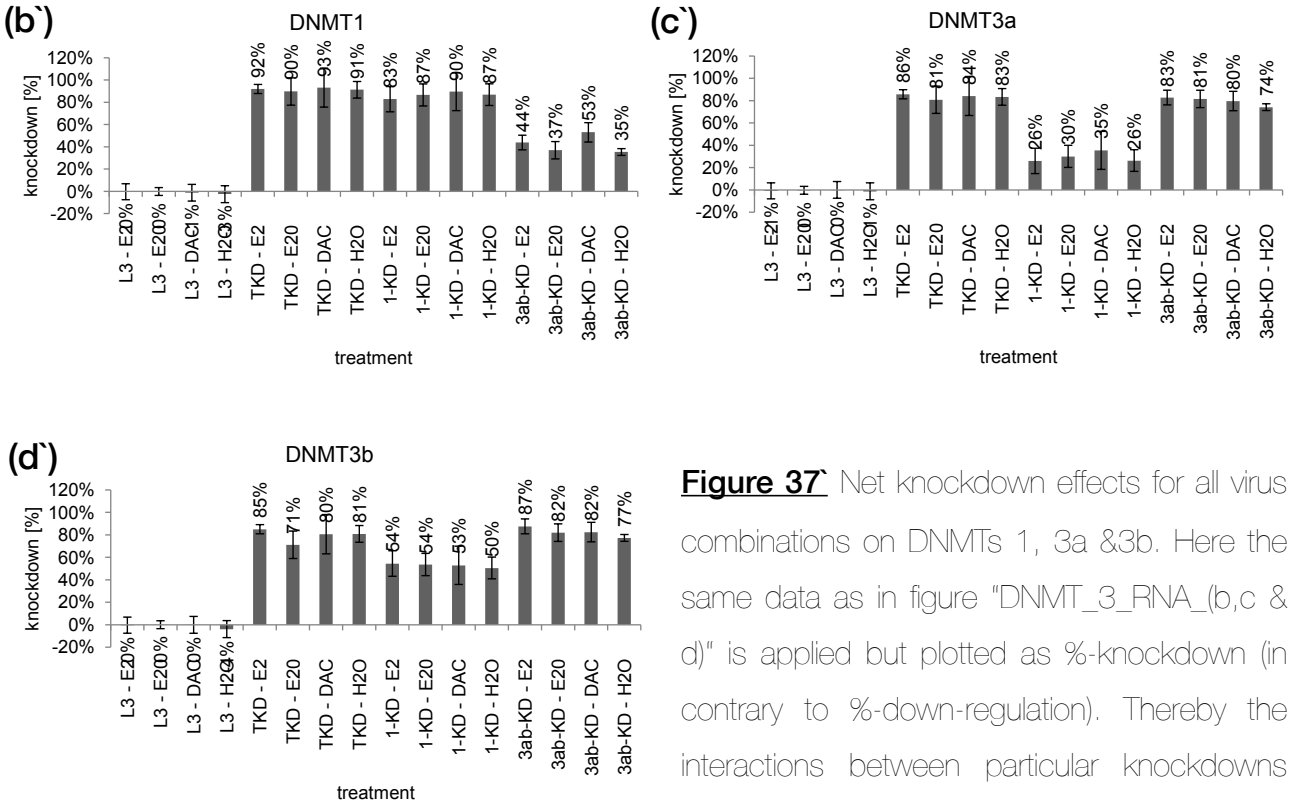

Figure 37` Net knockdown effects for all virus combinations on DNMTs 1, 3a &3b. Here the same data as in figure "DNMT_3_RNA_(b,c & d)" is applied but plotted as %-knockdown (in contrary to %-down-regulation). Thereby the interactions between particular knockdowns and attended genes get more obvious.

The silencing of one DNMT always co-silenced another DNMT. Thereby a heterogeneous effectivity can be monitored. DNMT 1 is off-target attended by combinatory DNMT 3a/b knockdown by 42 % (SEM = 4%) and DNMT 3b is off-target attended by DNMT 1 knockdown by 53 % (SEM = 4%). In contrary, weaker off-target attended is DNMT 3a by

DNMT 1 knockdown with only 29% (SEM = 2%). Hence, in a similar manner as observed through the expression enhancing reaction to inhibitor treatments (DAC,EGCG) the methyltransferases DNMT 1 and 3b show more reaction here than DNMT 3b. This again suggest a potential regulatory link DNMT 1 and 3b, although it must be emphasized, that this effect is a net knockdown correlation and that here are no explicit regulations on relative gene expression level present, as they would establish in Figure 37f-h.

Regarding the outcome for regulations in relative gene expression in this case, compared to the previous findings, it is less significant (Figure 37e-h). In the precedent assays a correlating transcription activity counter acting the inhibitory impact of DAC or EGCG on DNMT expression could be monitored. For this multi-knockdown scenario this effect can not be recovered. The foregoing observation might fail to establish due to the antagonistic impact of the DNMT-knockdowns contra the up-regulation, or simply because of the massive physiological disturbance under the sensible but need elevated MOI of 1200 (3 x 400). All in all for this scenario unfortunately no targeted gene regulation pattern constitutes.

Remains the epigenetic data for the third experimental series. In Figure 38 the appendant global methylation values are given.

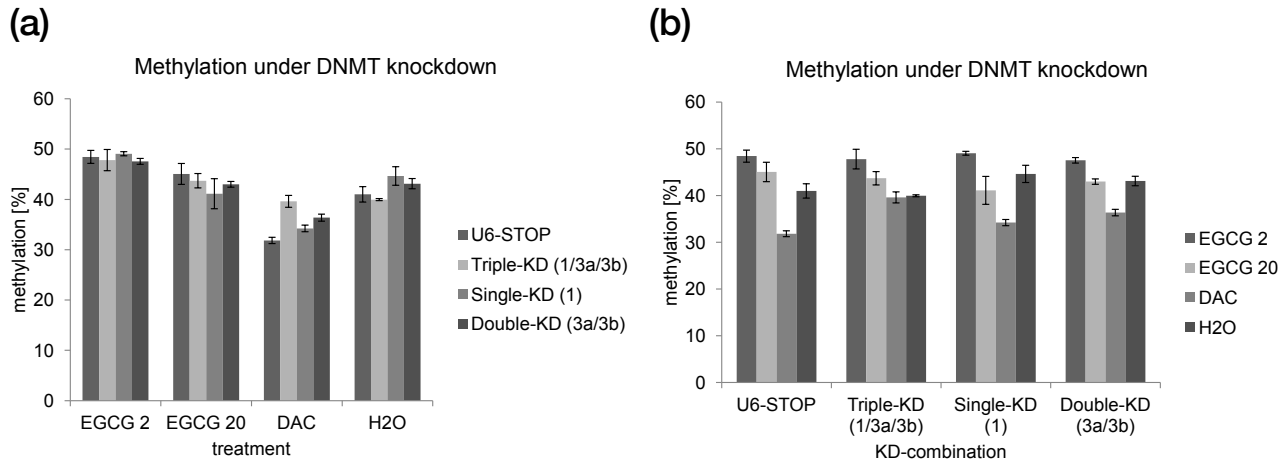

Figure 38 Corresponding methylation data to figure "DNMT_3_RNA" arranged after treatments (a) or (b) knockdown combinations. Epigenetic influence post drug treatments (2 mg/L EGCG, 20 mg/L EGCG, DAC & H_2O-control) in IPEC-J2 under DNMT knockdown combinations (*maintenance* DNMT (1), *de novo* DNMTs (3ab) or all three DNMTs (1,3a & 3b = TKD), MOI 3 x 400) versus knockdown control Ad5-U6-Stop (n = 3 wells x 2 RT-qPCR reactions).

In regard of the solid knockdown levels for all genes and under all treatment conditions of over 80 % a negative alteration in the methylation was highly expected. Surprisingly no suppression of epigenetic methylation derived from DNMT silencing can be assigned within the underlying data. Figure 38b shows transposed data from Figure 38a and thus explicitly underlines a pure drug dependency without any DNMT-knockdown influence. Thereby only DAC keeps up its demethylating and thus DNMT inhibitory properties, even if the varied DNMT knockdowns evoke the same effect as the negative control virus Ad5-U6-Stop. The question now is, which DNMTs are attended by DAC if the tree considered methyltransferases are all knocked down? At any rate methylation patterns are present, and DAC diminished. Maybe the estimated remaining 20 % of DNMTs 1 3a and 3b manage to keep up the methylation pattern even under knockdown conditions. Another attempt of explanation might be that primordial expressed DNMTs still reside within the epithelial cells from the time before the knockdown was applied and manage the methylation activities.

As observed previously the present hypo-methylation of 27 % established under EGCG impact without any knockout does not constitute when the 67LR is silenced. Therefrom the data points to a mediating effect of the 67LR for DNMT inhibition by EGCG. Hence, the EGCG-receptor postulation seems to be approved. Unfortunately this also happens for the knockdown control scenario. However, in regard of the third scenario these findings get dubious anyway. Under DNMT knockdown EGCG should be able to inhibit methylation due to a not silenced 67LR. Therefrom apparently the virus application itself disturbs the previously hypo-methylating activity of EGCG. Furthermore again the question rises on which methyltransferases shall EGCG act? Thus it seems most likely that methylation was already matured at the point of treatment, and this thesis calls the first case into question. Further the problem with this consideration is that DAC can not alter posteriori due to being only active when integrated into the DNA during the genesis of a new cell. An argumentation bringing all findings together without logical conflicts can not be assigned with this state of knowledge.

As physiological consequence regarding health contributory events in the EGCG context, the base epigenetic information is anyway axiomatically ambivalent. No primary coherence between beneficial or harmful consequences through global hypo-methylation can be predicted as cancer inducing pathways are activated by both tumor suppressor or oncogenes.

EGCG in metastasis

As described in chapter "*Green tea, epigallocatechin gallate and its receptor*" the 67 kDa laminin receptor, before getting into the spotlight as an EGCG-receptor, played a distinct role related to tumor progression and metastasis. Over-expressed on the surface of circulating cancer cells this membrane protein mediates target tissue binding and subsequent invasion. Synthetic peptides which bind competitively to the 67LR were shown to inhibit its metastatic potential *in vitro* (Iwamoto et al. 1987) and further down regulation of the receptor was assigned to prevent cancer cell migration (F. X. Chen et al. 2009). Outgoing from these findings and the postulation of the 67LR as a receptor for EGCG (Tachibana et al. 2004) the question for a connection arouse. To investigate the interplay a RNAi-knockdown model combined with RT-qPCR expression analysis was cast in order to evaluate the anti metastatic potential of EGCG via modulation of 67LR-expression in the intestinal epithelium. IPEC-J2 cells were treated with physiological as well as pharmacological concentrations of EGCG (1.0 g/l, 0.1 g/l, 0.02 g/l and 0.002 g/l) and the synergic effects between the tea catechin and the small RNAs interfering in gene expression was assigned (Müller n.d.).

In a first approach knockdown effects targeting the 67LR under 1.0 g/L EGCG treatment were measured versus the negative control virus Ad5-U6-Stop. Parallel the same experiment was cast with a second RNAi knockdown virus as a positive control. The outcome on gene expression level is shown in Figure 39a. A multitude of repetitions (7 assays x 3 wells) revealed that the small RNA induced suppression of 67LR transcripts was significantly enhanced in presence of EGCG, but not for the positive control knockdown. Whereas the knockdown evoked a transcript reduction down to 10 % without the tea catechin, only residual transcript level of 4 % was measured with EGCG. This step from 90 % to 96 % initially seems less impressive. But it needs a closer look. In Figure 39b the identical data from Figure 39a is applied, but in a different normalization mode. In Figure 39a the control groups refer to the control knockdown virus Ad5-U6-Stop within one EGCG concentration. Hence what is obtained are the net silencing effects. In contrary Figure 39b applies the media controls within one virus species as relative fixed point for normalization. As result now the net change in relative gene regulation via a drug treatment gets visible. In this view the slight knockdown enhancement under EGCG evolves to a giant leap and it is revealed, that the induced effect is an extra suppression of transcripts by 37 %.

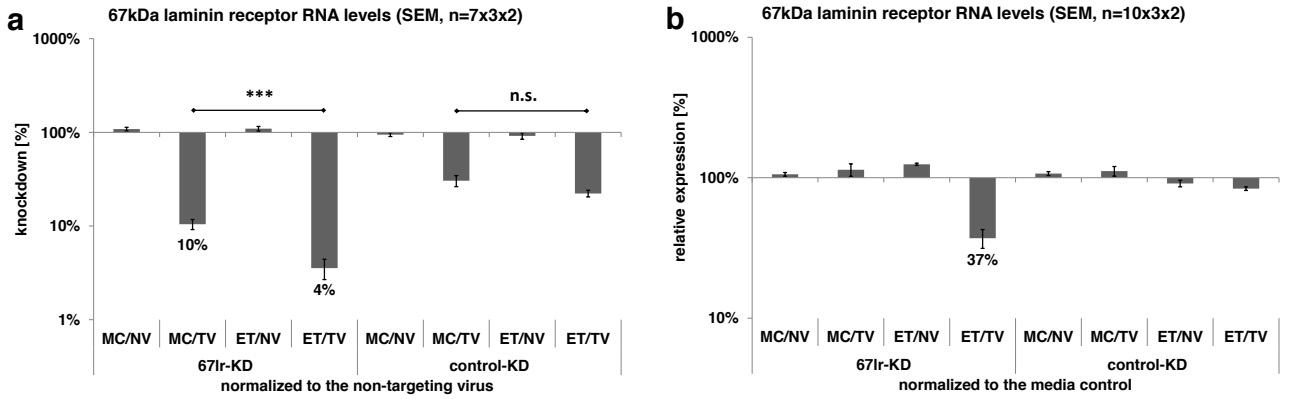

Figure 39 Comparison of the 67LR knockdown (67lr-KD) and the positive control knockdown (control-KD) under EGCG impact (ET = EGCG treatment, MC = media control, NV = Ad5-U6-Stop, TV = targeting RNAi virus). (a) Data normalized to Ad5-U6-Stop. This reveals net knockdown effects. b) Data normalized to media control. This reveals net relative change in gene expression induced by the drug treatment. ($p \leq 0.001$ = extremely significant (***), $p \leq 0.01$ = highly significant (**), $p \leq 0.05$ = significant (*), $p > 0.05$ = not significant (n.s.))

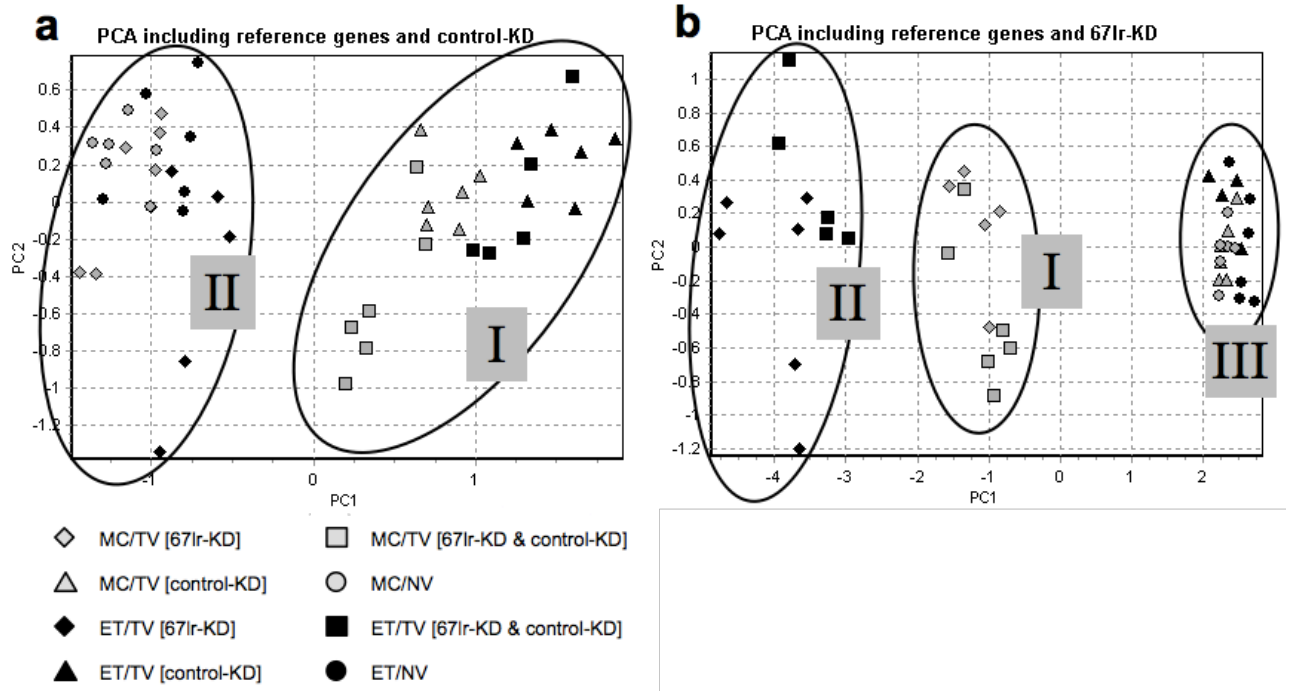

Figure 40 PCA comparing the impact of EGCG on the 67LR versus the positive control virus (black labels = EGCG treated, grey labels = samples without EGCG (same abbreviations as above). (a) Positive control virus induced knockdown (I = knockdown applied, II = negative control virus AD5-U6-Stop applied). (b) 67LR knockdown related effect (I = EGCG not present, II = EGCG treated, III = AD5-U6-Stop applied with and without EGCG).

In order to verify this observation independently from any kind of normalization mode principal component analysis (PCA) was applied. The plots derived from the statistical processing are shown in Figure 40. Thereby the two plots analyze the two knockdown scenarios, as is Figure 40a the positive control knockdown and in Figure 40b the 67LR targeting virus is applied. In Figure 40a two data clusters manifest, whereas in Figure 40b three clusters are present. And there the 67LR/EGCG-synergy crystalizes. For the positive control knockdown there is only the question is there silencing present or not, in case of Ad5-U6-Stop negative control. In contrast for 67LR an additional cluster separates among the knockdown targeted cloud. These are all samples which are attended by the extra suppression of transcripts under the synergistic impact of EGCG.

For a further evaluation of the findings the experiments were conducted with lower concentrations of EGCG as 1.0 g/L matches the conditions in fresh brewed tea, but not imperatively reflects actual concentrations of the small intestine *in vivo.* The significant co-regulatory effect on 67LR expression when interfering small RNAs and the tea catechin act together was also present there, for all concentrations applied (Figure 41).

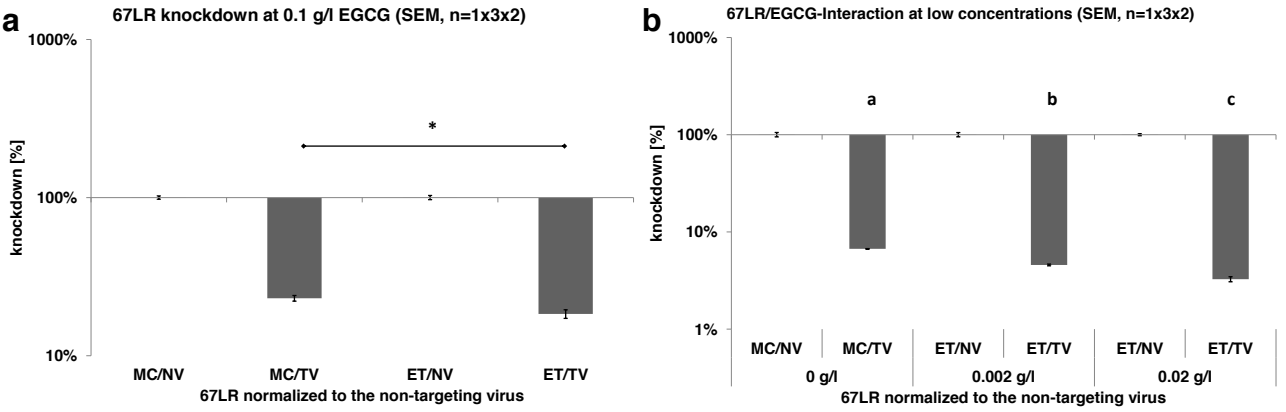

Figure 41 67LR/EGCG-synergy for lower EGCG concentrations. Same abbreviations and significance levels as above; letters a, b & c indicate extremely significant intermediate variances).

By means of mortality the still most vicious enemy in the combat against cancer is metastasis. EGCG significantly co-regulates the small RNA silenced expression of the metastasis associated 67LR in an epithelial cell line of the gastrointestinal tract. The cancer preventive potential of a tea catechin enriched diet may originate from this synergy. Ahead this principle of action may elucidate other, unsolved herbal induced health promoting effects.

Conclusions

Both investigated plant compounds are commonly known health promoters, both are applied orally and hence, both are absorbed through the small intestine epithelium. But how does their positive potential evolve?

Approaching this question by employment of cell culture *in vitro* models bearing targeted physiological manipulations by RNA interference, it must be notated that the inhered handiness and velocity of data generation is tremendous. This technique, acting on transcript level and further leaving a residual expression can enclose screening opportunities where the classical gene knockout evokes a lethal phenotype. Nevertheless it must be mentioned that investigations on protein level still retain an indispensable validity. Findings traced back to eventually remaining enzyme activity or problems when dealing with genes flickering in mRNA expression, are *a priori* disenchanted when the actual mediators of cellular functionality are assessed. However, the applied cell culture model managed to provide relevant insights about the involvement of the considered secondary plant metabolites in the intestinal physiology.

For cineole the question of an initial metabolization was clarified in so far, as the employed analytic could not assign any potential cineole derivates immediately emerging in this intestinal *in vitro* epithelium within the detection sensitivity. Thus, from this study it seems evident, that cineole itself must be the effector of orally applied administration, as it remains stable under these conditions. A very noteworthy finding for the volatile eucalyptus compound thereby is the absolute inert immune response of the intestinal *in vitro* model when exposed to a cineole dosage close to the here determined cell detaching concentration. In contrary stands the direct *in vivo* efficacy of a straight application of cineole preparations on airway mucosal layers. If the plant compound does not affect locally what is mediated beyond the lining of the gastrointestinal tract in the context of respiratory diseases? Accordingly the proximate scope should maybe focus liver inhered tissues in order to trace the metabolization and/or effector pathway of this medicinal agent to inner organs, for an approval wherefrom the body fluid metabolite levels after cineole ingestion found by other scientists derive.

The substantial occurrence of epigallocatechin gallate in green tea with around 1 g/L can be confirmed by measurements made during this work. However dealing with physiological

issues this compound leaves an ambiguous picture. Stimulation of early immune mediators, and in particular IL6, can be demonstrated within that study, although the applied loss-of-function model could on transcript level not distinguish a definite mode of action across the considered Nfκb or MAPK pathways. Further the predicted dependency of the shown effects from the postulated EGCG-Receptor named 67LR could not be approved by its systematic knockdown. In a greater context, considering together with its immunomodulatory impact additionally the assigned suppressive properties of EGCG referring to epigenetic methylation, its epidemiological proven healthy potential is not immediately obvious as to these alterations not obligatory a positive impact is linked. On the other hand, the finding of EGCG playing a role as a co-repressor of also metastasis linked factor 67LR in synergy with small RNA regulatory pathways, seems to bear a great potential due to its highly significant detectability even under a weak dosage. Clarifying follow up studies attending cancer cell lines would provide great suspense and further establish a basic approach for elucidation of many unsolved mechanisms of how herbal derived pharmacological compounds develop their principle of action, when considered in the small RNA regulatory context.

References

Abreu, M.T., 2010. Toll-like receptor signalling in the intestinal epithelium: how bacterial recognition shapes intestinal function. *Nature Reviews Immunology*, 10(2), pp.131–144.

Ahn, S.-C. et al., 2004. Epigallocatechin-3-gallate, constituent of green tea, suppresses the LPS-induced phenotypic and functional maturation of murine dendritic cells through inhibition of mitogen-activated protein kinases and NF-kappaB. *Biochemical and Biophysical Research Communications*, 313(1), pp.148–155.

Akira, S., 2009. Pathogen recognition by innate immunity and its signaling. *Proceedings of the Japan Academy Series B, Physical and biological sciences*, 85(4), pp.143–156.

Akira, S. & Takeda, K., 2004. Toll-like receptor signalling. *Nature Reviews Immunology*, 4(7), pp.499–511.

Akira, S., Uematsu, S. & Takeuchi, O., 2006. Pathogen recognition and innate immunity. *Cell*, 124(4), pp.783–801.

Alic, M., 1999. Green Tea for Remission Maintenance in Crohn's Disease? *The American journal of gastroenterology*, 94(6), pp.1710–1711.

Almstätter, I., 2010. Effects of the pharmacological agent and volatile aroma compound 1,8-cineole on porcine intestinal epithelium. *Master Thesis; Technische Universität München, Chair of Physiology - Weihenstephan (Prof. H.H.D. Meyer); Fraunhofer-Institut für Verfahrenstechnik und Verpackung - IVV, Sensory Analytics (Prof. A. K. Büttner)*.

Almstätter, I. et al., Determination of cell morphology under 1,8-cineole treatment in porcine intestinal cells. *13th Weurman Flavour Research Symposium (Book Chapter)*, (submitted 21.11.2011), pp.1–4.

Ameres, S.L., Martinez, J. & Schroeder, R., 2007. Molecular basis for target RNA recognition and cleavage by human RISC. *Cell*, 130(1), pp.101–112.

Angel, P. & Karin, M., 1991. The role of Jun, Fos and the AP-1 complex in cell-proliferation and transformation. *Biochimica et biophysica acta*, 1072(2-3), pp.129–157.

Asbaghian, S. et al., 2011. Comparison of volatile constituents, and antioxidant and antibacterial activities of the essential oils of Thymus caucasicus, T. kotschyanus and T. vulgaris. *Nat Prod Commun*, 6(1), pp.137–140.

Babu, P.V.A. & Liu, D., 2008. Green tea catechins and cardiovascular health: an update. *Current medicinal chemistry*, 15(18), pp.1840–1850.

Baldwin, I.T., 2003. Finally, Proof of Weapons of Mass Destruction. *Science's STKE*, 2003(203), pp.42pe–42.

Balentine, D.A., Wiseman, S.A. & Bouwens, L.C.M., 1997. The chemistry of tea flavonoids. *Critical Reviews in Food Science and Nutrition*, 37(8), pp.693–704.

Begnami, M.D. et al., 2010. Evaluation of cell cycle protein expression in gastric cancer: cyclin B1 expression and its prognostic implication. *Human Pathology*, 41(8), pp.1120–1127.

Beltz, L.A. et al., 2006. Mechanisms of cancer prevention by green and black tea polyphenols. *Anticancer Agents Med Chem*, 6(5), pp.389–406.

Bemelmans, J. & Land, D., 1979. *Review of isolation and concentration techniques* D. Land & H. Nursten, eds., London: Progress in flavour research.

Ben Farhat, M. et al., 2009. Variations in Essential Oil, Phenolic Compounds, and Antioxidant Activity of Tunisian Cultivated Salvia officinalis L. *Journal of agricultural and food chemistry*, 57(21), pp.10349–10356.

Berger, S.L. et al., 2009. An operational definition of epigenetics. *Genes & Development*, 23(7), pp.781–783.

Bett, A.J. et al., 1994. An efficient and flexible system for construction of adenovirus vectors with insertions or deletions in early regions 1 and 3. *Proceedings of the National Academy of Sciences of the United States of America*, 91(19), pp.8802–8806.

Blaszczyk, J. et al., 2001. Crystallographic and modeling studies of RNase III suggest a mechanism for double-stranded RNA cleavage. *Structure (London, England : 1993)*, 9(12), pp.1225–1236.

Boyle, R., McLean, S. & Davies, N.W., 2000. Biotransformation of 1,8-cineole in the brushtail possum (Trichosurus vulpecula). *Xenobiotica; the fate of foreign compounds in biological systems*, 30(9), pp.915–932.

Buchon, N. & Vaury, C., 2005. RNAi: a defensive RNA-silencing against viruses and transposable elements. *Heredity*, 96(2), pp.195–202.

Bull, S. et al., 1993. 7-Hydroxy-1,8-cineole and 7-Cineolic Acid. Two New Possum Urinary Metabolites. *Australian Journal of Chemistry*, 46(4), p.441.

Bumcrot, D. et al., 2006. RNAi therapeutics: a potential new class of pharmaceutical drugs. *Nature Chemical Biology*, 2(12), pp.711–719.

Carman, R. & Klika, K., 1992. Partially Racemic Compounds as Brushtail Possum Urinary Metabolites. *Australian Journal of Chemistry*, 45(4), p.651.

Castedo, M. et al., 2002. Cyclin-dependent kinase-1: linking apoptosis to cell cycle and mitotic catastrophe. *Cell death and differentiation*, 9(12), pp.1287–1293.

Castronovo, V., 1993. Laminin Receptors and Laminin-Binding Proteins During Tumor Invasion and Metastasis. *Invasion & Metastasis*, 13(1), pp.1–30.

Castronovo, V., Taraboletti, G. & Sobel, M.E., 1991. Functional domains of the 67-kDa laminin receptor precursor. *The Journal of biological chemistry*, 266(30), pp.20440–20446.

Cerutti, H. & Casas-Mollano, J.A., 2006. On the origin and functions of RNA-mediated silencing: from protists to man. *Current genetics*, 50(2), pp.81–99.

Chalk, A.M. & Sonnhammer, E.L.L., 2008. siRNA specificity searching incorporating mismatch tolerance data. *Bioinformatics*, 24(10), pp.1316–1317.

Chan, C. et al., 2009. A structural interpretation of the effect of GC-content on efficiency of RNA interference. *BMC Bioinformatics*, 10(Suppl 1), p.S33.

Chao, L.K. et al., 2005. Study on the Antiinflammatory Activity of Essential Oil from Leaves of Cinnamomum osmophloeum. *Journal of agricultural and food chemistry*, 53(18), pp. 7274–7278.

Chen, F.X. et al., 2009. Down-regulation of 67LR reduces the migratory activity of human glioma cells in vitro. *Brain Research Bulletin*, 79(6), pp.402–408.

Chen, M.-Y. et al., 2011. Decitabine and suberoylanilide hydroxamic acid (SAHA) inhibit growth of ovarian cancer cell lines and xenografts while inducing expression of imprinted tumor suppressor genes, apoptosis, G2/M arrest, and autophagy. *Cancer*, 117(19), pp.4424–4438.

Chen, T. & Li, E., 2006. Establishment and maintenance of DNA methylation patterns in mammals. *Curr Top Microbiol Immunol*, 301, pp.179–201.

Cheng, T., 2006. All teas are not created equal - The Chinese green tea and cardiovascular health. *International Journal of Cardiology*, 108(3), pp.301–308.

Chiang, L.-C. et al., 2005. Antiviral activities of extracts and selected pure constituents of Ocimum basilicum. *Clinical and experimental pharmacology & physiology*, 32(10), pp. 811–816.

Christman, J.K., Schneiderman, N. & Acs, G., 1985. Formation of highly stable complexes between 5-azacytosine-substituted DNA and specific non-histone nuclear proteins. Implications for 5-azacytidine-mediated effects on DNA methylation and gene expression. *The Journal of biological chemistry*, 260(7), pp.4059–4068.

Chung, J.Y. et al., 1999. Inhibition of activator protein 1 activity and cell growth by purified green tea and black tea polyphenols in H-ras-transformed cells: structure-activity relationship and mechanisms involved. *Cancer research*, 59(18), pp.4610–4617.

Conrad, C. & Rauhut, R., 2002. Ribonuclease III: new sense from nuisance. *The international journal of biochemistry & cell biology*, 34(2), pp.116–129.

Davison, A.J., Benko, M. & Harrach, B., 2003. Genetic content and evolution of adenoviruses. *The Journal of general virology*, 84(Pt 11), pp.2895–2908.

Deka, A. & Vita, J.A., 2011. Tea and cardiovascular disease. *Pharmacological Research*, 64(2), pp.136–145.

DePaola, N. et al., 2001. Electrical impedance of cultured endothelium under fluid flow. *Annals of biomedical engineering*, 29(8), pp.648–656.

Dhiman, R.K., 2011. The Green Tea Polyphenol, Epigallocatechin-3-Gallate (EGCG)—One Step Forward in Antiviral Therapy Against Hepatitis C Virus. *Journal of Clinical & Experimental Hepatology*, 1(3), pp.159–160.

Dolcet, X. et al., 2005. NF-kB in development and progression of human cancer. *Virchows Archiv*, 446(5), pp.475–482.

Donaldson, M.S., 2004. Nutrition and cancer: a review of the evidence for an anti-cancer diet. *Nutrition journal*, 3, p.19.

Duisken, M. et al., 2005. Metabolism of 1,8-cineole by human cytochrome P450 enzymes: identification of a new hydroxylated metabolite. *Biochimica et Biophysica Acta (BBA) - General Subjects*, 1722(3), pp.304–311.

Earnshaw, W.C., Martins, L.M. & Kaufmann, S.H., 1999. Mammalian caspases: structure, activation, substrates, and functions during apoptosis. *Annual Review of Biochemistry*, 68, pp.383–424.

Eferl, R. & Wagner, E.F., 2003. AP-1: a double-edged sword in tumorigenesis. *Nature Reviews Cancer*, 3(11), pp.859–868.

Elbashir, S.M., Harborth, J., et al., 2001a. Duplexes of 21-nucleotide RNAs mediate RNA interference in cultured mammalian cells. *Nature*, 411(6836), pp.494–498.

Elbashir, S.M., Lendeckel, W. & Tuschl, T., 2001b. RNA interference is mediated by 21- and 22-nucleotide RNAs. *Genes & Development*, 15(2), pp.188–200.

Engel, W., Bahr, W. & Schieberle, P., 1999. Solvent assisted flavour evaporation - a new and versatile technique for the careful and direct isolation of aroma compounds from complex food matrices. *European Food Research and Technology*, 209(3-4), pp.237–241.

Esteller, M., 2007. Epigenetic gene silencing in cancer: the DNA hypermethylome. *Human Molecular Genetics*, 16(R1), pp.R50–R59.

Fagarasan, S. & Honjo, T., 2003. Intestinal IgA synthesis: regulation of front-line body defences. *Nature Reviews Immunology*, 3(1), pp.63–72.

Fang, M.Z. et al., 2003. Tea polyphenol (-)-epigallocatechin-3-gallate inhibits DNA methyltransferase and reactivates methylation-silenced genes in cancer cell lines. *Cancer research*, 63(22), pp.7563–7570.

Filippov, V. et al., 2000. A novel type of RNase III family proteins in eukaryotes. *Gene*, 245(1), pp.213–221.

Fire, A. et al., 1998. Potent and specific genetic interference by double-stranded RNA in Caenorhabditis elegans. *Nature*, 391(6669), pp.806–811.

Flotho, C. et al., 2009. The DNA methyltransferase inhibitors azacitidine, decitabine and zebularine exert differential effects on cancer gene expression in acute myeloid leukemia cells. *Leukemia : official journal of the Leukemia Society of America, Leukemia Research Fund, U.K*, 23(6), pp.1019–1028.

Foray, L. et al., 1999. In vitro Cytotoxic Activity of Three Essential Oils from Salvia Species. *Journal of Essential Oil Research*.

Fu, M., 2004. Minireview: Cyclin D1: Normal and Abnormal Functions. *Endocrinology*, 145(12), pp.5439–5447.

Fujihara, M. et al., 2003. Molecular mechanisms of macrophage activation and deactivation by lipopolysaccharide: roles of the receptor complex. *Pharmacology & therapeutics*, 100(2), pp.171–194.

Fürst, R.W. et al., 2012. Is DNA methylation an epigenetic contribution to transcriptional regulation of the bovine endometrium during the estrous cycle and early pregnancy? *Molecular and Cellular Endocrinology*, 348(1), pp.67–77.

Galley, H.F. & Webster, N.R., 1996. The immuno-inflammatory cascade. *British journal of anaesthesia*, 77(1), pp.11–16.

Giaever, I. & Keese, C.R., 1984. Monitoring fibroblast behavior in tissue culture with an applied electric field. *Proceedings of the National Academy of Sciences of the United States of America*, 81(12), pp.3761–3764.

Government, U.S., 2011. *Usda Database for the Flavonoid Content of Selected Foods*, Books LLC.

Graham, F.L. et al., 1977. Characteristics of a human cell line transformed by DNA from human adenovirus type 5. *The Journal of general virology*, 36(1), pp.59–74.

Graham, H.N., 1992. Green tea composition, consumption, and polyphenol chemistry. *Preventive medicine*, 21(3), pp.334–350.

Greenwalt, C., Steinkraus, K. & Ledford, R., 2000. Kombucha, the fermented tea: Microbiology, composition, and claimed health effects. *Journal of Food Protection*, 63(7), pp.976–981.

Groschwitz, K.R. & Hogan, S.P., 2009. Intestinal barrier function: Molecular regulation and disease pathogenesis. *Journal of Allergy and Clinical Immunology*, 124(1), pp.3–20.

Grosshans, H. & Filipowicz, W., 2008. Molecular biology: the expanding world of small RNAs. *Nature*, 451(7177), pp.414–416.

Gruner, N., 2011. Untersuchung einer potentiellen Verstoffwechslung von 1,8-Cineol in der porcinen intestinalen Zelllinie IPEC-J2. *Diploma Thesis: Department of Chemistry and Pharmacy Friedrich-Alexander-Universität Erlangen-Nürnberg; Fraunhofer-Institut für Verfahrenstechnik und Verpackung IVV, Sensory Analytics (Prof. A.K. Büttner); Technische Universität München, Chair of Physiology - Weihenstephan (Prof. H.H.D. Meyer)*.

Hagmeyer, B.M. et al., 1993. Adenovirus E1A negatively and positively modulates transcription of AP-1 dependent genes by dimer-specific regulation of the DNA binding and transactivation activities of Jun. *The EMBO Journal*, 12(9), pp.3559–3572.

Hamaishi, K., Kojima, R. & Ito, M., 2006. Anti-ulcer effect of tea catechin in rats. *Biological & pharmaceutical bulletin*, 29(11), pp.2206–2213.

Hammond, S.M. et al., 2001. Argonaute2, a link between genetic and biochemical analyses of RNAi. *Science (New York, NY)*, 293(5532), pp.1146–1150.

Han, J. et al., 2006. Molecular basis for the recognition of primary microRNAs by the Drosha-DGCR8 complex. *Cell*, 125(5), pp.887–901.

Hannon, G.J., 2002. RNA interference. *Nature*, 418(6894), pp.244–251.

Harbowy, M.E. & Balentine, D.A., 1997. Tea Chemistry. *Critical Reviews in Plant Sciences*, 16(5), pp.415–480.

Hauber, I. et al., 2009. The main green tea polyphenol epigallocatechin-3-gallate counteracts semen-mediated enhancement of HIV infection. *Proceedings of the National Academy of Sciences of the United States of America*, 106(22), pp.9033–9038.

Hong, S., 2010. Connection between inflammation and carcinogenesis in gastrointestinal tract: Focus on TGF-β signaling. *World Journal of Gastroenterology*, 16(17), p.2080.

Horst, K. & Rychlik, M., 2010. Quantification of 1,8-cineole and of its metabolites in humans using stable isotope dilution assays. *Molecular Nutrition & Food Research*, 54(10), pp. 1515–1529.

Hutvágner, G. & Zamore, P.D., 2002. A microRNA in a multiple-turnover RNAi enzyme complex. *Science (New York, NY)*, 297(5589), pp.2056–2060.

Isaacs, C.E. et al., 2011. Digallate Dimers of (-)- Epigallocatechin Gallate Inactivate Herpes Simplex Virus. *Antimicrobial Agents and Chemotherapy*, 55(12), pp.5646–5653.

Iwamoto, Y. et al., 1987. YIGSR, a synthetic laminin pentapeptide, inhibits experimental metastasis formation. *Science (New York, NY)*, 238(4830), p.1132.

Iwasaki, A. & Medzhitov, R., 2004. Toll-like receptor control of the adaptive immune responses. *Nature Immunology*, 5(10), pp.987–995.

Jackson, A.L. et al., 2003. Expression profiling reveals off-target gene regulation by RNAi. *Nature Biotechnology*, 21(6), pp.635–637.

Jackson, A.L. et al., 2006. Widespread siRNA off-target transcript silencing mediated by seed region sequence complementarity. *RNA (New York, NY)*, 12(7), pp.1179–1187.

Jolliffe, I.T., 2002. Principal Component Analysis. In *Springer Series in Statistics*. Springer New York, pp. 1–9.

Joshua-Tor, L., 2004. siRNAs at RISC. *Structure (London, England : 1993)*, 12(7), pp.1120–1122.

Juergens, U.R. et al., 2003. Anti-inflammatory activity of 1.8-cineol (eucalyptol) in bronchial asthma: a double-blind placebo-controlled trial. *Respiratory medicine*, 97(3), pp.250–256.

Juergens, U.R. et al., 2004. Inhibitory activity of 1,8-cineol (eucalyptol) on cytokine production in cultured human lymphocytes and monocytes. *Pulmonary pharmacology & therapeutics*, 17(5), pp.281–287.

Jumblatt, M.M. & Neufeld, A.H., 1986. A tissue culture assay of corneal epithelial wound closure. *Invest Ophthalmol Vis Sci*, 27(1), pp.8–13.

Kaeffer, B. et al., 1993. Epithelioid and fibroblastic cell lines derived from the ileum of an adult histocompatible miniature boar (d/d haplotype) and immortalized by SV40 plasmid. *Eur J Cell Biol*, 62(1), pp.152–162.

Kapadia, R., Yi, J.-H. & Vemuganti, R., 2008. Mechanisms of anti-inflammatory and neuroprotective actions of PPAR-gamma agonists. *Frontiers in bioscience : a journal and virtual library*, 13, pp.1813–1826.

Karimi, M., Johansson, S. & Ekström, T.J., 2006. Using LUMA: a Luminometric-based assay for global DNA-methylation. *Epigenetics : official journal of the DNA Methylation Society*, 1(1), pp.45–48.

Karin, M., 1995. The regulation of AP-1 activity by mitogen-activated protein kinases. *The Journal of biological chemistry*, 270(28), pp.16483–16486.

Karin, M., Yamamoto, Y. & Wang, Q.M., 2004. The IKK NF-kappa B system: a treasure trove for drug development. *NATURE REVIEWS - Drug Discovery*, 3(1), pp.17–26.

Kazi, A. et al., 2002. Potential molecular targets of tea polyphenols in human tumor cells: significance in cancer prevention. *In Vivo*, 16(6), pp.397–403.

Keese, C.R. et al., 2002. Real-time impedance assay to follow the invasive activities of metastatic cells in culture. *BioTechniques*, 33(4), pp.842–4, 846, 848–50.

Khvorova, A., Reynolds, A. & Jayasena, S.D., 2003. Functional siRNAs and miRNAs exhibit strand bias. *Cell*, 115(2), pp.209–216.

Kielhorn, S. & Thorngate, J., III, 1999. Oral sensations associated with the flavan-3-ols (+)-catechin and (-)-epicatechin1. *Food quality and preference*, 10(2), pp.109–116.

Kirsch, F. et al., 2010. Transfer of a pharmacological aroma preparation into human milk - monitoring of substance profiles depending on physiological transition processes T. Hofmann, W. Meyerhof, & P. Schieberle, eds. *Advances and challenges in flavor chemistry & biology - Eigenverlag Deutsche Forschungsanstalt für Lebensmittelchemie*, p.257.

Kováts, E., 2004. Gas-chromatographische Charakterisierung organischer Verbindungen. Teil 1: Retentionsindices aliphatischer Halogenide, Alkohole, Aldehyde und Ketone. *Helvetica Chimica Acta*, (7), pp.1–18.

Krinke, L. & Wulff, D.L., 1990. The cleavage specificity of RNase III. *Nucleic Acids Research*, 18(16), pp.4809–4815.

Landthaler, M., Yalcin, A. & Tuschl, T., 2004. The human DiGeorge syndrome critical region gene 8 and Its D. melanogaster homolog are required for miRNA biogenesis. *Current biology : CB*, 14(23), pp.2162–2167.

Lee, K.W., Lee, H.J. & Lee, C.Y., 2002a. Antioxidant activity of black tea vs. green tea. *The Journal of nutrition*, 132(4), pp.785; author reply 786.

Lee, W.A. et al., 1996. Overexpression of the 67 kD laminin receptor correlates with the progression of gastric carcinoma. *Pathology, research and practice*, 192(12), pp.1195–1201.

Lee, Y. et al., 2004a. MicroRNA genes are transcribed by RNA polymerase II. *The EMBO Journal*, 23(20), pp.4051–4060.

Lee, Y. et al., 2002b. MicroRNA maturation: stepwise processing and subcellular localization. *The EMBO Journal*, 21(17), pp.4663–4670.

Lee, Y. et al., 2003. The nuclear RNase III Drosha initiates microRNA processing. *Nature*, 425(6956), pp.415–419.

Lee, Y.S. et al., 2004b. Distinct roles for Drosophila Dicer-1 and Dicer-2 in the siRNA/miRNA silencing pathways. *Cell*, 117(1), pp.69–81.

Ley, K. et al., 2007. Getting to the site of inflammation: the leukocyte adhesion cascade updated. *Nature Reviews Immunology*, 7(9), pp.678–689.

Li, S., Hattori, T. & Kodama, E.N., 2011. Epigallocatechin gallate inhibits the HIV reverse transcription step. *Antiviral chemistry & chemotherapy*, 21(6), pp.239–243.

Lim, L.P. et al., 2005. Microarray analysis shows that some microRNAs downregulate large numbers of target mRNAs. *Nature*, 433(7027), pp.769–773.

Lin, J.-K., 2002. Cancer chemoprevention by tea polyphenols through modulating signal transduction pathways. *Archives of pharmacal research*, 25(5), pp.561–571.

Lin, J.K., Liang, Y.C. & Lin-Shiau, S.Y., 1999. Cancer chemoprevention by tea polyphenols through mitotic signal transduction blockade. *Biochemical pharmacology*, 58(6), pp. 911–915.

Lin, Y.-S. et al., 2003. Factors affecting the levels of tea polyphenols and caffeine in tea leaves. *Journal of agricultural and food chemistry*, 51(7), pp.1864–1873.

Lingel, A. et al., 2004. Nucleic acid 3'-end recognition by the Argonaute2 PAZ domain. *Nature structural & molecular biology*, 11(6), pp.576–577.

Lingel, A. et al., 2003. Structure and nucleic-acid binding of the Drosophila Argonaute 2 PAZ domain. *Nature*, 426(6965), pp.465–469.

Liotta, L.A., 1986. Tumor invasion and metastases--role of the extracellular matrix: Rhoads Memorial Award lecture. *Cancer research*, 46(1), pp.1–7.

Liu, L. et al., 2010. Hypoxia promotes metastasis in human gastric cancer by up-regulating the 67-kDa laminin receptor. *Cancer science*, 101(7), pp.1653–1660.

Liu, Q. et al., 2003. R2D2, a bridge between the initiation and effector steps of the Drosophila RNAi pathway. *Science (New York, NY)*, 301(5641), pp.1921–1925.

Livak, K.J. & Schmittgen, T.D., 2001. Analysis of Relative Gene Expression Data Using Real-Time Quantitative PCR and the 2−ΔΔCT Method. *Methods*, 25(4), pp.402–408.

Lo, C.M., Keese, C.R. & Giaever, I., 1993. Monitoring motion of confluent cells in tissue culture. *Experimental cell research*, 204(1), pp.102–109.

Logan, J. & Edwards, K., 2009. *Real-time PCR: current technology and applications*,

Loizzo, M.R. et al., 2007. Cytotoxic activity of essential oils from labiatae and lauraceae families against in vitro human tumor models. *Anticancer research*, 27(5A), pp.3293–3299.

Lundien, M.C. et al., 2002. Induction of MCP-1 expression in airway epithelial cells: role of CCR2 receptor in airway epithelial injury. *Journal of clinical immunology*, 22(3), pp.144–152.

Maclachlan, I., 2008. siRNAs with guts. *Nature Biotechnology*, 26(4), pp.403–405.

Marraffini, L.A. & Sontheimer, E.J., 2010. CRISPR interference: RNA-directed adaptive immunity in bacteria and archaea. *Nature Reviews Genetics*, 11(3), pp.181–190.

Meier, J., 2011. Effects of RNAi induced 67LR- and DNMT-knockdowns in combination with demethylating agents on IPEC-J2 cells. *Master Thesis: Technische Universität München, Chair of Physiology - Weihenstephan (Prof. H.H.D. Meyer)*.

Miyazawa, M., Shindo, M. & Shimada, T., 2001. Oxidation of 1,8-cineole, the monoterpene cyclic ether originated from eucalyptus polybractea, by cytochrome P450 3A enzymes

in rat and human liver microsomes. *Drug metabolism and disposition: the biological fate of chemicals*, 29(2), pp.200–205.

Montuori, N. & Sobel, M.E., 1996. The 67-kDa laminin receptor and tumor progression. *Curr Top Microbiol Immunol*, 213 (Pt 1), pp.205–214.

Moon, H.-S. et al., 2007. Proposed mechanisms of (-)-epigallocatechin-3-gallate for anti-obesity. *Chemico-biological interactions*, 167(2), pp.85–98.

Mortusewicz, O. et al., 2005. Recruitment of DNA methyltransferase I to DNA repair sites. *Proceedings of the National Academy of Sciences of the United States of America*, 102(25), pp.8905–8909.

Mota, K.S.L. et al., 2009. Flavonoids with Gastroprotective Activity. *Molecules*, 14(3), pp.979–1012.

Murchison, E.P. & Hannon, G.J., 2004. miRNAs on the move: miRNA biogenesis and the RNAi machinery. *Current Opinion in Cell Biology*, 16(3), pp.223–229.

Müller, J., Synergetic downregulation of 67kDa laminin receptor by the green tea (Camellia sinensis) secondary plant compound epigallocatechin gallate: a new gateway in metastasis prevention? *BMC complementary and alternative medicine*, (submitted 08.03.2012), pp.1–20.

Müller, J. & Pfaffl, M.W., 2012. RNA interference off-target screening using principal component analysis (PCA). *Journal of Data Mining in Genomics & Proteomics*, (submitted 07.03.2012), pp.1–21.

Müller, J. et al., 2012. Inquiry of the metabolisation of 1,8-Cineole in an intestinal cell culture model and acquisition of its immune-modulatory effect via gene expression analysis. *Flavour and Fragrance Journal*, (revised 11.04.2012), pp.1–29.

Müller, J., Thirion, C. & Pfaffl, M.W., 2011. Electric cell-substrate impedance sensing (ECIS) based real-time measurement of titer dependent cytotoxicity induced by adenoviral vectors in an IPI-2I cell culture model. *Biosensors & bioelectronics*, 26(5), pp.2000–2005.

Myers, J.W. et al., 2003. Recombinant Dicer efficiently converts large dsRNAs into siRNAs suitable for gene silencing. *Nature Biotechnology*, 21(3), pp.324–328.

Nandakumar, V., Vaid, M. & Katiyar, S.K., 2011. (-)-Epigallocatechin-3-gallate reactivates silenced tumor suppressor genes, Cip1/p21 and p16INK4a, by reducing DNA methylation and increasing histones acetylation in human skin cancer cells. *Carcinogenesis*, 32(4), pp.537–544.

Nascimento, G.G.F. et al., 2000. Antibacterial activity of plant extracts and phytochemicals on antibiotic-resistant bacteria. *Brazilian Journal of Microbiology*, 31(4), pp.247–256.

Nelson, J. et al., 2008. The 67 kDa laminin receptor: structure, function and role in disease. *Bioscience Reports*, 28(1), p.33.

Nykänen, A., Haley, B. & Zamore, P.D., 2001. ATP requirements and small interfering RNA structure in the RNA interference pathway. *Cell*, 107(3), pp.309–321.

Okano, M., Xie, S. & Li, E., 1998. Cloning and characterization of a family of novel mammalian DNA (cytosine-5) methyltransferases. *Nature Genetics*, 19(3), pp.219–220.

Osborn, O. & Olefsky, J.M., 2012. The cellular and signaling networks linking the immune system and metabolism in disease. *Nature Medicine*, 18(3), pp.363–374.

Owen, R.L., 1999. Uptake and transport of intestinal macromolecules and microorganisms by M cells in Peyer's patches--a personal and historical perspective. *Seminars in immunology*, 11(3), pp.157–163.

Pandey, M., Shukla, S. & Gupta, S., 2010. Promoter demethylation and chromatin remodeling by green tea polyphenols leads to re-expression of GSTP1 in human prostate cancer cells. *International journal of cancer Journal international du cancer*, 126(11), pp.2520–2533.

Pham, J.W. & Sontheimer, E.J., 2005. Molecular requirements for RNA-induced silencing complex assembly in the Drosophila RNA interference pathway. *The Journal of biological chemistry*, 280(47), pp.39278–39283.

Pham, J.W. et al., 2004. A Dicer-2-dependent 80s complex cleaves targeted mRNAs during RNAi in Drosophila. *Cell*, 117(1), pp.83–94.

Pitman, R.S. & Blumberg, R.S., 2000. First line of defense: the role of the intestinal epithelium as an active component of the mucosal immune system. *Journal of gastroenterology*, 35(11), pp.805–814.

Platt, A.M. & Mowat, A.M., 2008. Mucosal macrophages and the regulation of immune responses in the intestine. *Immunology Letters*, 119(1-2), pp.22–31.

Prabuseenivasan, S., Jayakumar, M. & Ignacimuthu, S., 2006. In vitro antibacterial activity of some plant essential oils. *BMC complementary and alternative medicine*, 6, p.39.

Rao, J.N., Wang, J.-Y. & Jaladanki, R.N., 2010. *Regulation of Gastrointestinal Mucosal Growth*, Morgan & Claypool.

Reddy, L. et al., 1998. Assessment of rapid morphological changes associated with elevated cAMP levels in human orbital fibroblasts. *Experimental cell research*, 245(2), pp.360–367.

Sadlon, A.E. & Lamson, D.W., 2010. Immune-modifying and antimicrobial effects of Eucalyptus oil and simple inhalation devices. *Alternative medicine review : a journal of clinical therapeutic*, 15(1), pp.33–47.

Santos, F.A. & Rao, V.S., 2000. Antiinflammatory and antinociceptive effects of 1,8-cineole a terpenoid oxide present in many plant essential oils. *Phytotherapy research : PTR*, 14(4), pp.240–244.

Santos, F.P.S. et al., 2010. Decitabine in the treatment of myelodysplastic syndromes. *Expert review of anticancer therapy*, 10(1), pp.9–22.

Sato, H., Matsui, T. & Arakawa, Y., 2002. The protective effect of catechin on gastric mucosal lesions in rats, and its hormonal mechanisms. *Journal of gastroenterology*, 37(2), pp. 106–111.

Schierack, P. et al., 2006. Characterization of a porcine intestinal epithelial cell line for in vitro studies of microbial pathogenesis in swine. *Histochemistry and cell biology*, 125(3), pp. 293–305.

Schwarz, D.S. et al., 2003. Asymmetry in the assembly of the RNAi enzyme complex. *Cell*, 115(2), pp.199–208.

Sertel, S. et al., 2011. Krebshemmende Wirkung des ätherischen Salbei-Öls auf eine Plattenepithelzellkarzinom-Zelllinie der Mundhöhle (UMSCC1). *HNO*, 59(12), pp.1203–1208.

Shankar, S., Ganapathy, S. & Srivastava, R.K., 2007. Green tea polyphenols: biology and therapeutic implications in cancer. *Frontiers in bioscience : a journal and virtual library*, 12, pp.4881–4899.

Shao, Y. et al., 2007. Effect of target secondary structure on RNAi efficiency. *RNA (New York, NY)*, 13(10), pp.1631–1640.

Shaulian, E. & Karin, M., 2002. AP-1 as a regulator of cell life and death. *Nature cell biology*, 4(5), pp.E131–6.

Song, J.-J. et al., 2003. The crystal structure of the Argonaute2 PAZ domain reveals an RNA binding motif in RNAi effector complexes. *Nature Structural Biology*, 10(12), pp.1026–1032.

Spencer, J.P. et al., 2000. Decomposition of cocoa procyanidins in the gastric milieu. *Biochemical and Biophysical Research Communications*, 272(1), pp.236–241.

Spencer, J.P.E., 2003. Metabolism of tea flavonoids in the gastrointestinal tract. *The Journal of nutrition*, 133(10), pp.3255S–3261S.

Su, P. et al., 2008. Synergistic effect of green tea extract and probiotics on the pathogenic bacteria, Staphylococcus aureus and Streptococcus pyogenes. *World Journal of Microbiology and Biotechnology*, 24(9), pp.1837–1842.

Szyf, M., 2010. DNA methylation and demethylation probed by small molecules. *Biochimica et biophysica acta*, 1799(10-12), pp.750–759.

Tachibana, H. et al., 2004. A receptor for green tea polyphenol EGCG. *Nature structural & molecular biology*, 11(4), pp.380–381.

Takatsu, K., 2011. Interleukin-5 and IL-5 receptor in health and diseases. *Proceedings of the Japan Academy Series B, Physical and biological sciences*, 87(8), pp.463–485.

Takeuchi, O. & Akira, S., 2001. Toll-like receptors; their physiological role and signal transduction system. *International immunopharmacology*, 1(4), pp.625–635.

Tanaka, T. & Kouno, I., 2003. Oxidation of tea catechins: Chemical structures and reaction mechanism. *Food Science and Technology Research*, 9(2), pp.128–133.

Tiruppathi, C. et al., 1992. Electrical method for detection of endothelial cell shape change in real time: assessment of endothelial barrier function. *Proceedings of the National Academy of Sciences of the United States of America*, 89(17), pp.7919–7923.

Tsuchiya, H. et al., 1997. Simultaneous determination of catechins in human saliva by high-performance liquid chromatography. *Journal of chromatography. B, Biomedical sciences and applications*, 703(1-2), pp.253–258.

Tuschl, T., 2001. RNA interference and small interfering RNAs. *Chembiochem : a European journal of chemical biology*, 2(4), pp.239–245.

Underdown, B.J. & Schiff, J.M., 1986. Immunoglobulin A: strategic defense initiative at the mucosal surface. *Annual review of immunology*, 4, pp.389–417.

Valcic, S. et al., 1999. Antioxidant Chemistry of Green Tea Catechins. Identification of Products of the Reaction of (–)-Epigallocatechin Gallate with Peroxyl Radicals. *Chemical Research in Toxicology*, 12(4), pp.382–386.

van Rooij, E. & Olson, E.N., 2007. MicroRNAs: powerful new regulators of heart disease and provocative therapeutic targets. *The Journal of clinical investigation*, 117(9), pp.2369–2376.

Wang, Q., Peng, C. & Gong, J., 2011. Effects of enzymatic action on the formation of theabrownin during solid state fermentation of Pu-erh tea. *Journal of the science of food and agriculture*, 91(13), pp.2412–2418.

Wang, Y. et al., 2007. MicroRNA: past and present. *Frontiers in bioscience : a journal and virtual library*, 12, pp.2316–2329.

Whitehouse, M.W. et al., 1998. Emu oil(s): a source of non-toxic transdermal anti-inflammatory agents in aboriginal medicine. *Inflammopharmacology*, 6(1), pp.1–8.

Wilkins, R., Tucci, M. & Benghuzzi, H., 2011. Role of plant-derived antioxidants on NF-kb expression in LPS-stimulated macrophages - biomed 2011. *Biomedical sciences instrumentation*, 47, pp.222–227.

Wolf, F. et al., 2006. Dose-dependent effects of stable cyclin B1 on progression through mitosis in human cells. *The EMBO Journal*, 25(12), pp.2802–2813.

Worth, H., Schacher, C. & Dethlefsen, U., 2009. Concomitant therapy with Cineole (Eucalyptole) reduces exacerbations in COPD: A placebo-controlled double-blind trial. *Respiratory Research*, 10(1), p.69.

Wu, M. et al., 2009. Green tea drinking, high tea temperature and esophageal cancer in high- and low-risk areas of Jiangsu Province, China: a population-based case-control study. *International journal of cancer Journal international du cancer*, 124(8), pp.1907–1913.

Xavier, R.J. & Podolsky, D.K., 2007. Unravelling the pathogenesis of inflammatory bowel disease. *Nature*, 448(7152), pp.427–434.

Yamaguchi, K. et al., 2002. Inhibitory effects of (-)-epigallocatechin gallate on the life cycle of human immunodeficiency virus type 1 (HIV-1). *Antiviral research*, 53(1), pp.19–34.

Yan, K.S. et al., 2003. Structure and conserved RNA binding of the PAZ domain. *Nature*, 426(6965), pp.468–474.

Yang, C.S. & Wang, H., 2011. Mechanistic issues concerning cancer prevention by tea catechins A. H. Wu, ed. *Molecular Nutrition & Food Research*, 55(6), pp.819–831.

Yang, C.S. et al., 2011. Cancer prevention by tea: Evidence from laboratory studies. *Pharmacological Research*, 64(2), pp.113–122.

Yang, F. et al., 2001. The green tea polyphenol (-)-epigallocatechin-3-gallate blocks nuclear factor-kappa B activation by inhibiting I kappa B kinase activity in the intestinal epithelial cell line IEC-6. *Molecular pharmacology*, 60(3), pp.528–533.

Yuan, J.-M., Sun, C. & Butler, L.M., 2011. Tea and cancer prevention: Epidemiological studies. *Pharmacological Research*, 64(2), pp.123–135.

Zeng, Y. & Cullen, B.R., 2004. Structural requirements for pre-microRNA binding and nuclear export by Exportin 5. *Nucleic Acids Research*, 32(16), pp.4776–4785.

Zhang, K. & Nicholson, A.W., 1997. Regulation of ribonuclease III processing by double-helical sequence antideterminants. *Proceedings of the National Academy of Sciences of the United States of America*, 94(25), pp.13437–13441.

Acknowledgement

First of all I thank my doctoral advisors Prof. Dr. Dr. Heinrich H. D. Meyer and Prof. Dr. Michael W. Pfaffl for all what they have done for me.

Further I thank Prof. Dr. Andrea Büttner for participance as examiner during the defense of my doctor's thesis and for the scientific work we published together as outcome of our cooperation with the Fraunhofer-Institut für Verfahrenstechnik und Verpackung IVV

I also thank Prof. Dr. Dieter R. Treutter for participance as chairman during the defense of my doctor's thesis.

For funding I thank my parents and the Vereinigung zur Milchwissenschaftlichen Forschung an der Technischen Universität München e.V..

For teaching me RNAi-knockdown know-how I thank SIRION-BIOTECH GmbH and especially Dr. Christian Thirion and Dr. Michael Salomon.

For guiding and conducting GC-MS measurements for this work I thank Frauke Kirsch from the Chair of Food Chemistry of the Friedrich-Alexander-Universität Erlangen-Nürnberg.

For conducting the LUMA measurements I thank my colleague Rainer Fürst.

For technical assistance with the ECIS-device I thank Dr. Armin Biser from the IBIDI GmbH.

For help during my doctor's thesis I thank my master students Isabella Almstätter, Nathalie Gruner and Johannes Meier, my student apprentices Sibylle Schmitter and Juliane Hund and all members of the Lehrstuhl für Physiologie in Weihenstephan.

For the analyses of fresh brewed green tea I thank Christine Kaufmann and the Lehrstuhl für Chemisch-Technische Analyse und Chemische Lebensmitteltechnologie in Weihenstephan.

For disposal of the IPEC-J2 cells I thank Dr. Karsten Tedin.

For English proofreading I thank my companion Florian Walter

Mother nature I thank for *Camellia sinensis*

I would also like to thank everyone I forgot to mention here.

Finally I want to thank all my friends, my partner and my family for their being.

Scientific communications

Peer reviewed publications

Electric cell-substrate impedance sensing (ECIS) based real-time measurement of titer dependent cytotoxicity induced by adenoviral vectors in an IPI-2I cell culture model

Jakob Müller, Christian Thirion and Michael W. Pfaffl
Biosensors and Bioelectronics, 26(5), 2000-2005. (2011)

RNA interference off-target screening using principal component analysis

Jakob Müller and Michael W. Pfaffl
Journal of Data Mining in Genomics & Proteomics (published online: June 17, 2012)

Inquiry of the metabolisation of 1,8-Cineole in an intestinal cell culture model and acquisition of its immune-modulatory effect via gene expression analysis

Jakob Müller, Nathalie Gruner, Isabella Almstätter, Frauke Kirsch, Andrea Büttner and Michael W. Pfaffl
Flavour and Fragrance Journal (published online: September 26, 2012)

Synergetic downregulation of 67kDa laminin receptor by the green tea (Camellia sinensis) secondary plant compound epigallocatechin gallate: a new gateway in metastasis prevention?

Jakob Müller and Michael W. Pfaffl
BMC Complementary and Alternative Medicine (revised: July 11, 2012)

Peer reviewed book chapters

Determination of cell morphology under 1,8-cineole treatment in porcine intestinal cells

Isabella Almstätter, Jakob Müller, Michael W. Pfaffl and Andrea Büttner
13th Weurman Flavour Research Symposium, Zaragoza 2011, submitted 21.11.2011

Scientific posters

Titer dependent cytotoxicity of viral vectors measured in real time via ECIS-technology

Müller J., Thirion C. and Michael W. Pfaffl
5th qPCR-Event, Freising-Weihenstephan 2011

Gene-expression analysis of pro-inflammatory genes after 1,8-cineole treatment in porcine intestinal cells

Isabella Almstätter, Jakob Müller, Michael W. Pfaffl and Andrea Büttner
13th Weurman Flavour Research Symposium, Zaragoza 2011

Determination of cell morphology under 1,8-cineole treatment in porcine intestinal cells

Isabella Almstätter, Jakob Müller, Michael W. Pfaffl and Andrea Büttner
13th Weurman Flavour Research Symposium, Zaragoza 2011

Curriculum Vitae

Personal information

Name	Jakob Maximilian Müller
Place of birth	Nürnberg
Date of birth	August, 19th 1979

Education

2008 - 2012

Promotion, Technische Universität München: "Secondary plant metabolites and gut health: functional studies on porcine small intestine *in vitro* models"

2000 - 2007

Studies in biology, Technische Universität München: Major “Biochemistry”, Minor “Human biology”, Minor “Limnology”

1986 - 1999

Primary school & secondary school (Justus-von-Liebig-Gymnasium, Neusäß)

Appendix

Appendix 1

Electric cell-substrate impedance sensing (ECIS) based real-time measurement of titer dependent cytotoxicity induced by adenoviral vectors in an IPI-2I cell culture model

Appendix 2

RNA interference off-target screening using principal component analysis

Appendix 3

Synergetic downregulation of 67kDa laminin receptor by the green tea (Camellia sinensis) secondary plant compound epigallocatechin gallate: a new gateway in metastasis prevention?

Appendix 4

Inquiry of the metabolisation of 1,8-Cineole in an intestinal cell culture model and acquisition of its immune-modulatory effect via gene expression analysis

Appendix 5

Determination of cell morphology under 1,8-cineole treatment in porcine intestinal cells

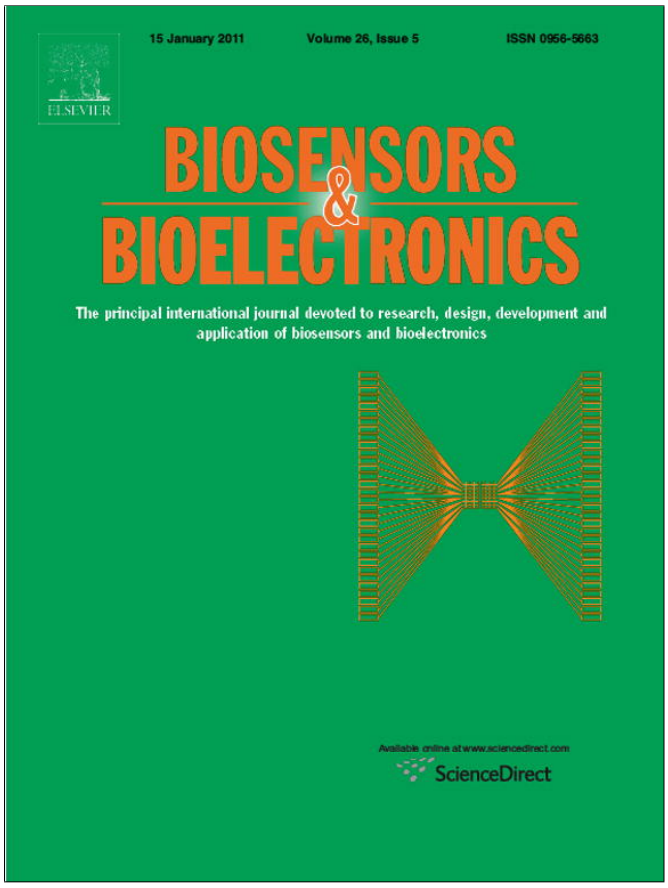

Biosensors and Bioelectronics 26 (2011) 2000–2005

Contents lists available at ScienceDirect

Biosensors and Bioelectronics

journal homepage: www.elsevier.com/locate/bios

Electric cell-substrate impedance sensing (ECIS) based real-time measurement of titer dependent cytotoxicity induced by adenoviral vectors in an IPI-2I cell culture model

Jakob Müller[a,*], Christian Thirion[b], Michael W. Pfaffl[a]

[a] Physiology Unit, Technische Universität München, Research Center for Nutrition and Food Science, Weihenstephaner Berg 3, 85350 Freising – Weihenstephan, Germany
[b] Friedrich-Baur-Institute, Klinikum der LMU, Department of Neurology, Marchioninistrasse 17, 81377 Munich, Germany

ARTICLE INFO

Article history:
Received 8 June 2010
Received in revised form 3 August 2010
Accepted 28 August 2010
Available online 9 September 2010

Keywords:
ECIS
Cytotoxicity
IPI-2I
Adenovirus 5
RNA interference
qPCR virus titration

ABSTRACT

Recombinant viral vectors are widespread tools for transfer of genetic material in various modern biotechnological applications like for example RNA interference (RNAi). However, an accurate and reproducible titer assignment represents the basic step for most downstream applications regarding a precise multiplicity of infection (MOI) adjustment. As necessary scaffold for the studies described in this work we introduce a quantitative real-time PCR (qPCR) based approach for viral particle measurement. Still an implicated problem concerning physiological effects is that the appliance of viral vectors is often attended by toxic effects on the individual target. To determine the critical viral dose leading to cell death we developed an electric cell-substrate impedance sensing (ECIS) based assay. With ECIS technology the impedance change of a current flow through the cell culture medium in an array plate is measured in a non-invasive manner, visualizing effects like cell attachment, cell–cell contacts or proliferation. Here we describe the potential of this online measurement technique in an in vitro model using the porcine ileal epithelial cell line IPI-2I in combination with an adenoviral transfection vector (Ad5-derivate). This approach shows a clear dose-depending toxic effect, as the amount of applied virus highly correlates ($p < 0.001$) with the level of cell death. Thus this assay offers the possibility to discriminate the minimal non-toxic dose of the individual transfection method. In addition this work suggests that the ECIS-device bears the feasibility to transfer this assay to multiple other cytotoxicological questions.

1. Introduction

Electrochemical impedance measurements in cell-based assays represent a method which is not yet widespread but bears a great potential for cell culture studies by providing the technical feature to monitor cell interactions, proliferation or cell death in real-time kinetics. Electrochemical impedance spectroscopy was first utilized for cell culture studies by Giaever and Keese (1984) who developed the ECIS-device. Thereby array like cell culture dishes covered with microelectrodes serve as adhesion substrate. By detecting the impedance change over time and/or altering the frequency of the current in the measurement, effects on cellular level can be monitored. The application can provide information about cell growth (Mitra et al., 1991), cell motility (Lo et al., 1993), cell barrier function (Tiruppathi et al., 1992) and in vitro toxicology (Ceriotti et al., 2007). It is also utilized in cancer research (Lovelady et al., 2007).

Our approach was to use this technique to determine the toxicity occurring as transfection side effect while using viral vectors for gene knockdown experiments. RNAi is a conserved cellular mechanism for post-transcriptional gene silencing induced by small RNA fragments. It was first described by Fire and Mello (Fire et al., 1998). RNAi is used in biotechnology to mediate gene knockdown in loss-of-function studies by small interfering RNAs (siRNA) (Tuschl, 2001). It can be elicited either by transfection of eukaryotic cells with siRNAs or by stimulating cells to express siRNAs by manipulating its genome via viral vectors. During our studies using adenoviral mediated RNAi (data not shown) in ECIS measurements on the ileal epithelial cell line IPI-2I (Schierack et al., 2006) we observed strong toxic effects by the viral infection itself leading to cell death. In consequence for normalization of the knockdown experiments there was the necessity for an assay, which determinates the toxicity level corresponding to a certain amount of viral vector.

The definite task was to assign the minimal multiplicity of infection (MOI), which causes no measurable difference in cell behavior. Therefore the blank RNAi-vector Ad5-U6Stop (without gene silencing function) served as effective substance in the described assay in order to monitor effects exclusively caused by the viral infection and not resulting from a gene knockdown. The Ad5-based vector bears gene deletions in the E1 and E3 regions (Russell, 2000) which are responsible for early viral gene expression. The result-

* Corresponding author. Tel.: +49 8161 71 3867; fax: +49 8161 71 4204.
E-mail address: jakob.mueller@wzw.tum.de (J. Müller).

0956-5663/$ – see front matter © 2010 Elsevier B.V. All rights reserved.
doi:10.1016/j.bios.2010.08.075

ing replication deficiency is complemented by the packaging cell line HEK293 (Graham et al., 1977) but not by IPI-2I. Due to this fact and regarding that our aim was to study a dose-depending effect we had a critical need for an accurate viral titer determination so that a precise MOI adjustment could be ensured. Besides classical methods for titer determination like plaque-assays or assays based on optical measurements (Graham and van der Eb, 1973; Philipson, 1961) and diverse other approaches (Crettaz et al., 2008; Palmer and Ng, 2004) we considered that regarding the time efficiency a qPCR-based titer measurement meets our requirements best. Among existing qPCR-based methods (Wang et al., 2008) no international established standard was available, thus we decided to develop an adenoviral titer measurement protocol based on the work of Ma et al. (2001).

The knowhow for the adenovirus production was gained in cooperation with Christian Thirion's workgroup. The basic knowledge for quantitative PCR measurements was contributed by Michael W. Pfaffl. The employment of these techniques in combination with the ECIS-based cytotoxicity assay for viral vectors was conceived and performed by Jakob Müller.

2. Experimental

2.1. Cells

For the cytotoxicity assay the ileal porcine cell line IPI-2I (Health Protection Agency Culture Collections, Salisbury, UK) was used. These cells were cultured in Dulbecco's modified Eagle medium (DMEM) (PAA, Pasching, Austria) supplemented with 10% FBS (PAA), 2 mM L-glutamine (PAA), insulin 0.024 U/ml (Sigma–Aldrich, St. Louis, USA), 100 U/ml penicillin/streptomycin (PAA) at 37 °C, 100% humidity and 5% CO_2. Cells were subcultured all 72 h at 80% confluence. Only IPI-2I passaged less than ten times were used. For virus production/amplification HEK293 cells (Cell Lines Service, Eppelheim, Germany) were used. HEK293 cells were maintained in the same manner but no insulin was added to the media.

2.2. Viral vector

The Ad5-U6stop virus was supplied by SIRION-BIOTECH (SIRION-BIOTECH, Martinsried, Germany). Its genome is based on a modified pAd/PL-DEST vector (Invitrogen, Karslruhe, Germany). The recombination region of pAD/PL-DEST contains the following insert: 5′-ACAAGTTTGTACAAAAAAGCAGGCTttaaaggaaccaattcagtcgactggatccGAATTCCAGCTAAAAAAGGCCAAAAACGGTgtttcgtccttccacaagatatataaagccaagaaatcgaaatactttcaagttacggtaagcatatgatagtccatttttaaaacataatttttaaaactgcaaactacccaagaaattattactttctacgtcacgtattttgtactaatatctttgtgtttacagtcaaattaattctaattatctttctaacagccttgtatcgtatatgcaaatatgaaggaatcatgggaaataggccctcttcctgcccgaccttggcgcgcgctcggcgcgcggtcacgctccgtcacgtggtgcgttttgcctgcgcgtcttgccactgggggtaccccgaatcactagatctaACCCAGCTTTCTTGTACAAAGTGGT-3′. The segments in capital letters at the flanks are the recombination sites (attB 1 and attB 2). The region in between contains an U6-promotor sequence. Upstream of this promoter resides a short cloning cassette, bearing a stop signal for RNA polymerase III (underlined capital letters) instead of a siRNA-hairpin sequence as the usual functional sequence in RNAi-knockdown vectors. Virus purification was carried out with the ViraBind™ Adenovirus Miniprep Kit (Cell Biolaps Inc., San Diego, USA). Virus amplification was performed in HEK293 cells as described in the kit manual. The virus stocks (here also called virus preparations) are stored at −80 °C in the kit elution buffer supplemented by 10% glycerol. The virus preparations are also used in this solution for the dilutions in the cytotoxicity assays or for the evaluation series of the qPCR-titration protocol.

2.3. qPCR-based viral particle titration

This protocol combines two steps. In the first step the genomes from a virus preparation are extracted selectively (Section 2.3.1) and in the following these genomes are quantified absolutely by qPCR (Section 2.3.2). The basic assumption is that one viral genome respectively one viral particle (VP) equates to one infectious Unit (IFU) (Thomas et al., 2006). The italic letters in brackets in Sections 2.3.1 and 2.3.2 refer to the equation in Section 2.3.2.

2.3.1. Selective Ad5-DNA extraction

10 μl samples (*a*) from virus preparations were digested 30 min at 37 °C with 1 μl DNase I (2000 U/ml, NEB, Ipswich, USA) according to the manufacturer's reaction conditions in a reaction volume of 4.6 μl. In the following step DNase I was inactivated by cofactor binding with 5.4 μl of 20 mM EGTA solution, pH = 8.0 (Sigma–Aldrich) over 10 min at 37 °C. In addition samples were further inactivated by incubating the reaction solution two times at 75 °C for 10 min every time followed by a 2 min incubation on ice. In a next step in order to release the viral DNA the capsid proteins are degraded by digestion with 6 μl Proteinase K (20 mg/ml, NEB) at 56 °C for 10 min again followed by 2 min incubation on ice. Subsequent 40 μl of Rotiphenol (Roth, Karlsruhe, Germany) was added and the samples were mixed by vortexing for 10 s one by one. The samples were centrifuged 2 min by max. rpm (Eppendorf centrifuge 541-D, rotor: F-45-24-11). A 40 μl share of the hydrophilic phase were mixed with 1/10 volume of 3 M sodium acetate, pH = 5.3 (Roth) and 2.5 × volume of absolute ethanol (Roth), again one sample after the other. This share was assigned as 2/3 of the whole hydrophilic phase and with this value included in the final titer calculation (*b*). These samples were incubated at −20 °C for 15 min (DNA precipitation) and then centrifuged at 4 °C, max. rpm for 15 min. The overhang was discarded and the pellet was washed two times with 70% ethanol (4 °C) each time followed by a 5 min centrifugation (4 °C, max. rpm). Then after a dry period of 10 min the DNA was dissolved in 20 μl H2O (*c*). The DNA concentration (*d*) was determined four times with the NanoDrop® ND-1000 (PeqLab, Erlangen, Germany) and the values were averaged. The extractions were performed in single probes but repeated on three different days. Viruses used for an experimental set were extracted simultaneously for maximization of comparability.

2.3.2. Absolute quantification of viral genomes

The samples from Section 2.3.1 represent a heterogeneous DNA pool. Due to the production procedure of the viral stocks this pool contains intact viral genomes derived from intact viral particles and fragmented DNA. The content of intact viral genomes respectively viral particles is ascertained in this step by absolute quantification against a standard curve via qPCR on the Corbett Rotorgene 3000 (Corbett Life Science, Sydney, Australia) in combination with the LightCycler® FastStart DNA Master SYBR Green I Kit (Roche, Penzberg, Germany). Primers (fwd-sequence: CTGCTCGATTTGATAAACATCCT, rev-sequence: CAGGCTAAGCATGGAATAGTTGAT; Eurofins MWG Operon, Ebersberg, Germany) targeted the human Ad5-pTP-gene (NCBI-RevSeq: AP_000203.1) (Davison et al., 2003). The standard curve was made from a pAd/PL-DEST plasmid stock (Invitrogen), diluted from 10^9 to 10^1 Plasmids/μl in yeast t-RNA (Invitrogen) stabilized TE-buffer (10 mM Tris, 1 mM EDTA, 10 ng/μl t-RNA, pH = 8.0) and stored at −80 °C. DNA samples were diluted to 10 ng/μl (*e*). 1 μl of sample respectively standard was inserted in the PCR. After a 10 min step at 95 °C the PCR program included under continuous fluorescence measurement 45 amplification cycles (denaturation 95 °C/10 s; annealing 60 °C/10 s; extension 72 °C/15 s) followed by a melting

curve from 40 °C to 95 °C (0.5 °C steps; dwell time: 2 s). The measurements were performed in triplicates which were averaged for titer calculation (g). In a back calculation the corresponding titers (VP/μl) of the viral stocks were determined under consulting the calculation that one Ad5-U6Stop genome (ds-DNA) has a mass of 20,776,102 Da or 3.45E−08 ng (f). The following equation for the titer was used: $T = (1/af) \times (cd/b) \times (fg/e)$, with T: viral titer (VP/μl), a: volume of initially inserted viral stock (μl), b: share of hydrophilic phase from selective DNA extraction, c: dissolving volume after selective DNA extraction (μl), d: DNA concentration after selective DNA extraction (ng/μl), e: concentration of DNA inserted in qPCR (ng/μl), f: mass of one Ad5-U6Stop genome (ng/VP) and g: measured genomes from qPCR (VP/μl). The measured titers for Ad5-U6Stop preparations here were in the range of 5.6×10^7 VP/μl.

2.4. Impedance measurement and toxicity assay

As platform served the ECIS-1600 (Applied BioPhysics, Troy, USA) with two 8W10E array plates (Ibidi integrated BioDiagnostics, Martinsried, Germany). Each of the eight wells of this array plates contains ten gold microelectrodes (250 μm diameter) detecting the current flow through the media. The substrate area is 0.8 cm^2 and the well's capacity is 600 μl. The array holder was placed in a standard cell culture incubator (37 °C, 100% humidity and 5% CO_2). The array plates were equilibrated over night with 300 μl of DMEM at cell culture conditions. Then 1×10^5 IPI-2I cells were seeded to each well in 300 μl media. The seeding cell solution was enumerated after seeding for a more precise determination of the initial cell density. Array plates were connected to the instrument immediately to record all effects of the cell settlement consistently. Based on multi-frequency optimization runs (data not shown) the ECIS-device was setup. The measurements were generally performed with a 30 kHz ac source with an amplitude of 10 mV. The electrodes provide a constant current of 1 μA. The used sampling interval was 60 s. After 20 h when a bend in the proliferation curve could be located the measurement was paused. This cell stadium was set as the point of time for viral infection. Therefore two wells were used for cell counting in order to calculate the viral load for the desired MOI. The cell count was carried out using a Neubauer counting chamber after trypsination of the cells. For infection 200 μl of the 300 μl DMEM/well were removed. Then 300 μl/well of prewarmed (37 °C) virus dilution (Ad5-U6Stop in DMEM) was applied. In the toxicity assay the MOI-levels of 100, 200, 400, 800 and 1600 were utilized. Culture media containing the same concentration of viral storage buffer like the MOI 1600 sample was applied as reference to ensure that the monitored effect is not a result from substances contained in the viral storage buffer. The different MOI-levels in each assay were performed in duplicates. After the inoculation the measurement was resumed and data collection was continued for 72 h post-infection. To avoid nutrient deficiency the culture media was renewed 56 h after infection. Therefore only 300 μl of media were replaced. At the end of the measurement another cell count was performed.

2.5. Data analysis

Data analyses were carried out in ECIS-Software-v1.2.8.PC (Applied BioPhysics), SigmaStat-3.0 & SigmaPlot-11.0 (Systat Software, Inc., Chicago, USA) Rotor-Gene-6-Software (Corbett Life Science) and Microsoft Office Excel 2007 (Microsoft). In ECIS-Software the MOI-duplicates were grouped and the graphs were normalized to the time of infection.

3. Results and discussion

3.1. qPCR-based viral particle titration

To analyze the dose dependency of physiological effects evoked by replication deficient viral vectors in real-time cell culture studies (ECIS) a precise MOI adjustment is required. Beneath cell counting the more critical factor thereby is the virus titration. Comparing classical methods we felt a strong demand for a more time efficient, standardize able and reproducible titer measurement. That led to a qPCR-based method. The obvious problem with qPCR-based approaches is that not the infective titer (IFU), which represents the caused infection events in an in vitro cell culture model, is determined. However the dimension of the discrepancy between present viral particles (VPs) and IFUs in a virus preparation remains unclear. It certainly depends on the preparation procedure and the subsequent handling of the viral stock.

How close a qPCR-based titration approximates the infectious reality is up to the methodical steps involved in the measurement. The basic principle for qPCR-based titration is to measure virus derived genomes after amplification via qPCR against a standard curve. The challenge is to selectively capture only genomes derived from intact viral particles. In order to accomplish that DNA from damaged viral particles or other origin must be detracted from the viral stocks. Initially our approach includes a selective DNA digestion step by DNase I. This intends to digest DNA not enveloped by capsid proteins. Proximate, the viral genomes are set free from the remaining intact viral particles by a capsid digestion with Proteinase K. DNase I is an endonuclease and so produces DNA fragments and not single nucleotides like exonucleases. The so matured DNA pool (here called "total-DNA") is heterogeneous. It consists of DNA fragments and intact viral genomes. With our approach we intend to selectively measure these intact genomes in the DNA pool, approximating the viral titer in an accurate and practicable manner. Anyway according to studies by Thomas (Thomas et al., 2006) the titers determined by qPCR correlate with infectious titers determined by plaque-assay or endpoint dilution assay.

For evaluation of our qPCR-titration four different Ad5-virus preparations were analyzed parallely. Total-DNA was extracted on three different days and total-DNA concentration was determined four times for each sample. Then qPCR-quantification was performed in triplicates. The results of this evaluation serial shown in Fig. 1 demonstrate relatively small errors, good reproducibility and a distinct functionality of the selective intact genome quantification within the heterogeneous DNA pool by qPCR. Fig. 1a shows that the amount of intact genomes does not correlate with the amount of total-DNA from a particular virus preparation. This implies that among different virus preparations a different share of viral particles is generated or destroyed during the production process. Further it shows that the corresponding intact remaining part of viral particles can be measured that way. In Fig. 1a no standard deviations are indicated. The accumulated error over the procedure is visualized in Fig. 1b. In this plot the errors done in every step of the titration protocol and thus the reproducibility between different extraction days related to any particular virus sample is itemized.

Total-DNA extractions prepared on three different days from all four different viruses deliver a mean CV-value of 5.54% due to the calculated mean DNA concentration among the three replicates for each virus. The four mean DNA concentrations delivering the dataset for this mean CV-value of the 2nd column in Fig. 1b are represented by the broad columns in Fig. 1a. Averaging the CV-values of the four calculated titers (each containing the qPCR measured values from the three different days of extraction) produced a mean CV-value of 8.99%. The four mean titers delivering the dataset for this mean CV-value of the 4th column in Fig. 1b are represented by

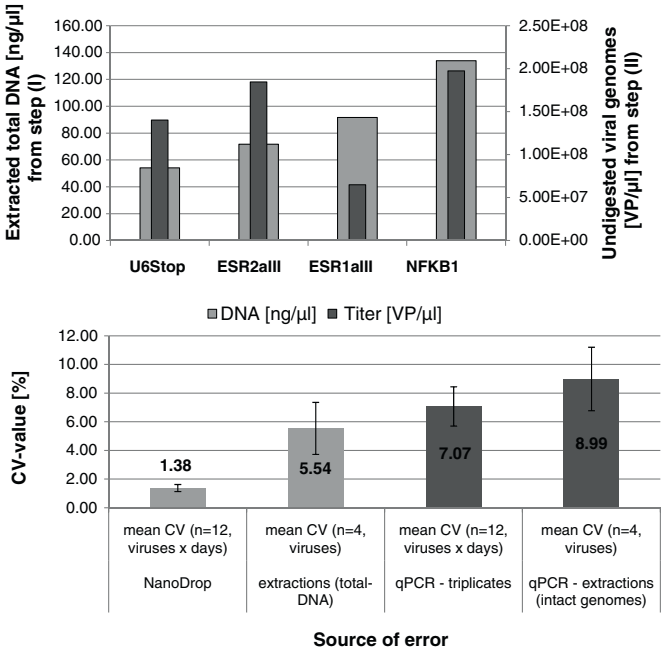

Fig. 1. (a) Total-DNA versus viral genomes. Total-DNA concentration (see Section 2.3.1) (primary ordinate) plotted against undigested viral genomes (see Section 2.3.2) (secondary ordinate) for four different Ad5-virus preparations. (b) Error analysis Ad5-qPCR-titer. Evaluation of error sources during the VP-titration. After each step of the procedure the CV-values resulting from the replicates are averaged (standard errors indicated). The 1st column represents the average of the CV-values from the four total-DNA measurements for each sample after selective Ad5-DNA extraction ($n = 12$; four viruses on three days). The 2nd column shows the error made between different days of total-DNA extraction. The four CV-values resulting from the three averaged concentration measurements for each of the four virus types ($n = 4$; four virus preparations). The 3rd column represents the mean CV-value resulting from the CV-values of the triplicates measured in qPCR for all samples after absolute quantification of viral genomes ($n = 12$; four viruses on three days). The 4th column results by averaging the four CV-values from the viral titers derived from the three extraction days ($n = 4$; four viruses).

the narrow columns in Fig. 1a. These mean CV-values show an independency between titration repetition and used analyte. The values of the 1st and 3rd column in Fig. 1b are general errors that occur by using the particular method, device or material (NanoDrop, qPCR-setup = device + reaction kit + triplicates). The values of the 2nd and 4th column in Fig. 1b show errors derived from the processing of an individual viral sample within this titration method. They should be considered consecutively according to the nonlinearity in Fig. 1a.

Eventually the aberration caused by the titration procedure remains relatively small and delivers repeatable results. A titration serial of this dimension or as well bigger can be executed within two days, which is far more time efficient than for example the classical plaque-assay that takes weeks to perform.

3.2. ECIS-based toxicity assay

In preliminary studies (data not shown) the behavior of IPI-2I in ECIS measurements was tested. At a density of 1×10^5 cells/well, 20 h post-cell seeding a characteristic bend in the impedance curves, changing from a higher to a lower slope could be monitored. Cell enumerations of non-treated samples at seeding time, after this characteristic bent and after 92 h showed that two different correlations between impedance signal and cell count are detected (Fig. 2a). According to the cell count data the increase in impedance between 0 h and 20 h must be attributed to effects of cell settlement. Within 0 h and 20 h no crucial increase in cell number took place. Interestingly, referred to the whole range of the impedance signal change the attachment phase already contributes approximately 50% to the total value. Regarding the subsequent cell count data it seems to be evident that not until 20 h post-cell seeding the impedance signal represents cell proliferation. In consequence the event of infection and the normalization of data were set to this point after the bent in the proliferation curve. Furthermore the second cell count was assumed as the base value for MOI calculation.

Due to the fact that the RNAi-vector is replication deficient in IPI-2I cells and so for loss-of-function studies it might be need to apply it in high concentrations in order to evoke an effective knockdown, the Ad-U6stop dilution series was prepared over a broad concentration range, including MOI 100, 200, 400, 800 and 1600. The infection was accompanied by a temporary signal deflection, but after about 2 h of re-equilibration the data curves returned to their previous values. The inoculations were left in the wells and thereupon ECIS data was collected continuously. After 56 h a media change got necessary because of nutrition deficiency. Then data collection was continued another 24 h (Fig. 2b). For all viral load levels excluding the control an inflection point occurs 24 h post-infection (PI). That could represent the incubation time of the adenoviral infection. After that point a constant decrease in the impedance signal was monitored with its decline correlating to the inserted MOI.

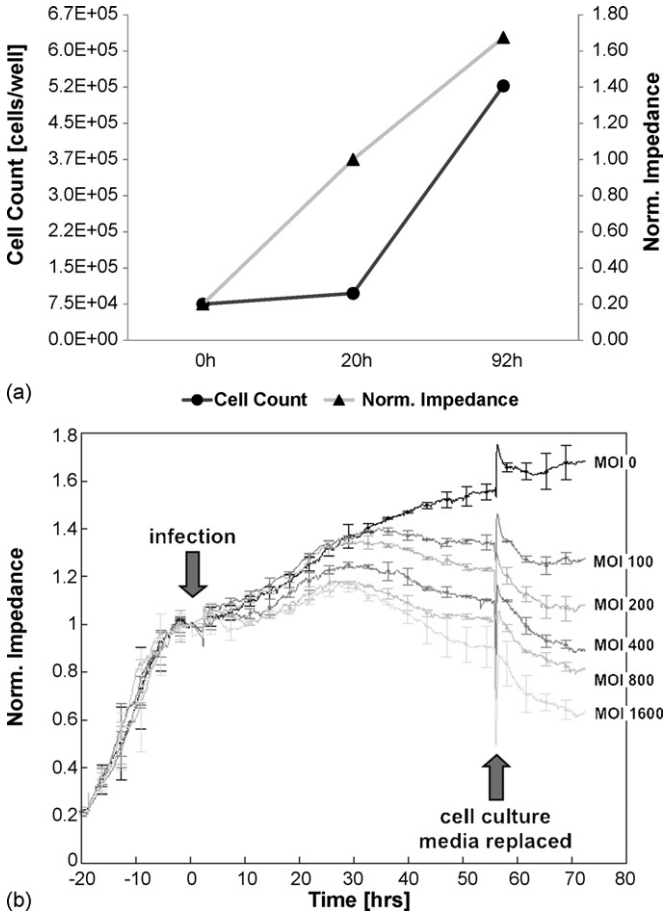

Fig. 2. (a) Impedance values and corresponding cell count. 1×10^5 IPI-2I/well were seeded into ECIS 8W10E arrays. Three cell counts were carried out: seeding time ($n = 4$, CV = 12.8%), 20 h post-seeding ($n = 4$, CV = 3.4%), and 92 h post-seeding ($n = 2$, CV = 6.7%). Impedance values of replicates are grouped in ECIS-software. (b) ECIS-cytotoxicity assay: IPI-2I infected with Ad5-U6Stop. Normalized impedance against time plot of an ECIS measurement of IPI2-2I cells in 8W10E array plates at standard cell culture conditions over 92 h. For reasons shown in (a) the x-axis starts with −20 h and 0 h is the time of infection. Cells were infected in duplicates with Ad-U6stop at MOI 0, 100, 200, 400, 800, 1600 and duplicates were grouped in ECIS-software. The inoculation (virus in DMEM) at 0 h remained in the wells until the media change (pure DMEM) at 56 h PI.

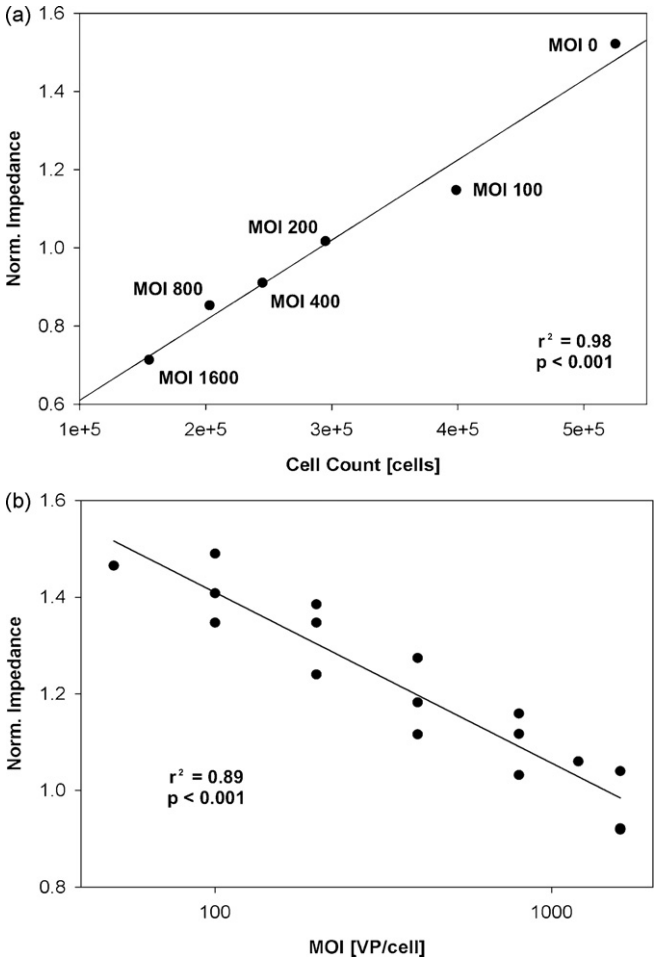

Fig. 3. (a) IPI-2I cells (72 h PI) with an MOI gradient of Ad5-U6Stop versus ECIS measured impedance. To confirm cell decease samples were enumerated four times 72 h PI with a hemocytometer and the cell count was plotted against the appending impedance values. The CV-values of the enumerations were 6–10%. A linear regression of the data delivered a regression coefficient of $r^2 = 0.98$ ($p < 0.001$). (b) ECIS measured impedance for IPI-2I infected with Ad5-U6Stop (72 h PI). Normalized impedance values after 72 h of viral impact plotted as a function of MOI (logarithmic abscissa!). A polynomial regression shows a regression coefficient of $r^2 = 0.89$ ($p < 0.001$).

Remarkably the signal decrease continued after the media change, indicating that the toxic effect of the infection was still present after the inoculation was removed and changed against blank cell culture media. Considering the fact that the cell count of the three highest MOI-levels at the end of the measurement was under the cell number at the time of infection, the decrease can be attributed to real cell decease and not only to lower proliferation rates or loss of adhesion of the cells on the substrate (Fig. 3a).

To see the correlation between the viral load and the resulting toxic effect the impedance values of three similar ECIS-cytotoxicity assays were plotted against the corresponding MOI (Fig. 3b). Therefore in all cases the impedance values 72 h PI were used and all data were normalized to the time of infection. The resulting polynomial regression shows a clear dose-depending effect. A regression coefficient of $r^2 = 0.89$ ($p < 0.001$) was ascertained. In case of this adenoviral model a logarithmic correlation with a very quick toxic response at relatively low MOI-levels (<MOI 100) can be monitored. However when the MOI rises to relatively high levels there is the evidence of a maximal toxic dose. This might be a state when all cells are saturated with viral particles. Presently we expand this ECIS-based model using other cell lines and RNAi-vectors that evoke gene knockdown. The data, which is still in ascertainment,

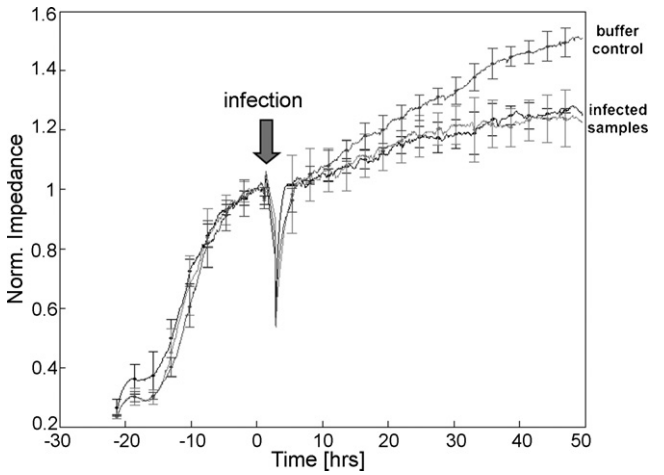

Fig. 4. IPI-2I infected with an equal MOI of different Ad5-viruses. Normalized impedance versus time plot. Each graph results from the grouped data of three parallel measured wells with IPI-2I cells infected with an equal dose of Ad5-PPARg and AD5-U6Stop. Infected groups show the same cell death levels whereas the buffer control group proliferates continuously.

underlines the functionality of this measuring system to assign cytotoxic effects of viral vectors. Similar toxicity subsequent to infection was monitored by using a PPARg targeting RNAi-virus versus the Ad-U6stop in equal MOIs (Fig. 4). It seems to be evident that with ECIS technology, used like in our work, the explicit toxic effects of transfection vectors can be quantified in a non-invasive manner, displaying disrupting incidents for the cell culture model in real-time. The data shown in Fig. 4 as well underlines the functionality of our titration method. Equal vector doses, determined by this titration protocol, affect the cell culture model comparably.

4. Conclusion

Concerning the adenovirus titration it remains to refer to the comparison study by Crettaz (Crettaz et al., 2008). According to that the qPCR-based approaches are the method of choice for the future. Our titration method underlines that with CV-values of 5–10%. The *Adenovirus Reference Material Working Group* (ARMWG) (Hutchins et al., 2000; Palmer and Ng, 2004) provides an adenoviral standard. If one day this virus is declared as international accepted standard it will make sense to ensure the correlation between VP and IFU on qPCR level.

Here we have shown another interesting application for ECIS measurements, an upcoming technique with a high potential for cell culture studies. We show that cytotoxicity of viral vectors can be quantified using ECIS technology. The grade of cell death caused by the inserted MOI in an individual cell culture model can be visualized in real-time. It is self-evident that this application can be transferred to similar studies in order to measure the impact of any active agent in cell culture models. Regarding the background of this work, the RNAi-knockdown model, it is intended to use ECIS technology to monitor *on-target-effects* of the induced RNA interference. That way the efficiency of different RNAi-sequences targeting a gene involved in cell growth may be evaluated. By providing real-time information about attachment and proliferation activities, cell death and thus the progress of an induced effect, ECIS represents a valuable tool for kinetic studies. It even bears the potential to reveal mechanisms causing the impact of a treatment.

Acknowledgements

This study was supported by a grant from the Vereinigung zur Förderung der Milchwissenschaftlichen Forschung an der Tech-

nischen Universität München e.V. The methodical knowhow for the knockdown model was provided by SIRION-BIOTECH (Am Klopferspitz 19, D-82152 Martinsried). Technical support for the ECIS-device came from IBIDI GmbH (Am Klopferspitz 19, D-82152 Martinsried). The authors want to thank especially Michael Salomon and Armin Bieser for their enduring assistance.

References

Ceriotti, L., Ponti, J., Colpo, P., Sabbioni, E., Rossi, F., 2007. Biosens. Bioelectron. 22 (12), 3057–3063.
Crettaz, J., Olague, C., Vales, A., Aurrekoetxea, I., Berraondo, P., Otano, I., Kochanek, S., Prieto, J., Gonzalez-Aseguinolaza, G., 2008. J. Gene Med. 10 (10), 1092–1101.
Davison, A.J., Benko, M., Harrach, B., 2003. J. Gen. Virol. 84 (Pt 11), 2895–2908.
Fire, A., Xu, S., Montgomery, M.K., Kostas, S.A., Driver, S.E., Mello, C.C., 1998. Nature 391 (6669), 806–811.
Giaever, I., Keese, C.R., 1984. Proc. Natl. Acad. Sci. U.S.A. 81 (12), 3761–3764.
Graham, F.L., Smiley, J., Russell, W.C., Nairn, R., 1977. J. Gen. Virol. 36 (1), 59–74.
Graham, F.L., van der Eb, A.J., 1973. Virology 52 (2), 456–467.
Hutchins, B., Sajjadi, N., Seaver, S., Shepherd, A., Bauer, S.R., Simek, S., Carson, K., Aguilar-Cordova, E., 2000. Mol. Ther. 2 (6), 532–534.
Lo, C.M., Keese, C.R., Giaever, I., 1993. Exp. Cell Res. 204 (1), 102–109.
Lovelady, D.C., Richmond, T.C., Maggi, A.N., Lo, C.M., Rabson, D.A., 2007. Phys. Rev. E: Stat. Nonlin. Soft Matter Phys. 76 (4 Pt 1), 041908.
Ma, L., Bluyssen, H.A., De Raeymaeker, M., Laurysens, V., van der Beek, N., Pavliska, H., van Zonneveld, A.J., Tomme, P., van Es, H.H., 2001. J. Virol. Methods 93 (1–2), 181–188.
Mitra, P., Keese, C.R., Giaever, I., 1991. Biotechniques 11 (4), 504–510.
Palmer, D.J., Ng, P., 2004. Mol. Ther. 10 (4), 792–798.
Philipson, L., 1961. Virology 15, 263–268.
Russell, W.C., 2000. J. Gen. Virol. 81 (Pt 11), 2573–2604.
Schierack, P., Nordhoff, M., Pollmann, M., Weyrauch, K.D., Amasheh, S., Lodemann, U., Jores, J., Tachu, B., Kleta, S., Blikslager, A., Tedin, K., Wieler, L.H., 2006. Histochem. Cell Biol. 125 (3), 293–305.
Thomas, M.A., Krajcsi, P., Lichtenstein, D.L., Tollefson, A.E., Wold, W.S.M., 2006. Mol. Ther. 13 (S1), S49–S50.
Tiruppathi, C., Malik, A.B., Del Vecchio, P.J., Keese, C.R., Giaever, I, 1992. Proc. Natl. Acad. Sci. U.S.A. 89 (17), 7919–7923.
Tuschl, T., 2001. Chembiochem 2 (4), 239–245.
Wang, F., Mathis, B.C., Montalvo, A., Wolf, J.J., Lewis, J.A., 2008. Methods Mol. Biol. 434, 25–36.

ISSN: 2153-0602

Journal of Data Mining in Genomics & Proteomics

The International Open Access Journal of Data Mining in Genomics & Proteomics

Available online at: OMICS Publishing Group (www.omicsonline.org)

Digital Object Identifier: http://dx.doi.org/10.4172/2153-0602.1000116

Data Mining in Genomics & Proteomics

Müller and Pfaffl, J Data Mining Genomics Proteomics 2012, 3:2
http://dx.doi.org/10.4172/2153-0602.1000116

Research Article Open Access

RNA Interference Off-target Screening using Principal Component Analysis

Jakob Müller* and Michael W. Pfaffl

Physiology Weihenstephan, Technische Universität München, Research Center for Nutrition and Food Science, Weihenstephaner Berg 3, 85350 Freising, Germany

Abstract

Off-target effects remain the major problem in any RNAi-knockdown application. Casting cell culture loss-of-function studies evaluated by heat map and principal component analysis (PCA) we realized that the PCA derived plots can clearly visualize off-target effects. Due to the inexistence of off-target effects in our cell culture model we created an *in silico* data model in order to demonstrate how PCA can be utilized therefore. With the presented *in silico* modulation it is possible to simulate the impact of various treatments on changing gene expression. Known effects caused by drug treatment or by inserted knockdowns could be clearly separated from unknown off-target effects. By creating various randomized gene expression data sets we demonstrate that PCA can assign more effective an off-target effect compared to a heat map gene regulation pattern.

Keywords: RNAi Off-target Screening; Principal Component Analysis; Heatmap; *In silico* Data Modelling; Virtual RT-qPCR

Abbreviations: Cq: Quantification Cycle; CV: Coefficient of Variation; EGCG: Epigallocatechin Gallate; HCA: Hierarchical Cluster Analysis; PCA: Principal Component Analysis; RNAi: RNA Interference; RT-qPCR: Reverse Transcription Quantitative Real-time Polymerase Chain Reaction; siRNA: Small Interfering RNA

Background

RNA interference (RNAi) is nowadays a common used technology for gene silencing. It is applied for therapeutic aims or identification of drug targets as well as for basic research on gene function. The still unsolved major problem with this technique is the potential to cause unspecific off-target gene regulations in the treated cell culture or organism. These off-target effects are well described in many studies [1-3]. Since its discovery [4] and utilisation [5,6] RNAi has become an easy tool to use in cell culture assays. Compared to knockout based loss-of-function studies RNAi-knockdowns can be applied easily as a combined application beside a drug treatment. The reaction of the cell culture model to the treatments can subsequently be assessed on RNA level. Conventionally expression proofing studies are performed by quantitative real-time RT-qPCR or hybridization arrays. To visualize the differential gene expression changes hierarchical cluster analysis (HCA) or heat maps are very common [7]. Effects of a single treatment, like a siRNA-sequence, on a very broad range of genes can be visualized that way. An alternative method of visualizing complex datasets is the principal component analysis (PCA). This statistical and visualization tool reduces the dimensionality of a dataset consisting of a large number of interrelated variables, while retaining as much as possible of the variation present in the dataset [8].

Using an adenoviral based RNAi knockdown-model, we casted a loss-of-function study (data not shown) identifying the influence of a plant secondary metabolite (EGCG) under various gene knockdowns in an immunological signalling pathway. The outcome of the experiments was among others analyzed by PCA. Doing this we observed by chance a synergetic side effect exclusively in those of our treatment groups in which one particular knockdown was combined with the drug appliance. These findings led to the idea that if we can separate the roots of an effect applying PCA we can use it vice versa and isolate RNAi originating gene regulations from drug effects and this means off-target screening.

For an approval of our assumption we tried to find an off-target gene regulation in our cell culture model caused by one of the viral induced siRNA-knockdowns we had in stock. But without access to genome wide transcriptional array results no off-target effect was found. Hence we decided to use *in silico* data modelling to demonstrate how PCA can be utilized beneficially for RNAi off-target screening.

Methods

Data modelling

The underlying dataset was justified to the gene expression data output of our standard cell culture assays. Thereby the extracted RNA initially undergoes a RT (Reverse Transcription) with subsequent qPCR (quantitative real-time polymerase chain reaction) gene expression analysis. Accordingly the layout of the data model was designed. It consists of eight treatment groups (a-h) each containing four replicates, leading to 32 samples (Table 1). The eight groups were divided into two sections, the drug-treated groups (b,d,f,h) and the media control treated groups (a,c,e,g). The sections in turn were sub-classified in four species each one characterized by a particular gene knockdown-combination. The four knockdown-combinations were

Knockdown-combination	kd-c	kd-I	kd-II	kd-I&II
Control (cell culture media)	a	c	e	g
Treatment (drug appliance)	b	d	f	h

Each treatment-variant (control, treatment) is combined with each knockdown-variant (kd-c, kd-I, kd-II, kd-I&II) leading to eight treatment groups (a - h), each n=4, leading to 32 samples

Table 1: Knockdown-assay layout.

***Corresponding author:** Jakob Müller, Physiology Weihenstephan, Technische Universität München, Research Center for Nutrition and Food Science, Weihenstephaner Berg 3, 85350 Freising, Germany, Tel: +49 8161 71 3867; Fax: +49 8161 71 4204; E-mail: jakob.mueller@wzw.tum.de

Received March 07, 2012; **Accepted** June 13, 2012; **Published** June 17, 2012

Citation: Müller J, Pfaffl MW (2012) RNA Interference Off-target Screening using Principal Component Analysis. J Data Mining Genomics Proteomics 3:116. doi:10.4172/2153-0602.1000116

composed from two target knockdowns (named "kd-I" or "kd-II") and one knockdown-control (named "kd-c"). The two treatment groups and the four knockdown-groups were combined pair wise (Table 1).

For each of the 32 samples a dataset of 21 genes was rendered using our self designed spreadsheet template (Microsoft Office Excel 2007, Additional file 1). The 21 genes where group-wise attributed to a supposed class of gene regulation. The classes differ in how genes respond, either to drug treatment or knockdown-appliance. Four of these classes where created: (class I) stabile expressed reference genes, (class II) target-genes knocked down by RNAi, (class III) genes regulated (up or down) by the drug treatment, (class IV) genes influenced by the drug treatment and additionally bearing a RNAi-off-target effect (Figures 1 and 2). The *in silico* expression data based on C_q-

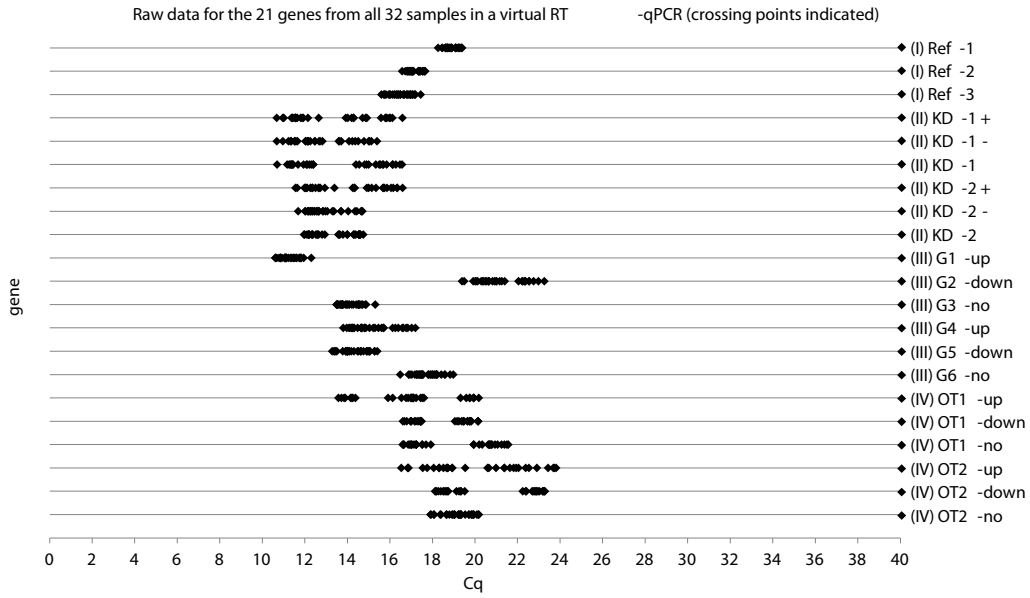

Figure 1: C_q-values plotted as virtual RT-qPCR. The one random output of our simulation which underlies all graphs in this work represents a raw dataset from a RT-qPCR gene expression analysis of 21 genes. The 32 C_q-values (originating from the eight different application combinations multiplied by the four replicates) are plotted gene wise on a line, like fluorescence-signals crossing a threshold in an *in vitro* RT-qPCR reaction. The random data distribution and within the emulated CV-value gets visible best in class I genes (unregulated reference-genes). Particular regulation effects become apparent by the separate clusters among the 32 data points of a gene.

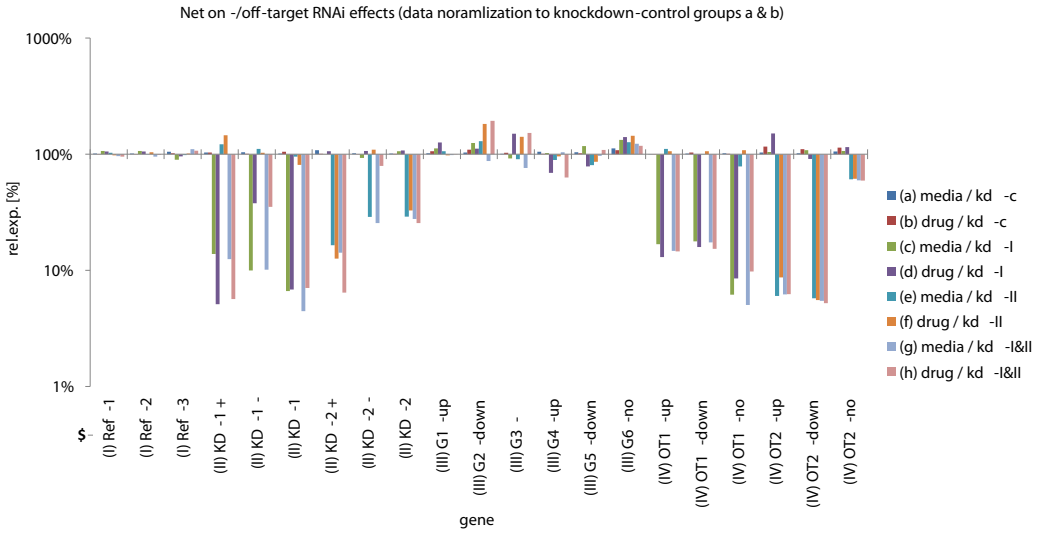

Figure 2: Knockdown-evaluation from the *in silico* data set. Relative expression levels of simulated genes after knockdown and/or drug appliance calculated by the $\Delta\Delta C_q$-method plotted against a logarithmic ordinate. Net knockdown-effects are exposed by normalizing data to knockdown control samples. The 21 genes are arranged in four classes: (class I) reference genes (Ref-1, Ref-2, Ref-3); (class II) knockdown-targets (KD-1+, KD-1-, KD-1, KD-2+, KD-2-, KD-2); (class III) drug targets (G1-up, G2-down, G3-no, G4-up, G5-down, G6-no); (class IV) drug targets with an additional off-target effect (OT1-up, OT1-down, OT1-no, OT2-up, OT2-down, OT2-no). The additional prefix specification "+" or "-" indicated at class II genes stands for an additional synergetic gene regulation effect which occurs when knockdown appliance is combined with drug appliance. The additional prefix specification "-up", "-down" or "-no" indicated at class III and IV genes stands for the direction of the predestinated gene regulation. For every gene eight expression levels are given corresponding to the eight treatment groups: a - h (Table 1).

values of every single sample for every individual gene was created by our random algorithm (Microsoft Office Excel 2007, Additional file 1). The C_q-value represents the number of cycles that are required by the fluorescence signal of a single sample in a qPCR-experiment to cross a defined threshold [9,10]. All factors which influence the C_q-value of a sample were randomly generated: the expression level of each gene, its variation coefficient, the range of up- or down-regulation, and the range of on-target or off-target knockdown. The data model delivers a dataset of 21 x 32 values (genes in columns x samples in rows). This *in silico* modelled dataset represents the raw data outcome of a corresponding RT-qPCR gene expression analysis obtained from our standard cell culture assays. For all plots presented the same raw dataset was used (Additional file 2). All variables influencing the data were completely randomized, but expression ranges, gene regulations and the inherent variability were chosen to be realistic based on the knowledge about gene expression we gained from our cell culture assays. The range of the gene regulation here was set from 1-10 folds, the knockdown-efficiency between 45% and 95% and the applied CV-value was justified to 35% of the emulated gene regulation. In order to evaluate the quality of the raw data the distribution of the 32 C_q -values (32 samples) corresponding to every gene is plotted in a virtual RT-qPCR (Figure 1).

Data processing

Gene expression analysis: The raw data was analyzed under the terms of the $\Delta\Delta C_q$-method [11], and then relative expression values (shown in percentage) were plotted gene-wise on a logarithmic ordinate.

Hierarchical cluster analysis: Heat maps of the modelled data were plotted in GenEx software (version 5.3.2.13, MultiD, Sweden) using the ΔC_q-values for each sample corresponding to the gene set [12].

Principal component analysis: The data processing using principal components analysis (PCA) was as well performed using GenEx software. Therefore the ΔC_q-values for each sample corresponding to the gene set were calculated and then pasted into the PCA-algorithm input box. According to the aim of the PCA (results and discussion) the data was mean centered to columns or transposed and then mean centered to rows [7].

Results and Discussion

For this work we designed a data emulator based on the layout of our cell culture assays. Every time used it delivers a unique dataset. Within this emulator the range of the RT-qPCR data constituting parameters can be set up. Subsequently the values are rendered randomly (Additional file 1). In order to show that this data is authentic compared to a cell culture experiment we plotted the raw data (C_q-values) in a virtual RT-qPCR (Figure 1). When this data is normalized to the control samples of the knockdown-treatments (group's a and b) the net knockdown-effects get visible (Figure 2). As a result this plot shows explicitly the knockdown-effect which weighs on a particular gene. The six genes in class II are all predestinated to be knockdown-targets by the simulation. Thus they show down-regulation after the normalization used in this plot. All other genes are no knockdown-targets. But nevertheless some of them show a significant down-regulation. These are the genes from class IV which bear an off-target effect. Slight regulations on the remaining genes (classes I and II) emerge from the random variation coefficient integrated in the data simulation. We inflicted additional gene regulations on some of the class II genes (Figure 2). The additional prefix specification "+" or "-" at the gene name indicates a synergetic

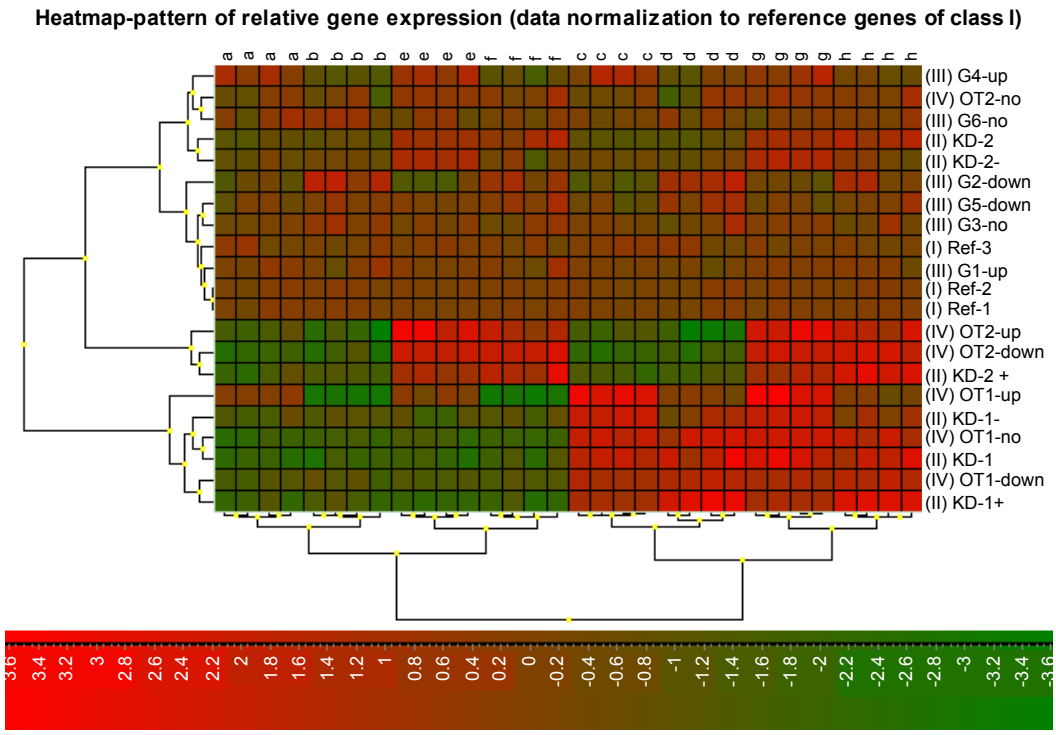

Figure 3: Heat map of relative expression data. ΔC_q-values (normalized against reference gene means) for all 32 samples corresponding to the 21 genes are plotted in GenEx software. Green indicates a relative up-regulation, red a relative down-regulation. The same dataset as in Figure 2 was applied.

effect on the gene regulation when the RNAi-knockdown and the drug appliance are inserted simultaneously. We include this special scenario, because it is a well known phenomenon in *in vitro* or *in vivo* models as we experienced it from our own cell culture assays (data not shown). The same gene expression data is plotted in a heat map in Figure 3. In this visualization mode the ΔC_q -values are directly used without any further normalization to control samples.

The randomly created dataset plotted in Figures 2 and 3 contains some special cases by chance. In the heatmap (Figure 3) we realize a separation between strong knockdown-effects evoked either by knockdown kd-I or knockdown kd-II. However only the genes influenced by knockdown kd-I can be globally separated clearly (KD-1, KD-1+, KD-1-, OT1, OT1-up, OT1-down). kd-II influenced genes fractionally merge undefined between red and green (KD-2, KD-2-, OT2-no). This happens due to the by chance relatively low knockdown-originated regulations on these genes. So, how can I adjust the undefined genes in order?

Therefore we additionally utilized PCA. A plot from a PCA will always have as much data points as the underlying dataset has rows. In every single data point you can include as much resources as you are interested in by integrating more or less columns of a dataset. In our case this means to consider more or less genes measured from one RNA-sample. Each gene will contribute its impact to the sample and influence its position in the PCA-plot. If a gene is strong regulated its impact is high. On the other hand a low regulated gene like a reference gene has poor impact on a sample. If such a gene (column) is included the position of a data point (sample) will not move in the PCA-plot. Figure 4a/b uses the same dataset as Figures 1,2 and 3. In the plots from Figure 4a/b the data was sorted as rows = samples. With the data arranged like this the PCA algorithm regards the impact which

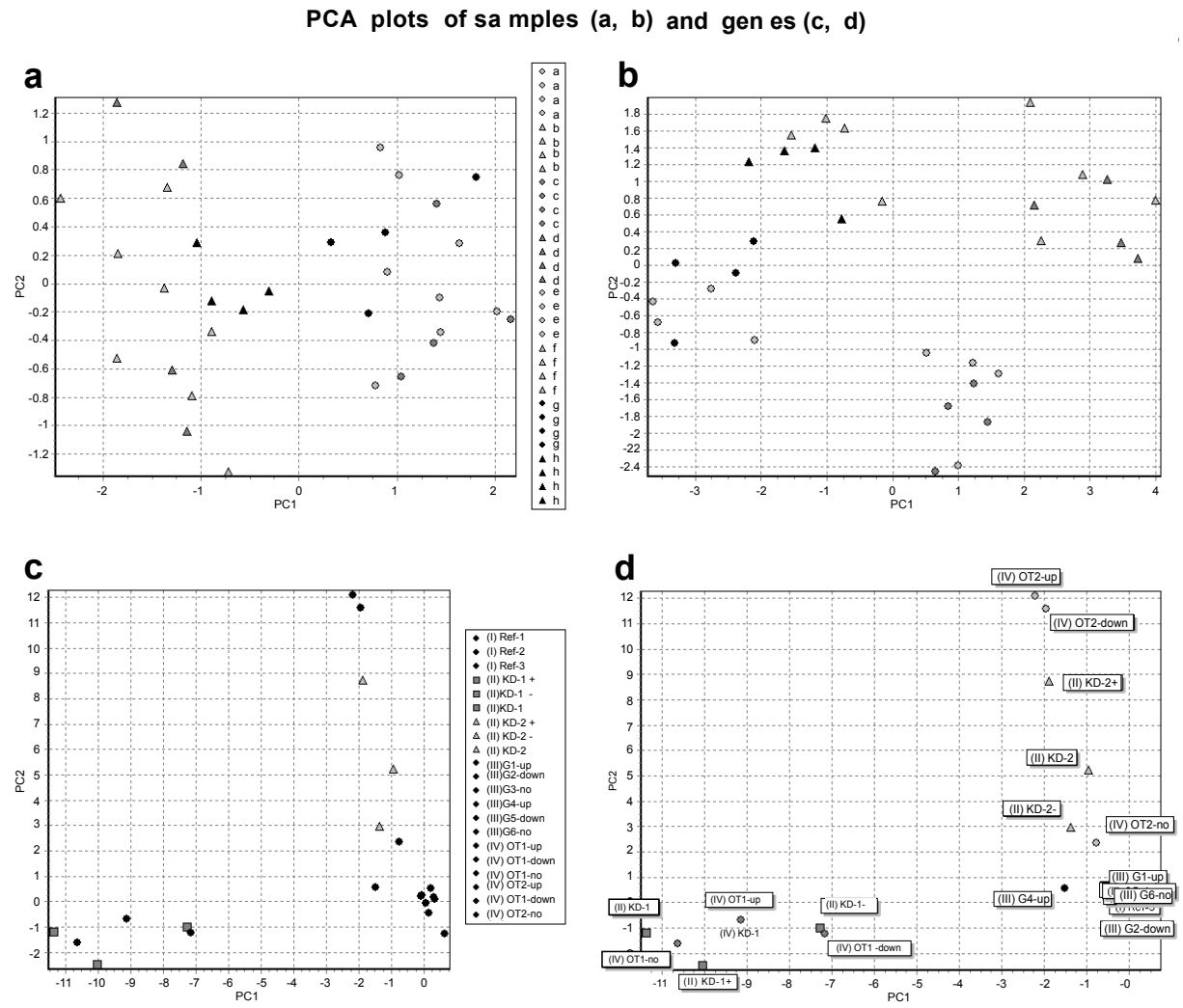

Figure 4: PCAs of the *in silico* data set from Figures 1,2 and 3. (a) PCA of all 32 samples (columns = genes, rows = samples) embracing exclusively genes of classes I and III. The samples cluster in two clouds according to media control (circles) or drug treatment (triangles). (b) PCA from the same data pool as in Figure 4a but including the class IV gene OT2-up. The incorporation of OT2-up divides the two clouds from Figure 4a by separating the samples which bear the off-target effect. (c) PCA with data transposed columns by rows including the complete dataset (32 samples x 21 genes). Genes of class II are indicated as squares (kd-I) or triangles (kd-II). Circles indicate genes from the three remaining classes. (d) Plot Identical with Figure 4c, but layout adjusted: gene names are given and class IV genes (with off-target effect) are now labeled in color according to the knockdown they originate from.

lies on each of the 32 samples. On the algorithm level that means the dimension of the collective gene regulation corresponding to a single sample is expressed as a vector. The resulting PCA-plot then simplifies the multi dimensional dataset and adjusts it to the biggest vectors. That way the major gene regulations are exposed in a two dimensional plot. The way one single gene can influence the plot from a PCA gets clear in Figures 4a/b. While in Figure 4a we can recognize two clouds, there are four clouds in Figure 4b. This is due to the impact that is load on the data points (samples) by integrating more or less resources (genes). In Figure 4a the PCA is cast only with genes that explicitly bear no knockdown-effect (classes I & III). As a result the data points cluster only in accordance with media (circles) or drug (triangles) appliance. In Figure 4b there is only one more column (only one class IV gene: OT2up) included into the dataset. This single load has enough impact to split the two clouds into four. The knockdown lying on OT2up represents a second vector of regulation. For those of the samples in Figure 4b which are treated with the knockdown kd-II the PCA algorithm exposes another vector because the provided effect (an off-target effect) is strong enough. For a screening that means if a gene set we want to analyze is not harassed by any off-target effects the PCA plot will remain in a treatment and a control cloud.

But we can go deeper into data analysis and retrieve more information about the gene regulation. In Figure 4c the PCA casted with the entire dataset is plotted. The major difference is that the data now is transposed columns by rows. In consequence every data point represents one gene including all 32 values from the corresponding samples. Three different kinds of symbols were attributed. Genes which are designated as knockdown-targets (class II) are labeled with squares (kd-I) or triangles (kd-II). All other genes (classes I, III & IV) are labeled as circles. The result is a pattern of the data branching into two directions (or vectors). In our model we have the advantage that we know which genes are additionally charged by an off-target effect (class IV genes). In an off-target screening this information would be the task. If we now label these genes with the color for the knockdown they bear we get a very clearly terminated evaluation (Figure 3d). Genes having an off-target effect from the knockdown kd-I cluster to the branch of kd-I target genes and accordingly behave genes with a kd-II originating off-target effect. This outcome is what we can use to screen for off-target effects using PCA. Genes clustering in a cloud containing a knockdown target are likely influenced by an off-target effect. They should be exclusively checked for off-target effects in an extra RT-qPCR experiment.

But where is the advantage compared to a heat map analysis? The trouble in any case is when weak regulated genes shall be assigned. At that point the vectors in a PCA plot provide us extra information. A very low regulated gene in our dataset is OT2-no. In addition to that the two knockdown targets KD-2 and KD-2- are only weakly down-regulated by the knockdown kd-II (Figures 2 and 3). If we look at these genes in the PCA-plots of Figure 4c/d we realize that this evaluation locates these genes in direction towards the cloud of genes affected by kd-II. Of course OT2-no merges slightly with the cloud of generally low regulated genes, but it settles at the border towards the kd-II containing cloud and explicitly not towards the kd-I influenced genes. In the heatmap these genes cannot be attributed to any treatment group and fade between other low regulated genes. At that point PCA can clearly provide more information about a gene regulation pattern than the HCA alone.

By using virtual RT-qPCR data modelling it is easy to create more similar datasets to demonstrate this evaluation method. For your concern we posted additional twelve PCA-plots online, even with extreme values for the regulative parameters or the CV-value (Additional file 2).

Conclusions

PCA in its innate manner takes that point of view on a dataset that visually maximizes the variation present in a dataset. As a result PCA cannot distinguish information which is not present in a dataset. But the task for the scientist is to pick the most vivid visualization mode for that what was measurable out of the processes which took place on biological level. Analyzing off-target effects using HCA and PCA gives us the advantage that a side effect can be easily attributed to its origin. In the PCA-plot the knockdown targets will cluster with genes regulated by the same cause. In a heat map only strong effects can be identified clearly. Weak regulations will fade between red and green. In addition the PCA assigns a direction to every source of gene regulation. Even when an effect is weak it will cluster towards that cloud of genes which are regulated by the same originator. Separated that way transcript expression patterns can efficiently be analyzed for siRNA specific gene regulations which means off-target screening in a very new mode.

Competing Interests

The authors declare that they have no competing interests.

Authors' Contributions

The idea of utilizing principal component analysis for RNAi-off-target screening was devised by JM. The data modelling spread sheet was designed by JM. The manuscript was drafted by JM and supervised by MP.

Acknowledgements

This study was supported by a grant from the Vereinigung zur Förderung der Milchwissenschaftlichen Forschung an der Technischen Universität München e.V. I vigorously thank Katrin Danowski for basic and Dr. Ales Tichopad for advanced guidance with the GenEx software.

References

1. Jackson AL, Bartz SR, Schelter J, Kobayashi SV, Burchard J, et al. (2003) Expression profiling reveals off-target gene regulation by RNAi. Nat Biotechnol 21: 635-637.
2. Jackson AL, Burchard J, Schelter J, Chau BN, Cleary M, et al. (2006) Widespread siRNA "off-target" transcript silencing mediated by seed region sequence complementarity. RNA 12: 1179-1187.
3. Lim LP, Lau NC, Garrett-Engele P, Grimson A, Schelter JM, et al. (2005) Microarray analysis shows that some microRNAs downregulate large numbers of target mRNAs. Nature 433: 769-773.
4. Fire A, Xu S, Montgomery MK, Kostas SA, Driver SE, et al. (1998) Potent and specific genetic interference by double-stranded RNA in Caenorhabditis elegans. Nature 391: 806-811.
5. Tuschl T, Zamore PD, Lehmann R, Bartel DP, Sharp PA (1999) Targeted mRNA degradation by double-stranded RNA in vitro. Genes Dev 13: 3191-3197.
6. Zamore PD, Tuschl T, Sharp PA, Bartel DP (2000) RNAi: double-stranded RNA directs the ATP-dependent cleavage of mRNA at 21 to 23 nucleotide intervals. Cell 101: 25-33.
7. Bergkvist A, Rusnakova V, Sindelka R, Garda JM, Sjogreen B, et al. (2010) Gene expression profiling-Clusters of possibilities. Methods 50: 323-335.
8. Jolliffe IT (2002) Introduction, Principal Component Analysis. Springer New York.
9. Bustin SA, Benes V, Garson JA, Hellemans J, Huggett J, et al. (2009) The MIQE guidelines: minimum information for publication of quantitative real-time PCR experiments. Clin Chem 55: 611-622.
10. Freeman WM, Walker SJ, Vrana KE (1999) Quantitative RT-PCR: pitfalls and potential. Biotechniques 26: 112-122, 124-125.

11. Livak KJ, Schmittgen TD (2001) Analysis of relative gene expression data using real-time quantitative PCR and the 2(-Delta Delta C(T)) Method. Methods 25: 402-408.

12. Pfaffl MW, Vandesompele J, Kubista M (2009) Data Analysis Software. Caister Academic Press, Norwich, UK.

Title page

Title:

Synergetic downregulation of 67kDa laminin receptor by the green tea (Camellia sinensis) secondary plant compound epigallocatechin gallate: a new gateway in metastasis prevention?

Authors:

Jakob Müller

Physiology Weihenstephan, Technische Universität München, Research Center for Nutrition and Food Science, Weihenstephaner Berg 3, 85350 Freising, Germany

Michael W. Pfaffl

Physiology Weihenstephan, Technische Universität München, Research Center for Nutrition and Food Science, Weihenstephaner Berg 3, 85350 Freising, Germany

Corresponding Author:

Jakob Müller

eMail: jakob.mueller@wzw.tum.de

Tel.: 00498161713867

Fax: 00498161714204

Web: http://www.wzw.tum.de/physio/

Address: Physiology Weihenstephan, Technische Universität München, Research Center for Nutrition and Food Science, Weihenstephaner Berg 3, 85350 Freising, Germany

Abstract

Background. In traditional Chinese medicine, green tea is considered to have a life-prolonging effect, possibly as a result of its rich content of antioxidant tea polyphenols, and hence has the potential to prevent cancer. This study investigated the role of the major tea secondary plant compound epigallocatechin gallate (EGCG) for its inhibitory effects on the metastasis-associated 67kDa laminin receptor (67LR).

Methods. To clarify the impact of EGCG on siRNA-silenced expression of 67LR, we applied an adenoviral-based intestinal *in vitro* knockdown model, porcine IPEC-J2 cells. Quantitative real-time polymerase chain reaction was performed to analyze 67LR gene expression following treatment with physiological and pharmacological concentrations of EGCG (1.0 g/l, 0.1 g/l, 0.02 g/l and 0.002 g/l).

Results. We report co-regulation of EGCG and 67LR, which is known to be an EGCG receptor. siRNA selectively and highly significantly suppressed expression of 67LR under the impact of EGCG in a synergetic manner.

Conclusions. Our findings suggest that 67LR expression is regulated by EGCG via a negative feedback loop. The explicit occurrence of this effect in synergy with a small RNA pathway and a plant-derived drug reveals a new mode of action. Our findings may help to provide insights into the many unsolved health-promoting activities of other natural pharmaceuticals.

Keywords: cancer; EGCG; IPEC-J2; miRNA; RNA interference

Background

Studies assessing the beverage brewed from the leaves of the tea plant Camellia sinensis and its health-promoting effect are almost innumerable. It is assumed that among other constituents, the major effector of ‘green’ tea is the polyphenol epigallocatechin gallate (EGCG). One liter of green tea in a common preparation (1g tea/100ml water) contains approximately 300–1000 mg of this secondary plant compound [1, 2]. Therewith, it provides the major share of all tea catechins. The role of green tea, and particularly EGCG, as part of a cancer-preventive diet has been well researched [3-5]. Molecular targets of the green tea polyphenols are proposed [6-8], but solid knowledge about the underlying anticancer mechanisms is still missing. In 2004, a new candidate associated with EGCG was revealed [9]: the 67kDa laminin receptor (67LR). Tachibana et al. showed that this protein specifically binds EGCG among other tea catechins. Furthermore, a transmembrane signaling pathway was postulated in which EGCG induces the activation of myosin phosphatase through 67LR and hence develops its anticancer potential via inhibition of cell proliferation [10].

Indeed, in the scope of cancer research, 67LR has been well studied [11]. It is well known that this protein is overexpressed on the surface of cancer cells [12-15]. Thus, the involvement of 67LR in metastasis formation has been highly investigated. During this process, an invading tumor cell binds to its target tissue mediated by the local surface proteins. As laminin is a major component of the basement membrane, it was shown that enhanced expression of 67LR promotes metastasis [16]. This can be explained by the whole mechanism of the tumor invasion process. After the attachment of the circulating cancer cell, a rearrangement of the basement membrane occurs. Thereby one determining factor is the binding of laminin to 67LR. As a local consequence, laminin undergoes conformational changes and can subsequently be degraded by proteases [17]. Thereafter, the tumor cell can invade the target tissue. While examining the role of 67LR in target tissue binding during metastasis it could be shown that a 67LR-derived peptide called peptide G increases the metastatic potential in cell culture experiments [18]. Considering the fact that peptide G represents the laminin binding site of 67LR, this underlines the invasion model. In contrast, a

synthetic laminin pentapeptide (YIGSR) corresponding to the binding domain of laminin was assigned as a competitive metastasis inhibitor [19].

Taken together, it becomes clear that downregulation of 67LR provides a gateway for metastasis prevention. In the work of Chen et al. this basic effect has already been demonstrated [20]. Considering the multiple clues for the cancer-preventative effect of green tea, and regarding the interaction of EGCG and 67LR, we focused on the question as to whether tea catechin can influence the expression of 67LR in the gastrointestinal tract. We conducted qRT-PCR expression analysis combined with an RNAi-knockdown model to evaluate the anti-metastatic potential of EGCG via modulation of 67LR expression in vitro using the porcine intestinal epithelial cell line IPEC-J2.

Methods

Knockdown assays

The jejunal-derived JPEC-J2 cells [21] were maintained in Dulbecco's modified eagle medium (DMEM)/Ham's F-12 (1:1) (PAA, Pasching, Austria) supplemented with 5% fetal bovine serum (FBS; PAA), 2mM L-glutamine (PAA) and 100 U/ml penicillin/streptomycin (PAA) at 37 °C,100% humidity and 5% CO_2. This cell line was kindly provided by Dr Karsten Tedin (FU Berlin). Only cells that had been passaged ten times or less were used. The cell culture assay was designed on multiwell tissue culture plates (48W) from Greiner Bio-One (Frickenhausen, Germany) with a substrate area of $1cm^2$. In these, 5×10^4 IPEC-J2 cells were seeded in 500µl of cell culture media, and after 48 h of settlement the desired knockdown treatment was applied together with fresh media. For gene knockdown, we used adenoviral vectors which induce siRNA expression in the target cell line in an optimized multiplicity of infection (MOI) of 400 [22]. We obtained the methodology for the gene silencing technology from SIRION-BIOTECH (Martinsried, Germany), with which we produced an individual knockdown virus targeting 67LR transcript [NCBI accession number: NM_001037146], termed '67lr-KD' in this manuscript. A second targeting knockdown was designed as a positive control, designated 'control-KD', and targeted IKBKB [NCBI accession number: NM_001099935]. A third knockdown served as negative control and represented a non-targeting virus (named 'NV"'). The NV was identical to the two targeting knockdown viruses (overall named 'TV') but was unable to induce RNA interference due to leakage of a siRNA-insert. This negative control solely evoked the effects accompanying viral infection. At 48 h post-infection, we treated the cells with different concentrations (1.0 g/l, 0.1 g/l, 0.02 g/l, 0.002 g/l) of EGCG (Sigma-Aldrich St. Louis, USA) diluted in 400µl fresh media, following washing with 600µl of prewarmed PBS (pH 7.5, without Ca & Mg; PAA). Here, EGCG treatment is abbreviated to 'EGCG', and the corresponding media control to 'MEDIA'. For the assay layout, EGCG treatment and the media control were combined with a targeting virus or the non-targeting virus control, respectively. For the targeting viruses, both variants (targeting 67LR and the positive control) were applied. The resulting assay layout consisted of the

following treatment groups: MEDIA/NV, MEDIA/TV, EGCG/NV & EGCG/TV; with TV = 67lr-KD or control-KD. All treatment variations were performed in triplicate (three cell culture wells). Cells were harvested for total RNA extraction 6 h after EGCG treatment. This included another washing step of the cell layer with PBS, followed by direct cell lysis with 350µl of RLT buffer (RNeasy Mini Kit, Qiagen, Hilden, Germany). RNA was prepped according to the manufacturers' instructions and then diluted to 10ng/µl (NanoDrop ND-1000 spectrophotometer, PEQLab Biotechnologie GmbH, Erlangen, Germany) for subsequent gene expression analysis.

Gene expression analysis

Prior to gene expression analysis by quantitative real-time polymerase chain reaction (qRT-PCR), the RNA integrity was checked using a RNA nano LABchip on an Agilent 2100 Bioanalyzer (Agilent, Santa Clara, United States). Samples were prepared using a SuperScript III Platinum SYBR Green One-Step qRT-PCR Kit (Invitrogen, Karlsruhe, Germany), and analyzed using a Corbett Rotorgene 3000 (Corbett Life Science, Sydney, Australia). The sample volume of 10µl contained 38ng RNA, 5µl SYBR-Mix and 10 pmol primer mix (67LR [NCBI accession number: NM_001037146], forward primer: AGCGAGCTGTGCTGAAGTTT & reverse primer: GTGAGCTCCCTTGTTGTTGC; IKBKB [NCBI accession number: NM_001099935], forward primer: GGCGAACAGAGATTAATACACAAA & reverse primer: GTGCCGAAGCTCCAGTAGTC). The cycler program included a 10 min reverse transcription reaction at 50°C followed by a 5 min denaturation step at 95°C. Subsequently, under continuous fluorescence measurement, 40 amplification cycles (denaturation 95°C/10 s, annealing 60°C/10 s, extension 72°C/15 s) were performed, followed by a terminal melting curve measurement from 40°C to 95°C (in 0.5°C steps with a lag time of 2 sec). All qRT-PCR experiments were performed in duplicate (two one-step qRT-PCRs). The raw data were obtained using Rotor-Gene 6 software (Corbett Life Science, Sydney, Australia) via the implemented comparative quantification algorithm. Furthermore, the melting curve analysis of the Rotor-Gene 6 software was consulted for control of primer specificity. Relative changes in gene expression (shown as percentages) were determined under the terms of the $^{\Delta\Delta}$Cq method [23]. The Cq value

displayed for the cycle number was required by the fluorescence signal of a single qPCR sample to cross a predefined threshold [24, 25]. The chosen reference genes were Histone H3 ([NCBI accession number: XM_003356519], forward primer: ACTGGCTACAAAAGCCGCTC, and reverse primer: ACTTGCCTCCTGCAAAGCAC) and GAPDH ([NCBI accession number: XM_003358301], forward primer: AGATCCAGGATAAGGAAGGCA, and reverse primer: GCTCCACCTCCAGGGTGAT). All primers were generated by Eurofins MWG Operon (Ebersberg, Germany).

Statistical data evaluation

The plots visualizing gene expression indicate mean values from repeated measurements. Thereby, the replicates are specified as ”n = (a) x (b) x (c)”. These variables stand for the number of assays included (a), the cell culture replicates (b) and the qRT-PCR reactions conducted (c). Significant changes through treatments were ascertained with paired *t*-tests (SPSS 19.0, IBM Corporation, Armonk, USA), and resulting *P*-values are indicated by asterisks, as follows: $P \leq 0.001$ = extremely significant (***), $P \leq 0.01$ = highly significant (**), $P \leq 0.05$. = significant (*), $P > 0.05$ = not significant (n.s.). For Figure 3b, one-way ANOVA was performed (SPSS 19.0, IBM Corporation, Armonk, USA) to test the differences between the EGCG concentrations; the letters a, b, and c indicate extremely significant intermediate variances ($P \leq 0.001$). The assay data were additionally analyzed by principal component analysis (PCA) using GenEx software (version 5.3.2.13, MultiD, Göteborg, Sweden). Therefore, mean centered $^{\Delta}$Cq values were applied [26]. PCA is a statistical visualization method for multivariable data sets, which reduces the dimensionality while exposing the maximal variation embedded [27].

Results and discussion

In our cell culture assays, we combined pairwise drug treatments (EGCG *vs.* media control) with knockdowns (target genes *vs.* control virus). Thereby, the relative gene regulation (calculated by $2^{-\Delta\Delta Cq}$ given as percentage relative to control) caused by a combinatory treatment with target virus and/or EGCG was evaluated for every single treatment variant in reference to its particular control group. By this method, the net knockdown efficiency was calculated by normalizing target knockdown-treated samples containing one individual concentration of EGCG to the samples containing the same EGCG concentration but that were treated with the non-target control virus. In the same manner, the net effect of a drug treatment becomes clear when it is normalized within one virus treatment group to its media control partner. Figure 1 shows the mean values from repetitions of our cell culture assay, thereby data in Figure 1a was offset against the knockdown controls within one treatment (EGCG or media) variant to obtain the net knockdown on the corresponding target gene. The plot shows that the resulting downregulation was approximately 90% in wells treated solely with medium and the target virus for 67LR (MEDIA/TV, 67lr-KD) (mean of seven independent experiments). Interestingly, 67lr-KD efficiency was altered when EGCG was applied instead of pure media (EGCG/TV, 67lr-KD). The gene-silenced cells that were co-treated with EGCG showed an additional reduction in 67LR expression to result in a knockdown efficiency of 96%. At first, the step from 90% to 96% seems less impressive, but on closer analysis it represents a large change. For all expression plots, the value is presented on a logarithmic scale. Regarding the fact that relative change in mRNA expression is calculated, a remaining transcript level of 10% must be reduced by more than 50% to fall down to 4%.

In follow-up measurements, we clarified if this observation originated from an artifact resulted from the methodology applied. Therefore, we performed the assay with another target-knockdown, which did not target 67LR (shown in Fig. 1a as ‘control KD’). In this setting, EGCG had no significant effect on enhancing the knockdown efficiency, leading to the assumption that the combination of 67LR protein and its binding partner EGCG can promote synergetic downregulation. To demonstrate the co-action between 67LR and EGCG, the data underlying Figure 1a was adjusted to the media control within one knockdown scenario in the

plot from Figure 1b. Thus, the extent of the synergetic effect evoking 63% of relative residual 67LR mRNA expression as a mean value from ten independent experiments was revealed. In contrast the other treatment combinations where EGCG was applied in absence of the 67LR knockdown did not lead to substantial changes in relative expression.

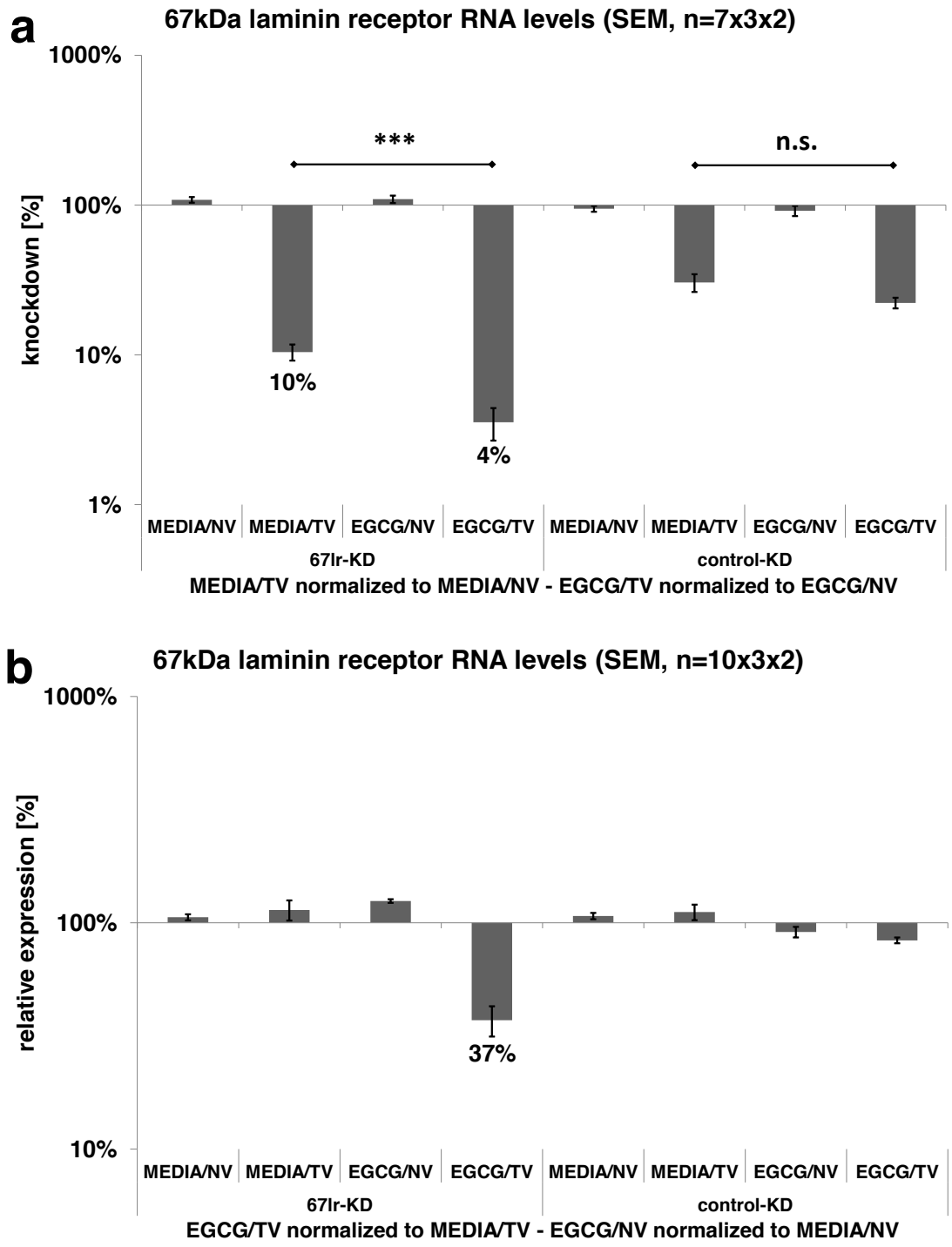

Figure 1. *Knockdown assays comparing 67lr-KD and control-KD under EGCG treatment. a) Pooled data from seven assays normalized to the non-targeting virus samples. This normalization revealed net knockdown effects. b) Pooled data from ten assays normalized to the media control samples. This normalization revealed the net regulation induced by the drug treatment. (Legend: EGCG = EGCG treatment, MEDIA = media control, NV = non-targeting virus, TV = targeting virus, 67lr-KD = 67LR knockdown, control-KD = control knockdown).*

To confirm our observations independent of normalization to any control groups (virus/drug), we consulted principal component analysis (PCA). With this statistical data evaluation it is possible to analyze the outcome of an assay by sample [26]. The PCA considers the collective variation in gene expression an RNA sample bears in reference to all genes measured from it. Therefore, our expression data were inserted in the PCA as raw data solely corrected against the reference genes but not against any control groups of the underlying cell culture assay. The findings from this independent kind of data analysis were in accordance with those from the relative fold changes shown in Figure 1ab. The PCA-plot in Figure 2 shows data from an assay that also includes eight treatment variants (MEDIA/NV, MEDIA/TV, EGCG/NV & EGCG/TV; with TV = 67lr-KD and/or control-KD) each replicated six times (3 cell culture wells × 2 qRT-PCR reactions). For each of these 48 datapoints (samples), the gene expression of two reference genes and two target genes (67lr-KD, control-KD) was ascertained. In Figure 2a, the gene expression data including the reference genes and the control-KD gene was analyzed. The resulting image of the PCA shows data clustering in two clouds: (I) with (MEDIA/TV [control-KD] & EGCG/TV [control-KD]) or (II) without (MEDIA/NV, EGCG/NV & MEDIA/TV [67lr-KD], EGCG/TV [67lr-KD]) the considered control KD. In contrast, the PCA considering the reference genes and the 67LR knockdown (67lr-KD) (Fig. 2b) reveals three data clusters: (I) the 67kd-KD combined with medium treatment (MEDIA/TV [67lr-KD]), (II) the 67kd-KD combined with EGCG treatment (EGCG/TV [67lr-KD]) and (III) samples not containing the considered 67LR-knockdown but treated with either media or EGCG (MEDIA/NV, EGCG/NV & MEDIA/TV [control-KD]). Thus, the additional separation into a third cloud is again induced exclusively under the synergy of 67lr-KD and EGCG.

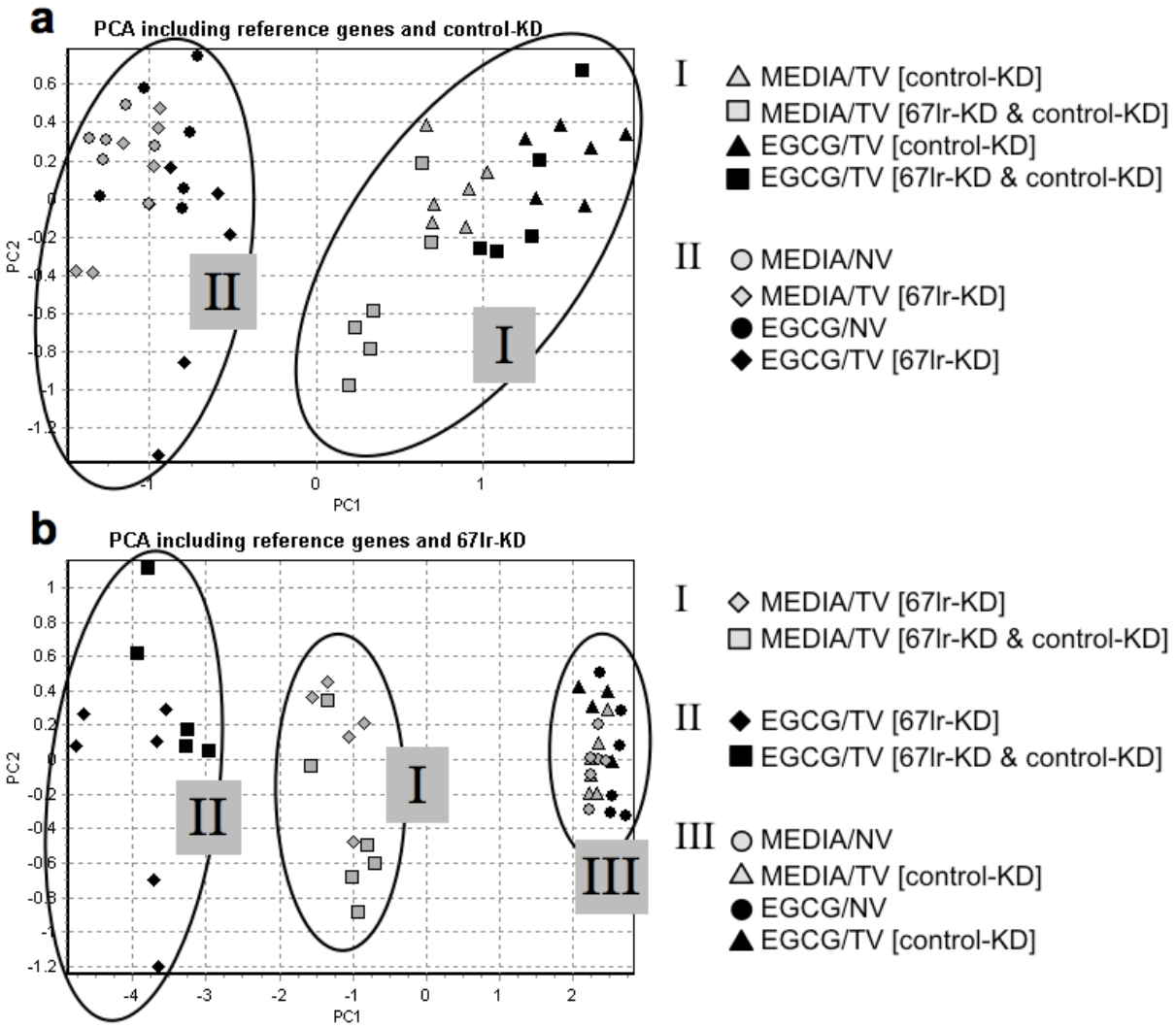

Figure 2. *Principal component analysis comparing the influence of EGCG on 67LR versus the control gene. a) For the control gene, the impact of the drug treatment was dependent on whether a gene knockdown was applied (I) or not (II). b) For the 67LR gene, siRNA-induced downregulation altered the extent of its synergy with EGCG (I) and a new data cluster was separated from the samples solely treated with the 67lr-KD (II). When no knockdown was applied, EGCG did not affect the gene regulation (III) in accordance with Figure 2a. (Color code: black labels indicate samples containing EGCG, grey labels indicate no EGCG; Legend: EGCG = EGCG treatment, MEDIA = media control, NV = non-targeting virus, TV = targeting virus, 67lr-KD = 67LR knockdown, control-KD = control knockdown).*

The next question was to ascertain if EGCG was able evoke the same effect at concentrations lower than that measured in freshly brewed green tea [1, 2]. Therefore, we added EGCG at concentrations from one (0.1 g/l) up to three potencies (0.02 g/l & 0.002 g/l) below the actual tea content (Fig. 3). Again, we observed 67LR/EGCG synergy, but this effect was less distinct. At an EGCG concentration of 0.1 g/l, we observed a 3.7-fold reduction in downregulation of 67LR (Fig. 3a), and at 0.02 g/l & 0.002 g/l, we were still able to measure a significant effect (P=0.001; Fig. 3b).

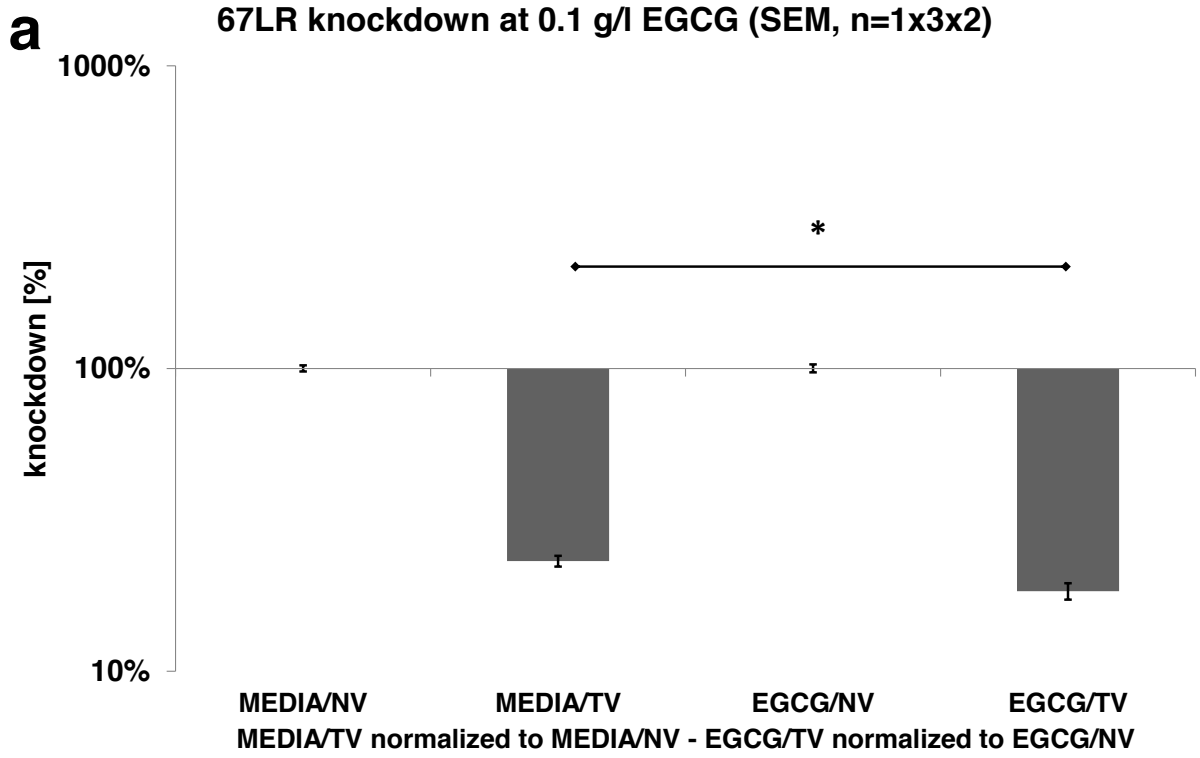

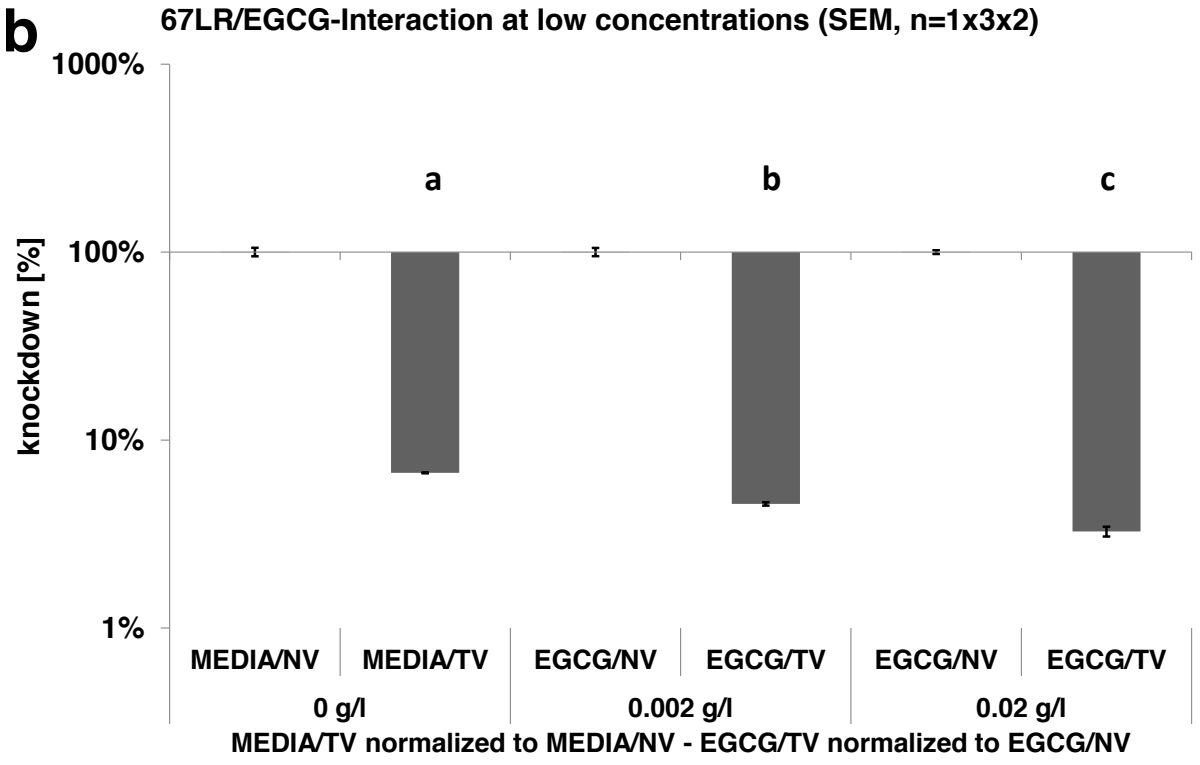

Figure 3. *67LR/EGCG-synergy when the secondary plant metabolite was added at potencies below the actual EGCG-content of freshly brewed green tea. (Legend: EGCG = EGCG treatment, MEDIA = media control, NV = non-targeting virus, TV = targeting virus, 67lr-KD = 67LR knockdown, control-KD = control knockdown).*

Since the discovery of intra- and intercellular short ribonucleic acids, many different species of non-coding but functional active small RNAs have been identified [28]. Among these, miRNAs and siRNAs are involved in negative gene regulation. However, with increasing knowledge from in vitro studies, pathways that once initially seemed distinct have become blurred, revealing the extent of the complexity as to how small RNAs act in gene regulation. miRNAs were originally described to bind the 3´UTR alone, but there is now evidence that miRNAs can also act upon the coding region of a transcript [29]. Within the complex machinery of posttranscriptional gene regulation, it has been shown that certain miRNA signatures can serve as biomarkers for oncology [30]. Thus, small RNA synthesis or leakage can affect cancer and influence metastasis positively or negatively depending on the targeted gene.

Our results indicate EGCG significantly influences siRNA-induced downregulation of 67LR expression. Since a close relation of this protein and its transcript has been ascertained [31], these findings show a correlation between the plant compound and its receptor [9] via a negative feedback loop. Reasonably the anti metastatic potential of green tea as a daily diet develops best outgoing from the gastrointestinal tract. In regard to its carcinogenic potential, enhanced expression levels of 67LR have been associated with metastasis formation in different tissues, including the intestine [32].

Considering our findings that EGCG acts synergistically and promotes siRNA-induced downregulation of 67LR protein, a new concept of how secondary plant metabolites act in cancer prevention can be established. The complex feedback control system of miRNA regulation of oncogenes might be influenced selectively in synergy with plant compounds, and may provide clues to the potential anti-carcinogenic mechanism of EGCG. [2].

Conclusions

Metastasis presents the largest challenge in terms of mortality in the treatment of cancer. In this study, we identified a significant correlation of EGCG co-regulation with siRNA-silenced expression of 67LR in a porcine intestinal cell line. As pigs are monogastric animals, IPEC-J2 cells represent a model conferrable to the human gastrointestinal tract. As part of a cancer-preventive diet, green tea may act via synergic action of small RNA regulation and the properties of an herbal-derived drug, EGCG. This synergy may help to provide clues as to the mode of action of pharmacologically-applied plant compounds.

List of abbreviations

3´UTR, three prime untranslated region; 67LR, 67kDa laminin receptor; EGCG, epigallocatechin gallate; MOI, multiplicity of infection; PCA, principal component analysis; RNAi, RNA interference; RT-qPCR, quantitative reverse transcription real-time polymerase chain reaction; siRNA, small interfering RNA; EGCG, EGCG treatment; MEDIA, media control; NV, non-targeting virus; TV, targeting virus; 67lr-KD, 67LR knockdown; control-KD, control knockdown.

Competing interests

The authors declare that they have no competing interests.

Authors' contributions

The assays in this study where designed and conducted by JM. The data evaluation was performed by JM. The manuscript was drafted by JM and supervised by MP.

Acknowledgments

This study was supported by a grant from the Vereinigung zur Förderung der Milchwissenschaftlichen Forschung an der Technischen Universität München e.V.. The authors gratefully thank Dr. Karsten Tedin for providing us with the IPEC-J2 cells. Furthermore, we thank Katrin Danowski for guidance with the SPSS software and Johannes Meier for performing additional knockdown-assays.

References

1. Sang S, Lambert JD, Ho CT, Yang CS: **The chemistry and biotransformation of tea constituents**. *Pharmacol Res* 2011, **64**(2):87-99.
2. Yang CS, Wang H, Li GX, Yang Z, Guan F, Jin H: **Cancer prevention by tea: Evidence from laboratory studies**. *Pharmacol Res* 2011, **64**(2):113-122.
3. Donaldson MS: **Nutrition and cancer: a review of the evidence for an anti-cancer diet**. *Nutr J* 2004, **3**:19.
4. Shankar S, Ganapathy S, Srivastava RK: **Green tea polyphenols: biology and therapeutic implications in cancer**. *Front Biosci* 2007, **12**:4881-4899.
5. Yuan JM, Sun C, Butler LM: **Tea and cancer prevention: epidemiological studies**. *Pharmacol Res* 2011, **64**(2):123-135.
6. Beltz LA, Bayer DK, Moss AL, Simet IM: **Mechanisms of cancer prevention by green and black tea polyphenols**. *Anticancer Agents Med Chem* 2006, **6**(5):389-406.
7. Kazi A, Smith DM, Daniel K, Zhong S, Gupta P, Bosley ME, Dou QP: **Potential molecular targets of tea polyphenols in human tumor cells: significance in cancer prevention**. *In Vivo* 2002, **16**(6):397-403.
8. Park AM, Dong Z: **Signal transduction pathways: targets for green and black tea polyphenols**. *J Biochem Mol Biol* 2003, **36**(1):66-77.
9. Tachibana H, Koga K, Fujimura Y, Yamada K: **A receptor for green tea polyphenol EGCG**. *Nat Struct Mol Biol* 2004, **11**(4):380-381.
10. Umeda D, Yano S, Yamada K, Tachibana H: **Green tea polyphenol epigallocatechin-3-gallate signaling pathway through 67-kDa laminin receptor**. *J Biol Chem* 2008, **283**(6):3050-3058.
11. Montuori N, Sobel ME: **The 67-kDa laminin receptor and tumor progression**. *Curr Top Microbiol Immunol* 1996, **213 (Pt 1)**:205-214.
12. Hand PH, Thor A, Schlom J, Rao CN, Liotta L: **Expression of laminin receptor in normal and carcinomatous human tissues as defined by a monoclonal antibody**. *Cancer Res* 1985, **45**(6):2713-2719.

13. Malinoff HL, Wicha MS: **Isolation of a cell surface receptor protein for laminin from murine fibrosarcoma cells**. *J Cell Biol* 1983, **96**(5):1475-1479.

14. Sobel ME: **Differential expression of the 67 kDa laminin receptor in cancer**. *Semin Cancer Biol* 1993, **4**(5):311-317.

15. Terranova VP, Rao CN, Kalebic T, Margulies IM, Liotta LA: **Laminin receptor on human breast carcinoma cells**. *Proc Natl Acad Sci U S A* 1983, **80**(2):444-448.

16. Liotta LA: **Tumor invasion and metastases - role of the extracellular matrix: Rhoads Memorial Award lecture**. *Cancer Res* 1986, **46**(1):1-7.

17. Nelson J, McFerran NV, Pivato G, Chambers E, Doherty C, Steele D, Timson DJ: **The 67 kDa laminin receptor: structure, function and role in disease**. *Biosci Rep* 2008, **28**(1):33-48.

18. Berno V, Porrini D, Castiglioni F, Campiglio M, Casalini P, Pupa SM, Balsari A, Menard S, Tagliabue E: **The 67 kDa laminin receptor increases tumor aggressiveness by remodeling laminin-1**. *Endocr Relat Cancer* 2005, **12**(2):393-406.

19. Iwamoto Y, Robey FA, Graf J, Sasaki M, Kleinman HK, Yamada Y, Martin GR: **YIGSR, a synthetic laminin pentapeptide, inhibits experimental metastasis formation**. *Science* 1987, **238**(4830):1132-1134.

20. Chen FX, Qian YR, Duan YH, Ren WW, Yang Y, Zhang CC, Qiu YM, Ji YH: **Down-regulation of 67LR reduces the migratory activity of human glioma cells in vitro**. *Brain Res Bull* 2009, **79**(6):402-408.

21. Schierack P, Nordhoff M, Pollmann M, Weyrauch KD, Amasheh S, Lodemann U, Jores J, Tachu B, Kleta S, Blikslager A *et al*: **Characterization of a porcine intestinal epithelial cell line for in vitro studies of microbial pathogenesis in swine**. *Histochem Cell Biol* 2006, **125**(3):293-305.

22. Müller J, Thirion C, Pfaffl MW: **Electric cell-substrate impedance sensing (ECIS) based real-time measurement of titer dependent cytotoxicity induced by adenoviral vectors in an IPI-2I cell culture model**. *Biosens Bioelectron* 2011, **26**(5): 2000-2005.

23. Livak KJ, Schmittgen TD: **Analysis of relative gene expression data using real-time quantitative PCR and the 2(-Delta Delta C(T)) Method**. *Methods* 2001, **25**(4): 402-408.

24. Freeman WM, Walker SJ, Vrana KE: **Quantitative RT-PCR: pitfalls and potential**. *Biotechniques* 1999, **26**(1):112-122, 124-115.

25. Bustin SA, Benes V, Garson JA, Hellemans J, Huggett J, Kubista M, Mueller R, Nolan T, Pfaffl MW, Shipley GL *et al*: **The MIQE guidelines: minimum information for publication of quantitative real-time PCR experiments**. *Clin Chem* 2009, **55**(4): 611-622.

26. Bergkvist A, Rusnakova V, Sindelka R, Garda JM, Sjogreen B, Lindh D, Forootan A, Kubista M: **Gene expression profiling - Clusters of possibilities**. *Methods* 2010, **50**(4):323-335.

27. Jolliffe IT: **Introduction, Principal Component Analysis**. In.: Springer New York; 2002: 1-9.

28. Finnegan EJ, Matzke MA: **The small RNA world**. *J Cell Sci* 2003, **116**(Pt 23): 4689-4693.

29. Fang Z, Rajewsky N: **The impact of miRNA target sites in coding sequences and in 3'UTRs**. *PLoS One* 2011, **6**(3):e18067.

30. Aigner A: **MicroRNAs (miRNAs) in cancer invasion and metastasis: therapeutic approaches based on metastasis-related miRNAs**. *J Mol Med (Berl)* 2011, **89**(5): 445-457.

31. Wewer UM, Liotta LA, Jaye M, Ricca GA, Drohan WN, Claysmith AP, Rao CN, Wirth P, Coligan JE, Albrechtsen R *et al*: **Altered levels of laminin receptor mRNA in various human carcinoma cells that have different abilities to bind laminin**. *Proc Natl Acad Sci U S A* 1986, **83**(19):7137-7141.

32. Rao M, Manishen WJ, Maheshwari Y, Sykes DE, Siyanova EY, Tyner AL, Weiser MM: **Laminin receptor expression in rat intestine and liver during development and differentiation**. *Gastroenterology* 1994, **107**(3):764-772.

Special Issue Paper

Flavour and Fragrance Journal

Received: 2 January 2012, Revised: 3 June 2012, Accepted: 4 June 2012 Published online in Wiley Online Library

(wileyonlinelibrary.com) DOI 10.1002/ffj.3109

Investigation into the metabolism of 1,8-cineole in an intestinal cell culture model and acquisition of its immune-modulatory effect via gene expression analysis†

Jakob Müller,[a]* Natalie Gruner,[b] Isabella Almstätter,[a] Frauke Kirsch,[b] Andrea Buettner[b,c] and Michael W Pfaffl[a]

ABSTRACT: 1,8-Cineole, a common and widely used odorant with antiphlogistic and anti-inflammatory properties, was investigated in this study with regard to potential physiological effects targeting mainly its intestinal effects. Accordingly, the aim of the study was to utilize a combinatory methodological approach to both monitor potential biotransformatory effects on a chemo-analytical basis, as well as physiological and immunological tools to monitor further effects of biofeedback. Reverse transcription quantitative real-time polymerase chain reaction was used to monitor the occurrence of relative expression changes for particular marker genes, following 1,8-cineole treatment. Furthermore, a potential effect of 1,8-cineole on the proliferation and fitness of the intestinal cells using impedance sensing was studied. Generally, our studies showed that the applied model system did neither lead to any significant metabolite formation, nor did the applied dosages result in any major modifications with regard to gene expression. Also, it was shown that cineole had no effect on the intestinal porcine epithelial cells applied in pharmacological or physiological concentrations; neither during the attachment and spreading process nor on confluent cell layers. Only the exposure to high concentrations of cineole (> 1 g/l) affected the cells and led to massive cell detachment. Overall, our studies show that even common higher 1,8-cineole dosages do not seem to lead to any major physiological or aversive response, only until a critical concentration is reached that then directly leads to cell death within the intestinal model. Copyright © 2012 John Wiley & Sons, Ltd.

Keywords: hydroxycineole; metabolism; gas chromatography–mass spectrometry; RT-qPCR; ECIS; stable isotope dilution assay

Introduction

1,8-Cineole (also named eucalyptol or 1,3,3-trimethyl-2-oxabicyclo [2.2.2]octane) is a potent and characteristic odour substance in diverse plant materials that are also part of the human diet. It is also frequently used for its positive physiological effects in aroma formulations and as a pharmacological agent.[1,2]

1,8-Cineole is the major constituent of oil from leaves of the eucalyptus tree (*Eucalyptus* sp.), and concentrations may reach 84%.[2] As a result, *Eucalyptus* sp. is the major natural source of this volatile secondary plant compound. However, other edible plants such as thyme (*Thymus* sp.) or sage (*Salvia* sp.) also contain this odorous substance.[3,4] Among other applications 1,8-cineole is used as a therapeutic agent in connection with respiratory diseases.[5,6] Today, different pharmacological preparations based on 1,8-cineole are available (e.g. Soledum® from Klosterfrau Healthcare Group, Köln, Germany; GeloMyrtol® from G. Pohl-Boskamp GmbH & Co, Hohenlockstedt, Germany). They are usually applied orally as enteric coated dragées. In this contained form, the drug traverses the stomach and is eventually released into the small intestine where absorption takes place.

The anti-inflammatory, antiphlogistic and anti-infectious capacity of 1,8-cineole is a proven and commonly utilized effect.[2,5,7] Nevertheless, other potential physiological aspects of 1,8-cineole have not been addressed so far. However, when keeping the relatively high dosages of common 1,8-cineole treatments in mind, it is more than justified to look for other possible effects, or at least to exclude the potential occurrence of any negative physiological significance.

With regard to the further fate of cineole in the human body after ingestion, some studies demonstrated that 1,8-cineole is metabolized by the cytochrome P450 system in the mammalian liver.[8,9] Also, metabolite profiles in plasma were investigated with regard to their qualitative and quantitative composition.[10] However, the potentially diverse physiological and immunological roles of 1,8-cineole remained largely unclarified.

* Correspondence to: Jakob Müller, Physiology Weihenstephan, Technical University Munich, Research Center for Nutrition and Food Science, Weihenstephaner Berg 3, 85350 Freising, Germany. E-mail: jakob.mueller@wzw.tum.de

† *This article is published in Flavour and Fragrance Journal as Part II of Special Issue: 13th Weurman Flavour Research Symposium, Zaragoza, Spain, 27th–30th September 2011, edited by Vicente Ferreira (University of Zaragoza).*

[a] Physiology Weihenstephan, Technical University Munich, Research Center for Nutrition and Food Science, Weihenstephaner Berg 3, 85350 Freising, Germany

[b] Department of Chemistry and Pharmacy – Emil Fischer Center, University of Erlangen–Nuremberg, Schuhstr. 19, 91052 Erlangen, Germany

[c] Fraunhofer Institute for Process Engineering and Packaging (IVV), 85354 Freising, Germany

The small intestine primarily represents a physiological interface where the first immune response is initiated. Accordingly, one aim of our study was to elucidate whether 1,8-cineole is metabolized immediately after its uptake through the intestinal epithelium and to determine which local physiological pathways are further affected. To achieve this goal, the porcine epithelial cell line IPEC-J2 served as a model for our study.[11] These cells originate from the mid-jejunal epithelium of a neonatal, unsuckled piglet (*Sus scrofa domestica*). Due to the fact that pigs are monogastric animals, this model provides a close similarity to the human intestinal tract.

As the experimental set-up we treated the cells with pharmacologically oriented dosages (0.1 g/l and 1 g/l) of 1,8-cineole in order to achieve distinct effects. The 1,8-cineole concentrations chosen were carefully selected based on different values in the literature and provided by established pharmaceutical formulations. The basis of all calculations was an intake volume of 500 ml. Based on this volume all amounts of cineole in nutrition or medicine were calculated for their volumes in the particular culture vessel. For example, one capsule of Soledum® with 100 mg 1,8-cineole or Soledum forte® with 200 mg consumed with a 500 ml volume, results in a concentration of 0.2 g/l or 0.4 g/l, respectively. Two capsules of GeloMyrtol® contain 60 mg 1,8-cineole, which corresponds to a concentration of 0.12 g/l. Accordingly, concentrations were selected to encompass the span of these concentration ranges. Additionally, it should be kept in mind that under 'real-life' conditions the ingested capsule most likely opens instantaneously within the small intestine, where it is designed to dissolve. Accordingly, it is most likely that the full dosage (100 or even 200 mg of cineole) can be liberated locally at once so that the initial local concentration is likely to be very high. The higher concentration was also chosen as being close to the maximal non-lethal concentration (1.2 g/l) of 1,8-cineole for IPEC-J2 cells as determined within the present study. The chosen time intervals for exposure were also selected to be in accord with time periods that are representative of gastrointestinal passage periods (control experiment at 0 h of incubation, then sampling at 3 h, 6 h, 9 h and 24 h). Gas chromatography–mass spectrometry (GC-MS) was used to determine the potential of an initial metabolism of the target substance in the chosen tissue culture model. The metabolite profiles were collected quantitatively and qualitatively as well as over time. Additionally, we applied reverse transcription quantitative real-time polymerase chain reaction (RT-qPCR) in order to monitor the potential of relative expression changes for particular proliferation, apoptosis, and immune relevant marker genes subsequent to the 1,8-cineole treatment.

Summarizing the above, the current paper deals with combining chemo-analytical and physiological approaches to characterize potential intestinal effects of food ingredients, specifically odorants. Thereby, we focused on the application of techniques that had not previously been used in a comparative setting in order to monitor the odorant effects, and to highlight new potential strategies in this rapidly developing field of research.

Experimental

Chemicals and Materials

α2-Hydroxy-1,8-cineole, 7-hydroxy-1,8-cineole and 9-hydroxy-1,8-cineole and tri-fold deuterated 2α-hydroxy-1,8-cineole were kindly supplied by Horst and Rychlik.[10] α3-Hydroxy-1,8-cineole was a generous gift from C.J. Wallis and R.M. Carman (University of Queensland, Brisbane, Australia). 2,3-Dehydro-1,8-cineole, 2-oxo-1,8-cineole, 3-oxo-1,8-cineole, β2-hydroxy-1,8-cineole and 4-hydroxy-1,8-cineole were synthesized as described by Kirsch *et al.*[12] *n*-Alkanes C6–C28 for determination of retention indices were from Aldrich (Steinheim, Germany). Dichloromethane p.a. and anhydrous sodium sulfate were from Th. Geyer GmbH & Co. KG (Renningen, Germany).

Cell Culture

As the intestinal model the non-transformed porcine jejunal cell line IPEC-J2[11] was used. (This cell line was obtained from Dr Karsten Tedin, FU Berlin.) The cells were cultured in Dulbecco's modified Eagle medium (DMEM)/Ham's F-12 (1:1) (PAA, Pasching, Austria) supplemented with 5% fetal bovine serum (PAA), 2 mM L-glutamine (PAA) and 100 U/ml penicillin–streptomycin (PAA) at 37°C,100% humidity and 5% CO_2. Cells were sub-cultured after 72 h at 80% confluency. Only IPEC-J2 cells passaged fewer than ten times were used.

Cineole Metabolism Assay

For the cineole metabolism assays the IPEC-J2 were seeded in 75 cm^2 (250 ml) cell culture dishes (Greiner Bio-One) at a density of 1×10^6 cells/20 ml media. After 72 h, when a confluence level of 95% was attained, the medium was renewed and subsequently the cells were treated. Two different cineole concentrations were applied: 0.1 g/l and 1.0 g/l. After incubation for 0 h, 3 h, 6 h, 9 h and 24 h the cells were detached with a cell scraper.

Metabolite Extraction

For the dichloromethane extraction of potentially metabolized cineole, 20 ml of the medium containing the detached cells were mixed with 20 ml (1:1) dichloromethane in a glass separating funnel, and subsequently extracted. During addition of the solvent the cells dissolved immediately. To those samples which were used for cineole quantification an internal standard in dichloromethane (tri-fold deuterated 2-α-hydroxy-1,8-cineole, 400 ng/ml) was added before the first extraction. Three successive extractions were applied and the three solvent fractions were pooled.

Sample Preparation for Gas Chromatography Analysis by Solvent Assisted Flavour Evaporation

Solvent-assisted flavour evaporation[13] was applied for the fast and careful isolation of cineole and potential metabolites from the respective cell culture samples. The pooled dichloromethane phases were subjected to the distillation process. Each sample extract was dried over anhydrous Na_2SO_4 and then distilled using the solvent-assisted flavour evaporation apparatus at 50°C and approximately 1×10^{-4} mbar. Evaporated volatiles were frozen with liquid nitrogen and, after thawing, the extracts were further concentrated by microdistillation according to Bemelmans[14] at 50°C to a total volume of about 100 µl.

To evaluate the possible presence of metabolites in the cineole standard, the cineole reference substance was diluted to achieve the maximum concentration in the final sample extracts (100 mg/ml). Then, this sample was evaluated by using GC-MS analysis to screen for the presence of potential metabolites.

Gas Chromatography–Mass Spectrometry

GC-MS analysis was performed with an Agilent MSD quadrupole system (GC 7890A and MSD 5975C; Agilent Technologies, Waldbronn, Germany) with a GERSTEL CIS 4C injection system and GERSTEL MPS 2 autosampler (GERSTEL GmbH & Co. KG, Duisburg, Germany). The software used for recording and analysis was MSD ChemStation E.02.00.493 (Agilent Technologies). The analytical capillaries used were DB-FFAP and DB-5

(30 m length, 0.25 mm inner diameter, 0.25 μm film thickness; J&W Scientific, Fisons Instruments, Mainz–Kastel, Germany). An uncoated, deactivated fused silica capillary was used as a precolumn (0.53 mm inner diameter, 0.5 to 3.5 m length) and changed regularly according to accumulated impurities. Helium was used as the carrier gas.

Total flow of the system was 1.3 ml/min, which went directly into the mass spectrometer. The temperature of the mass spectometer transfer line was set to 200°C, the temperature of the source was 200°C and that of the quadrupole to 150°C. The CIS injection system was used like a cold on-column injector and its temperature was set to a start temperature of 40°C. Electron ionization mass spectra were generated in full scan mode (*m/z* range 40 to 250) at 70 eV ionization energy.

The oven starting temperature was 40°C, held for 2 min. Then, the temperature was raised at 6°C/min until 170°C and again at 40°C/min to 230°C with 5 min holding time for DB-FFAP, or directly to 250°C with 5 min holding time for DB-5. The injection volume was 1 μl.

Identification of Potential Metabolites

Metabolites of 1,8-cineole were identified by comparison of retention indices on two analytical capillaries of different polarities (DB-FFAP and DB-5) and by comparison of electron ionization mass spectra with those of synthesized references.

Quantification of Potential Metabolites

Absolute quantification of metabolites with calibration curves for each substance was not possible due to limited amounts of the synthesized reference material. For relative quantification the peak area (extracted ion chromatogram) of the respective metabolite was normalized to that of the internal standard (deuterated 2-α-hydroxy-1,8-cineole) and multiplied with the employed concentration of the standard. This approach resulted in good estimations for the metabolite 2-α-hydroxy-1,8-cineole and was still acceptable for the other metabolites since in these experiments solely quantitative dimensions and not exact values were crucial.

Electric Cell-substrate Impedance Sensing

For determination of the minimal lethal dose for 1,8-cineole in the IPEC-J2 cell culture, electric cell-substrate impediance sensing (ECIS) technology[15] was applied. An ECIS-1600 (Applied BioPhysics, Troy, NY, USA) served as a platform, in combination with 8W10E arrays (Ibidi Integrated BioDiagnostics, Martinsried, Germany). These special eight-well cell culture dishes offer a substrate area of 0.8 cm^2 and are kept in the cell culture incubator under standard conditions (see above). In each well 1×10^5 cells were inoculated within 300 μl of media. Each cell culture well is coated with 10 gold microelectrodes, 250 μm in diameter, which detect the current flow through the media. The device was set to 30 kHz employing an AC source delivering 1 μA and an amplitude of 10 mV. The sampling interval was 60 s. In order to smooth the curves the data volume was later reduced by applying mean values for every 3 min during the time course. At confluence (the state at which cells in a cell culture dish have grown until they completely cover the bottom of the dish), the point of time was declared as the treatment starting point (indicated as 0 h in the figures). Different cineole concentrations (0.3, 0.5, 0.7, 1.0, 1.3, 1.7 and 2.0 g/l) were added diluted in cell culture media. Thereby, this step represented at the same time a media change. This addition of fresh media solution is an important step due to depletion of the media during the growth process of the cells from seeding until confluence is reached. The measurements for one concentration were performed in duplicate. All together the measurement recorded a time course for 72 h (12 h cell growth until confluence and 60 h under 1,8-cineole impact).

RT-qPCR Gene Expression Analysis

For the gene expression analysis 1×10^5 IPEC-J2 cells were seeded into CELLSTAR® 48-well cell culture dishes (Greiner Bio-One, Frickenhausen, Germany) in a volume of 600 μl. After 24 h when a confluence of 80% was reached they were treated with different cineole concentrations (0.0 g/l, 0.1 g/l and 1.0 g/l). The cineole was applied mixed with new cell culture media. All treatments were performed in triplicate. The cineole treated samples were incubated for 0, 3, 6 and 9 h, respectively.

Prior to RNA extraction the cineole-treated cell layer was washed with 600 μl of pre-warmed phosphate-buffered saline (pH 7.5, without calcium and magnesium) (PAA, Pasching, Austria). Afterwards, cells were harvested directly in 350 μl lysis buffer (RNeasy® Mini Kit; Qiagen, Hilden, Germany) and RNA was extracted according to the manufacturer's kit manual. RNA concentration was determined using the NanoDrop® ND-1000 spectrophotometer (PEQLab Biotechnologie GmbH, Erlangen, Germany) and RNA integrity was checked with the Agilent 2100 Bioanalyzer using the RNA nano LABchip (Agilent, Santa Clara, CA, USA). As an RT-qPCR platform the Corbett Rotorgene 3000 (Corbett Life Science, Sydney, Australia) was used in combination with the SuperSkript® III Platinum® SYBR® Green One-Step qRT-PCR Kit (Invitrogen, Karlsruhe, Germany). A sample volume of 10 μl containing 38 ng RNA, 5 μl SYBR-Mix and 10 pmol primermix (forward + reverse) (Eurofins MWG Operon, Ebersberg, Germany) was inserted. After a 10 min reverse transcription reaction at 50°C and a 5 min denaturation step at 95°C the PCR program included, under continuous fluorescence measurement, 40 amplification cycles (denaturation 95°C/10 s, annealing 60°C/10 s, extension 72°C/15 s) followed by a melting curve from 40°C to 95°C (in 0.5°C steps with a dwell time of 2 s). The measurement was performed in duplicate and data was collected with the Rotor-Gene 6 software (Corbett Life Science). The relative change in gene expression (shown as a percentage) was determined under the terms of the $\Delta\Delta C_q$ method.[16] The C_q value represents the number of cycles which are required by the fluorescence signal of a qPCR sample to cross a defined threshold.[17,18] Stably expressed histone H3 and ubiquitin served as reference genes. All analysed genes and corresponding primer sequences are shown in Table 1. Additionally, the data obtained were evaluated by principal component analysis (PCA) using the GenEx software (MultiD, Gothenburg, Sweden). Therefore the ΔC_q values were inserted and data was mean-centred to rows.[19] This statistical visualization tool reduces the dimensionality of a multivariable dataset while exposing the maximum expansion of variation present in a dataset.[20]

Results and Discussion

Monitoring of a Potential Biotransformation of 1,8-Cineole During Application to the Intestinal Cell Culture

Commercially available cineole, enriched from natural resources, might contain traces of natural derivatives. For this reason, the cineole standard was investigated with regard to the potential presence of derivatives or metabolites of 1,8-cineole prior to the actual incubation experiments. Indeed, nine derivatives of cineole could be detected in the cineole standard used in this study, albeit in trace concentrations of a factor of 10^4 to 10^6 lower than the 1,8-cineole itself as will be discussed below. These substances were 2,3-dehydro-1,8-cineole, 2-oxo-1,8-cineole, 3-oxo-1,8-cineole, α2-hydroxy-1,8-cineole, β2-hydroxy-1,8-cineole, α3-hydroxy-1, 8-cineole, 4-hydroxy-1,8-cineole, 7-hydroxy-1,8-cineole and 9-hydroxy-1,8-cineole.[12]

Additionally, control experiments with a dose of 1.0 g/l were carried out both on cineole in aqueous solution as well as in the culture medium of the intestinal cell line applied in this study, under the same incubation conditions at 37°C and 5% CO_2 atmosphere. In each case, the same profile of 1,8-cineole derivatives was detectable, as already found for the cineole standard itself. This was true for water and culture medium samples, respectively, all

Table 1. Forward (fwd) and reverse (rev) primer sequences for target and reference genes

Gene name	Abbreviation		Primer sequence	Fragment length (bp)	Accession number
Reference genes					
Histone H3	H3	fwd	ACTGGCTACAAAAGCCGCTC	232	XM_003356519
		rev	ACTTGCCTCCTGCAAAGCAC		
Ubiquitin	UQ	fwd	AGATCCAGGATAAGGAAGGCA	198	XM_003358301
		rev	GCTCCACCTCCAGGGTGAT		
Target genes					
Caspase 3	Casp3	fwd	GCAACGTTTCTAAAGAAGACCATAG	64	NM_001077840
		rev	CCATGGCTTAGAAGCACACAAATAA		
Caspase 9	Casp9	fwd	CTGACTGCCAAGCAAATGG	104	XM_003127619
		rev	GCCTGACAGCCGTGAGAG		
Cyclin B1	CycB1	fwd	GGATCACCAGGAACACGAAA	187	NM_001170768
		rev	GCTTCCTTTTTCAGAGGCAGT		
Cyclin D1	CycD1	fwd	GACGAGCTGCTGCAAATG	188	XM_003480653
		rev	GAAATGAACTTCACGTCTGTGG		
Interleukin 1 beta	IL1β	fwd	AGAAGAGCCCATCGTCCTTG	139	NM_001005149
		rev	GAGAGCCTTCAGCTCATGTG		
Interleukin 5	IL5	fwd	TGGAGCTGCCTACGTTAGTG	105	NM_214205
		rev	TCGCCTATCAGCAGAGTT		
Interleukin 6	IL6	fwd	GCAATGAGAAAGGAGATGTGT	138	XM_003357471
		rev	GCAGGTCTCCTGATTGAACC		
Interleukin 8	IL8	fwd	GGCAGTTTTCCTGCTTTCTGC	153	XM_003361958
		rev	CAGTGGGGTCCACTCTCAAT		
Transforming growth factor beta 1	TGFβ	fwd	ACGTCACTGGAGTTGTGCGG	159	XM_002701901
		rev	TTCATGCCGTGAATGGTGGCG		
Tumour necrosis factor-alpha	TNFα	fwd	CCCCTGTCCATCCCTTTATT	200	NM_214022
		rev	AAGCCCCAGTTCCAATTCTT		

being investigated at 0, 3, 6, 9 and 24 h to monitor potential changes. Comparative evaluation by peak integration during GC-MS analysis revealed that no obvious changes in the composition of 1,8-cineole derivative profile occurred from the treatment in each case, which suggests that both 1,8-cineole as well as the trace derivative constituents observed were stable under the experimental conditions applied. Thus it could be ascertained that neither cineole nor its derivatives were retained by any media constituents such as proteins contained therein. Other studies by our group on cellular and intestinal models (unpublished data), as well as our own and previous investigations of other groups on absorption and distribution processes of cineole *in vivo*[10,12] additionally demonstrated that cineole is readily taken up by intestinal cells and further transmitted into the human organism where it is detectable either in serum, breast milk or exhaled breath after uptake through the intestine. Accordingly, the lack of relevant metabolite detection cannot be attributed to impaired uptake of cineole by the intestinal cells.

Overall, it could be shown that both for the water control samples as well as for the culture medium control samples, all cineole derivative concentrations were drastically lower than the concentration of 1,8-cineole (1 g/l) itself. Thereby, 3-oxocineole and 2-oxocineole were the constituents with the relatively highest concentration in a range of around 200 μg/l, both in water and in culture medium. All other derivatives were present with concentrations of around 100 μg/l (α2-hydroxy-1,8-cineole) or even below (data not shown), only α2-hydroxy-1,8-cineole showed some tendency to somewhat higher values of about 200 μg/l in culture medium in comparison to about 100 μg/l in the water control. Nevertheless, it still needs to be kept in mind that determination of these trace constituents was already close to the detection limit so that such changes need to be considered as insignificant in relation to the very high dosage of the cineole treatment applied within this study. Overall it can be concluded that none of the cineole derivatives is an artefact formed due to the sample treatment conditions applied in this study.

Then, potential metabolite profiles of the odorant 1,8-cineole were monitored at the same time steps as for the control samples (0, 3, 6, 9 and 24 h of incubation) while being applied to the intestinal cell line culture in culture medium. The same derivatives (α2-hydroxy-1,8-cineole, β2-hydroxy-1,8-cineole, α3-hydroxy-1,8-cineole, 7-hydroxy-1,8-cineole, 9-hydroxy-1,8-cineole, 2-oxo-1,8-cineole, 3-oxo-1,8-cineole, 2,3-dehydro-1,8-cineole, 4-hydroxy-1,8-cineole) were detected in all samples under investigation. Quantitative evaluation of the peak areas confirmed that those cineol derivatives were only detectable as trace constituents in all cases at concentrations below 600 μg/l (Figure 1). By means of these experiments it could be demonstrated that these metabolites were, again, predominantly attributable to the trace impurities of the applied cineole standard but were not additionally formed to any relevant extent during application to the intestinal cell culture.

Only in some cases was there a tendency of a recordable increase (Figure 1): α2-hydroxy-1,8-cineole amounted from a start concentration of around 150 μg/l to a final concentration of about 550 μg/l after 24 h incubation, corresponding to an increase of a factor of about 3.7. Moreover, 4-hydroxy-1,8-cineole and 9-hydroxy-1,8-cineole, with initial concentrations at

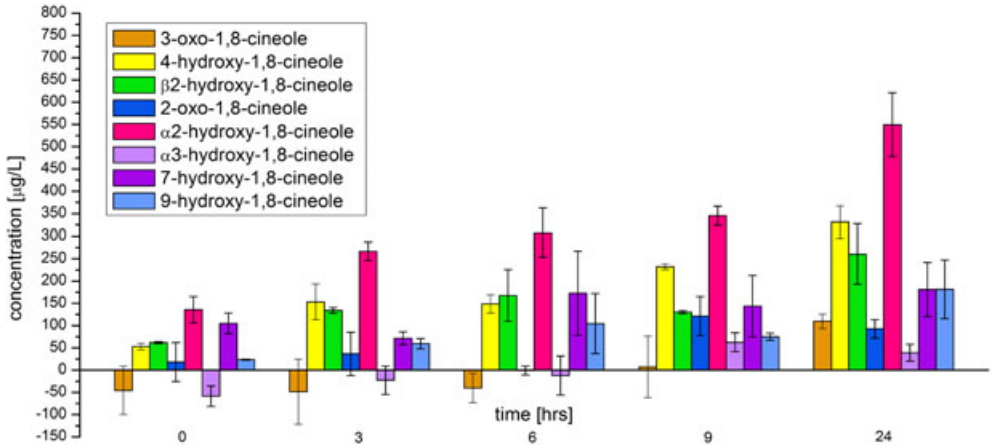

Figure 1. 1,8-Cineole derivative values as determined after incubation with 1,8-cineole (1.0 g/l dosage) in a IPEC-J2 intestinal cell line model with sampling at 0, 3, 6, 9 and 24 h of incubation. Data are expressed as values after subtraction of control values that were determined in parallel

time point 0 h of about 50 µg/l and about 25 µg/l, respectively, finally revealed values of about 350 µg/l and 175 µg/l, respectively, for the last time point (24 h). This would even correspond to an increase factor of 7 in both cases. At first sight these changes seem to represent partially enormous increases, still the comparatively dramatically higher concentration of 1,8-cineole needs to be kept in mind when rating these findings with regard to their relevance. For 2,3-dehydro-1,8-cineole chromatographic separation was very poor and showed considerable variance so that no decisive quantitative results could be obtained for this substance. However, semi-quantitative estimation revealed that also no distinct increase or decrease in concentration was observable during exposure of 1,8-cineole to the intestinal cell culture (data not shown). The negative values obtained for 3-oxo-1,8-cineole and α3-hydroxy-1,8-cineole can be attributed to the fact that all values were in a very low range around the detection limit, and that the respective blank values, with their relative variations, were subtracted from these actual values.

Overall, application of a 10-fold lower concentration of 0.1 g/l cineole also did not lead to any effective metabolite formation, which is comparable to the higher dosage investigated.

Summarizing the above, it could be shown that there might have been some slight indication of a metabolic activity observable under the incubation experiments applied; nevertheless, there were no obvious changes observable due to biotransformation in the presence of the applied intestinal cell line and under the experimental conditions used.

Maximum Non-lethal Cineole Concentration Determined at a Cellular Level via Electric Cell-substrate Impedance Sensing

The influence of 1,8-cineole on the proliferation and fitness of the epithelial cells was examined using non-invasive real-time tracking with the ECIS system.[21] The underlying principle is to trace the activity concerning surface interaction and attachment using a specific cell culture dish which can measure the attending change in impedance through the surrounding media. Increasing assemblage of cells growing to confluence and tighter lamination of cells on the electrodes increases the impedance, whereas detaching cells decrease the signal. The result is a picture of events at a cellular level in real time. Accordingly it is possible to determine toxic effects of a treatment, leading to cell detachment and death in a concentration-dependent manner.[22]

Figure 2a shows the IPEC-J2 obtained cineole treatment shortly before their confluent state. At that point of time eight cineole concentrations containing a control were applied (0.0, 0.3, 0.5, 0.7, 1.0, 1.3, 1.7 and 2.0 g/l). A notable result is that within this

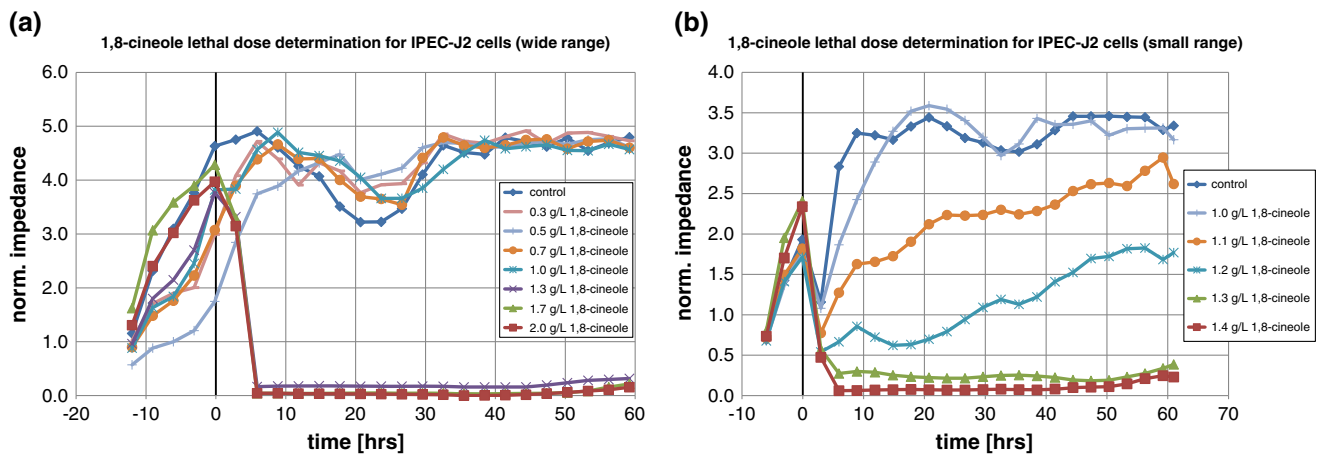

Figure 2. Electric cell-substrate impedance sensing (ECIS) measurement of cineole-treated JPEC-J2 cells. Inserted are low (a) and high (b) resolution ranges of cineole concentration. In both cases 1.0 g/l has no visible impact on the cell layer. The highest non-lethal concentration is revealed in plot (b) with 1.2 g/l

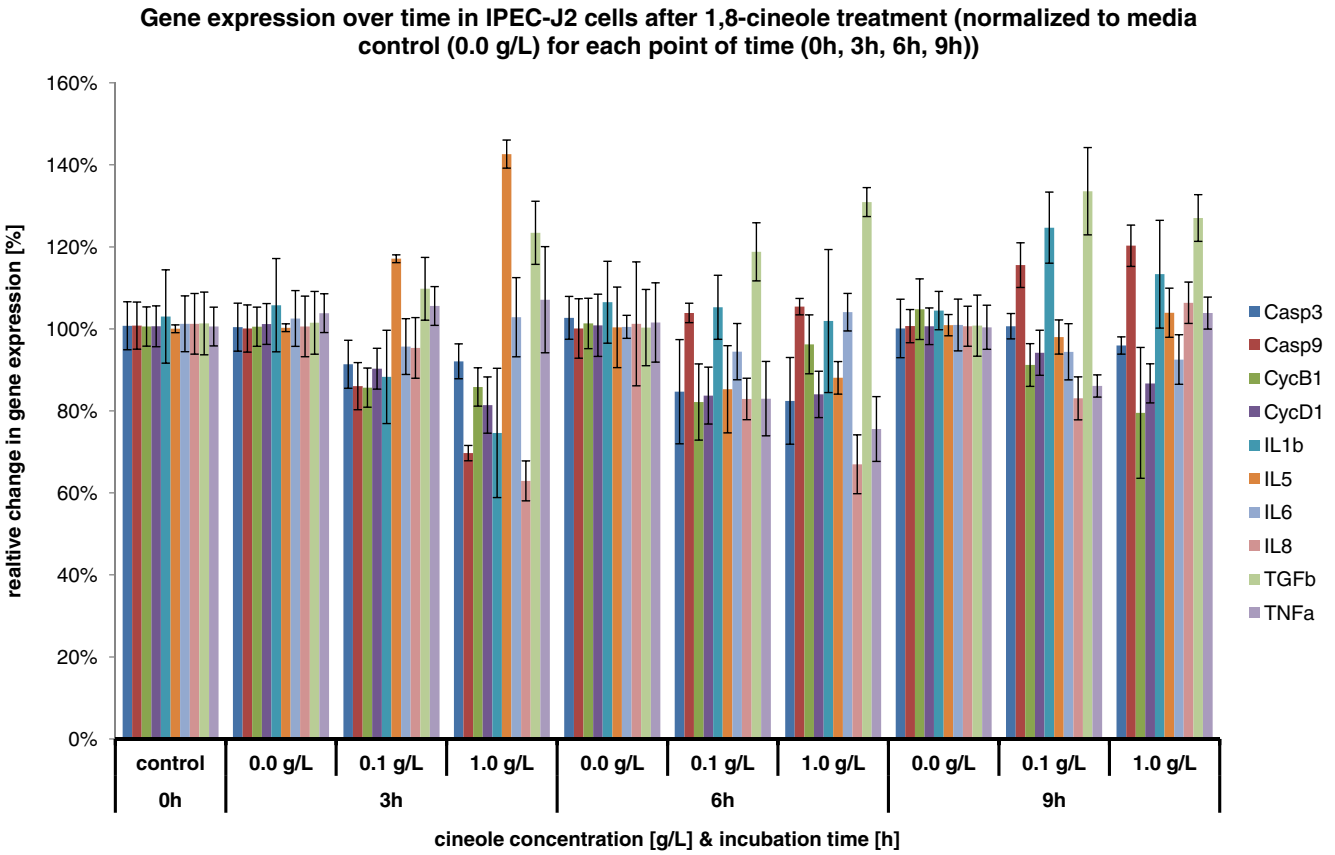

Figure 3. Reaction of the IPEC-J2 cells to the 1,8-cineole treatment on transcript level monitored over time. Relative change in gene expression (shown as a percentage) for the dataset normalized to the particular untreated samples of each time point is plotted. In each case 10 genes are displayed. The value corresponding to one gene within one treatment variant derives from the mean of three (SEM, $n = 3$) cell culture replicates (wells), according error bars are indicated. The duplicates of the RT-qPCR measurement are averaged for $2^{-\Delta\Delta Cq}$ calculation but not incorporated within the error bars (because of high reproducibility: mean CV value of 0.8%). A value of 100% on the ordinate represents constant gene expression subsequent to the 1,8-cineole treatment. The 0.0 g/l treatment groups to each point of time are slightly fluctuating around that value as a result of the natural variation and the technical error sources weighing on each sample

narrow range of cineole concentrations only two effect variants occurred. Up to 1.0 g/l of cineole the treatment was without any visible effect in the ECIS measurement and so for the integrity of the cell layer. The next higher cineole concentration (1.3 g/l) instantly led to complete cell detachment. With these concentrations no effect in between was measurable. Regarding the signal decay after 20 h in Figure 2a all samples were affected by the treatment; however, considering the control samples this occurred independently of the cineole concentration applied.

In order to assess whether there are intermediate events we conducted the assay with an even higher resolution of cineole concentration (1.0, 1.1, 1.2, 1.3 and 1.4 g/l). Figure 2b shows that for the concentration range between 1.0 and 1.3 g/l recovery of cell attachment could be monitored. These findings are in accord with the sudden toxic effect above 1.0 g/l from Figure 2a. Hence, we could establish that the maximal non-lethal dose of 1,8-cineole for IPEC-J2 cells is 1.2 g/l.

Gene Expression Analysis (RT-qPCR)

As we were surprised by the distinct effector level of cineole in our ECIS measurements we conceived to go one step deeper and evaluate the impact at the molecular level. Due to the fact that detachment of the IPEC-J2 cells occurs when the cineole concentration exceeds 1.2 g/l there should be a response on gene expression level. Therefore 10 marker genes were chosen: the proliferation markers cyclins CycB1 and CycD1, the growth factor TGFβ and, further regarding the aspect of apoptosis, the caspases Casp3 and Casp9. In respect of modulatory effects of 1,8-cineole on the immune system, the primary mediators IL1β and TNFα[23] and the secondary mediators IL6 and IL8[24] were analysed. Gene expression levels of IL5 were assessed, especially because of its role in asthmatic diseases.[5,25]

Figure 3 shows the relative change in gene expression for the two inserted 1,8-cineole concentrations over time. Considering physiologically relevant amplitudes of gene regulations only two genes, *IL1β* (fold down-regulation of 0.7 at 3 h and 1.0 g/l) and *IL8* (fold down-regulation of 0.6 at 6 h and 1.0 g/l) (see Table 2), were of interest. All other genes did not show a distinguished modulation after 1,8-cineole treatment. Regarding the function of these genes as primary (*IL1β*) and secondary (*IL8*) mediators we could assign an immunosuppressive effect of 1,8-cineole in compliance to Sadlon and Lamson.[2] If the time sample interval of 3 h was missed further early effects between 0 h and 3 h remained undetermined in this study. However, it must be pointed out that this finding is limited to the 1,8-cineole concentration of 1.0 g/l and therefore is potentially unrealistic as a pharmaceutical appliance. Interestingly, in this connection no up-regulation of apoptotic markers was observed for the concentration close to the lethal dose.

Table 2. Gene regulation of the investigated marker genes is displayed as x-fold regulation (calculated by $2^{-\Delta\Delta Cq}$): expression data are shown after two different normalizations visualized in Figures 3 and 4a

Time point (h)	Dose (g/l)	Casp3	Casp9	CycB1	CycD1	IL1â	IL5	IL6	IL8	TGFβ	TNFα
Data corresponding to Figure 3 [a]											
0	0.0	1.01	1.01	1.01	1.01	1.03	1.00	1.01	1.01	1.01	1.01
3	0.0	1.00	1.00	1.01	1.01	1.06	1.00	1.03	1.01	1.01	1.04
	0.1	0.91	0.86	0.86	0.90	0.88	1.17	0.96	0.95	1.10	1.06
	1.0	0.92	0.70	0.86	0.81	0.75	1.43	1.03	0.63	1.23	1.07
6	0.0	1.03	1.00	1.01	1.01	1.06	1.00	1.01	1.01	1.00	1.02
	0.1	0.85	1.04	0.82	0.84	1.05	0.85	0.94	0.83	1.19	0.83
	1.0	0.82	1.05	0.96	0.84	1.02	0.88	1.04	0.67	1.31	0.76
9	0.0	1.00	1.01	1.05	1.01	1.04	1.01	1.01	1.01	1.01	1.00
	0.1	1.01	1.16	0.91	0.94	1.25	0.98	0.94	0.83	1.34	0.86
	1.0	0.96	1.20	0.80	0.87	1.13	1.04	0.93	1.06	1.27	1.04
Data corresponding to Figure 4a [b]											
0	0.0	1.01	1.01	1.01	1.01	1.03	1.00	1.01	1.01	1.01	1.01
3	0.0	1.12	1.31	1.30	1.13	1.02	0.77	1.10	2.76	1.38	1.35
	0.1	1.02	1.13	1.11	1.01	0.85	0.90	1.02	2.62	1.49	1.38
	1.0	1.03	0.91	1.11	0.91	0.72	1.09	1.10	1.73	1.68	1.40
6	0.0	1.22	0.99	2.17	1.72	0.90	1.03	1.24	2.70	1.45	1.68
	0.1	1.01	1.03	1.76	1.42	0.89	0.88	1.17	2.21	1.72	1.37
	1.0	0.98	1.04	2.06	1.43	0.86	0.91	1.28	1.79	1.89	1.25
9	0.0	1.12	0.94	4.27	1.98	0.76	0.81	1.38	1.78	1.40	1.38
	0.1	1.12	1.08	3.71	1.85	0.91	0.79	1.29	1.47	1.86	1.18
	1.0	1.07	1.13	3.24	1.70	0.82	0.84	1.27	1.88	1.77	1.43

[a]Data corresponding to Figure 3 are normalized to the media control (0.0 g/l) for each point of time (0 h, 3 h, 6 h, 9 h).
[b]Data corresponding to Figure 4a are normalized to the absolute control ('control', $t = 0$).

For a deeper analysis of the measured expression values we applied additional evaluations. The data in Figure 3 are normalized to the corresponding media control for each point of time. Because of the low fluctuations in the expression pattern we decided to normalize all data to the media control of time point 0 h (Figure 4a). This revealed the shift of the genes in the cell culture over time. Regarding the three concentrations (including 0.0 g/l) for one point of time a clear time effect could now be assigned. The application of 1,8-cineole evoked an expression pattern similar to the 0.0 g/l samples. It was shown that several genes were regulated during the 9 h of incubation, but substantially independent of the 1,8-cineole treatment. Conspicuous is the up-regulation of *CycB1* (4.3-fold at 9 h). This gene has its function as activator of the cyclin-dependent kinase 1/cyclin B1 complex in the cell cycle during the progression from the G2 phase to the M phase.[26] Relative accumulation of its transcript over the 9 h of incubation may appear due to dense confluence of the cell layer. The incipient cell cycle arrest may temporarily cause the increased expression levels as normally CycB1 is not degraded until the anaphase.[27]

The fact that the expression changes over time were more dominant than any gene regulation originating from the 1,8-cineole treatment was demonstrated most definitely when a PCA was applied to the dataset (see the section 'RT-qPCR gene expression analysis'). In Figure 4b the C_q values normalized solely with the reference genes are shown in a PCA plot. This means that the datasets were considered sample-wise with respect to the amplitude of all regulative effects lying on one sample. This visualization mode clearly exposes the fact that the background gene regulation of the cell culture (Figure 4a) clearly exceeded the weak immunomodulatory findings from the 1,8-cineole application (Figure 3). This means that for our model we cannot assign a proven physiological effect of 1,8-cineole concerning the monitored marker genes.

Conclusion

Our data show that application of the methods used may be useful in elucidating potential physiological response mechanisms at the cellular and molecular levels to food ingredients, especially odorants. The combinatory approach may be a promising tool for gaining a comprehensive understanding of odorant–physiology interactions. Nevertheless, with regard to the studied target substance, 1,8-cineole, surprisingly few physiological effects were monitored within this study during exposure of the investigated intestinal cell lines to 1,8-cineole, unless a lethal concentration was reached. Obviously, the intestinal system in this case does not react, with direct initial contact, by an immediate defence or response mechanism, even if concentrations approach potentially harmful levels that may finally lead to apoptosis. This is at least true for the intestinal cell models investigated within this study, and for the assays applied. Further studies in this field will need to further elucidate and verify this seemingly obvious passivity to the generally pharmacologically active substance 1,8-cineole, and to focus on other potentially pharmacologically active substances, specifically other odorants.

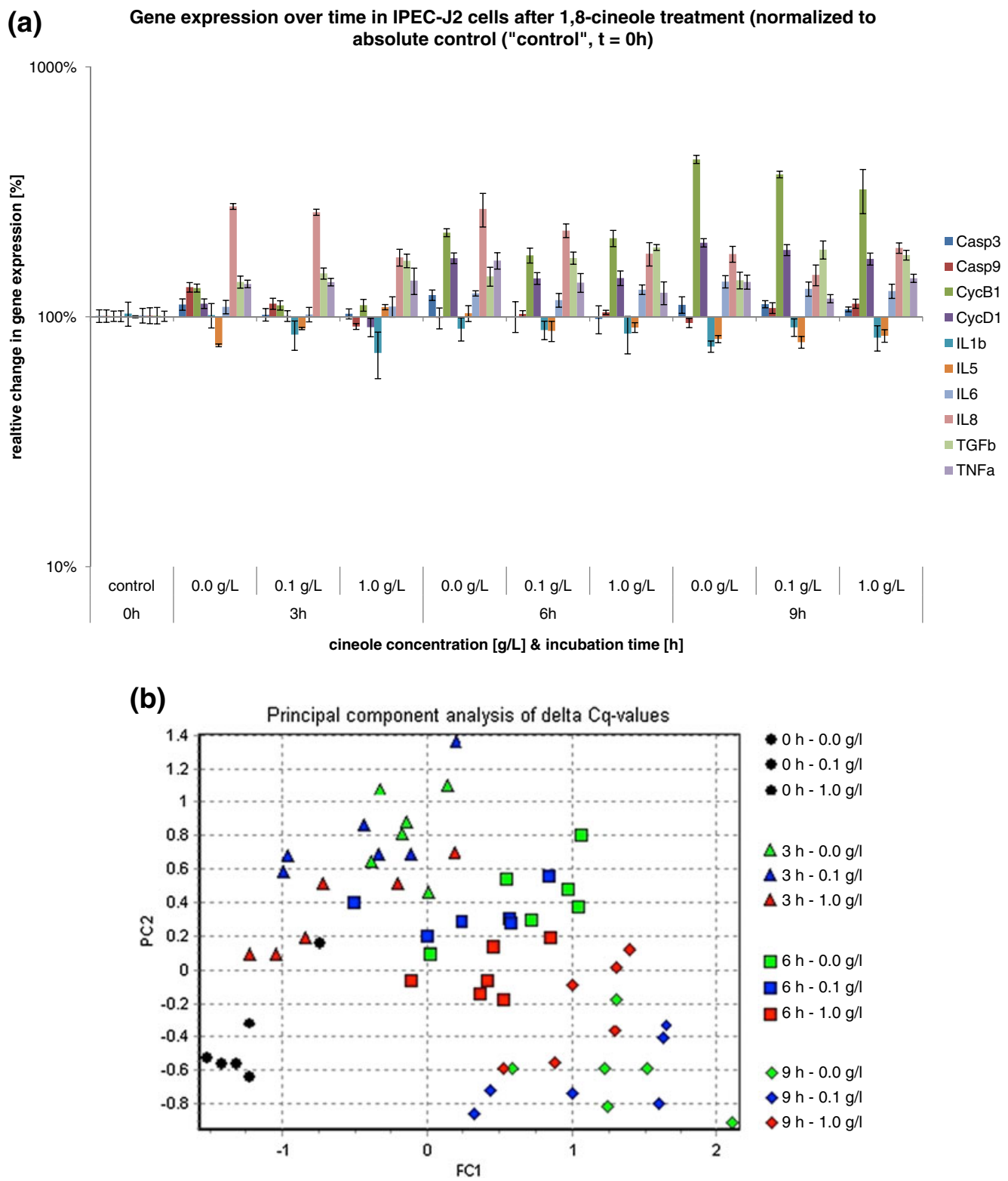

Figure 4. Dataset analysed independently of the media control expression level of a single point of time. (a) In contrast to Figure 3 all data are now normalized to the expression level of the untreated cells at time point 0 h. Further to the ordinate a logarithmic scale was applied and the abscissa was set to 100%. Gene regulation now appears above or below the value of constant expression. The sample group named 'control' reveals the reference point for the normalization. The amplitude for the fold regulation after this normalization mode is much higher compared to Figure 3 (up to 4.3-fold, see Table 2). Errors indicated are in accordance to the experimental set-up (SEM, $n = 3$, RT-qPCR duplicates excluded for error calculation). (b) PCA of the whole dataset using ΔC_q values (= C_q values normalized to reference genes) mean centred to columns (= genes). In this PCA the data are considered for the extent of variation which affects one sample referred to its origin (treatment group). Equal shapes represent an equal point of time, equal colours for an equal dose of 1,8-cineole. The maximum impact which brings variation to the expression levels for one sample is visible in clusters of data points. Here data only clusters due to the shapes and not colour-wise

Acknowledgements

This study was supported by a grant from the Vereinigung zur Förderung der Milchwissenschaftlichen Forschung an der Technischen Universität München e.V. The IPEC-J2 cell culture was generously supplied by Dr Karsten Tedin. The authors are most grateful to Juliane Hundt for the carrying out the RT-qPCR experiments.

References

1. K. Inoue, H. Takano. *Basic Clin. Pharmacol. Toxicol.* **2011**, *108*, 295.
2. A. E. Sadlon, D. W. Lamson. *Altern. Med. Rev.* **2010**, *15*, 33.
3. S. Asbaghian, A. Shafaghat, K. Zarea, F. Kasimov, F. Salimi. *Nat. Prod. Commun.* **2011**, *6*, 137.
4. S. Sertel, T. Eichhorn, P. K. Plinkert, T. Efferth. Anticancer activity of Salvia officinalis essential oil against HNSCC cell line (UMSCC1). *HNO* **2011**, *59*(12), 1203–1208.
5. U. R. Juergens, U. Dethlefsen, G. Steinkamp, A. Gillissen, R. Repges, H. Vetter. *Respir. Med.* **2003**, *97*, 250.
6. H. Worth, C. Schacher, U. Dethlefsen. *Respir. Res.* **2009**, *10*, 69.
7. Z. Yang, N. Wu, Y. Fu, G. Yang, W. Wang, Y. Zu, T. Efferth. *J. Biomol. Struct. Dyn.* **2010**, *28*, 323.
8. M. Duisken, F. Sandner, B. Blomeke, J. Hollender. *Biochim. Biophys. Acta* **2005**, *1722*, 304.
9. M. Miyazawa, M. Shindo, T. Shimada. *Drug Metab. Dispos.* **2001**, *29*, 200.
10. K. Horst, M. Rychlik. *Mol. Nutr. Food Res.* **2010**, *54*, 1515.
11. P. Schierack, M. Nordhoff, M. Pollmann, K. D. Weyrauch, S. Amasheh, U. Lodemann, J. Jores, B. Tachu, S. Kleta, A. Blikslager, K. Tedin, L. H. Wieler. *Histochem. Cell Biol.* **2006**, *125*, 293.
12. F. Kirsch, K. Horst, J. Beauchamp, M. Rychlik, A. Buettner. In *Advances and Challenges in Flavour Chemistry & Biology*, T. Hofmann, W. Meyerhof, P. Schieberle (eds). Eigenverlag Deutsche Forschungsanstalt für Lebensmittelchemie: Garching, **2011**; 257.
13. W. Engel, W. Bahr, P. Schieberle. *Eur. Food Res. Technol.* **1999**, *209*, 237.
14. J. M. H. Bemelmans. In *Progress in Flavour Research*, D. G. Land, H. E. Nursten (eds). Applied Science Publishers: London, **1979**; 79.
15. I. Giaever, C. R. Keese. *Proc. Natl. Acad. Sci. U. S. A.* **1984**, *81*, 3761.
16. K. J. Livak, T. D. Schmittgen. *Methods* **2001**, *25*, 402.
17. S. A. Bustin, V. Benes, J. A. Garson, J. Hellemans, J. Huggett, M. Kubista, R. Mueller, T. Nolan, M. W. Pfaffl, G. L. Shipley, J. Vandesompele, C. T. Wittwer. *Clin. Chem.* **2009**, *55*, 611.
18. W. M. Freeman, S. J. Walker, K. E. Vrana. *Biotechniques* **1999**, *26*, 112.
19. A. Bergkvist, V. Rusnakova, R. Sindelka, J. M. Garda, B. Sjogreen, D. Lindh, A. Forootan, M. Kubista. *Methods* **2010**, *50*, 323.
20. I. T. Jolliffe. *Principal Component Analysis. In Springer Series in Statistics*. Springer: New York, **2002**; pp. 1–9.
21. P. Mitra, C. R. Keese, I. Giaever. *Biotechniques* **1991**, *11*, 504.
22. J. Müller, C. Thirion, M. W. Pfaffl. *Biosens. Bioelectron.* **2011**, *26*, 2000.
23. H. F. Galley, N. R. Webster. *Br. J. Anaesth.* **1996**, *77*, 11.
24. R. de Waal Malefyt, J. Abrams, B. Bennett, C. G. Figdor, J. E. de Vries. *J. Exp. Med.* **1991**, *174*, 1209.
25. K. Takatsu. *Proc. Jpn. Acad. Ser. B Phys. Biol. Sci.* **2011**, *87*, 463.
26. M. Castedo, J. L. Perfettini, T. Roumier, G. Kroemer. *Cell Death Differ.* **2002**, *9*, 1287.
27. F. Wolf, C. Wandke, N. Isenberg, S. Geley. *EMBO J.* **2006**, *25*, 2802.

Determination of cell morphology under 1,8-cineole treatment in porcine intestinal cells

Isabella Almstätter [a], Jakob Müller [a], Michael W. Pfaffl [a] and Andrea Büttner [b,c]

[a]*Physiology Weihenstephan, Z I E L Research Center for Nutrition and Food Sciences, Technical University of Munich, Weihenstephaner Berg 3, D-85354 Freising, Germany*

[b]*Department of Chemistry and Pharmacy - Emil Fischer Center, University of Erlangen-Nuremberg, Schuhstr. 19, D-91052 Erlangen, Germany*

[c]*Sensory Analytics, Fraunhofer Institute for Process Engineering and Packaging (IVV), Giggenhauserstr. 35, D-85354 Freising, Germany*

e-mail: andrea.buettner@ivv.fraunhofer.de

Keywords: jejunal; ileal; IPEC-J2; IPI-2I; wound healing; apoptosis; ECIS

ABSTRACT

A potential effect of 1,8-cineole on the morphology and growth behaviour of the cells lining the first segments of the intestinal system should be studied. It was shown that morphologically cineole had no effect on jejunal and ileal porcine cells applied in pharmacological or physiological concentrations, neither on cells during attachment and spreading, nor on confluent cell layers. Solely the exposure to high concentrations of cineole adversely affected the cells and led to subsequent apoptosis. In a wound healing assay a potential protective or growth promoting effect by cineole could not be detected.

1. INTRODUCTION

The most important natural reservoir of the volatile aroma compound 1,8-cineole are the leafs of the eucalyptus tree (Eucalyptus spec.) [1]. Applications for cineole are various, for example as flavouring agent [2] or antioxidant in food, beverages, cosmetics and drugs. In the therapy of respiratory tract diseases, cineole is a very popular pharmacological agent acting as expectorant and mucolytic, and is also suggested to have an anti-inflammatory effect [3]. The first contact of cineole with the consuming organism in vivo depends on the administration form. If consumed as drug in enteric coated capsules, the small intestinal system, in particular the epithelia of the jejunum and ileum, are the first sites of contact. Based on that fact, the chosen in vitro models were two porcine small intestinal epithelial cell lines, the jejunal IPEC-J2 and the ileal IPI-2I cells, as the human and swine intestinal tracts are highly similar. Up to now, the effect of cineole on intestinal epithelium, most specifically the morphology and growth behaviour of the cells, was not examined. Technical tool was the ECIS system for non-invasive real-time observation of cell cultures [4].

2. MATERIALS AND METHODS

Cell cultures. The IPEC-J2 cell line is a permanent, non-transformed porcine jejunal cell line originated from midjejunal epithelium isolates of a neonatal, unsuckled piglet [5]. The IPI-2I cell line is a transformed porcine ileal cell line derived from the ileum of an adult histocompatible miniature male boar [6]. The IPEC-J2 cells were cultured in DMEM Ham's F12 supplemented with 5% Foetal Bovine Serum (FBS) and 2 mM L-glutamine, the IPI-2I cells in DMEM with 10% FBS, 4 mM L-glutamine and 0.024 U/ml insulin, both with 1% penicillin/streptomycin antibiotic mix at 37°C in humidified atmosphere of 5% CO_2 [7]. 1,8-cineole was applied to growing cells in pre-mixed medium in different pharmacological and physiological concentrations (ten-fold increase from 0.00002 to 2 g/L).

Electric Cell Substrate Impedance Sensing (ECIS). The influence of the cineole treatment on the morphology and growth behaviour of epithelial cells was examined by non-invasive real-time tracking of cell attachment and proliferation with the electric cell substrate impedance sensing system (ECIS). Principle is to trace all changes of surface attachment in a specific cell culture dish by measurement of the impedance. With increasing confluency the impendance in the wells increases, if attached cells die and detach, the impedance decreases. So the resulting impedance profile is a real-time follow-up of changing cell densities. The ECIS culture dishes were inoculated with 10^5 cells per well for both cell lines and the IPEC-J2 reached full confluency with plateau impedance level after about 16h, the IPI-2I after about 22h. When the cells reached this plateau, the cineole treatment was applied (Figure 1).

Wound Healing Assay. The migration velocity of a cell line towards unpopulated areas of a culture dish was formerly examined by a scratch or scrape assay [8]. The ECIS-based wound healing assay can replace these mechanical ways of wounding by pointed application of an elevated electrical field (6 V, 20 sec) [9]. The technique allows real-

time monitoring of wound healing, migration of surrounding cells to repopulate the empty area, by detection of increasing impedances. Aim of this assay was to find out whether pre-applied cineole has any protective effect on the cells or whether the growth velocity after wounding under cineole treatment differs. The assay was performed with the IPEC-J2 cells and a treatment concentration of 1.2 g/l, the maximal not-lethal cineole concentration for this cell line.

3. RESULTS

Quantitative real-time monitoring of attachment and spreading [10] for signs of cytotoxicity after cineole treatment in different concentrations was performed with the ECIS system in non-invasive manner (Figure 1) [11]. Firstly, the growth velocity to build a confluent cell monolayer was determined. The jejunal cells grew a bit faster than the ileal cells. Treatment of both cell lines with 2 g/l cineole led to subsequent cell death which was also found in an assay with Chinese hamster ovary cells [12]. Interestingly all concentrations below 1.3 g/l had no effect. Neither in jejunal nor in ileal cells their growth behaviour or morphology was influenced, being also confirmed by microscopy (Figure 2).

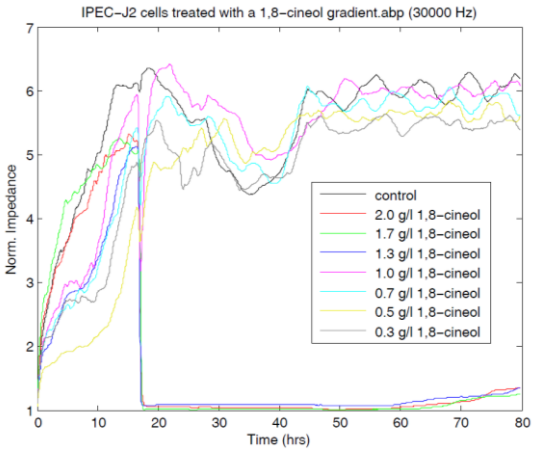

Figure 1. ECIS measurement of IPEC-J2 cells treated with 1,8-cineol.

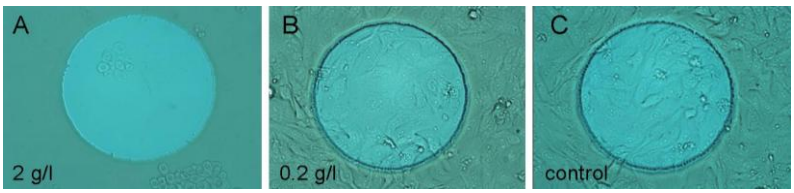

Figure 2. IPEC-J2 cells after 72h of 1,8-cineole treatment in a 20x magnification.

The wound healing assay with the ECIS system was used to identify possible protective or inhibitory effects of cineole on spreading IPEC-J2 cells. Therefore the assay was performed with the maximal non-lethal cineole concentration of 1.2 g/l. No

morphological changes in terms of an altered attachment and spreading behaviour of the jejunal cells could be detected in cineole containing medium. After wounding there was also no effect of cineole pre-treatment, neither on the inwards movement velocity of surrounding cells nor in their attachment and spreading. This result is contrary to earlier results demonstrating a gastro-protective effect of cineole [13], however with much higher doses than used in this study. The cineole treatment during the healing process also did not alter the healing process.

4. DISCUSSION AND CONCLUSION

This was the first study investigating the effect of the pharmacological compound 1,8-cineole on intestinal epithelial cells and potential alterations of cell attachment, morphology and survival. It was demonstrated that morphologically and behaviourally cineole in pharmacological or physiological concentrations had no effect on jejunal and ileal porcine epithelial cells, neither during cell attachment and spreading, nor on confluent cell layers. Also, no potential protective or growth promoting effect of cineole could be confirmed in a wound healing assay. Solely the exposure to high concentrations of cineole adversely affected the cells and led to subsequent apoptosis. Such high doses can lead to serious poisoning in humans if consumed orally [14]. It could be suggested that even a concentration of 1.2 g/l cineole is not high enough to induce adverse effects to the intestinal epithelium directly or after wounding and has neither a preventive nor a growth inhibiting effect on the cells.

Acknowledgement for funding: V. z. Förderung der Milchwiss. Forschung an der TUM e.V.

References

1. Asbaghian, S; Shafaghat, A; Zarea, K; Kasimov, F; Salimi, F; Nat Prod Commun. 2011; 6(1), 137-140
2. Horst, K; Rychlik, M; Mol Nutr Food Res. 2010; 54: 1515-1529
3. Juergens, UR; Dethlefsen, U; Steinkamp, G; Gillissen, A; Repges, R; Vetter, H; Respir Med. 2003, 97(3), 250-256
4. Müller, J; Thirion, C; Pfaffl, MW; Biosens Bioelectron. 2011, 26(5), 2000-2005
5. Rhoads, JM; Chen, W; Chu, P; Berschneider, HM; Argenzio, RA; Paradiso, AM; Am J Physiol. 1994, 266(5 Pt 1), G828-838
6. Kaeffer, B; Bottreau, E; Velge, P; Pardon, P; Eur J Cell Biol. 1993, 62(1), 152-162
7. Mariani, V; Palermo, S; Fiorentini,S; Lanubile, A; Giuffra, E; Vet Immunol Immunopathol. 2009, 131(3-4), 278-284
8. Jumblatt, MM; Neufeld, AH; Invest Ophthalmol Vis Sci. 1986, 27(1), 8-13
9. Keese, CR; Wegener, J; Walker, SR; Giaever, I; PNAS. 2004, 101(6), 1554-1559
10. Mitra, P; Keese, CR; Giaever, I; Biotechniques. 1991, 11(4), 504-510
11. Giaever, I; Keese, CR; PNAS. 1991, 88(17), 7896-7900
12. Ribeiro, DA; Matsumoto, MA; Marques, ME; Salvadori,DM; Oral Surg Oral Med Oral Pathol Oral Radiol Endod. 2007, 103(5), e106-109
13. Santos, FA; Rao, VS; Dig Dis Sci. 2001, 46(2), 331-337
14. Tibballs, J; Med J Australia. 1995, 163, 177-180